Measurements and Analysis of the Microwave Dielectric Properties of Tissues

Anne Margaret Campbell

Department of Physics and Astronomy

University of Glasgow

Presented for the degree of Doctor of Philosophy

to the University of Glasgow

October 1990

To my wonderful family

Eddie, Maureen

John, Stephen

and Jenny

Acknowledgements

Table of Contents

Chapter 3 *Dielectric properties of biological tissues 2*

Data review 35

Summary

Knowledge of the microwave dielectric properties of human tissues is essential for the understanding and development of medical microwave techniques. In particular, microwave thermography relies on processes fundamentally determined by the high frequency electromagnetic properties of human tissues. The specific aim of this work was to provide detailed information on the dielectric properties of female human breast tissue at 3 — 3.5GHz, the frequency of operation of the Glasgow microwave thermography equipment.

At microwave frequencies the frequency variation of the dielectric properties of biological tissues is thought to be determined mainly by the dipolar relaxation of tissue water. Water exists in different states of binding within the tissue; the relaxation of each component of this water may be parameterised by the Debye or Cole-Cole equations. At a single frequency an average relaxation frequency may be calculated for a given tissue type.

Mixture equations may be used to describe the dielectric properties of two-phase mixtures in terms of the dielectric properties and volume fractions of the component phases. Biological tissues are very much more complex than these two phase models. However, comparisons of the observed dielectric properties as a function of water content, with models calculated from mixture theory allow some qualitative conclusions to be drawn regarding tissue structure.

Human and animal dielectric data at frequencies between 0.1 and 10GHz have been collected from the literature and are displayed in tabular form. These comprehensive tables were used to examine the widely-held assumption an animal tissue is representative of the corresponding human tissue. This assumption was concluded to

be uncertain in most cases because of lack of available data, and perhaps wrong for certain tissue types.

The tables were also used to compare *in vivo* and *in vitro* dielectric data. These may be expected to be different because the tissue is in a physiologically abnormal state *in vitro*. However at microwave frequencies *in vitro* data was found to be representative of the tissue *in vivo* provided gross deterioration of the tissue is avoided.

A new resonant cavity perturbation technique was designed for dielectric measurements of small volumes of lossy materials at a fixed frequency of 3.2GHz. This technique may be used to measure materials of a wide range of permittivities and conductivities with accuracies of 3 — 4%. The major sources of error were found to be tissue heterogeneity and sample preparation procedures.

Using this technique *in vitro* dielectric measurements were made on human female breast tissues. A large number of data were gathered on fat and normal breast tissues, and on benign and malignant breast tumours.

Each data set was parameterised using the Debye equation. Results from this suggest that all breast tissues measured in this work contain a component of bound water. A smaller proportion of water is bound in fat than is bound in other tissues.

Comparisons were made of the dielectric properties of breast tissues with values calculated from mixture theories. Permittivity data largely fall within bounds set by mixture theory: conductivity data often fall outside these limits. This may imply that physiological saline is not a good approximation to tissue waters; or it may imply that another relaxation process is occurring in addition to the dipolar relaxation of saline.

Comparisons of tissue type indicate that a dielectric imaging system could be designed which would detect breast diseases, but that severe problems could arise in distinguishing disease types from dielectric imaging alone.

Chapter 1

Introduction

Knowledge of the microwave dielectric properties of human tissues is essential for our understanding of certain medical techniques and for some biophysical processes. In particular, microwave thermography and microwave hyperthermia techniques rely on processes fundamentally determined by the high-frequency electromagnetic properties of tissues.

1.1 Microwave thermography

Microwave thermography is a technique which allows estimation of internal body temperatures from measurement of the natural thermal radiation emitted by body tissues. This technique has a number of potentially important medical applications for the detection, diagnosis and treatment monitoring of diseases which produce regional or localised temperature changes in the body's normal temperature distribution. For instance, initial studies of its clinical application have included osteo-articular diseases, vascular disorders, diseases of the acute abdomen, and cancers in the breast, thyroid and brain (Barrett et al, 1980; Edrich , 1979; Land et al, 1986; Abdul-Razzak et al, 1987; Brown, 1989). Microwave thermography, in contrast to other thermographic imaging techniques, detects electromagnetic radiation which has penetrated medically useful distances, of the order of several centimetres, through body tissues, thus allowing a passive, non-invasive measurement of subcutaneous temperatures (Land, 1987a, 1987b).

The Glasgow microwave thermography system operates at frequencies of 3 — 3.5GHz. This choice of measurement frequency allows a reasonable penetration depth (about 0.8cm in muscle, and about 5cm in fat), and reasonable lateral spatial resolution (about 0.7 to 2cm near the antenna). If microwave thermography is to be

1

widely used and to fulfill its potential as a clinical technique, accurate retrieval of the subcutaneous temperature profile is essential. Temperature retrieval is achieved using models of the underlying tissue structure which depend crucially on the dielectric and thermal properties of the tissue (Brown, 1989; Hawley et al, 1988).

1.1.1 Microwave thermography in breast disease

A promising application of microwave thermography is in the detection of early (asymptotic) breast cancer. A very large number of women develop breast cancer at some point throughout their lives: one in every fifteen women on the west coast of Scotland (Blamey, 1984); and one in every eleven women in the United States of America (Burn, 1984). In industrialised countries breast cancer is the leading cause of cancer deaths among both pre- and post-menopausal women and its incidence is increasing (Davis et al, 1990). Despite publicity about self examination, it is unusual for women to present with lesions at a curable stage: most women are diagnosed with symptomatic breast cancer, too late to have any chance of being cured. The only real hope in these circumstances lies in regular screening of women at risk (Forrest et al, 1986).

At present the most consistently accurate and reliable method of detecting breast cancer is by mammography, the examination of the breast by means of low energy radiography (Rotherberg, 1986; Forrest et al , 1986). However, a recent statistical study by Edeiken (1988), showed that mammography has a very high false-negative rate: in over one fifth of cases in a sample of 499 women with cancer proven by biopsy, a mammogram gave a false-negative result. When the sample group was separated into pre- and post-menopausal women, the false-negative rate was 44% for younger ages and 13% for the older group.

There is clearly a need for new screening methods such as microwave thermography to provide aid in clinical diagnosis. Microwave thermography should be particularly useful when used in younger women who are more likely to have dense glandular tissue (see Section 5.2) in which detection of lesions by mammography is

difficult; and also as a preliminary screening method to identify high risk women who may then be given mammography. This would reduce the number of women exposed to x-rays and the risk associated with this.

The new dielectric data presented in Chapter 5 were taken mainly from measurements of human female breast tissue, with the specific aim of providing information to improve temperature retrieval in microwave thermography. Knowledge of the microwave properties of normal and diseased breast tissues at 3GHz will allow better models of tissue structure to be designed, thus achieving more accurate results in the retrieval of subcutaneous temperature profiles. This in turn should improve the ability of the technique to detect breast disease and to distinguish between benign and malignant tumours. This type of information will also be of use to other groups who design thermal imaging systems. For instance, Leroy's group in Lille, France, has designed a multiprobe radiometer operating at 3GHz in order to detect breast lesions. At present temperature retrieval is performed using the relative differences between radiometric data from diseased and normal tissues, without detailed knowledge of the tissue dielectric properties (Bocquet et al, 1988; Mamouni et al, 1986).

A recent report on noninvasive thermometry (Bardati et al, 1989) recommended that microwave properties of tissues, particularly fat, bone and connective tissues, should be investigated at frequencies of 1 to 9GHz. It was recommended that the accuracy of measurement should be at least ±10%. Data from these and other tissue types are examined in Chapter 5; dielectric properties were measured to a higher accuracy than was recommended by Bardati et al (1989).

1.2 Microwave hyperthermia

An area closely related to microwave thermographic imaging is microwave hyperthermia. This is a technique in which carcinomas are diminished or destroyed through heating by radiofrequency or microwave electromagnetic fields. Temperatures should be maintained at 42 — 45 °C during heating. Above these

3

temperatures, normal tissues may be irrevocably destroyed; below these temperatures, heating may stimulate tumour growth. Microwave thermography has considerable potential as a new technique for monitoring temperatures during application of the field. It is not yet routinely used for this purpose because sufficient temperature resolution with depth has not yet been achieved, and because microwave thermography equipment and hyperthermia applicators have not yet been integrated. Development of microwave thermography for this application is very important because it would remove a number of problems connected with current invasive methods of temperature monitoring (discomfort to patients, choice of optimum probe position and accurate positioning, and limited information about tissue temperatures away from the vicinity of probes).

Absorption and penetration of the waves are dependent on tissue composition and interfaces. This makes dosimetry very difficult to measure, since it depends on tissue dielectric properties. At microwave frequencies it is well known that tumours are selectively vulnerable to heat treatment, but estimations are needed of the heating doses (temperature and time) necessary to eradicate tumours and of the extent to which normal tissues are spared or destroyed by the microwave field. Thus, in order to permit the design and predict the range and safety of a microwave hyperthermia treatment system, biophysical data, including high frequency relative permittivity and electrical conductivity are needed. It is extremely important that values and ranges for normal and pathological tissues are established (Atkinson, 1983; Dickson and Calderwood, 1983; Guy and Chou, 1983; Hand, 1987).

One of the frequencies of operation of microwave hyperthermia equipment is 2.45GHz, close to the frequency of measurement (3.2GHz) of the tissues presented here.

1.3 Microwave tomographic techniques

Microwave tomography is another area in which knowledge of the dielectric

properties of tissues is essential. This is an active imaging technique for temperature or dielectric measurement using an inverse scattering reconstruction. The tissue region of interest is illuminated by a known microwave source, and the microwave field scattered by the tissue is measured; this potentially allows a reconstruction of the dielectric structure of the illuminated tissue. Equipment has been developed at 3GHz and at 2.45GHz, but is still in a fairly early stage of development (Bolomey et al, 1984; Bolomey, 1986; Aitmehdi et al, 1986; Jofre et al, 1988). In order to understand local field variations in the tomographic reconstruction, a good knowledge is needed of the microwave properties of tissues and their temperature variation (Bolomey, 1986).

One possible area of expansion with tomographic techniques is detection of breast cancer. If carcinomas within an individual exhibit dielectric properties sufficiently different from normal tissues in the same individual, it may be possible to detect them by dielectric retrieval. Knowledge of the dielectric properties of breast cancers would be essential for this field of application.

1.4 Related applications of biomedical significance

1.4.1 Phantoms

Tissue phantoms are used in the testing of hyperthermia applicators, in the design of microwave antennas and in the design of of power deposition patterns for thermal dosimetry. It is very important that the phantoms used have the correct dielectric properties; this is achievable only if the properties of actual tissues are known (Cetas, 1983).

1.4.2 Microwave hazards

A basic understanding of bioeffects is needed for estimation of microwave hazards. Microwave and radiofrequency radiation has been associated, or has been

claimed to be associated, with a wide variety of psychological and physiological changes, ranging from subtle behavioural changes at low intensity exposures, to death from exposure to high intensity thermogenic fields (Cleary, 1983). These effects depend not only on the field strength but on the coupling of the body to the field. Thus microwave hazards can be properly assessed only with detailed knowledge of tissue dielectric properties and structure (Spiegel et al, 1989; Hoque and Gandhi, 1988).

1.5 Arrangement of thesis contents

In the following chapters some aspects of the dielectric properties of tissue are discussed and some new measurements are presented:

In Chapter 2 theoretical models which describe mixtures of materials and their components are assessed and compared, and their application to biological materials is discussed.

In Chapter 3 the available data from the literature on dielectric properties of animal and human tissues are examined in detail. This chapter includes a comparison between human and animal tissue properties, a topic which has not been discussed before in the literature. Comprehensive data tables, the first such tables for ten years, are also presented.

In Chapter 4 a new resonant cavity perturbation technique for tissue measurements at 3.2GHz is presented . The theory behind the technique is discussed and equipment calibrations and experimental procedure are described.

In Chapter 5 new data on the dielectric properties of human tissue at 3.2GHz are presented. One hundred and two measurements of female breast tissue were made (fat, normal and diseased) on thirty seven different patients; two measurements on male breast tissue were made, from one individual patient; and two measurements on cartilage and one on bone were made, from another individual patient. Low water content tissues (fat and bone) and high water content tissues (normal tissues; benign

and malignant tumours) are analysed separately. The new data are compared with theoretical models from Chapter 2, and with data from the literature tables in Chapter 3. A summary of results is presented, giving values and ranges for the normal and pathological tissue studied.

Finally in Chapter 6, a summary is given of the work presented in this thesis, with some discussion and suggestions for future work in this field.

Chapter 2

Dielectric Properties of Biological Tissues 1
Theory

2.1 Introduction

Researchers have found it difficult to devise a theory which adequately describes the dielectric properties of biological materials. This problem has long been examined at several different levels of complexity and scale. Equations have been derived for microscopic structures and macroscopic structures, using both theoretical and semi-empirical methods. It remains a difficult problem for most systems and is soluble only for simple structures.

This chapter reviews the various attempts in the literature to produce suitable dielectric theories. In Section 2.2, a brief discussion is given of tissue structure and composition in order that the immense complexity of biological tissue, and therefore of its dielectric properties, may be perceived. Section 2.3 introduces the concepts needed to describe materials in a static field; this is extended in Section 2.4 to time-dependent fields. In these two sections equations are given which relate microscopic and macroscopic polarisation, and general relaxation theory is used to discuss dielectric dispersion. Section 2.5 then gives a fairly comprehensive review of mixture theory, including in Section 2.5.6, an examination of the experimental justification for such theories.

2.2 Tissue structure and composition

Biological tissue is a complex mixture of water, ions, membranes, and macromolecules of a wide range of shapes and sizes. There are four fundamental types of tissue: the first is epithelial tissue, consisting of sheets of cells covering surfaces and

lining cavities; secondly, connective tissue which consists of highly fibrous, only slightly cellular supporting, connecting and padding materials including bone, cartilage, tendons and fat; thirdly, muscular tissue which contains elongated fibres able to contract; and finally nervous tissue, which is specialised for the reception of stimuli and conduction of impulses. Blood may be considered as a fifth tissue type but is really a specialised connective tissue. This classification (Windle, 1976) is arbitrary since no tissue exists in pure form: epithelium contains nerves; connective tissue contains nerves and blood vessels; and muscular tissue could not function without these and connective tissue sheaths.

The basic building block of all tissues is the cell, specialised for each different type of tissue to perform specific functions. The cell is made up of a mass of protoplasm, containing proteins, polysaccharides, nucleic acids and lipids, bound by a delicate membrane. Molecules of the protoplasm are suspended in water, known as intracellular water, which comprises about 75% of the mass of most living cells. The cells themselves are suspended in an aqueous environment, made up mainly of interstitial (or intercellular) water. In the human body intracellular water comprises 67% of its total water content, interstitial water 25%. The remaining 8% is contained in plasma (extracellular water). A delicate balance exists between the constituents of these three types of fluid. They vary in ionic composition (Table 2.1) but plasma and interstitial may be treated as being 0.9% sodium chloride solution. Intracellular water has a very different ionic profile having a high concentration of potassium ions among others (Windle 1976).

It is interesting to observe that although the human body is 50 — 70% water, with some tissues containing a much higher percentage, most body tissues are solid or semi-solid. A comparison may be made between a mixture of equal quantities of sugar and water, and a mixture of 10% gelatine (an animal product) in water: the sugar produces a solution while the gelatine results in a stiff jelly. Thus gelatine gives water a fairly rigid structure. This rigid structure is caused by the presence of 'bound water' or 'water of

Anion or Cation	Ion	Plasma	Interstitial	Intracellular
Cations	Na⁺	142	145	10
	K⁺	4	4	160
	Ca²⁺	5	5	2
	Mg²⁺	2	2	26
TOTAL		153	156	198
Anions	Cl⁻	101	114	3
	HCO₃⁻	27	31	10
	HPO₄⁻	2	2	100
	Protein	16	1	65
	SO₄²⁻	1	1	20
	organic acids	6	7	0
TOTAL		153	156	198

Table 2.1.   Ionic profile of body fluids in meq/l (Data from Brooks and Brooks, 1980)

$$1 \text{ meq} = \frac{\text{atomic weight}}{\text{ionic charge} \times 1000}$$

hydration'. Similarly, in the body, the presence of bound water explains the solid and semi-solid characteristics of tissue. This will be discussed in more detail in Chapter 3.

2.3 Static fields

There are two basic responses of a medium to a steady field : charges of opposite sign are displaced with respect to each other by amounts proportional to the electric field strength, leading to a dielectric polarisation P; or constituent charges in the medium move relatively freely under the influence of the field leading to a static conductivity, σ_s. Many materials, including biological materials, produce both types of response.

The dielectric response of a material is the result of either dipolar or space-charge polarisation. Dipolar polarisation is caused by the separation of a pair of opposite charges in either permanent dipoles (in polar molecules such as methanol or water) or induced dipoles in non-polar molecules. Space charge polarisation is caused by free charges in the material either introduced from outside the material or at interfaces within the material.

Three types of dipolar polarisation may occur in a material: electronic polarisation, which is caused by the displacement of an electron orbital relative to the nucleus; atomic polarisation, due to mutual displacements of atoms within the same molecule; and orientational polarisation, so-called because of the tendency of dipolar molecules with permanent dipole moments to align themselves with the field, a tendency opposed by thermal agitation and interactions with neighbouring molecules. Biological materials usually contain permanent dipoles and so potentially possess all three types of polarisability (Grant, 1984). However, only orientational polarisation is important at microwave frequencies: the other effects occur at much higher frequencies of imposed field. Space-charge polarisation, which is not a dipolar effect, is also important at microwave frequencies, in particular at interfaces within a heterogeneous material. These will be discussed in more detail in the next two sections.

The relative permittivity (or dielectric constant) and conductivity of a material are

the charge and current densities induced in a material in response to an applied electric field of unit amplitude. From Maxwell's (1881) equations these are written:

$$D = \varepsilon_0 E + P = \varepsilon_0 \varepsilon_s E \qquad (2.1)$$

$$j = \sigma_s E \qquad (2.2)$$

where E is the electric field, P is the electric polarisation, and j is the current density in a material with static relative dielectric constant ε_s and static conductivity σ_s. $\varepsilon_0 = 8.85.10^{-12}$ F m^{-1} is the permittivity of free space (Lorraine and Corson, 1970).

These equations are valid for isotropic homogeneous materials with a linear response to the field, where the system under examination is much larger than the molecular dimensions. In a real system, nonlinear terms in E^2, E^3 and higher orders exist, but provided E is small they are negligible (Kraus, 1984; Foster and Schwan., 1989).

Relating the microscopic polarisation to the macroscopic polarisation is a difficult problem, because generally the local field, E_l , experienced by a molecule is very different from the macroscopic field, E. E_l is a function of both the applied field and the permanent and induced dipole moments of the molecule and its neighbours. For a number of non-polar molecules N per unit volume the polarisation is:

$$P_{\text{induced dipole}} = N \alpha E_l \qquad (2.3)$$

where α is the molecular polarisability. Combining this with (2.1) it is found that:

$$\varepsilon_s = 1 + \frac{N \alpha E_l}{\varepsilon_0 E} \qquad (2.4)$$

This equation and a simple relation between local and microscopic fields (Hasted, 1973):

$$E_l = \left(\frac{\varepsilon_s + 2}{3}\right) E$$ (2.5)

form the basis for the well-known Clausius-Mossotti formula for static permittivity:

$$\frac{\varepsilon_s - 1}{\varepsilon_s + 2} = \frac{N_0 \, \alpha}{3 \, v \, \varepsilon_0}$$ (2.6)

where v is the molar volume and N_0 is Avogadro's number.

Debye (1929) derived an equation for rigid polar molecules which can orient in an applied field. Using a simple expression for the polarisation and Boltzmann's law to describe the distribution of dipole moments, he found that:

$$\frac{\varepsilon_s - 1}{\varepsilon_s + 2} = \frac{N_0}{3 \, \varepsilon_0 \, v} \left(\alpha + \frac{\mu_g^2}{3 \, k \, T}\right)$$ (2.7)

where μ_g is the permanent dipole moment of the molecules, T is the temperature and κ is Boltzmann's constant.

However, Debye's equation failed to reproduce the static dielectric constants of dense fluids. This led Onsager (1936) to attempt a different representation of the inner field. He represented the molecule as a point dipole in a spherical cavity of molecular size, dispersed in a medium of permittivity ε_{med}, deriving the equation:

$$\frac{(\varepsilon_s - \varepsilon_{med}) (2 \varepsilon_s + \varepsilon_{med})}{\varepsilon_s (\varepsilon_{med} + 2)^2} = \frac{N_0 \mu_g^2}{\varepsilon_o 9 \kappa T} \qquad (2.8)$$

These three equations were superseded by the Kirkwood-Frohlich equation (Kirkwood, 1936; Frohlich, 1949) which takes into account local forces between neighbouring dipoles. A statistical calculation of the average local field in the molecule showed that fluctuations in the induced molecular moment gave rise to deviations in the local field (2.5). This in turn produced the equation:

$$\frac{(\varepsilon_s - \varepsilon_{med.}) (2 \varepsilon_s + \varepsilon_{med})}{\varepsilon_s (\varepsilon_{med} + 2)^2} = \frac{N_0 g \mu_g^2}{\varepsilon_0 9 \kappa T v} \qquad (2.9)$$

where g is known as the Kirkwood correlation parameter: it is an expression of intermolecular angular correlation in a material.

Cole (1957) deduced the same equation and generalised it to apply to alternating fields. When $\varepsilon_{med} = 1$ (2.9) reduces to the Kirkwood (1936) formula; when $g = 1$ (2.9) reduces to the Onsager formula. For a mixture of polar molecules the derivation may be extended. For instance, for two types of material A and B, (2.9) may be written (Grant et al, 1978):

$$\frac{(\varepsilon_s - \varepsilon_{med}) (2 \varepsilon_s + \varepsilon_{med})}{\varepsilon_s (\varepsilon_{med} + 2)^2} = \frac{1}{9 \kappa T v \varepsilon_0} \left\{ g_A N_A \mu_g^2 + g_B N_B \mu_g^2 \right\} \qquad (2.10)$$

where subscripts A and B refer to materials A and B respectively.

Generally, these equations relating microscopic and macroscopic polarisations are not easily applied to biological materials. Tissues, in particular, are highly complex and little understood dielectrically, making it impossible to derive, for instance, any

meaningful measurement of the molecular dipole moments of the constituent parts. However, simpler materials have been studied, such as animal proteins in solution, which allow estimations of molecular parameters (Grant et al, 1978). This type of study of the simpler components of a substance is necessary in order to understand the more complex systems of which they are components.

2.4 Time-dependent fields

2.4.1 Relaxation theory

Dielectric polarisation in a material is caused by the physical displacement of charge and takes time to develop. Thus the response of the medium to a voltage is a relaxation process (Fig 2.1), the complexity of which depends on the process of charge displacement. This relaxation process generally becomes apparent when the applied field gives rise to a polarisation which lags behind the field and which relaxes at about the same rate as the field alternates.

Dielectric relaxation is the exponential decay with time of the polarisation in a dielectric when an externally imposed field is removed. A relaxation time, τ, may be defined as the time in which this polarisation is reduced to 1/e times its natural value, where e is the natural logarithmic base. Dielectric relaxation is the cause of a dispersion in which the dielectric constant decreases as the frequency increases.

At microwave frequencies the most important relaxation process is that involving orientational polarisation , where molecules or molecular groups rotate; this depends on the internal structures of the molecules and on the molecular arrangement. When the polar molecules are very large, or when the frequency of the field is great, or when the viscosity of the medium is high, the molecules do not rotate rapidly enough to attain equilibrium with the field. The polarisation then acquires a component out of phase with the field, resulting in thermal dissipation of energy. This ohmic or loss current
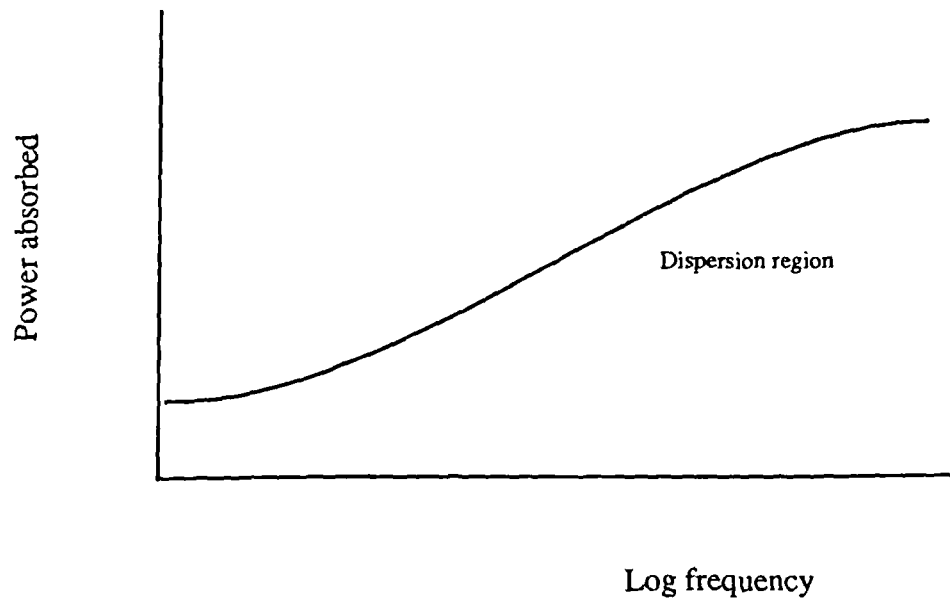
Figure 2.1   Relaxation spectrum of a simple material

describes the absorption properties of the medium (Smythe, 1955; Von Hippel, 1954). To represent this type of lossy material, a complex representation of the dielectric constant is necessary:

$$\varepsilon^* = \varepsilon' - j\,\varepsilon'' \qquad (2.11)$$

where the real part, ε', is the permittivity and the imaginary part, ε'', is the dielectric loss or loss factor. This may also be expressed as a complex conductivity:

$$\sigma^* = \sigma + j\,\omega\,\varepsilon_0\,\varepsilon' \qquad (2.12)$$

The variables ε'' and σ contain contributions from both dielectric relaxation and ionic conductance processes which are impossible to separate at an isolated frequency, although relative contributions can be isolated using information obtained at different frequencies:

$$\sigma = \sigma_i + \sigma_D$$

$$\varepsilon'' = \frac{\sigma}{\varepsilon_0\,\omega} \qquad (2.13)$$

$$\varepsilon_D'' = \frac{\sigma_D}{\varepsilon_0\,\omega}$$

where i and D refer to ionic and dispersion processes respectively.

In the simplest case the polarisation of a sample will relax towards the steady state as a first order process characterised by the relaxation time τ. The form of the dielectric constant for this process was derived by Debye (1929):

$$\varepsilon^* = \varepsilon_\infty + \frac{(\varepsilon_s - \varepsilon_\infty)}{1 + j\omega\tau} \qquad (2.14)$$

where ε_s and ε_∞ are the low frequency and high frequency limits of the dielectric constant respectively. Equation (2.14) may be separated into real and imaginary parts:

$$\varepsilon' = \varepsilon_\infty + \frac{(\varepsilon_s - \varepsilon_\infty)}{1 + \omega^2\tau^2}$$

$$\qquad (2.15)$$

$$\varepsilon'' = \frac{(\varepsilon_s - \varepsilon_\infty)\omega\tau}{1 + \omega^2\tau^2}$$

These equations are often expressed in terms of a characteristic frequency f_c rather than relaxation time τ. The two are related by the equation:

$$f_c = (2\pi\tau)^{-1} \qquad (2.16)$$

Equations (2.15) are illustrated in Fig 2.2 for water at 20 °C. In Tables 3.1 and 3.2 relaxation parameters for water, and the values of ε' and ε'' at 3GHz are given for temperatures between 20 and 40 °C.

The Debye equations may be represented in the complex ε', ε'' plane as a semicircle stretching from $\varepsilon' = \varepsilon_s$, $\varepsilon'' = 0$ to $\varepsilon' = \varepsilon_\infty$, $\varepsilon'' = 0$ (Cole and Cole, 1941, 1942). An example of such a plot is shown in Figure 2.3(a). (This type of plot is usually known as a Cole-Cole plot.)

A distribution of relaxation times is expected in real material, which may be a mixture of a number of different substances, or a solution, or may have a nonlinear relaxation process. The Cole-Cole (Cole and Cole, 1941, 1942) equation, which allows for a distribution of relaxation times, is then used. This is an empirical equation which serves to parameterise data:
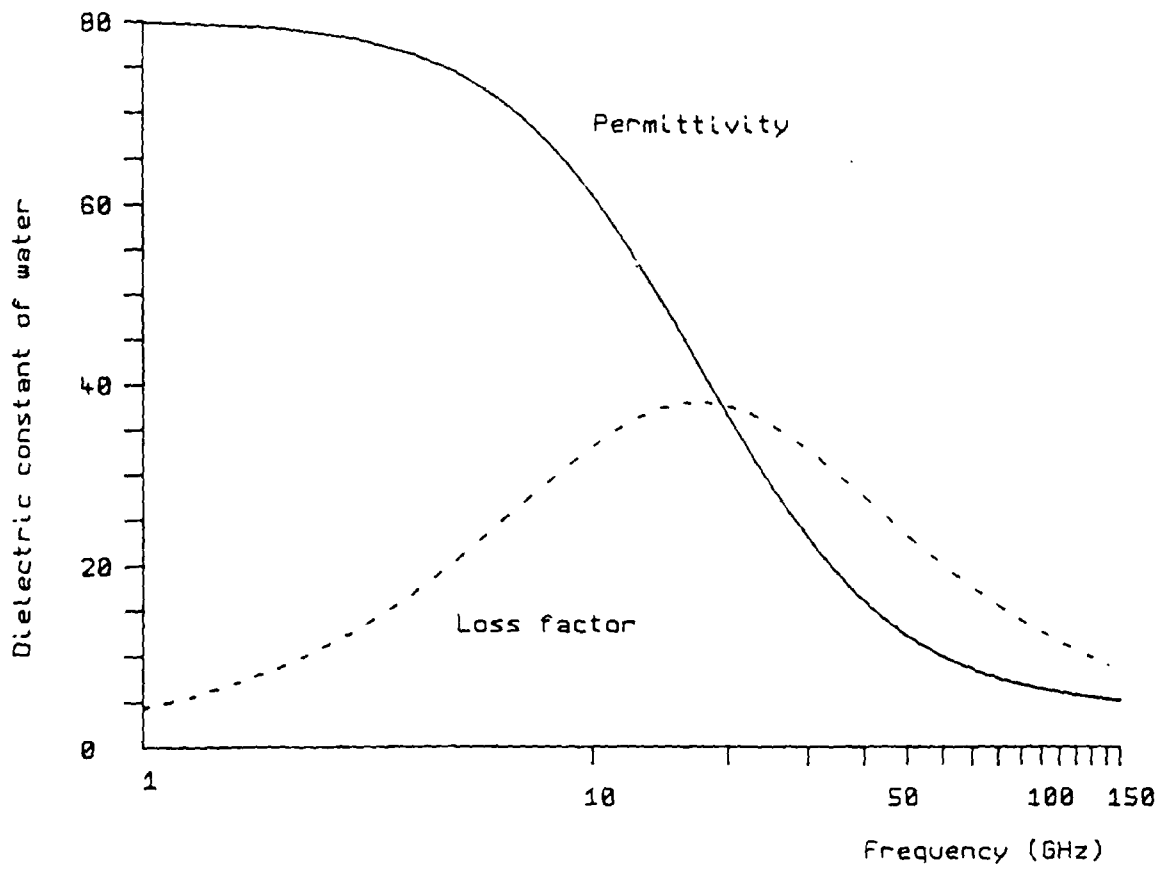
Figure 2.2   Debye dispersion of water at 20 °C

$$\varepsilon^* = \frac{\varepsilon_s - \varepsilon_\infty}{1 + (j\,\omega\,\tau)^{1-\alpha}} \quad , \qquad 0 \le \alpha \le 1 \qquad (2.17)$$

It may be separated into real and imaginary parts:

$$\varepsilon' = \varepsilon_\infty + \frac{(\varepsilon_s - \varepsilon_\infty)\left[1 + (\omega\,\tau)^{1-\alpha} \sin\frac{\alpha\pi}{2}\right]}{1 + 2\,(\omega\,\tau)^{1-\alpha}\sin\frac{\alpha\pi}{2} + (\omega\,\tau)^{2\,(1-\alpha)}} \ .$$

$$(2.18)$$

$$\varepsilon'' = \frac{(\varepsilon_s - \varepsilon_\infty)\,(\omega\,\tau)^{1-\alpha}\cos\frac{\alpha\pi}{2}}{1 + 2\,(\omega\,\tau)^{1-\alpha}\sin\frac{\alpha\pi}{2} + (\omega\,\tau)^{2\,(1-\alpha)}}$$

The Cole-Cole equation corresponds to a symmetrical distribution of relaxation times, characterised by α. A Cole-Cole plot of ε'' versus ε' would remain semi-circular but its centre would lie below the $\varepsilon'' = 0$ axis at an angle $\alpha\pi/2$ to it [Fig 2.3(a)]. The Cole-Davidson equation (Davidson and Cole, 1951) allows an asymmetrical distribution of relaxation times:

$$\varepsilon^* = \varepsilon_\infty + \frac{(\varepsilon_s - \varepsilon_\infty)}{(1 + j\,\omega\,\tau)^{1-\alpha}} \qquad (2.19)$$

This equation, again empirical, is used for materials such as glycerine and other viscous fluids, and gives rise to a skewed arc in the $\varepsilon'-\varepsilon''$ plane [Fig 2.3(b)]. It is seldom used for biological materials in which the main component is water, a non-viscous substance.

More recently, Havriliak and Watts (1986) derived the following empirical equation for the dielectric relaxation of polymers:
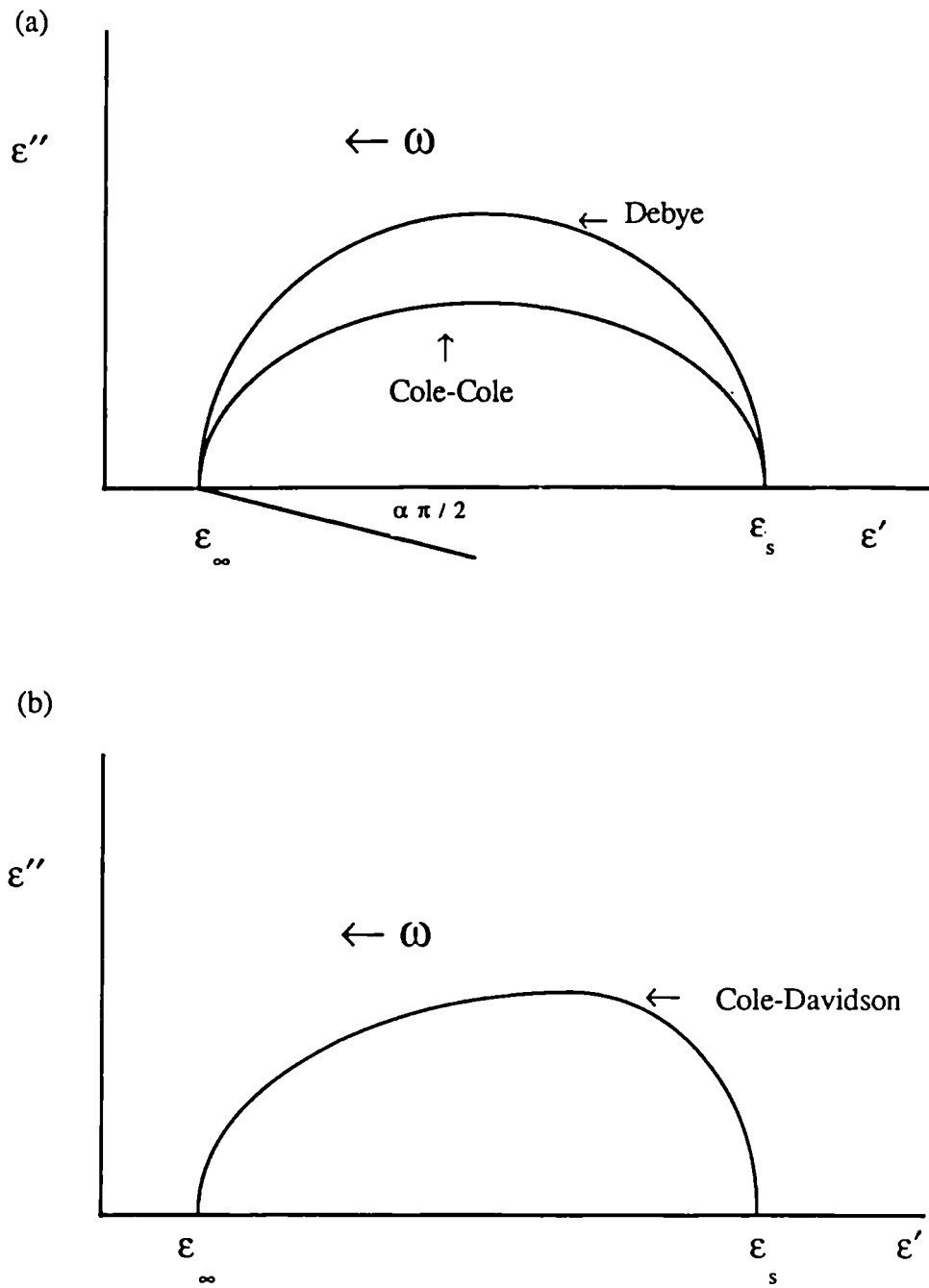
Figure 2.3 Cole-Cole plots of (a) the Debye and Cole-Cole equations
and (b) the Cole-Davidson equation

$$\varepsilon^* = \varepsilon_\infty + \frac{\varepsilon_s - \varepsilon_\infty}{\{1 + (j\,\omega\,\tau)^\alpha\}^\beta} \qquad (2.20)$$

where α and β are formally related to the distribution of relaxation times. When $\alpha = 1$, their equation reduces to the Cole-Davidson equation; when $\beta = 1$, it reduces to the Cole-Cole equation. Again, this equation is not used in data analysis of biological materials, which produce data more easily parameterised by the Cole-Cole equations.

Each relaxation time in the Cole-Cole, the Cole-Davidson and the Havriliak-Watts equations would, isolated, behave in the manner of the Debye equations.

2.4.2 Dispersion mechanisms in biological tissue

I. Dipolar relaxation

The discussion of general relaxation theory in Section 2.4.1 may be used to describe the partial orientation of permanent dipoles in an alternating field. In tissues several dipolar relaxation effects are observed. Globular proteins show dispersion at frequencies less than about 10MHz; partial orientation of polar side-chains contribute to a dispersion between 0.1 and 1GHz; water exhibits single time-constant dipolar relaxation with a characteristic frequency of 25GHz at 37° C; and bound water appears to exhibit a dispersion at frequencies below that of the tissue bulk water (Foster and Schwan, 1986). The observed dielectric properties of tissue are discussed in more detail in Chapter 3.

II Space-charge polarisation

(a) Interfacial polarisation

In a heterogeneous material a dispersion occurs due to the charging of interfaces within the material, which produces a relaxation frequency dependent on the differences in bulk properties of the constituent materials. This effect is important in the analysis of microwave dielectric properties of tissues (Foster and Schwan, 1989) and is the subject

of Section 2.5.7.

(b) Counterion diffusion

This is a surface phenomenon arising from ionic diffusion in the electrical double layers close to charged surfaces. Because of the theoretical complexity this process has not been analysed in any detail in relation to tissues; it was discussed qualitatively by Foster and Schwan (1986), who believe that counterion diffusion processes may explain why tissue data show relaxations much broader than predicted by the Debye theory. This effect is most important at sub-microwave frequencies.

2.5 Mixture equations

2.5.1 Principle of generalised conductivity

An immense amount of work has been done over the last century by workers trying to understand the electrical and thermal properties of disperse systems. The usual problem is to describe the effective properties of a two-phase dispersion in which one phase consists of particles dispersed in a second continuous phase. Both phases are usually regarded as homogeneous within themselves. Many materials have these general properties, so that describing them is of interest in such diverse areas of science as emulsion technology, colloid science, geophysics and remote sensing, food technology, biological physics and medical physics.

Different investigators have had different interests and have consequently derived mixture equations independently for static permittivity, static conductivity, magnetic permeability, thermal conductivity and diffusivity. However, all these so-called 'transport coefficients' may be grouped together so that a solution derived for one particular coefficient is applicable to any other as long as the system characteristics are identical in both cases. This is known as the 'Principle of Generalised Conductivity'

(Dukhin, 1971; Dukhin and Shilov, 1974; Clausse, 1983): it is justified by the formal coincidence of the differential equations of steady-state flux in each case (Table 2.2). Using the language of the thermodynamics of irreversible processes, the generalised conductivity, k, is a phenomenological or kinetic coefficient linking the flux vector J to the thermodynamic force F:

$$J = k \, F \tag{2.21}$$

If the material contains no source densities then:

$$\text{div } J = 0 \tag{2.22}$$

For linear, homogeneous and isotropic materials:

$$\text{div } F = 0 \tag{2.23}$$

At an interface between two phases 1 and 2, the normalised components of the flux are equal:

$$J_{n1} - J_{n2} = 0 \tag{2.24}$$

which implies that :

$$k_1 \, F_{n1} - k_2 \, F_{n2} = 0 \tag{2.25}$$

The tangential forces of the thermodynamic force are also equal:

$$F_{t1} - F_{t2} = 0 \tag{2.26}$$

Equations (2.21), (2.22), (2.25) and (2.26) constitute a general formulation of the particular equations for each of the 'transport coefficients'. For oscillating electric fields this general formulation holds for the quasi-static approximation if k represents the complex permittivity, ε^*. Lewin (1947) showed that the quasi-static approximation holds for disperse systems if the dimensions of the included particles are small compared with the wavelength of the imposed electric field. Thus the equation expressing the complex permittivity of a complex system is identical in formulation to that of the static permittivity. Consequently, any formula valid for static permittivity may easily be transposed to the case of complex permittivity. Since this thesis is concerned with dielectric phenomena all mixture equations will be expressed in terms of static permittivity, which may be interchanged when necessary with complex permittivity.

Generalised Conductivity	Flux Vector J	Thermodynamic Force F	Kinetic Coefficient k
electrostatic	electric displacement D	electric field intensity E	static permittivity ε_s
elerodynamic	conduction current density j	electric field intensity E	static conductivity σ_s
magnetostatic	magnetic flux density B	magnetic field intensity H	magnetic permeability μ
heat conduction	heat flow q	temperature gradient grad T	heat conduction coefficient λ
diffusion	diffusion flow M	concentration gradient grad C	diffusion coefficient D

Table 2.2

Parameters of generalised conductivity for transport coefficients

The complex permittivity of a heterogeneous system, ε^*, characterises the macroscopic field. Therefore the electric field must be understood as averaged over a volume containing a large number of disperse particles such that the medium is homogeneous and may be characterised by a definite value of dielectric constant. If E and D are the average field intensity and electric displacement then ε^* is defined:

$$E = \varepsilon^* D \qquad (2.27)$$

2.5.2 Bounds

Formal upper, ε_s^+, and lower, ε_s^-, bounds on the effective permittivity of a mixture were first derived by Wiener (1912). These are set by simple capacitance theory where a capacitor is filled with fibres stretching either from plate to plate or parallel with the plates:

$$\frac{1}{\varepsilon_s^-} = \frac{\phi}{\varepsilon_{1s}} + \frac{1-\phi}{\varepsilon_{2s}} \qquad \text{parallel}$$

$$(2.28)$$

$$\varepsilon_s^+ = \phi\,\varepsilon_{1s} + (1-\phi)\,\varepsilon_{2s} \qquad \text{series}$$

where ϕ is the volume fraction of medium 1.

Later Hashin and Shtrikman (1961) obtained more rigorous limits by applying variational methods to maximise or minimise the Gibbs free energy of a dielectric body. When $\varepsilon_{1s} > \varepsilon_{2s}$,

$$\frac{\varepsilon_s^+ - \varepsilon_{1s}}{\varepsilon_s^+ + 2\,\varepsilon_{1s}} = \frac{\varepsilon_{2s} - \varepsilon_{1s}}{\varepsilon_{2s} + 2\,\varepsilon_{1s}} \, \phi$$

$$(2.29)$$

$$\frac{\varepsilon_s^- - \varepsilon_{2s}}{\varepsilon_s^- + 2\,\varepsilon_{2s}} = \frac{\varepsilon_{1s} - \varepsilon_{2s}}{\varepsilon_{1s} + 2\,\varepsilon_{2s}} \, (1- \phi)$$

When $\varepsilon_{1s} < \varepsilon_{2s}$ exchanging the superscripts in (2.29) gives the limiting conditions. A comparison of the Wiener and Hashin-Shtrikman limits is shown in Figure 2.4.

2.5.3 Maxwell's equation

Maxwell (1881) was the first to derive a mixture equation, in this case for the thermal conductivity of a dilute suspension of identical spheres. His equation became the basis of most subsequent formulations. Wiener (1912) and Wagner (1914) derived the same equation for different transport coefficients.

Consider a medium of static permittivity ε_{2s} in which spherical particles of static permittivity ε_{1s} and radius a_i randomly fill a spherical volume of radius R [See Fig 2.5 (a)]. This volume is large enough that a great number of particles is contained within it; also, the average distance apart of the particles greatly exceeds their radius. The system is submitted to a uniform electric field, E_0. The dipole moment, p_i, of each particle is calculated neglecting mutual polarisation :

$$p_i = (\frac{4}{3} \pi a_i^3) \; 3\,\varepsilon_0 \; \frac{\varepsilon_{1s} - \varepsilon_{2s}}{\varepsilon_{1s} + 2\,\varepsilon_{2s}} \; E_0 \; \varepsilon_{2s}$$

$$(2.30)$$

Summing over all particles N_i with radius a_i in the volume gives:
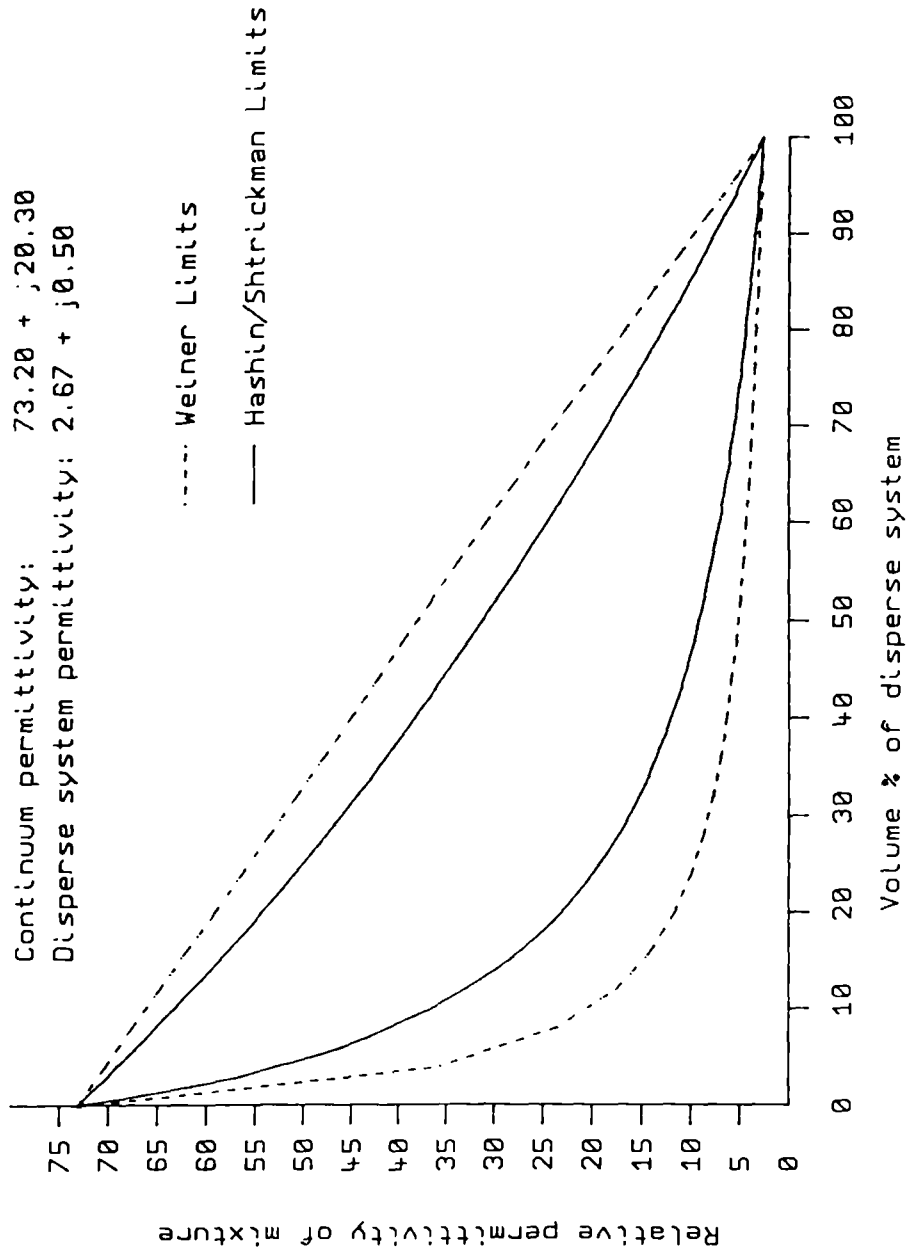
Figure 2.4   Comparison of Weiner and Hashin/Shtrikman
upper and lower bounds

(a)

$\mathbf{E}_0 \rightarrow$

ε_{2s}

(b)

$\mathbf{E}_0 \rightarrow$

ε_{2s}
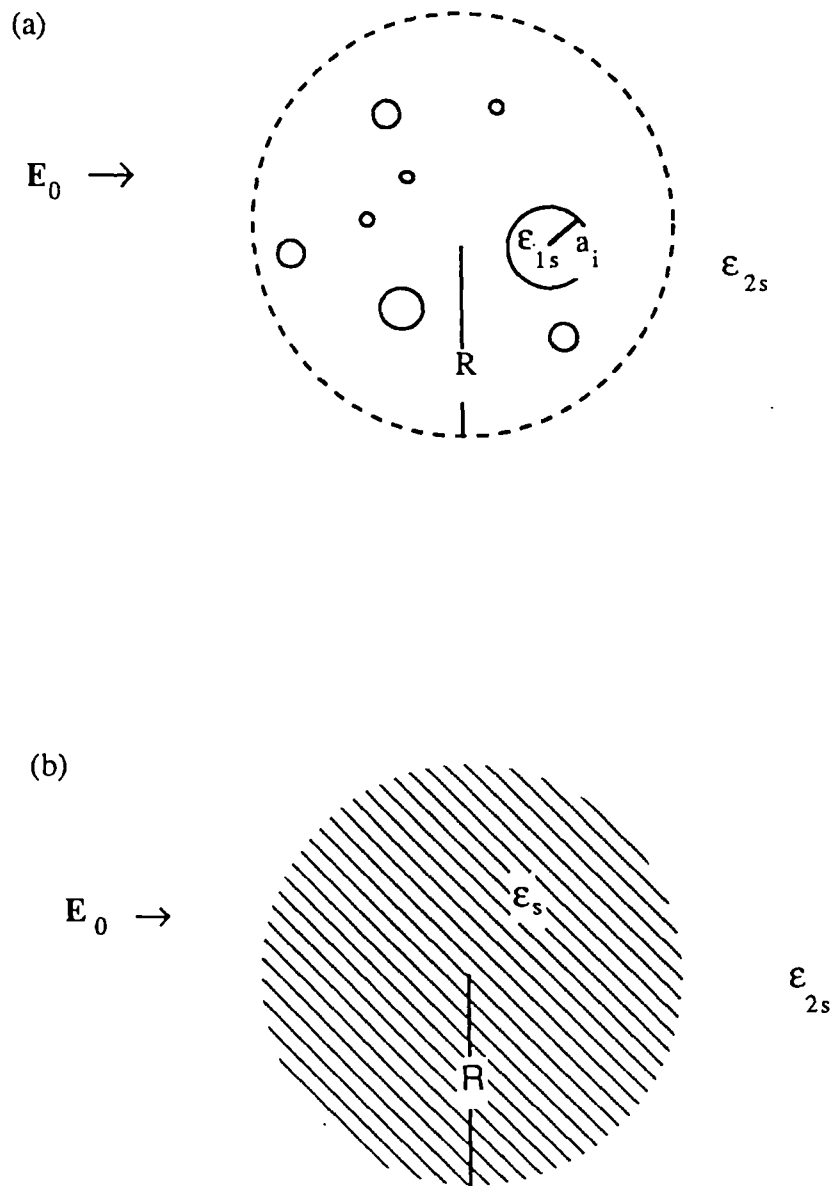
Figure 2.5   Schematic representation of Maxwell's model
                    (a) real situation , (b) equivalent body

$$P_T = \sum_i N_i \, p_i \qquad (2.31)$$

The dipole moment P' of the spherical volume is calculated assuming it to be macroscopically homogeneous and characterised by permittivity ε_s [See Fig 2.4(b)]:

$$P' = (\frac{4}{3}\pi R^3) \; 3 \, \varepsilon_0 \; \frac{\varepsilon_s - \varepsilon_{2s}}{\varepsilon_s + 2 \, \varepsilon_{2s}} \; E_0 \; \varepsilon_{2s} \qquad (2.32)$$

Equating P' with P_T yields the Maxwell mixture equation:

$$\frac{\varepsilon_s - \varepsilon_{2s}}{\varepsilon_s + 2 \, \varepsilon_{2s}} = \frac{\varepsilon_{1s} - \varepsilon_{2s}}{\varepsilon_{1s} + 2 \, \varepsilon_{2s}} \; \phi \qquad (2.33)$$

This equation is also known as the Maxwell-Wagner equation, the Wagner equation and the Wiener equation.

Equation (2.33) is in a form similar to (2.29). It is thus clear that the static permittivity of a statistically isotropic and homogeneous mixture, where $\varepsilon_{1s} > \varepsilon_{2s}$, is bounded above by the static permittivity of a dispersion of spherical particles ε_{2s} in a continuous medium of static permittivity ε_{1s}; and is bounded below by the static permittivity of a dispersion of spherical particles of static permittivity ε_{1s} in a continuous medium of static permittivity ε_{2s}.

Fricke (1924, 1925a) introduced into the Maxwell equation a geometrical form factor, x, which allows the particles to be oblate or prolate spheroids:

$$\frac{\varepsilon_s - \varepsilon_{2s}}{\varepsilon_s + x \, \varepsilon_{2s}} = \frac{\varepsilon_{1s} - \varepsilon_{2s}}{\varepsilon_{1s} + x \, \varepsilon_{2s}} \; \phi \qquad (2.34)$$

The factor x is a function of the axial ratio of the ellipsoids and the ratio of the static permittivities of the two phases. [See Stratton (1941) for a discussion of the effect of conducting or dielectric ellipsoids in an electric field.] Equation (2.34) is usually known as the Fricke or the Maxwell-Fricke equation.

The theory was extended again in 1940 by Velick and Goran to allow for ellipsoids with all three axes different. Their solution is very complex and takes into account particle orientation in flowing media. This approach would be useful when a great deal of information about particle geometry is available.

Another application of Maxwell's equation was first considered by Maxwell himself (1881). He calculated the equivalent conductance of a shell-covered sphere (See Fig 2.6). If the equivalent permittivity of the core is ε_s^c, that of the shell ε_s^s, that of the shell-covered sphere ε_s may be calculated:

$$\frac{\varepsilon_s - \varepsilon_s^s}{\varepsilon_s + 2\,\varepsilon_s^s} = (\frac{R}{R+d})^3 \; \frac{\varepsilon_s^c - \varepsilon_s^s}{\varepsilon_s^c + 2\,\varepsilon_s^s} \tag{2.35}$$

where R is the radius of the core and d the thickness of the shell.

This formulation allows the Maxwell equation to be extended to a weak suspension of shell-covered spheres by applying (2.33) and (2.35) consecutively (Fricke, 1925a). Later Fricke (1955) applied this technique to the case of a dilute suspension of spheres surrounded by multiple membranes. More recently, Irimajiri et al (1979) used (2.35) to derive a multi-stratified shell model for the dielectric constant of large single cells.

2.5.4 Bruggeman's equation

For more concentrated dispersions the electrical interactions among the particles are not negligible. Mutual polarisation of the particles may easily be taken into account for a rigidly ordered system but for a randomly ordered spatial distribution of particles the situation is very much more difficult. In this sort of system the particles are polarised
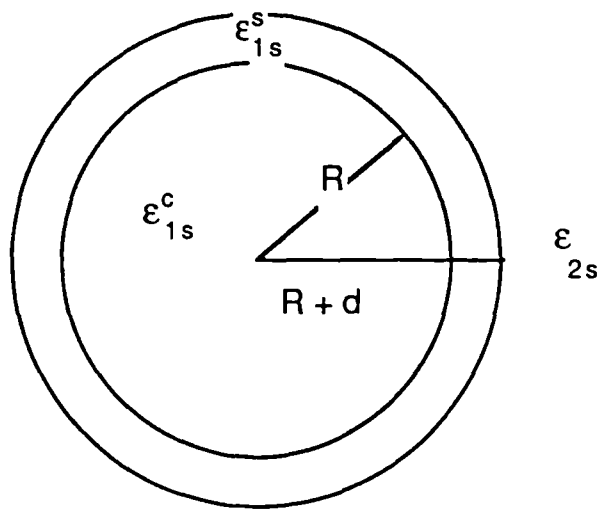
Figure 2.6   Shell-covered sphere in Maxwell's formulation

under the influence of both the macroscopic field and the local field of the neighbouring particles.

Bruggeman (1935) devised an integral procedure which consisted of building up the spherical dispersion system by successive additions of infinitesimal amounts of the disperse phase. At a given state the static permittivity of the system is ε_s and the disperse phase volume fraction is ϕ'. A further addition of the disperse phase, $\delta\phi'$, produces a variation in ε_s of $\delta\varepsilon_s$. The new value of the system static permittivity, $\varepsilon_s +$ $\delta\varepsilon_s$, is expressed by Maxwell's equation (2.33), where ε_s is replaced by $\varepsilon_s + \delta\varepsilon_s$, ε_{2s} by ε_s, and ϕ by $\delta\phi'/(1-\phi)$, which is the volume fraction of the added amount of disperse phase. Maxwell's equation then becomes:

$$\frac{2\varepsilon_s + \varepsilon_{1s}}{3\varepsilon_s (\varepsilon_s - \varepsilon_{1s})} \delta\varepsilon_s = \frac{\delta\phi'}{1-\phi'} \qquad (2.36)$$

Integrating this from ε_{2s} (the continuum permittivity) to ε_s and from 0 to ϕ yields the Bruggeman equation:

$$\left\{ \frac{\varepsilon_{1s} - \varepsilon_{2s}}{\varepsilon_{1s} - \varepsilon_s} \right\}^3 \frac{\varepsilon_s}{\varepsilon_{2s}} = \frac{1}{(1-\phi)^3} \qquad (2.37)$$

The extension of the Bruggeman equation to complex permittivities was first suggested by Hanai (1968), who later extended the theory to shell-covered spheres using a compound of the Maxwell (2.33) and Bruggeman (2.37) formulas. This method may easily be extended, if necessary, to spheres covered by multiple shells or membranes by successive applications of the Maxwell equation (2.33), followed by application of the Bruggeman (2.37) formula.

More recent work using this integral formulation was done by Boned and Peyrelasse (1983) who calculated the complex permittivity of a random distribution of ellipsoids dispersed in a continuum. In order to use their results, detailed knowledge of

the ellipsoidal geometry is necessary. No experimental comparisons were made in this paper.

Until recently the Bruggeman equation has been solved numerically [see Clausse (1983) for details of a numerical solution], although an analytical solution is possible, which may easily be extended to allow for complex permittivities. Smith and Scott (1990) published a solution to Bruggeman's equation for only one parameter, the dielectric constant of the mixture. Another method is presented in Appendix A, generalised so that (2.35) may be solved for any of the three parameters, ε_s, ε_{1s} or ε_{2s}, as long as the other two are known. A simple method for choosing roots is also given. A comparison of the Maxwell and Bruggeman formulas is shown in Figure 2.7, with the Wiener limits shown for reference.

2.5.5 Other equations

Rayleigh (1892) derived an equation for cylindrical or spherical particles arranged uniformly at the lattice points of a simple cubic lattice. His equation, as corrected by Runge (1925) may be written:

$$\varepsilon_s = \varepsilon_{2s} \left\{ 1 + 3\phi \left[\frac{\varepsilon_{1s} + 2\,\varepsilon_{2s}}{\varepsilon_{1s} - \varepsilon_{2s}} - \phi - 0.525 \frac{\varepsilon_{1s} - \varepsilon_{2s}}{\varepsilon_{1s} + \frac{4}{3}\varepsilon_{2s}} \phi^{10/3} \right]^{-1} \right\} \tag{2.38}$$

Equation (2.38) is the beginning of a series expansion. Other workers have produced similar equations, notably Lewin (1947), who used it to model ferromagnetic materials; Meredith and Tobias (1960), who extended Rayleigh's equation to further terms in the series so that it would be applicable at high concentrations; and Sihvola (1989) and Sihvola and Lindell (1990) who extended (2.38) to take into account shell-covered particles, for applications to freezing rain and melting hail. These models are unlikely to be useful for biological materials, which are heterogeneous random systems of molecules.
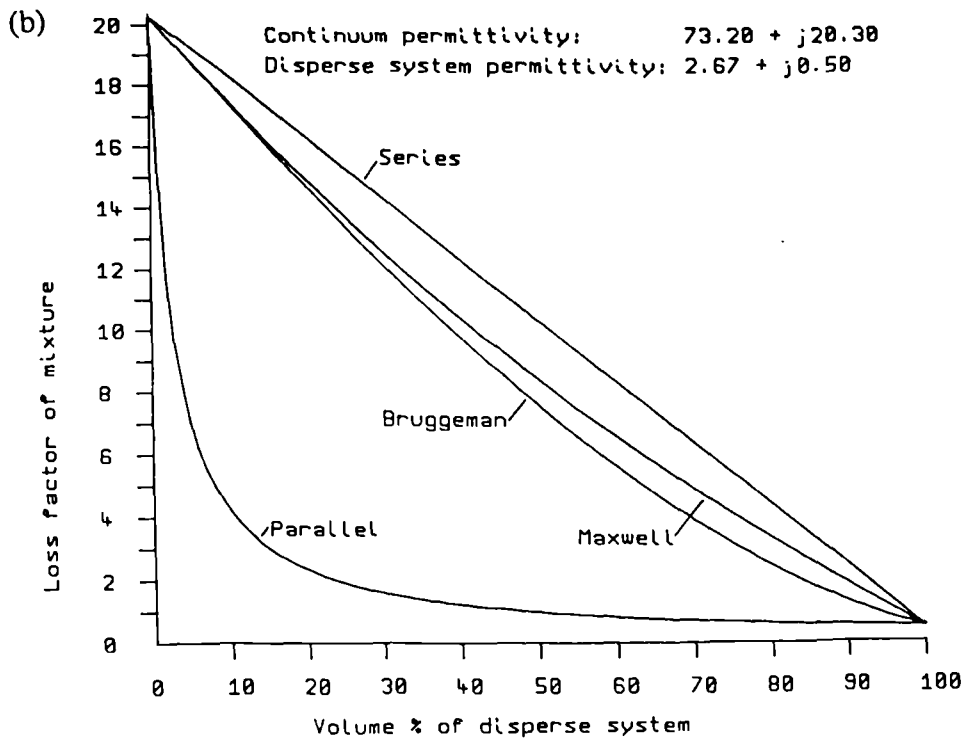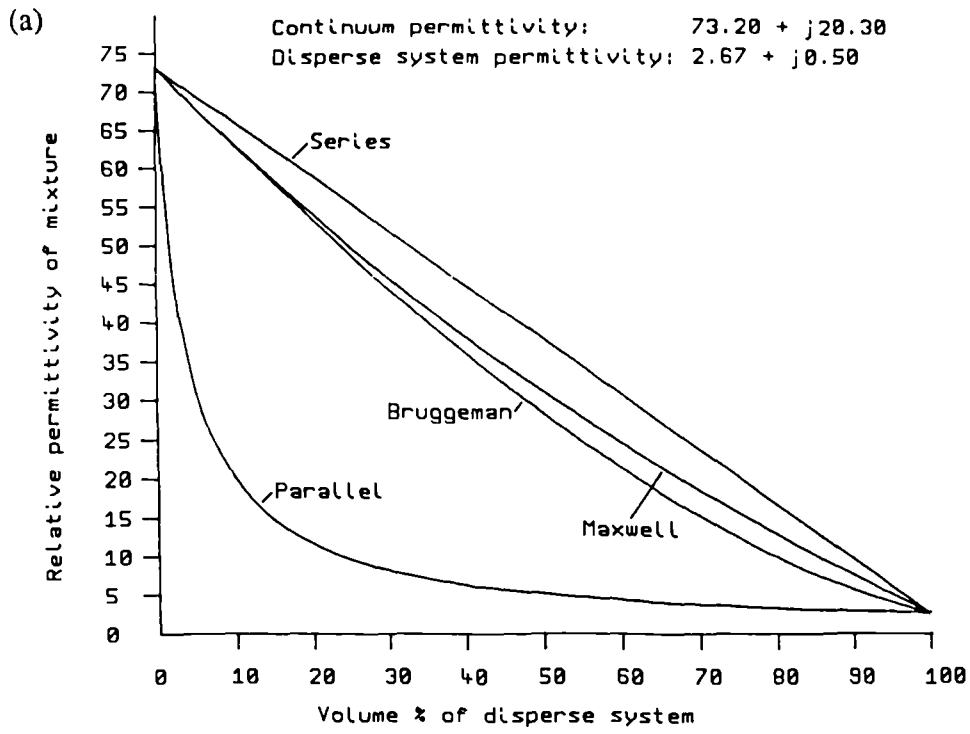
Figure 2.7   Comparison of the Maxwell and Bruggeman mixture formulas
as a function of volume of the disperse system
for (a) relative permittivity and (b) conductivity

Using (2.5) to describe the local field, Bottcher (1945) derived the following equation for crystalline powders:

$$\frac{\varepsilon_s - \varepsilon_{2s}}{3\,\varepsilon_s} = \phi\,\frac{\varepsilon_{1s} - \varepsilon_{2s}}{2\,\varepsilon_s + \varepsilon_{1s}} \qquad (2.39)$$

This equation was also derived by Polder and van-Santen (1946) as a limiting case of their solution for a dilute suspension of ellipsoidal particles.

Looyenga (1965) considered a mixture with dielectric constant $\varepsilon_s - \Delta\varepsilon$, to which small spheres of dielectric constant $\varepsilon_s + \Delta\varepsilon$ are added, until the dielectric constant ε_s is reached. This produced the equation:

$$\varepsilon_s^{1/3} = \varepsilon_{2s}^{1/3} + \phi\,(\varepsilon_{1s} - \varepsilon_{2s})^{1/3} \qquad (2.40)$$

This equation, although known as Looyenga's equation, had in fact been derived in another form, and more rigorously, by Landau and Lifshitz (1959). Dukhin (1971) criticised (2.40), because in Looyenga's derivation the system is considered random and ordered simultaneously. Landau and Lifshitz imposed limits on the equation's applicability whereas Looyenga assumed it to be general.

Another equation which has been in favour is Lichtenecker's logarithmic law (Lichtenecker, 1929; Lichtenecker and Rother, 1931) which may be written:

$$\log \varepsilon_s = \phi \log \varepsilon_{1s} + (1 - \phi) \log \varepsilon_{2s} \qquad (2.41)$$

This is derived by considering the dielectric structure to be a random spatial distribution of particles in an embedding medium. Volumetric coefficients of permittivity of the continuum, the inclusions and the mixture are defined. These are then assumed to be proportional to their respective volumes, for an elemental volume, and linearly related.

Integrating the linear relation produces (2.41).

Dukhin (1971) criticised (2.41) for the same reasons that he criticised Looyenga's equation: the derivation assumes the system to be random and ordered simultaneously. Clausse (1983) also criticised (2.41), on the grounds of its symmetry. Only under very special circumstances for certain statistical mixtures, are symmetric equations valid, whereupon interchanging ϕ and $(1-\phi)$ and ε_{1s} and ε_{2s} the equation remains the same. In the case of a mixture of discrete particles in a continuum symmetric equations cannot hold and may be shown to lead to absurd conclusions (Clausse, 1983). Experimentally, symmetric equations have been shown to be invalid for oil and water mixtures: W/O (water particles in oil) and O/W (oil particles in water) emulsions exhibit very different dielectric properties (Clausse, 1983).

Apparently unaware of these criticisms, Neelakantaswamy et al (1983) rederived (2.41) and then extended it to include a geometrical form factor (Kisdnasamy and Neelakantaswamy, 1984). They were later forced to recognise the criticisms (Neelakantaswamy et al, 1985), although defending it on the grounds that it was supported by experimental data (see Section 2.5.6). They proposed a new equation:

$$\varepsilon_s = C(\varepsilon_{1s}, \varepsilon_{2s}, \phi) \, \varepsilon_{s+}^{n(a/b)} \, \varepsilon_{s-}^{[1-n(a/b)]} \qquad (2.42)$$

where ε_{s+} and ε_{s-} are the Weiner limits ε_s^+ and ε_s^- (2.28), a/b is the axial ratio of the ellipsoids and C is a weighting factor. The factor n is the fraction of the stochastic system which behaves as if polarised in the direction of the electric field; the remaining (1-n)th factor is polarised orthogonally. Neelakantaswamy and his co-workers have not further extended their work in this area.

A completely different approach was taken by Brown (1955) who used a method from statistical mechanics to derive a power series for ε_s. Later, other authors used his method, in particular, Gunther and Heinrich (1965), Chiew and Glandt (1983) and Cichoki and Felderhof (1988), who extended Brown's work to allow for very

complicated systems. These authors showed that particle geometry and sizes, complex local particle fields, and random aggregation of particles, all have important effects on mixture permittivities. These statistical solutions are not in general use due to the complexity of the formulas and the need for detailed system information.

2.5.6 Experimental verification

Many of the above theories were devised to study specific problems, so that there were usually contemporaneous experimental studies. Fricke and Morse (1925) tested Fricke's equation (2.34) on suspensions of cream in skimmed milk by comparing the measured volume fractions with those calculated from his theory: they found good agreement up to volume fractions as high as 60%. In another paper (Fricke, 1925a) results of measurements on suspensions of dog erythrocytes were used to test the theory for dilute mixtures of membrane-covered particles in a continuum (2.35): using this approach the thickness of the membrane surrounding the erythrocyte cell was roughly determined. Velick and Goran (1940) tested their extended Fricke model for ellipsoidal inclusions on suspensions of avian erythrocytes in a sodium chloride solution: again good agreement was found between theory and experiment for volume fractions up to 60%. More recently, Bianco et al (1979) used Fricke's equation to determine the permittivity and loss factor of human erythrocytes (from a mixture of erythrocytes in plasma) at five different frequencies between 0.1 and 2GHz and five different volume fractions between 14 and 84%. Using x as an empirical factor [x = 1.5 at low frequencies; x = 1.9 at high frequencies (Cook, 1952)], they measured ε' and ε" at each frequency for the different volume fractions, calculated the means, and examined the standard deviations. The largest standard deviation, 12%, was in ε' at 1GHz. The loss factor results were rather better, the worst standard deviation in this case being 8% at 2GHz. Cole et al (1969) tested both the Maxwell and Rayleigh equations on suspensions of non-conducting spheres over a wide range of volume fraction, 30 — 90%, finding good agreement to within accuracies of about 1% over the whole range. From these and other experimental studies it seems that the simple

29

Maxwell and Fricke relations may be used even up to fairly high concentrations of dispersed particles.

In his 1955 paper, Fricke gave experimental results, again on suspensions of erythrocytes, to verify his model for particles with multi-stratified shells. Later this same model was used by Irimajiri et al (1979) to examine dielectric results on large single cells at low frequencies; he used the theory to determine successfully the number of membranes surrounding the cell.

Bruggeman's formula has been extensively tested by Hanai and his colleagues for W/O (water in oil) and O/W (oil in water) emulsions, and for biological suspensions (Hanai and Koizumi, 1975; Hanai et al, 1979; Asami et al, 1980; Hanai et al, 1980). Previously, Hanai (1968) in a review article found excellent agreement with Bruggeman's equation using reported data on sand suspensions, O/W emulsions, glass bead suspensions and dog-blood suspensions at volume fractions as high as 90%.

Lewin (1947) found that measurements on powders agreed at up to 75% volume fraction with his Rayleigh-type equation, while Sihvola (1989) used results from radiofrequency scattering of melting hail and freezing rain to make a successful qualitative comparison with his extended Rayleigh equation.

Other workers have studied Bottcher's and Looyenga's equations, finding the former suitable at high volume fractions (>75%) and the latter useful at low volume fractions (<35%) (Benadda et al., 1982).

Neelakantaswamy et al (1983) tested Lichtenecker's logarithmic law (2.41) on powder dielectrics by comparing the calculated and measured dielectric dispersion, finding good agreement. (See Section 2.4.7 for a discussion of dispersions in mixtures.) They also compared their results with the Bottcher and Looyenga equations, finding good agreement using the restrictions on volume fraction set by Benadda et al (1982). In a later paper (Kisdnasamy et al, 1984) the reported results of Bianco et al (1982) (discussed above) were used to test the logarithmic law, with excellent agreement in the whole volume fraction range (14 — 84 %): the maximum deviation

from the measured values was 2%. This certainly lends credence to the claim (Neelakantaswamy et al, 1985) that the logarithmic law is supported by experimental evidence.

A summary is given in Table 2.2 of the different mixture equations discussed in this section, their authors and range of applicability. Unfortunately it is not possible to give a very detailed summary which includes ranges of accuracy, covering volume fractions, frequency and permittivity ranges. Few experimental data on particles dispersed at different volume fractions are available: more studies are necessary on different types of material suspensions at different volume fractions and frequencies, before the applicability of the various mixture equations may be assessed.

2.5.7 Maxwell-Wagner polarisation

Also known as interfacial or migration polarisation, this is a dielectric phenomenon typical of heterogeneous dielectrics with at least one conducting component. Any theoretical mixture formula giving the complex permittivity of a heterogeneous system may be shown to give rise to a dielectric relaxation which may be expressed by any of the relaxation equations given in Section 2.4. For example, Maxwell's equation (2.33) may be written in the form:

$$\varepsilon^* = \varepsilon_2^* \; \frac{\varepsilon_1^* + 2\varepsilon_2^* + 2\phi(\varepsilon_1^* - \varepsilon_2^*)}{\varepsilon_1^* + 2\varepsilon_2^* - \phi(\varepsilon_1^* - \varepsilon_2^*)} \tag{2.43}$$

where the static permittivity is exchanged for complex permittivity by the principle of generalised conductivity.

Assuming that no intrinsic dielectric relaxation is exhibited by either component, their complex permittivities may be written:

Author	Equation number	Type of mixture	Range	Comments
Wiener (1912)	(2.28)		bounds	
Hashin and Shtrikman (1961))	(2.29)		bounds	More rigorous derivation than for (2.28)
Maxwell (1881)	(2.33)	suspension of spheres	dilute	
Fricke (1924)	(2.34)	suspension of ellipsoids	dilute	Agrees with experiments up to 60% volume
Bruggeman (1935)	(2.37)		concentrated	Integral method Agrees with experiments up to 90% volume fraction
Rayleigh (1892)	(2.38)	uniform distribution of spheres	dilute	Series expansiom May be useful up to 75% volume fraction
Bottcher (1945)	(2.39)	suspension of ellipsoids	concentrated	Useful above 75% volume fraction
Looyenga (1965)	(2.40)		dilute	Discredited by Dukhin (1971) but experimental verification below 35% volume fraction
Lichtenecker (1935)	(2.41)	semi-stochastic	general	Symmetric:invalid for W/O type mixtures, but experimental verification on powder dielectrics
Neelakantaswamy et al (1985)	(2.42)	semi-stochastic	general	Intractable : no experimental verification
Brown (1955) Gunther and Heinrich (1983) Chiew and Glandt (1983) Cichoki and Felderhof (1988)		stochastic	general	Extremely complex equations Need for detailed system information

Table 2.3   Summary of mixture equations for a two-phase dispersion

$$\varepsilon_1^* = \varepsilon_{1s} - j\,\frac{\sigma_1}{\omega\,\varepsilon_0}$$

<div align="right">(2.44)</div>

$$\varepsilon_2^* = \varepsilon_{2s} - j\,\frac{\sigma_2}{\omega\,\varepsilon_0}$$

Equation (2.44) may be transformed into a Debye type equation with an ohmic term:

$$\varepsilon^* = \varepsilon_h + \frac{\varepsilon_1 - \varepsilon_h}{1 + j\dfrac{f}{f_c}} + \frac{\sigma_1}{j\,\varepsilon_0\,\dfrac{f}{f_c}}$$

<div align="right">(2.45)</div>

where:

$$\varepsilon_h = \varepsilon_{2s}\,\frac{\varepsilon_{1s} + 2\,\varepsilon_{2s} + 2\,\phi\,(\varepsilon_{1s} - \varepsilon_{2s})}{\varepsilon_{1s} + 2\,\varepsilon_{2s} - \phi\,(\varepsilon_{1s} - \varepsilon_{2s})}$$

$$\sigma_1 = \sigma_2\,\frac{\sigma_1 + 2\,\sigma_2 + 2\,\phi\,(\sigma_1 - \sigma_2)}{\sigma_1 + 2\,\sigma_2 - \phi\,(\sigma_1 - \sigma_2)}$$

$$\varepsilon_1 = \varepsilon_{2s}\,\frac{\sigma_1}{\sigma_2} + \frac{9\,\phi\,\sigma_2\,(\varepsilon_{1s}\sigma_2 - \varepsilon_{2s}\sigma_1)}{[\sigma_1 + 2\,\sigma_2 - \phi\,(\sigma_1 - \sigma_2)]^2}$$

and

$$f_c = \frac{1}{2\,\pi\,\varepsilon_0}\,\frac{\sigma_1 + 2\,\sigma_2 - \phi\,(\sigma_1 - \sigma_2)}{\varepsilon_{1s} + 2\,\varepsilon_{2s} - \phi\,(\varepsilon_{1s} - \varepsilon_{2s})}$$

Here ε_h corresponds to ε_∞, and ε_1 to ε_s in (2.14); f_c is the characteristic frequency defined in (2.16), and σ_s corresponds to an ionic conductivity.

The situation becomes more complicated when this interfacial polarisation interferes with intrinsic dielectric relaxations exhibited by one or both phases. Interfacial effects can dominate the properties of colloids and emulsions, but in biological materials at microwave frequencies, the effects of dipolar relaxation of liquid water are believed to be more important. More information on these processes may be

found in Foster and Schwan (1986), Clausse (1983) and other reviews.

2.5.8 Application to biological materials

The above mixture equations have been developed for two phase systems, whereas biological materials like tissue are very much more complex (as discussed in Section 2.2). Thus these mixture equations can never exactly reproduce results on biological systems, their main use being a qualitative guide to the tissue structure. At microwave frequencies the main contribution to the permittivity is expected to be from water which exhibits dipolar relaxation in the GHz region (this is discussed in more depth in the next chapter). The other components of the tissue are expected to be less important, since most other biological materials show dispersions at lower frequencies. In particular, for measurements at a single microwave frequency, detailed models such as those which describe shell-covered particles are not expected to be necessary, since the shell effect in blood and tissues should be small. [This has been shown to be more important in the radiofrequency region of the spectrum (Foster and Schwan, 1989).]

Attempts to discover system structure in any detailed way cannot be made using measurements at a single frequency: only by separating out the different dispersions over a very wide range of frequencies will this type of information be revealed. At an isolated microwave frequency, however, some useful information may be derived: for instance, comparison of total water content with that expected from models may give information about bound water and may also indicate which models are most useful for biological applications.

2.6 Summary

In this chapter, several theoretical approaches to understanding the dielectric properties of materials have been described. Equations relating microscopic and macroscopic polarisation in static fields were compared: these are likely to be most

33

useful when trying to estimate molecular parameters of simple substances. Dielectric relaxation was discussed and various empirical equations for different types of substance were compared: the most useful of these for biological materials is the Cole-Cole equation (2.17). A review was given of the various mixture equations devised over the past century. It was concluded that for general two-phase mixtures, the most useful models were those of Maxwell (1881), Fricke (1925a) and Bruggeman (1935). For data in which detailed system information is known, there are several other models available. New experiments are required which examine the relation of relative volumes of different two phase mixtures to any of the 'generalised conductivities' of the mixture, at different frequencies: this would allow a more rigorous assessment of the range of applicability of each model. Biological materials cannot be categorised as two-phase mixtures, so that predictions from mixture theories must be considered as qualitative guides.

Chapter 3

Dielectric Properties of Biological Tissue 2
Data Review

3.1 Introduction

This chapter examines in detail the observed dielectric properties of tissues at microwave frequencies. In order to put these into context, the properties of water and physiological saline are first discussed, in Section 3.2, and an overall picture of the frequency variation of tissue permittivity is given in Section 3.3. The work of the major groups in the field is summarised in Section 3.4, followed by a detailed comparison between the dielectric properties of human and animal tissues in Section 3.4.1. This comparison makes use of data which have been collected from the literature and which are presented in Tables 3.6 and 3.7. Further discussions follow, including a comparison of *in vitro* and *in vivo* measurements and an analysis of the relationship of tissue water content to permittivity and conductivity. Finally, in Section 3.5, a discussion is given of the properties of bound water in biological materials.

3.2 Water and physiological saline

Water is one of the most important constituents in living organisms having many properties necessary for the existence and continuance of life. For instance, it has very good temperature stability, essential for animal and plant life, which may be exposed to sudden dramatic changes in temperature; its surface tension allows capillary action in plants to transfer nutrients from soil; and, at a molecular level, water determines to some extent the structure and properties of biological macromolecules. Only a very brief discussion of the dielectric properties of water is given here. More material is available in the literature: in particular, the comprehensive reviews of Hasted (1972, 1973) provide detailed information.

The water molecule, H_2O, possesses a permanent dipole moment (1.83D) which determines the properties of the bulk molecule through the Kirkwood-Frohlich equation (2.9) in weak fields. (In strong fields the equations of Section 2.3 must be modified to include other effects.) The frequency dependent behaviour of pure water may be described using the Debye or the Cole-Cole relations [(2.14) and (2.17)].

Since dielectric measurements have been summarised and reviewed in Hasted (1973) only essential data are given here. Firstly, the static dielectric constant was accurately measured by Malmberg and Maryott (1956) as a function of temperature. The best fit to their data is given by:

$$\varepsilon_s = 87.740 - 0.4008\ T + 9.398.10^{-4}\ T^2 - 1.410.10^{-6}\ T^3 \qquad (3.1)$$

where T is the temperature in °C. The temperature coefficient $d(\ln \varepsilon_s)/dT$ derived from this equation is almost constant at - 4.55 ($\pm$ 0.03) $.10^{-3}$ from 0 to 100°C. The other parameters in the Debye and Cole-Cole equations for water were calculated by Hasted (1973) using a regression analysis of the collected microwave data to that date. All four parameters are summarised in Table 3.1. Other workers (for example Schwan et al, 1976) have also calculated these parameters finding very similar values. Levels of uncertainty are less than 1% in ε_s, about 25% in ε_∞, about 2% in f_c, and about 50% in α (Schwan et al, 1976): these lead to small uncertainties in the microwave dielectric properties of water, of about 2 — 3%. A Debye dispersion for pure water at 20°C is shown in Figure 2.2. Comparing the two equations, Debye and Cole-Cole, at 3GHz, it was found that the differences in the calculated values of permittivity and loss factor were very small: less than 0.4% in ε' and less than 1.8% in ε'' over the temperature range 0 to 40°C. Values of ε' and ε'' for water at 3GHz have been calculated for temperatures between 20 and 40°C and are shown in Table 3.2.

Surprisingly, the parameters ε_s and ε_∞ for ice are very similar to those for water. At 0°C , $\varepsilon_{s\ ice} = 92$ and $\varepsilon_{\infty\ ice} = 3.1$, while $\varepsilon_{s\ water} = 87.7$ and $\varepsilon_{\infty\ water} = 4.5$. However, an immense difference is found in the relaxation time, τ: at 0°C $\tau_{ice} = 20\ \mu s$ whereas

T (°C)	ε_s	ε_∞	τ (x 10^{-11})	α
0	87.74	4.46	1.79	0.014
10	83.82	4.10	1.26	0.014
20	80.09	4.23	0.93	0.013
25	78.29	4.22	0.81 ·	0.013
30	76.52	4.20	0.72	0.012
35	74.80	4.18	0.64	0.011
40	73.12	4.16	0.58	0.009

Table 3.1   Relaxation parameters for water derived from the Cole-Cole equations.   Data from Hasted (1973)

T (°C)	ε'	ε''
20	77.5	13.0
25	76.3	11.2
30	75.0	9.81
35	73.6	8.55
37	73.0	8.20
40	72.2	7.57

Table 3.2   The permittivity and loss factor of water at 3 GHz for temperatures between 20 and 40 °C

τ_{water} = 20 ps. This is indicative of the different strengths of bonding of molecules in the two states: in liquid water molecules are relatively free to rotate without hindrance from bonds with neighbouring molecules, whereas in ice the molecules are strongly bound and unable to rotate freely.

Salts are dissolved in the water of the human body (Table 2.1) and have a marked effect on that water's dielectric properties: the static dielectric constant and the relaxation time are reduced and an ionic conductance is introduced. The physical basis for the lowering of ε_s and τ is more than a volume effect arising from the addition of non-polar molecules, and cannot be quantified by a mixture equation: the ions orient the water molecules around them in the applied field thus lowering the static dielectric constant and relaxation time. This may be expressed (Hasted, 1973) in terms of a dielectric decrement, δ:

$$\varepsilon_{ss} = \varepsilon_{sw} + \delta\, c \qquad\qquad (3.2)$$

where ε_{ss} is the static dielectric constant of the solution, ε_{sw} is the static dielectric constant of water and c is the concentration or molarity expressed in moles/kg of water. Similarly, a reduction in the relaxation time may be expressed using a decrement, $\delta\tau$:

$$\tau_s = \tau_w + c\, \delta\tau \qquad\qquad (3.3)$$

where τ_s is the relaxation time of the solution and τ_w the relaxation time of water. Comparisons of dielectric decrements of different ions are useful when comparing properties of different electrolytic solutions.

The accepted method of calculating the values of ε_s and τ for salt solutions was set out by Stogryn (1971), who used equations of the form:

$$\varepsilon_s\,(T,N) = \varepsilon_s\,(T,0)\ a\,(N)$$
$$2\pi\,\tau\,(T,N) = 2\pi\,\tau\,(T,0)\ b\,(N,T) \qquad\qquad (3.4)$$

where ε_s (T,0) is the static dielectric constant of water calculated from (3.1); τ(T,0) is a function which fits the experimental data gathered on the relaxation time of water as a function of temperature; and N is the normality of the solution. (For a NaCl solution, 1 Normal = 1 mole/litre.) The functions a (N) and b (N) are given by:

$$a (N) = 1.000 - 0.2551\ N + 5.151\ 10^{-2}\ N^2 - 6.889\ 10^{-3}\ N^3$$
$$b (N, T) = 0.1463\ 10^{-2}\ N\ T + 1.000 - 0.04896\ N - 0.02967\ N^2 + 5.664\ 10^{-3}\ N^3$$

(3.5)

Experimental measurements reviewed in Hasted (1973) show that the decrements of Na^+ ions (found in plasma and interstitial water) and K^+ ions (found in intracellular water) are the same. Any differences in conductivity between the different body electrolytes are mainly due to the different negative ions — largely Cl^- in plasma and interstitial water, and various proteins in intracellular water. It is clear that plasma and interstitial water may be treated as 0.9% NaCl solutions (physiological saline), but it is not obvious that intracellular water may be considered in this way. Indirect evidence (Cook, 1951) would suggest that its conductivity is less than that of 0.9% saline. However, at present there is no quantifiable evidence to prove this: therefore, in this thesis, for the purposes of modelling tissues, all three types of body electrolytes are assumed to be 0.9% NaCl solutions.

Using (3.4) and (3.5), values for ε_s and τ of physiological saline (= 0.9% or 0.154 Normal NaCl solution) were calculated at temperatures between 20 and 40°C. The relaxation time τ was found to be almost identical to that of pure water over this range and so may be taken to be those values shown in Table 3.1. A comparison of the values of ε_s calculated for pure water and physiological saline is shown in Table 3.3.

Introducing an ionic conductance, σ_s, into the Cole-Cole equations requires the addition of an extra term on the right hand of the equation for ε". These equations are then written:

38

T (°C)	ε_s (saline)	ε_s (water)
20	77.04	80.09
25	75.31	78.29
30	73.60	76.52
35	71.95	74.80
37	70.33	73.12
40	70.33	73.12

Table 3.3   Static dielectric constant of a 0.9% NaCl solution and of pure water

T (°C)	σ_s (mS/cm)
20	14.0
25	15.5
30	17.0
35	18.6
37	19.3
40	20.3

Table 3.4   Ionic conductivity of a 0.9% (0.154 Normal) NaCl solution

$$\varepsilon' = \varepsilon_\infty + \frac{(\varepsilon_s - \varepsilon_\infty)\left[1 + (\omega\tau)^{1-\alpha}\sin\frac{\alpha\pi}{2}\right]}{1 + 2(\omega\tau)^{1-\alpha}\sin\frac{\alpha\pi}{2} + (\omega\tau)^{2(1-\alpha)}}$$

$$(3.6)$$

$$\varepsilon'' = \frac{(\varepsilon_s - \varepsilon_\infty)(\omega\tau)^{1-\alpha}\cos\frac{\alpha\pi}{2}}{1 + 2(\omega\tau)^{1-\alpha}\sin\frac{\alpha\pi}{2} + (\omega\tau)^{2(1-\alpha)}} + \frac{\sigma_s}{\omega\varepsilon_0}$$

The ionic conductivity is assumed to be frequency independent [as demonstrated by many workers, eg Foster and Schwan (1986)] and may be calculated as a function of temperature using Stogryn's (1971) equations. The values of σ_s for temperatures between 20 and 40°C are shown in Table 3.4.

The parameter ε_∞ apparently is independent of salinity (Stogryn, 1971). This is to be expected, because at the highest frequencies water molecules cannot be made to oscillate significantly, so that the tendency for ions to impede the oscillation is unimportant. ε_∞ therefore takes the values shown in Table 3.1.

Using (3.6) values of permittivity and loss factor of physiological saline at 3GHz were calculated for temperatures between 20 and 40°C and are displayed in Table 3.5. These values, therefore, are a good approximation to the dielectric properties at 3GHz of plasma, interstitial and intracellular fluids in the body.

3.3 Observed dielectric dispersions in tissue

Tissue dielectric dispersions have been extensively discussed in the literature and biophysical mechanisms have been proposed to explain them (Foster and Schwan, 1989, 1986; Pethig, 1984; Pethig and Kell 1987; Grant et al, 1978). Tissues typically display three or four separate dielectric dispersions between audio and infrared frequencies, such as those shown in Figure 3.1. These dispersions are usually called alpha, beta, gamma and delta dispersions after Schwan's (1957) classification. A

T (°C)	ϵ'	ϵ''
20	74.5	20.9
25	73.4	20.1
30	72.1	19.6
35	70.8	19.4
37	70.2	19.4
40	69.4	19.4

Table 3.5   The permittivity and loss factor of a 0.9% NaCl solution at 3 GHz for temperatures between 20 and 40 °C
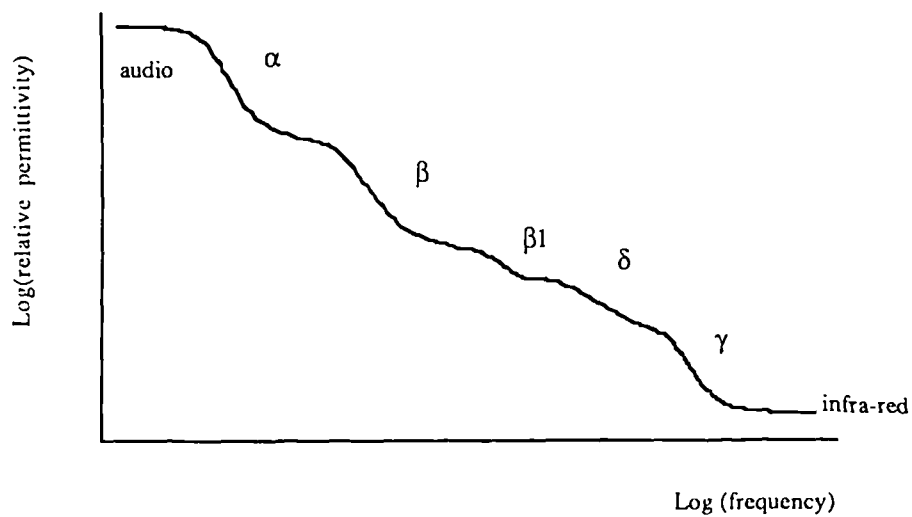
Figure 3.1   Frequency variation of the permittivity of a typical high water content tissue. Symbols are explained in the text.

dielectric decrement $\Delta\varepsilon$ is often used to quantify the dispersion:

$$\Delta\varepsilon = \varepsilon_s - \varepsilon_\infty \qquad\qquad (3.7)$$

where ε_s and ε_∞ are the end points of the particular dispersion. The alpha, beta,gamma and delta dispersions may therefore be described by total dielectric decrements $\Delta\varepsilon_\alpha$, $\Delta\varepsilon_\beta$, $\Delta\varepsilon_\gamma$ and $\Delta\varepsilon_\delta$ respectively. Each dispersion region may be described by the relaxation (3.6), the spread of relaxation times being determined by the different physical processes involved.

The α-dispersion, observed at audio frequencies ($f_c \approx 100\text{Hz}$, $\tau \approx 1.6\text{ms}$), is characterised by very high values of the relative permittivity and a large dielectric decrement, both of the order of 10^6. This dispersion is thought to be caused by ionic diffusion processes and by membrane conductance phenomena. At these low frequencies the tissue is very resistive ($\sigma \approx 0.25\text{Sm}^{-1}$) despite the high permittivity values, so that the increase in conductivity ($\leq 0.01\text{Sm}^{-1}$) is only slight over the dispersion region, tissue relaxation being swamped by ionic conductivity. The α-dispersion disappears quickly after excision of tissue and has been used to test the freshness of raw food (Hasted, 1973). More details may be found in Schwan (1981) who reviewed knowledge and understanding of this effect.

The β-dispersion occurs at radiofrequencies in tissues ($f_c \approx 500\text{kHz}$, $\tau \approx 300\text{ns}$) with a dielectric decrement of $\Delta\varepsilon_\beta \approx 10^4$. Blood displays this dispersion at higher frequencies ($f_c \approx 3\text{MHz}$, $\tau \approx 50\text{ns}$) with a dielectric decrement of $\Delta\varepsilon_\beta \approx 2000$. This effect is thought to be caused by the charging of cell membranes with smaller contributions arising from the dipolar relaxation of proteins in tissue. [This latter effect is sometimes analysed as a separate dispersion, called the $\beta 1$-dispersion (Grant, 1984).] The larger permittivity values observed in tissues compared to blood are due to larger cell sizes. Observation of the β-dispersion can give valuable information on the coupling of externally imposed fields and 'in situ' field strengths in tissue: a fairly comprehensive discussion of this is given in Foster and Schwan (1989).

The γ-dispersion occurs at microwave frequencies ($f_c \approx 25\text{GHz}$, $\tau \approx 6$ ps), with a total dielectric decrement for high water content tissues of $\Delta\varepsilon_\gamma \approx 50$; the corresponding increase in conductivity is about 70 Sm^{-1}. This dispersion is caused by the dipolar relaxation of plasma, intracellular and interstitial fluids in tissue, a process which was examined in Chapter 2 and quantified for water and physiological saline in Section 3.2.

The δ-dispersion occurs in the frequency range 0.1 to 5GHz and is rather poorly defined because it overlaps the strong β- and γ-dispersions. Its dielectric decrement is typically $\Delta\varepsilon_\delta \approx 15$ with an associated increase in conductivity of between 0.4 and 0.5Sm^{-1} (Foster and Schwan, 1986). The δ-dispersion is thought to be caused by the dipolar relaxation of bound water (water of hydration). Bound water consists of those molecules close to macromolecular surfaces which are unable to rotate freely: it has a reduced static dielectric constant and relaxation time. It is not known whether other processes have an effect at these frequencies: rotational relaxation of polar side-chains and counterion diffusion processes both have been suggested as mechanisms (Foster and Schwan, 1986). Bound water is discussed more fully in Section 3.5.

3.4 Measured dielectric properties of tissue

For more than 150 years the bulk dielectric properties of tissue have been of interest to researchers. The earliest recorded measurements were made by Peltier in 1834 (cited by du-Bois Reymond, 1849) who discovered the capacitive properties of animal bodies. In this century, a data set has been built up since the 1950's stimulated by developments in instrumentation made during World War 2.

Measurements on human tissues were first reported by England and Sharples (1949) and by Cook (1951), authors who were particularly interested in possible therapeutic uses of microwaves. About the same time Schwan began to study the properties of blood and tissue, both human and animal (Schwan and Li, 1953, 1956). Since then, with the help of his colleagues in Pennsylvania, Schwan has greatly expanded understanding of the electrical properties of all types of biological material,

41

with papers published on cell suspensions, blood and tissues, at frequencies ranging from about 1mHz to 18GHz. He has published several reviews in which the many papers from his group are cited (Foster and Schwan, 1989; Foster and Schwan, 1986; Schwan and Foster, 1980; Schwan, 1957).

Another group which has greatly contributed to the available dielectric data on tissue is that of Stuchly and his co-workers in Canada. Their main studies in this field have been reported over the last 10 years and include the first comprehensive review of tissue data (Stuchly and Stuchly, 1980). As with Schwan's group, the Canadian group has a wide-ranging interest in the interaction of electromagnetic waves with biological materials. Relevant papers are cited later in this section.

In Britain, most data have come from Grant's laboratory in the University of London. With his colleagues, Grant has examined the structural parameters of biological molecules and of biological water; the properties of normal and cancerous tissue for hyperthermia studies; and the properties of lens tissue for investigations of microwave hazards. Most of this work has been carried out at frequencies between 10MHz and 18GHz, apart from one paper which reports data at 35GHz (Steel and Sheppard, 1988). Pertinent data from this group's publications are examined later in this section.

Several other groups have worked or are working in this field, most notably Burdette and his colleagues in Illinois and Atlanta, who developed an *in vivo* technique for dielectric measurement. Their particular interest is in the analysis of microwave hazards. Their papers and those of other groups are examined later in this section.

Data from the above authors and others have been gathered and are presented in tabular form in Tables 3.6 and 3.7. These tables cover human and animal tissue dielectric data for the frequency range 0.1 to 10GHz; that is, covering the δ- and part of the γ-dispersion ranges. They update the Stuchly and Stuchly (1980) paper for this frequency range, except that no data on protein solutions and only limited data on blood are included. As in the earlier tabulation, much of the data have been read from graphs, which may impose some limitations on their accuracy. None, however, have been

interpolated or extrapolated or calculated from author's models. Data from the earlier (Stuchly and Stuchly, 1980) paper are included for completeness. (These data may include extrapolated points.) Also, data from earlier work, not included by Stuchly and Stuchly, are presented here.

Although some other data reviews have appeared in the intervening years, they are limited in extent. Pethig's (1984) review contains data from ten papers which are mostly extrapolated or interpolated to 0.9 and 2.45GHz, and gives no information on species type. Foster and Schwan's (1986, 1989) reviews are not as extensive as the present one: they contain information from only about eleven references for the same frequency range, include extrapolated and interpolated data, and are set out in a confusing way. The tables presented here draw data from more than forty sources and are presented with alphabetical ordering for ease of consultation.

Two other points should be made about the data contained in these two tables (3.6 and 3.7). One paper, Schwan and Li (1953), is regularly cited as a source for human dielectric data at 37°C: however, the measurements were made at 27°C and later adjusted by Schwan (1957) using temperature coefficients derived from another source. In the present tables the original data are presented. Secondly, an error in the reporting of data by Stuchly and Stuchly (1980) has been corrected: they reported data from Osswald (1937) at 100MHz as human dielectric data using Schwan (1964) as the source. This data was in fact measured using swine and cattle and is reported as such in the present tabulation.

3.4.1 The tabulated data

Tables 3.6 and 3.7 show that for some tissue types (e.g. brain, ocular tissue and muscle) many data are available, while for others (e.g. fat and bone) very few data have been published. Data on human tissue are scarce and most of them come from early papers. Most authors work with animal rather than human tissue, presumably because of its greater availability, and also because there is a widely held assumption that the electrical properties of mammalian tissues are indicative of human tissue. It is

43

Table 3.6   Dielectric properties of human tissue gathered from the literature at frequencies 0.1 to 10 GHz.

Data 'in vitro' unless stated 'in vivo'.   Conductivity in mS cm-1.   Temperature in °C.

Tissue type	T	f(GHz):	0.1	0.2	0.5	1.0	2.0	3.0	4.0	10.0	Reference	Comments
Whole Blood	25	ε'	69	65	61	59	58	56			Jenkins et al (1989)	
		σ	--	--	--	9.2	17	27				
	27	ε'		67	64*	63^					Schwan et al (1953)	*0.4 GHz, ^0.9 GHz
		σ		10	11	13						
	37	ε'						53		45*	England (1950) — et al (1949)	*9.43 GHz
		σ						25		105		
	15	ε'						60		42*	Stuchly et al (1980)	*9.4 GHz
		σ						33		140		
	25	ε'						58		46*		
		σ						29		120		
	35	ε'						56		48*		
		σ						27		100		
Bone	37	ε'					8.4*	8.4	7.8^		Cook (1951)	*1.8 GHz, ^3.6 GHz mid-shaft tibia
		σ					1.5	2.2	3.3			
	37	ε'								7.4*	England et al (1949)	*9.43 GHz femur
		σ								8.1		
Bone Marrow	37	ε'								4.2	England et al (1949)	
		σ								11		
	37	ε'				4.3-7.3		4.2-5.8		4.4-5.4*	Stuchly et al (1980)	*8.5 GHz
		σ				0.4-1.0		1.2-2.3		1.7-4.7		

Tissue type	T	f(GHz) :	0.1	0.2	0.5	1.0	2.0	3.0	4.0	10.0	Reference	Comments
Brain	37	ε'					32*	32	^33		Lin (1975)	*2.45 GHz, ^3.9 GHz
		σ					21	29	34			
	23	ε'	--								Rajewsky (1938)	
		σ	3.3-5.0									
Breast Carcinoma	37	ε'	80 (a)								Surowiec et al (1988)	Infiltrating ductal carcinoma. (a) central
		σ	9.3									(b)surrounding tissue (<6 mm from tumour)
	37	ε'	60 (b)									(c)peripheral (25 mm from tumour)
		σ	11									(d)central (mainly adipose tissue but with infiltrating tumour cells)
	37	ε'	8.0 (c)									
		σ	0.62									
	37	ε'	23 (d)									80-85% water
		σ	1.0									
	37	ε'						62		42*, 38* 95, 92	England (1950) — et al (1949)	*9.4 GHz
		σ						25				
	37	ε'						57		42*, 41* 106, 110		scirrus
		σ						30				
	37	ε'								38* 92		
		σ										
	37	ε'								38* 89		
		σ										

Tissue type	T	f(GHz):	0.1	0.2	0.5	1.0	2.0	3.0	4.0	10.0	Reference	Comments
Breast-normal	37	ε'	6.5								Surowiec et al (1988)	
		σ	0.41									
Fat		ε'			6.0	6.2		6.0*			Jenkins et al (1989)	*2.5 GHz in vivo
		σ			1.1	1.2		2.3				
	27	ε'		4.5-7.5	4-7 *	3.2-6^					Schwan et al (1953)	*0.4 GHz, ^0.9 GHz
		σ		0.20-0.67	0.25-0.77	0.29-0.91						
	37	ε'					4.2* (a)	3.9 (a)	4.1^ (a)		Cook (1951)	*1.8 GHz, ^4.6 GHz **3.6 GHz (a)breast (b)abdominal wall (c)near faecal fistula (d)sole of foot
		σ					1.1	1.5	1.9			
	37	ε'						4.9 (b)	4.2 ** (b)			
		σ						2.4	2.0			
	37	ε'					7.2* (c)	7.0 (c)	5.8^ (c)			
		σ					2.3	2.9	4.8			
	37	ε'					11* (d)	12 (d)	7.7^ (d)			
		σ					3.0	3.8	2.3			
	37	ε'						5.2 (a)		4.0* (a)	England (1950), — et al (1949)	*9.43 GHz (a) breast (b) leg
		σ						2.6		5.3		
	37	ε'						7.2 (a)		4.1* (b)		
		σ						2.9		4.7		
	37	ε'	8-13			5.3-7.5	5.8*	3.9-7.2	4.7^	3.5-4.5**	Stuchly et al (1980)	*2.45 GHz, ^5 GHz **8.5 GHz
		σ	0.67			0.83-1.5	1.1	1.1-2.3	1.9	2.7-4.2		

Tissue type	T	f(GHz):	0.1	0.2	0.5	1.0	2.0	3.0	4.0	10.0	Reference	Comments
Kidney	37	ε'	80 (84)								Surowiec et al (1987)	Data at 16±7 hours after death. Bracketed values transformed to 1-2 hours after death. 83.9% water
		σ	11 (12)									
	27	ε'		62	55-57*	53-56^					Schwan et al (1953)	*0.4 GHz, ^0.9 GHz
		σ		9.6	10	12						
	23	ε'	--								Rajewsky (1938)	
		σ	6.5-10									
Liver	37	ε'	71 (74)								Surowiec et al (1987)	Data at 16 ±7 hours after death. Bracketed values transformed to 1-2 hours after death. 77.3 % water
		σ	5.8 (7.0)									
	27	ε'		50-56	46-53*	44-52^					Schwan et al (1953)	*0.4 GHz, ^0.9 GHz
		σ		5.9-8.0	6.7-8.3	8.3-11						
	23	ε'	--								Rajewsky (1938)	
		σ	5.1-6.7									
	37	ε'			43-51	46-47		42-43		34-38*	Stuchly et al (1980)	*8.5 GHz
		σ			--	9.5-10		20		50-57		
Lung	27	ε'		35	36*	35^					Schwan et al (1953)	*0.4 GHz, ^0.9 GHz
		σ		5.3	6.1	7.3						
	23	ε'	7.1-10								Rajewsky (1938)	Deflated lung
		σ										
Muscle		ε'			49	49		49*			Jenkins et al (1989)	*2.5 GHz in vivo Sartorius muscle
		σ			8.6	9.5		13				
	37	ε'	72								Surowiec et al (1987)	Cardiac muscle. Data taken 16±7 hours after death. 78.9% water
		σ	8.9									

Tissue type	T	f(GHz) :	0.1	0.2	0.5	1.0	2.0	3.0	4.0	10.0	Reference	Comments
Muscle	27	ϵ'		56	54-56 *	53-55^					Schwan et al (1953)	*0.4 GHz, ^0.9 GHz (a) cardiac muscle
		σ		8.3-9.1	9.5-10	12						
	27	ϵ'		59-63 (a)	54-58* (a)	53-57^ (a)						
		σ		7.7-9.1	8.7-10	10-12						
	37	ϵ'					51* (a)	51 (a)	47^ (a)		Cook (1951)	*1.8 GHz, 4.6GHz (a) soleus (b) pectoralis major
		σ					24	30	52			
	37	ϵ'					50* (b)	50 (b)	47^ (b)			
		σ					23	29	42			
	37	ϵ'					52* (b)	52 (b)	49^ (b)			
		σ					21	32	50			
	37	ϵ'								34*	England et al (1949)	*9.4GHz skeletal
		σ								79		
	37	ϵ'								33*		
		σ								84		
	23	ϵ'	--								Rajewsky (1938)	(a)skeletal (b)cardiac
		σ	6.5-7.7(a)									
	23	ϵ'	--									
		σ	6.0-7.4(b)									
	37	ϵ'				49-52	48*	45-48	44^	40-52**	Stuchly et al (1980)	*2.45 GHz, ^5 GHz **8.5 GHz
		σ				13	18	22-23	39	71		

Tissue type		T	f(GHz):	0.1	0.2	0.5	1.0	2.0	3.0	4.0	10.0	Reference	Comments
Ocular Tissue Lens	nuclear	37	ε'	48	44	39	36	33	31	29*		Dawkins et al (1981)	**0.53 GHz for ε', 0.56 GHz for σ, ^2.2GHz for σ, ^^3.2 GHz for σ, *4.3 GHz for ε', 4.7 GHz for σ.
			σ	3.2	4.1	5.6	7.4	13^	19^^	28			
	cortical	37	ε'	62	58	50**	47	44	41	38*			
			σ	6.0	7.1	5.4	10	15	21	32			
Skin			ε'					40	44*		37	Xu et al (1987)	*2.5 GHz in vivo
			σ					21	27		76		
			ε'								22	Hey-Shipton et al (1982)	in vivo
			σ								98		
			ε'				42	40*	38^	37**		Tanabe et al (1976)	*1.8 GHz, ^3.2 GHz **3.8 GHz. in vivo
			σ				6.1	13	22	30			
			ε'		51*, 53*	47^, 48^	43, 48**					Schwan et al (1953)	*0.25 GHz, ^0.4 GHz **0.9 GHz (both measurements)
			σ		7.1 6.9	7.4, 8.6	9.2,11						
		37	ε'					52* (a)	51 (a)	46^(a)		Cook (1951)	*1.8 GHz, ^4.6 GHz (a)near faecal fistula (b)breast (c)instep sole
			σ					21	25	41			
		37	ε'					40* (a)	40 (b)	39^(b)			
			σ					18	21	34			
		37	ε'						42 (c)	40^ (c)			
			σ						22	32			

Tissue type	T	f(GHz) :	0.1	0.2	0.5	1.0	2.0	3.0	4.0	10.0	Reference	Comments
Skin	37	ε'						41		36* (a)	England (1950), — et al (1949)	*9.4 GHz (a)breast (b)leg
		σ						28		86		
	37	ε'						50		34* (b)		
		σ						25		81		
	37	ε'						52				
		σ						28				
	37	ε'	65	57	47	43-46	43*	40-45	41	36^	Stuchly et al (1980)	*2.45 GHz, ^8.5 GHz
		σ	7.2-8.3	8.0	7.4	9.1-11	19	20-27	39	71		
Spleen	37	ε'	73 (76)								Surowiec et al (1987)	Data at 16±7 hours after death. Bracketed data transformed to 1-2 hours after death. 79.0% water
		σ	11 (10)									
	23	ε'	--								Rajewsky (1938)	
		σ	7.1-9.1									

interesting to examine this assumption at microwave frequencies by comparing the human and animal data from Tables 3.6 and 3.7 for different tissue types.

(a) Fat

Figures 3.2(a) and (b) show the collected permittivity and conductivity data on fat as a function of frequency. Only two sets of measurements exist on animal tissues, both canine, compared to four data sets on human tissues. The graph of permittivity dispersion shows canine fat relative permittivity to be very much higher than that of human fat over the range 0.1 to 2GHz (ε'= 13 to 19 for canine fat; ε' = 3.1 to 7.5 for human fat). Human fat appears to exhibit very little dispersion over this range. The disparity in human and canine fat data indicates that canine fat probably has a higher water content than human fat and so cannot be regarded as typical of the human tissue.

Figure 3.2(b), the graph of conductivity as a function of frequency, is very curious. All the data lie between 0.2 and 5.3mS/cm apart from those data measured by Burdette et al (1986a) which are an order of magnitude higher (20 to 58mS/cm in the range 0.1 to 2.0GHz). No mention was made by Burdette et al of these unusually high conductivity values: the authors instead discussed their high permittivity values compared to human data (2-3 times greater), proposing the observed differences to be due to higher water content of the tissue *in vivo*. However since both ε' and σ should be affected in the same way by a difference in water content it seems likely that such high conductivity values are caused by experimental error rather than an intrinsic property of tissue *in vivo* as compared to *in vitro*. A similar problem with Burdette's work was discussed by Stuchly et al (1982a) who compared dielectric data from different animal species. They found that data from Burdette et al (1980) differed greatly from their own measurements on cat and rat tissues, and showing his permittivity and conductivity data to be inconsistent, they suggested that Burdette's technique may have been at fault at the calibration stage. Other authors have also expressed doubts about Burdette's work: Foster and Schwan (1989) pointed out that his conductivity data on kidneys seem inconsistent with data of other workers while

(a)

(b)
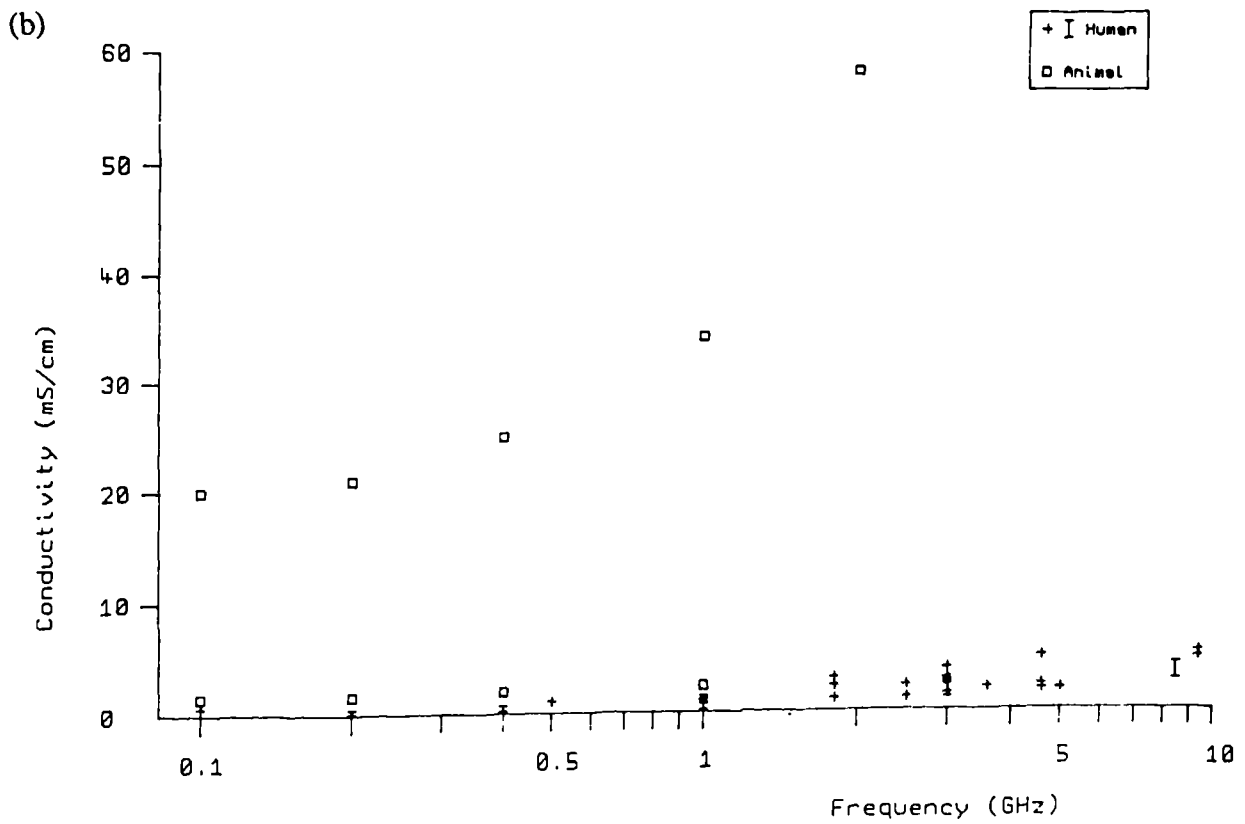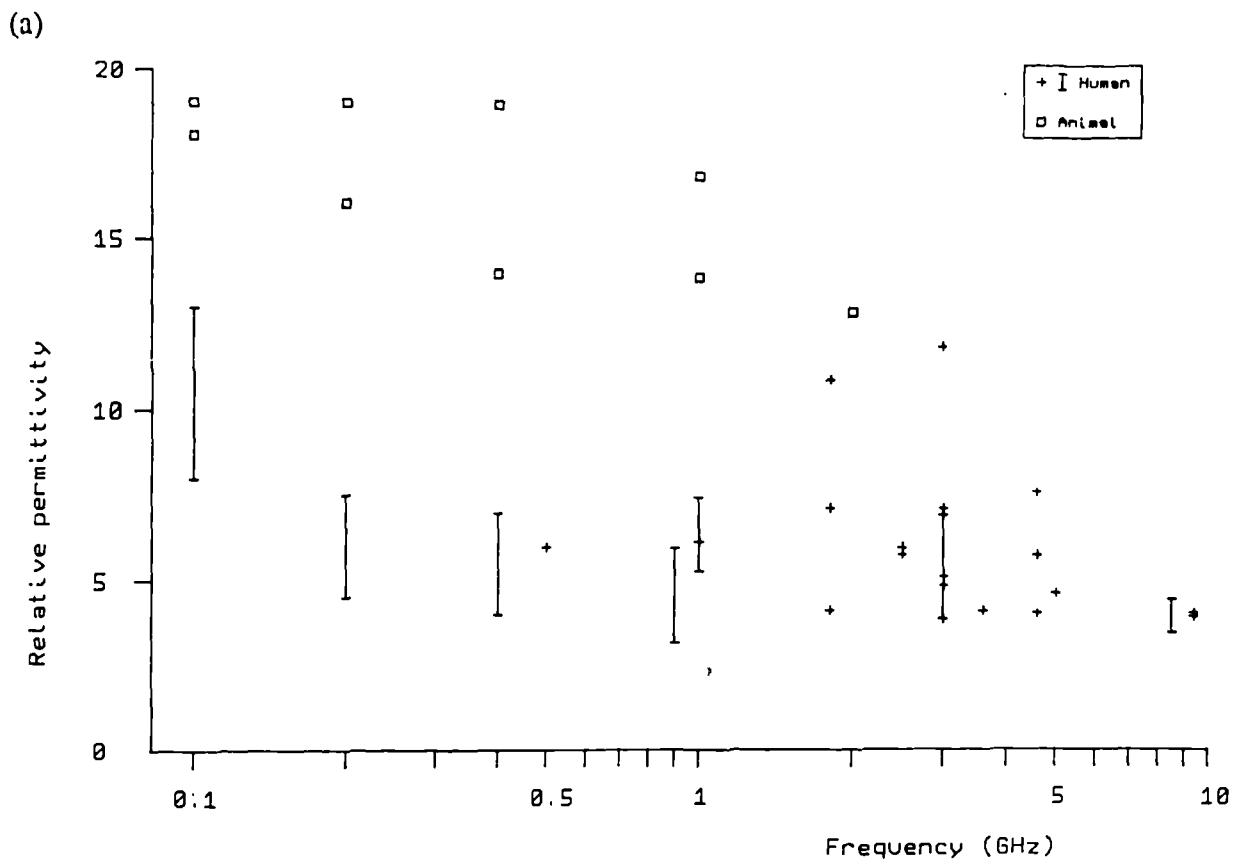
Figure 3.2   Variation with frequency of (a) relative permittivity
                    and (b) conductivity of fat data collected from the literature

Grant (1984) criticised his experimental technique. Burdette used an *in vivo* technique. Measurement probes were fabricated from coaxial cables with an extended centre conductor attached to connectors of different shapes and sizes. Measurements were made with a network analyser. The most probable sources of error are at the connector, where insufficient knowledge of field reflection coefficients at the connector/tissue interface, at internal tissue interfaces, and at the connector/network analyser interface could lead to erroneous interpretation of data.

There is a possibility that actual differences existed in the canine fat measured by Burdette et al (1986a) and human and canine fat of other authors, but such large differences are extremely unlikely. More studies on fat dielectric dispersions would help clarify this matter.

(b) Malignant tumours

Figures 3.3(a) and (b) show the collected permittivity and conductivity data on tumour tissues as a function of frequency. There exist only limited data on human tumour tissue at microwave frequencies with useful contributions from only two authors (Surowiec et al, 1988; England 1949, 1950) who made measurements on breast carcinomas. One other data set exists (Chaudhary et al, 1984) [2] which is not reported in Table 3.7. This author's work was omitted because samples of tissue were collected in physiological saline: inevitably the resulting data at microwave frequencies was representative of physiological saline rather than of breast carcinoma. Four sets of data are available on animal tumours from rat, mouse and canine tumours.

England's (1949, 1950) data on human tissue compare quite favourably with the collected animal data although permittivities appear slightly higher in human tissue at 3GHz. From his data it may be surmised that little difference is likely to be found between human and animal tumours at microwave frequencies, although because so few data are available this must be a very tentative conclusion. The data of Surowiec et al (1988) at 100MHz, however, seem very much lower than the collected animal data. Their values, ranging from 8 to 80 in ϵ' (compared with 83 to 100 for animal tissue)
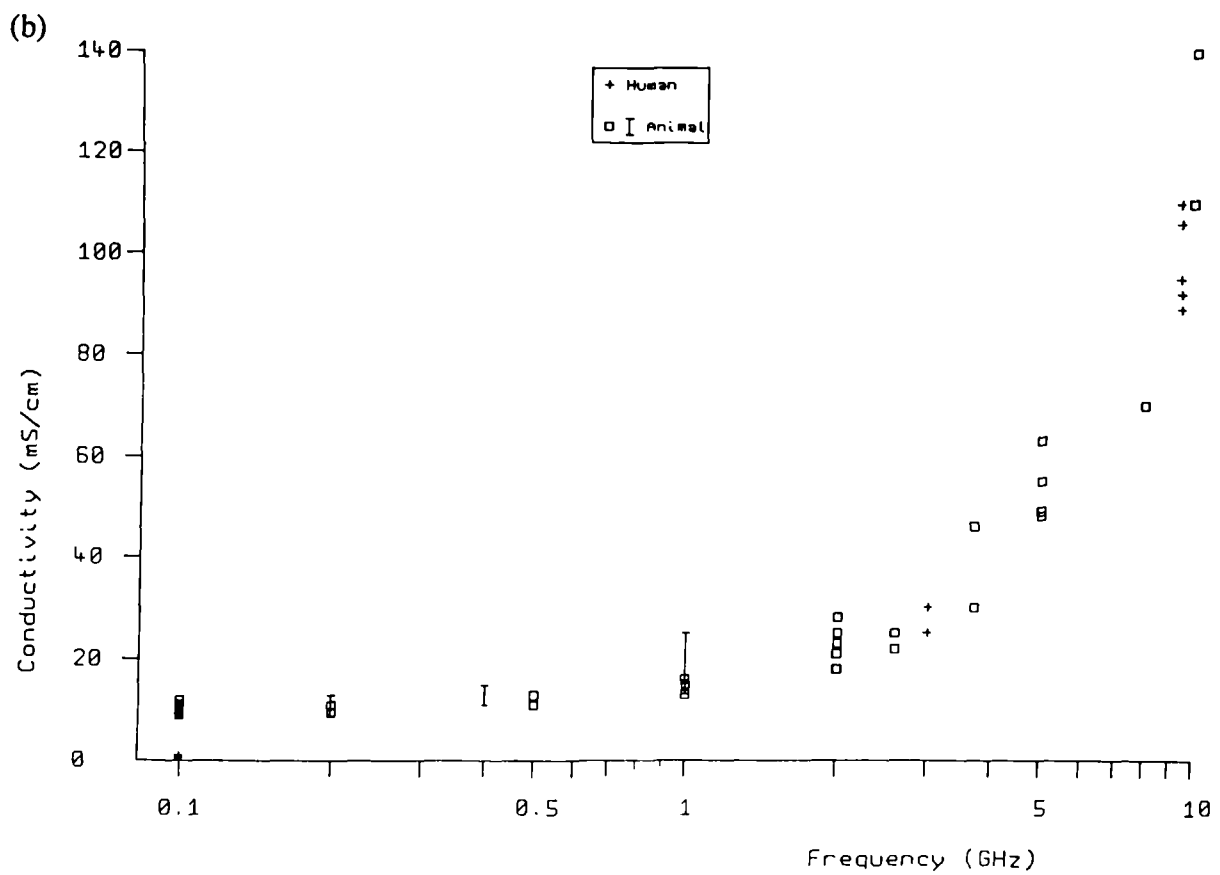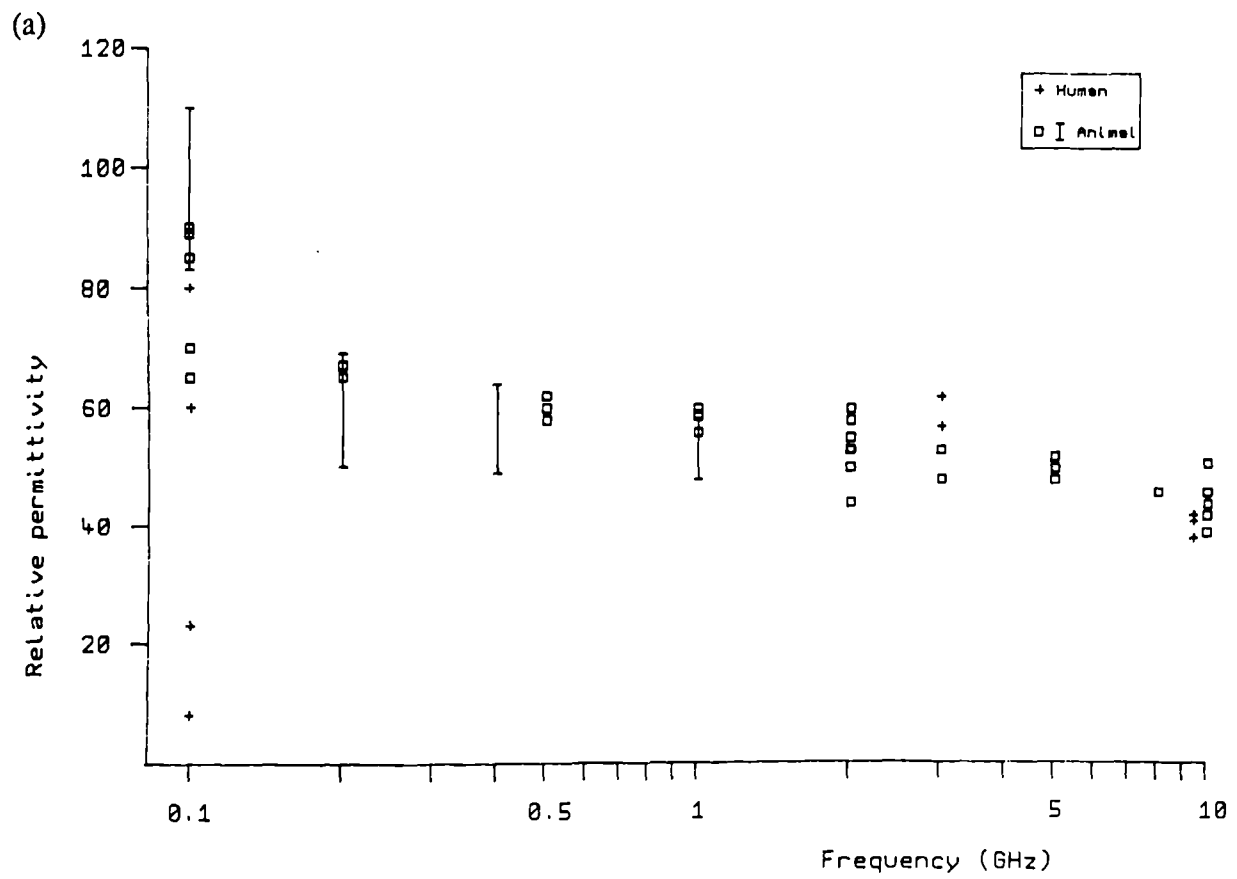
Figure 3.3   Variation with frequency of (a) relative permittivity and
(b) conductivity for tumour data collected from the literature

and from 0.6 to 12mS/cm in σ (compared with 8.5 to 12mS/cm for animal tissues) may reflect their examination of surrounding and necrotic tissue as well as malignant tissue. It is possible that only one data point is truly representative of malignant tissue ($\epsilon' = 80$, $\sigma = 11$mS/cm).

It is considered that the new data presented in Chapter 5 will form a useful addition to these existing data on tumours.

(c) Brain

Nine studies of canine, rat and mouse brain tissues have been reported over the last decade with a spread of values for ϵ' and σ resulting at each frequency . (At 3GHz ϵ' ranges from 36 to 68 and σ ranges from 12 to 23mS/cm.) This variation seems independent of species and is likely to be a function of tissue water content, itself a function of animal age (Thurai et al, 1984). In the same animal grey brain tissue has a higher water content than white brain tissue and consequently has a higher permittivity and conductivity. The results for macerated or homogenised tissue lie between these two extremes. Published data on human brain tissue are extremely limited by comparison, consisting of only three data points (at 2.45, 3 and 4GHz). These data come from a study by Lin (1975) in which no information was given about the location or type of brain tissue used, or its water content. Comparing the values of ϵ' from this study with the collected animal data indicates that the human brain tissue was perhaps white and therefore of lower water content. However the conductivity data are inconsistent with this conclusion, lying at the highest part of the range for animal tissues. Figure 3.4 shows a graph of conductivity versus permittivity of the collected data at 3GHz: this graph clearly shows that the point from Lin (1975) lies far from the range of animal data. An intrinsic difference may exist between the animal and human brain tissues: it is more likely that the observed discrepancy was an artifact of the particular experiment. Clearly more experimental data are needed on human brain tissue. One other point on Figure 3.4 lies away from the main range of data: this is a data point taken from Burdette et al (1986a) whose work was criticised above in the
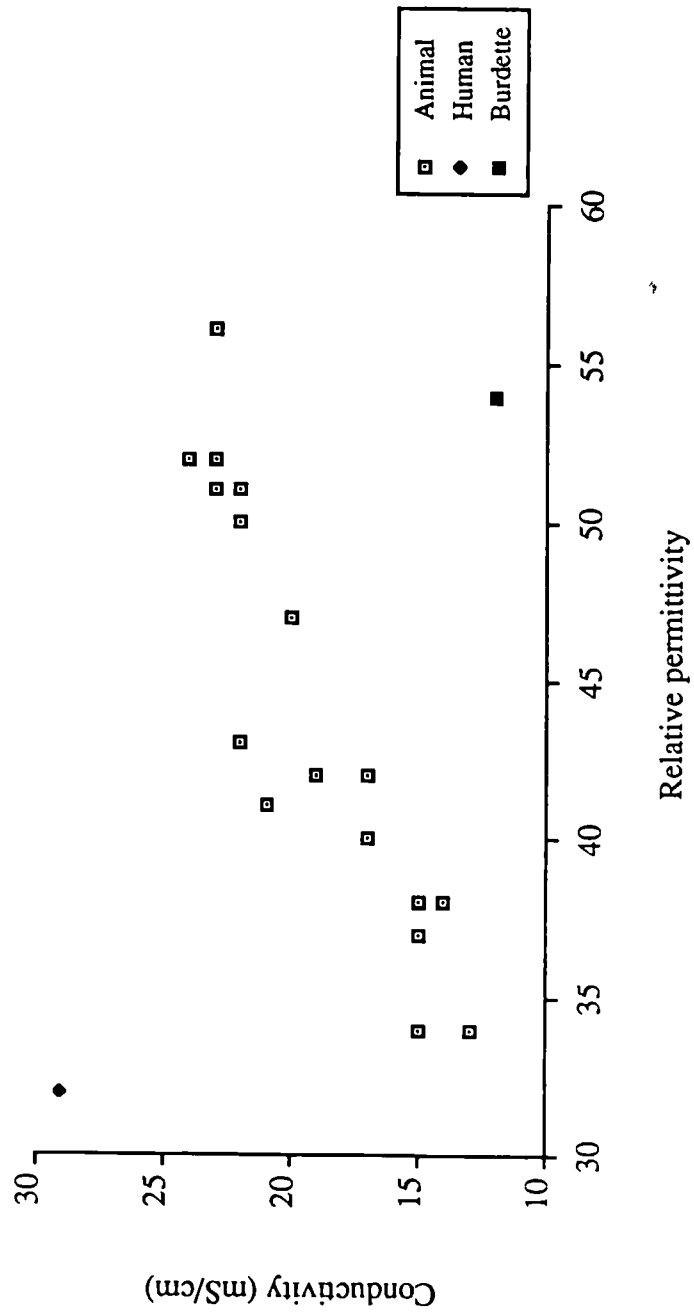
Figure 3.4   The variation of conductivity with permittivity for all brain tissue at 3GHz

section on fat.

(d) Skin

More microwave dielectric data has been published on human skin than on animal skin. At least seven studies of human skin , three *in vivo*, have been made since 1949, in comparison to just two of animal skin (canine and rat). As with other high water content tissues, skin displays a fairly wide range of dielectric properties as shown in Figures 3.5(a) and (b). One set of measurements, by Zywietz et al (1986), shows markedly lower permittivitiies and conductivities than the other studies. They measured the average water content of the skin tissue to be 54.2%, which might be expected to give rise to higher dielectric properties than those observed (ε' ranges from 8.8 to 17.3 and σ from 0.41 to 1.7mS/cm in the frequency range 0.2 to 2GHz in their study). The authors comment that their *in vivo* technique may have probed below the skin layer to a fat layer, although the largest part of the signal came from the skin. Their technique was based on that of Burdette(1980), which was discussed in Section 3.4.1(a). Their data cannot be dismissed without further animal measurements. However it is possible that the authors of this study were correct in criticising their technique, and that little difference exists between the properties of human and animal tissue.

(e) Muscle

A large body of data on muscle tissue has been reported in the last decade.Twelve sets of data on animal tissues — canine, bovine, mouse, swine — and six sets of measurements on human tissues exist. These are compared in Figures 3.6(a) and (b). Although the data on human muscle appear to be slightly lower in permittivity, no clear distinction can be made between the observed dispersions of the animal and human tissue.

(f) Kidney

Very few data have been published on human kidney at microwave frequencies,
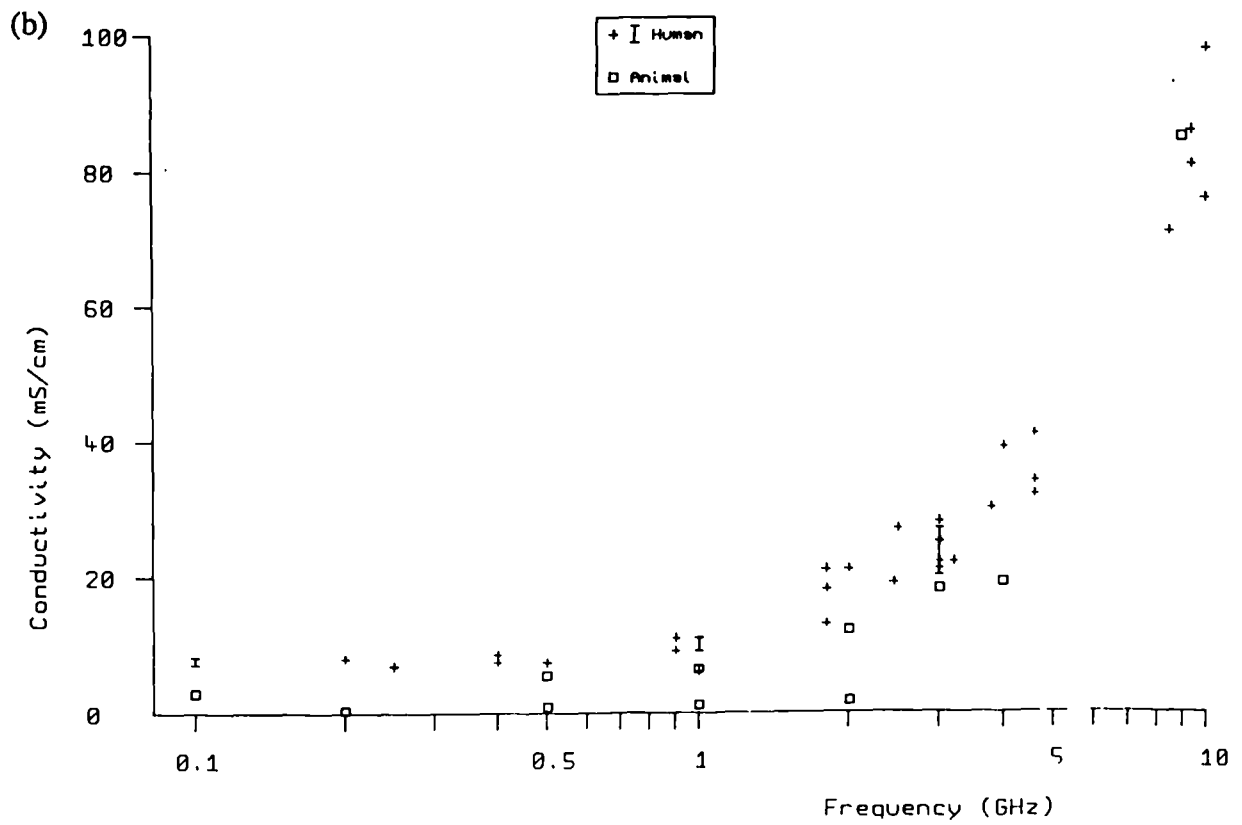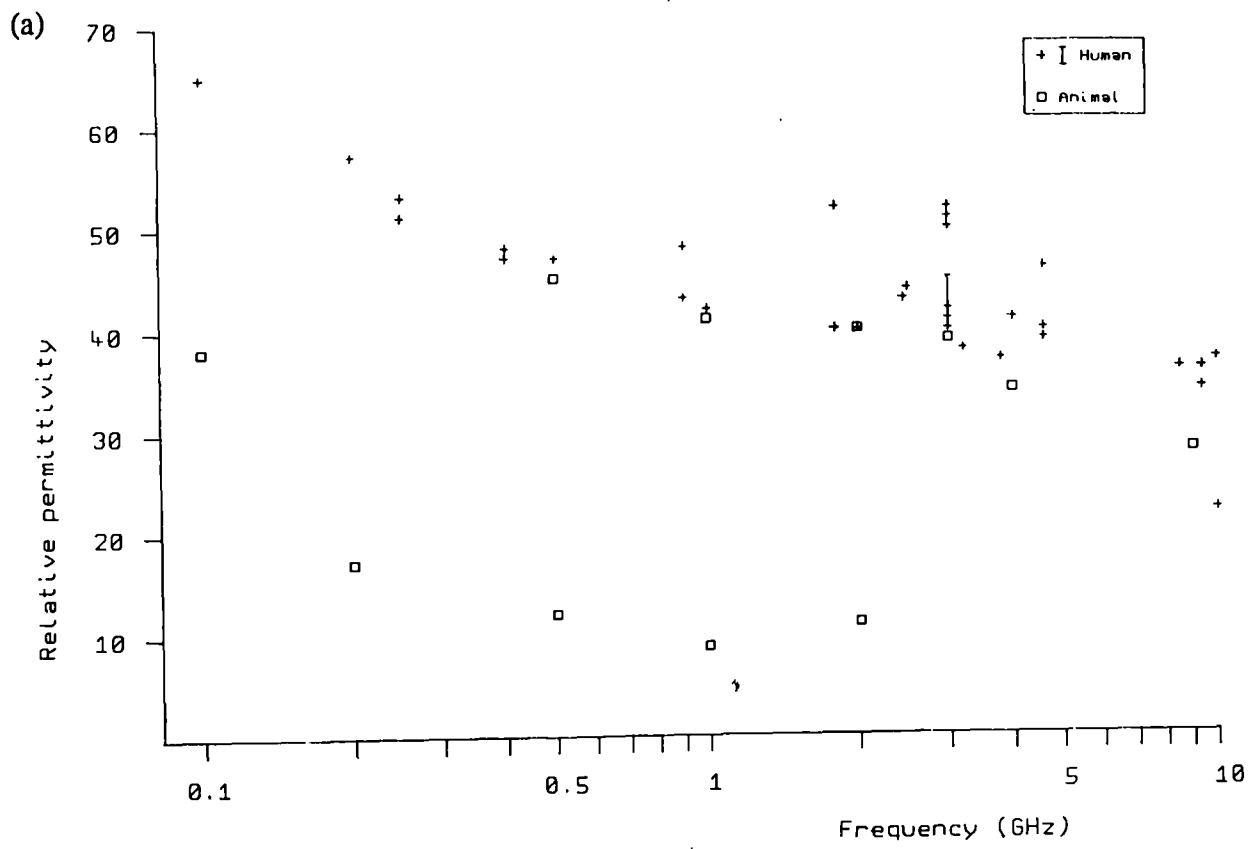
Figure 3.5   Variation with frequency of (a) relative permittivity and
   (b) conductivity for skin data collected from the literature
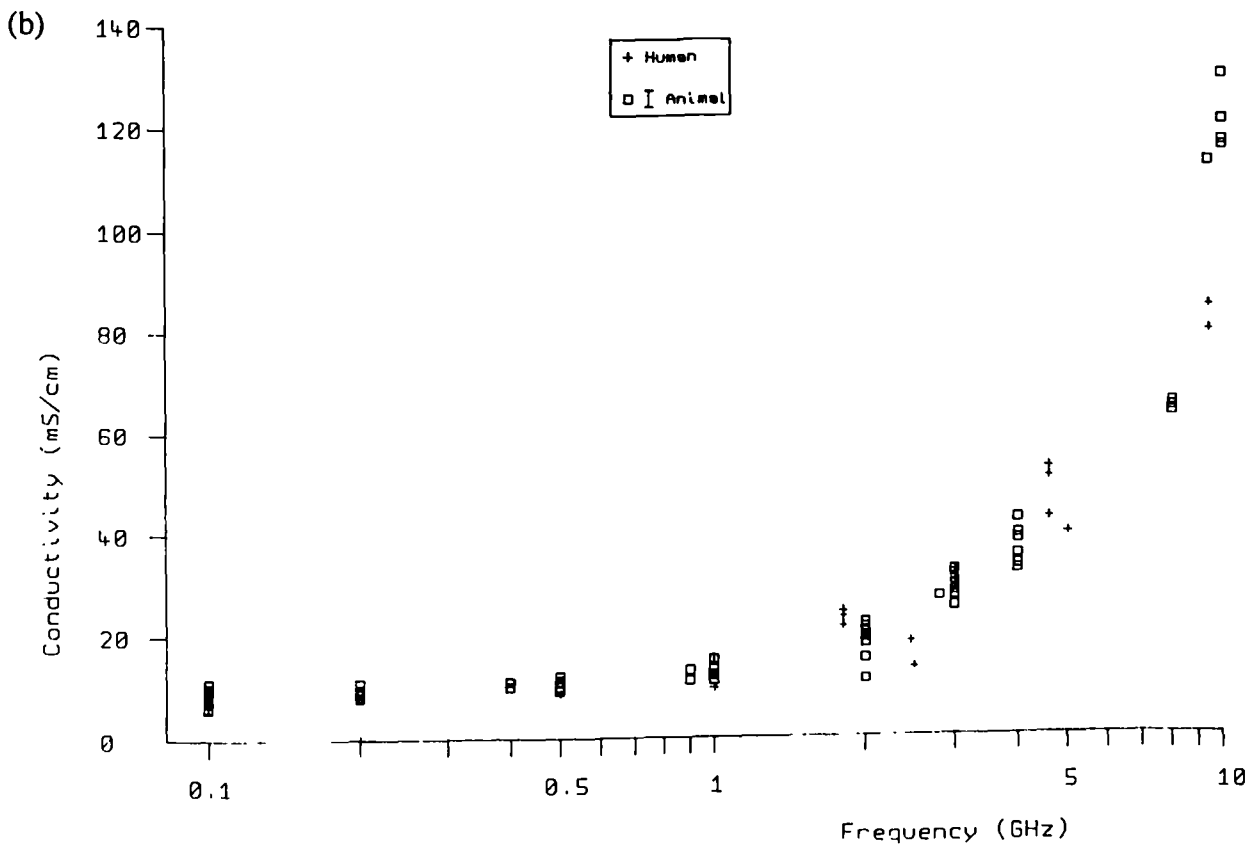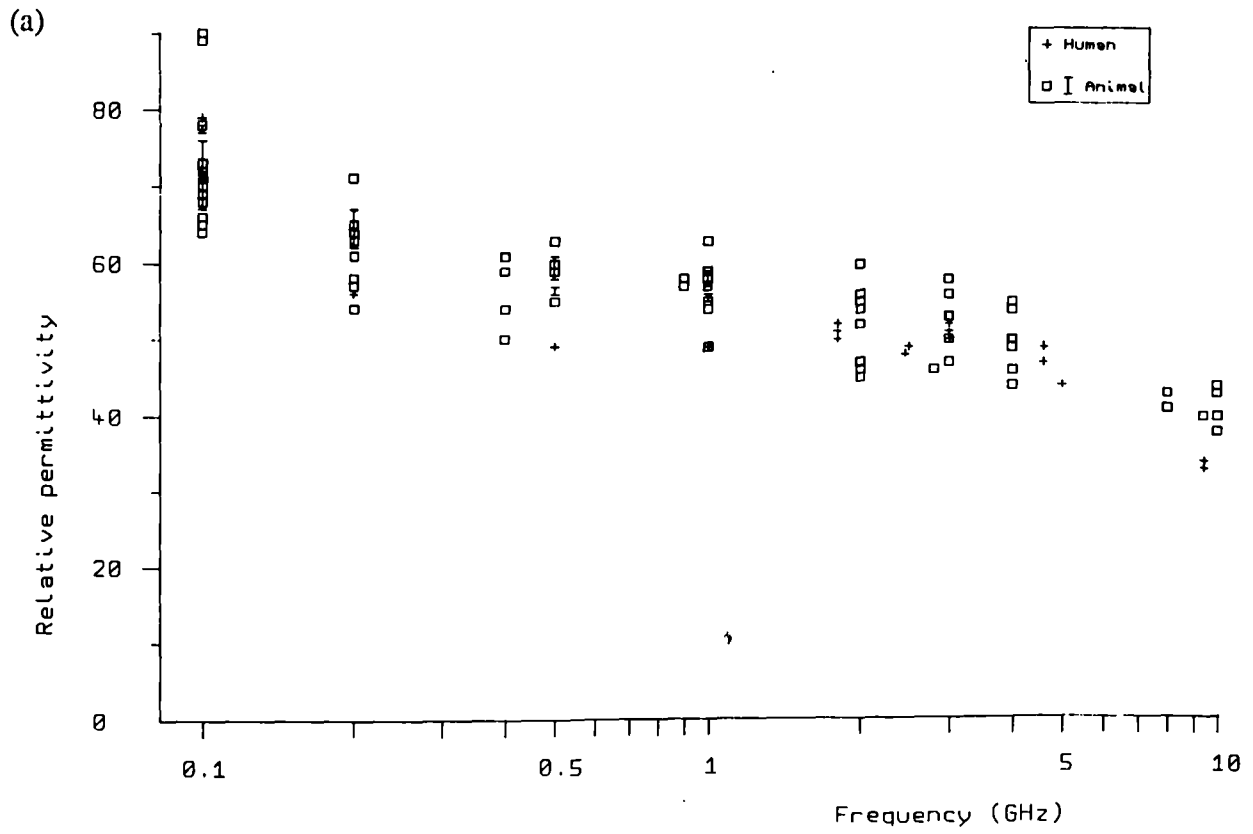
Figure 3.6   Variation with frequency of (a) relative permittivity and (b) conductivity for muscle data collected from the literature

compared to about twelve sets on canine, bovine, rabbit, rat and swine kidneys. Those human data which have been published appear to be consistent with data from animal kidneys.

(g) Lens

Lens cortex and nucleus measurements of rabbit and bovine eyes have been made by several authors, while only one set of data exists on human lens (Dawkins et al 1981). Lens cortex has a higher water content than lens nucleus so that the two tissues must be considered separately. No noticeable difference can be seen in the human and animal measurements on lens cortex. However the data on human lens nucleus show higher permittivities and conductivities than the corresponding rabbit and bovine tissues. Such few data are available on lens nuclear tissue (three on animal and one on human nucleus) that no proper comparison can be made.

(h) Liver

Again, only a limited number of measurements have been published on human liver, most of which come from early studies by Schwan. By contrast, eleven studies of canine, bovine and rat liver tissues have been published in the last decade. The early human permittivity data are a little lower than recent animal permittivity data while human and animal conductivity data are consistent. It seems likely that little difference exists in the microwave properties of human and animal liver.

(i) Other Tissues

The other tissue data in Tables 3.6 and 3.7 are insufficient to allow a detailed animal/human comparison to be made.

From the above discussions of the different tissue types, the main conclusion must be that, in general, too few data have been published on human tissues to be sure that animal measurements are a good substitute. For most tissue types animal tissue data

Table 3.7   Dielectric properties of mammalian tissue gathered from the literature at frequencies 0.1 to 10 GHz

Data 'in vitro' unless stated 'in vivo'.   Conductivity in mS cm-1.   Temperature in °C.

Tissue type	T	f(GHz) :	0.1	0.2	0.5	1.0	2.0	3.0	4.0	10.0	Reference	Comments
Artery bovine	37	ε'					47	47	46		Brady et al (1981)	
		σ					19	25	33			
Blood rat	23	ε'	84		64		63	64		51	Burdette et al (1980)	in vivo Burdette's data criticised in text
		σ	9.1		9.6		20	30				
rat	23	ε'	75	65	53	58	56*	55	52^	45	Stuchly et al (1980)	*2.45 GHz, ^5.0 GHz
		σ	11	12	13	14	21	26	46	122		
Bone rat	37	ε'	23								Kosterich et al (1983)	Fluid saturated bone
		σ	57									
Bone Marrow calf	25	ε'	20	20	18	18					Smith et al (1985)	
		σ	2.6	2.6	3.0	3.5						
Brain canine white	20	ε'	60		37	41	43	38	36	30*	Xu et al (1987)	* 9.0 GHz
		σ	3.5		3.9	8.0	13	14	18	67		
grey	20	ε'	78		64	59	60	56	52	45*		
		σ	6.2		8.5	11	21	23	26	147		
canine: pia mater	36	ε'		69	64*	57	51		48		Burdette et al (1986a)	*0.4 GHz in vivo Burdette's data criticised in text
		σ		9.5	9.9	13	18		32			
pia mater -over vessel	36	ε'		72	60*	59	54		50			
		σ		11	12	14	18		30			

Tissue type	T	f(GHz) :	0.1	0.2	0.5	1.0	2.0	3.0	4.0	10.0	Reference	Comments
Brain canine homogenised	25	ε'					47*				Burdette et al (1986b)	*2.45 GHz in vivo Burdette's data criticised in text
		σ					17					
	30	ε'					43*					
		σ					15					
	37	ε'					44*					
		σ					15					
mouse cerebral cortex	37	ε'	80-120		47-58	45-61		39-56			Thurai et al (1984)	77.1-86.5 % water Range of 4 samples
		σ	6.0-10		8.6-11	9.2-15		14-29				
mouse: cerebellum	37	ε'	85	62	48	44	42*	42^	39**		Nightingale et al (1983)	*1.9 GHz, ^2.7 GHz **3.7 GHz cerebellum -76.5 % water cerebrum -73.7 % water stem -72.3 % water
		σ	5.1	6.2	7.6	9.4	13	17	24			
cerebrum	37	ε'	74	58	45	42	40*	40^	38**			
		σ	4.6	5.6	7.0	9.0	12	17	25			
stem	37	ε'	72	57	43	40	38*	^37	35**			
		σ	4.5	5.5	6.9	8.9	12	15	21			
cat cortex	35	ε'	71	68	58**	55^^	52	50	50	46*^	Stuchly et al (1982a)	*0.12 GHz, ^0.24 GHz **0.4 GHz, ^^0.9 GHz *^8.0 GHz
		σ	9.6	9.8	11		16	22	32	66		
rat cortex	35	ε'	70*	60^								
		σ	8.0	8.7								
swine and cattle	37	ε'	81-83								Osswald (1937)	
		σ										

Tissue type		T	f(GHz):	0.1	0.2	0.5	1.0	2.0	3.0	4.0	10.0	Reference	Comments
Brain														
cat	grey	33	ε'	65-80	58-63	48-52	47-51					Suchly et al (1981)	in vivo
			σ	5.2-8.5	6.0-8.2	7.1-9.3	8.9-12						
	white	35	ε'	58-64	49-50	39-40	37-39						
			σ	4.8-5.1	5.2-5.4	6.1-6.2	8.1-8.2						
rabbit	white	37	ε'					35*	34^	34**	30*^	Steel et al (1985)	*2.4GHz, ^3.2 GHz **3.7 GHz, ^^3.9 GHz *^9.5 GHz
			σ					12	15	16	63		
	grey	37	ε'					47*	47	47	40*^		
			σ					16	20	27	87		
	macerated	37	ε'					42	42	40	37*^		
			σ					13	19	24	72		
	white	20	ε'					37*	38	47^^	31*^		
			σ					9.7	15	21	77		
	grey	20	ε'					51*	51	50^^	38*^		
			σ					16	22	32	105		
	macerated	20	ε'					43	42	40^^	35*^		
			σ					13	19	26	88		
mouse	macerated	37	ε'						41^	40	35*^		
			σ						21	25	73		

Tissue type		T	f(GHz) :	0.1	0.2	0.5	1.0	2.0	3.0	4.0	10.0	Reference	Comments
Brain													
canine	white	37	ε'	66, 57								Stoy et al (1982)	
			σ	4.8, 3.6									
	grey	37	ε'	90									
			σ	6.9									
cat	cortex	36	ε'	73 (85)	68	58*	55^	53	52 (52)	50	44 (45)**	Kraszewski et al (1982)	*0.4 GHz, ^0.9 GHz **8 GHz, ^^0.3 GHz in vivo Bracketed values in vitro
			σ	9.0 (9.5)	10	11	12	17	23 (24)	31	67 (65)		
rat		32	ε'	85	58^^	55	53^	51	51	50	44		
			σ	7.5	8.7	9.8	11	15	23	31	108		
mouse		37	ε'		61*	47^	44	41**	42^^	39*^		Nightingale et al (1980)	*0.17 GHz, ^0.51 GHz **1.9 GHz, ^^2.6 GHz *^3.7 GHz
			σ		6.2	7.4	9.4	13	17	24			
canine	white	37	ε'				37		34		28	Schwan et al (1980)	white - 72% water grey - 82% water
			σ				7.5		13		67		
	grey	37	ε'				45		43		37		
			σ				11		22		100		
	unknown	22	ε'	52									
			σ	2.7									
rat		32	ε'	84	69	57	56	54	54	54	44	Burdette et al (1980)	in vivo Burdette's data criticised in text
			σ	6.5	3.6	3.9		7.8	12	17	61		

Tissue type		T	f(GHz) :	0.1	0.2	0.5	1.0	2.0	3.0	4.0	10.0	Reference	Comments
Brain canine	white	37	ε'	68			36	37		31	30	Foster et al (1979)	*0.9 GHz
			σ	4.7			7.8	9.7		12-18	62		
	grey	37	ε'	90			46*	49		41	39		
			σ	7.0			10	13		24-30	95		
	white	25	ε'	59				37		34	28		
			σ	3.9				9.5		19	69		
	grey	25	ε'	75				50		34	39		
			σ	5.8				12		33	95		
Fat canine		35	ε'	19	19	19*	17	13				Burdette et al (1986a)	*0.4 GHz in vivo Burdette's data criticised in text.
			σ	20	21	25	34	58					
equine or canine		25	ε'	18	16	14*	14					Smith et al (1985)	*0.4 GHz 21% water
			σ	1.6	1.7	2.0	2.4						
Heart canine		20	ε'	61		57	53	53	52	52	39*	Xu et al (1987)	*9.0 GHz
			σ	4.6		7.9	12	19	22	29	145		
rat			ε'								40*	Karolkar et al (1985)	*9.4 GHz 71% water
			σ								75		
Intestine rat			ε'								62*	Karolkar et al (1985)	*9.4 GHz 97% water
			σ								145		
Kidney canine		20	ε'	68		60	56	54	53	49	43*	Xu et al (1987)	*9.0 GHz
			σ	5.3		9.1	9.6	19	23	28	162		
canine			ε'	79 (83)	67 (66)	59 (56) *	54 (51)	51 (47)		48 (44)		Burdette et al (1986a)	*0.4 GHz in vivo Bracketed values in vitro. Burdette's data criticised in text.
			σ	11 (7.9)	11 (7.9)	11 (8.4)	15 (11)	24 (17)		41 (30)			

Tissue type	T	f(GHz):	0.1	0.2	0.5	1.0	2.0	3.0	4.0	10.0	Reference	Comments
Kidney bovine	24	ε'	80 (62)								Surowiec et al (1985)	78.8% water Bracketed values calculated from authors' fit.
		σ	6.7 (6.8)									
rat		ε'								40*	Karolkar et al (1985)	*9.4 GHz 66% water
		σ								99		
canine	37	ε'	89, 95								Stoy et al (1982)	
		σ	9.4, 11									
cat cortex	36	ε'	85 (66)	50 (50) (a)	54 (53) *	43 (42)^	41 (41)	48 (47)	40 (38) (a)	41 (41) **	Kraszewski et al (1982)	*0.4 GHz, ^0.9 GHz **8.0 GHz in vivo Bracketed values in vitro cat 76.4 % water except (a) 73.7 % water
		σ	7.5 (7.0)	6.9 (7.2)	7.6 (7.4)	8.3 (8.0)	13 (13)	23 (22)	23 (21)	62 (59)		
rat	32	ε'	73		54	53^	51	51	50	40		
		σ	8.0		9.1	10	16	23	31	97		
cat	35	ε'	56-72	51-52	44-45	43					Stuchly et al (1981)	in vivo
		σ	6.6-7.2	7.1-7.2	7.4-7.7	9.5-9.7						
bovine	37	ε'					51	48	44		Brady et al (1981)	
		σ					18	26	31			
swine and cattle	37	ε'	87-92								Osswald (1937)	
		σ										
Liver canine	20	ε'	57		58	55	52	49	46	38*	Xu et al (1987)	*9.0 GHz bovine
		σ	3.2		6.4	8.6	17	23	30	142		
bovine	24	ε'	60 (51)								Surowiec et al (1985)	Data in brackets calculated from authors' fit 73.6 % water
		σ	4.9 (4.6)									
rabbit	25	ε'	66	58	56	52					Smith et al (1985)	
		σ	5.3	5.7	6.5	8.3						
rat		ε'								34*	Karolkar et al (1985)	*9.4 GHz 63% water
		σ								76		

Tissue type	T	f(GHz) :	0.1	0.2	0.5	1.0	2.0	3.0	4.0	10.0	Reference	Comments
Liver cat	36	ε'	82 (68)	60 (63)	55 (55)*	51 (50)^	50 (50)	47 (49)	46 (47)	41 (43)**	Kraszewski et al (1982)	*0.4 GHz, ^0.9 GHz **8.0 GHz in vivo Bracketed values in vitro.
		σ	6.3 (7.0)	7.1 (9.1)	7.8 (9.6)	10 (11)	16 (17)	21 (23)	27 (28)	57 (59)		
rat	32	ε'	71		50	48^	47	46	45	35		
		σ	6.4		8.1	9.3	15	21	29	89		
canine	37	ε'	77								Stoy et al (1982)	
		σ	7.2									
	25	ε'	68									
		σ	6.2									
rabbit	37	ε'	79									
		σ	7.0									
cat	35	ε'	71	60	55*	51^	50	46	45	40**	Stuchly et al (1982a)	*0.4 GHz, ^0.9 GHz **8.0 GHz
		σ	6.3	6.5		9.3	16	20	27	55		
rat	35	ε'			50*							
		σ			6.5							
cat	35	ε'	65-68	56-58	49-50	47-49					Stuchly et al (1981)	in vivo
		σ	6.0-7.1	6.5-7.4	7.3-7.9	9.5-1.0						
bovine	37	ε'					44	43	42		Brady et al (1981)	
		σ					16	22	29			
canine	37	ε'	64				46		42*	37	Schepps (1981)	*5 GHz 79.5 % water
		σ	6.8				11		18	100		
rat		ε'	75								Stuchly et al (1980)	
		σ	7.1									

Tissue type	T	f(GHz) :	0.1	0.2	0.5	1.0	2.0	3.0	4.0	10.0	Reference	Comments
Liver swine and cattle	37	ε'	76-79								Osswald (1937)	
		σ	5.6-6.5									
Muscle canine	20	ε'	73		61	52	54	53	49	41*	Xu et al (1987)	*9.0 GHz
		σ	7.1		10	11	19	25	31	130		
rat (skeletal)	32	ε'			60	58	52				Zywietz et al (1986)	in vivo 73.9% water
		σ			10	13	18					
rat		ε'								40*	Karolkar et al (1985)	*9.4 GHz 70% water
		σ								112		
rat	37	ε'	71	58	54*	49					Peloso et al (1984)	*0.4 GHz
		σ	8.7	9.2	11	12						
mouse	37	ε'	72	57	55	55	51	46	43^	36	Rogers et al (1983)	* conductivity at 2.6 GHz, ^3.7 GHz
		σ	8.2	8.4	9.3	15		27*				
rat	37	ε'	89, 90								Stoy et al (1982)	
		σ	11									
canine	37	ε'	64, 66									
		σ	7.8, 7.5									
rat	37	ε'	70									
		σ	8.2									
cat	34	ε'	69	64		58^	55	53	49	41**	Stuchly et al (1982a)	*0.4 GHz, ^0.9 GHz **8.0 GHz
		σ	9.3	9.3		11	18	25	33	63		
rat	34	ε'		61	59*	58						
		σ		9.7	11	12						

Tissue type	T	f(GHz) :	0.1	0.2	0.5	1.0	2.0	3.0	4.0	10.0	Reference	Comments
Muscle cat	36	ε'	68 (65)	64 (63)	61 (61) *	59 (57)^	55 (54)	53 (53)	50 (50)	41 (43)**	Kraszewski et al (1982)	*0.4 GHz, ^0.9 GHz **8.0 GHz in vivo Bracketed data in vitro. cat 75.1 % water rat 76.9 % water
		σ	9.0 (9.0)	9.0 (9.0)	11 (10)	12 (12)	19 (18)	27 (28)	35 (33)	64 (65)		
rat	31	ε'	73		59	57^	56	56	54	44		
		σ	9.7		11	13	20	29	39	115		
cat (skeletal)	31	ε'	67-72	62-67	58-61	57-59					Stuchly et al (1981)	in vivo
		σ	9.5-9.9	9.7-10.6	11-12	14-15						
(smooth)	35	ε'	77-78	65	56-57	55-56						
		σ	9.4-9.7	9.8	11	13						
bovine	37	ε'					47	47	46		Brady et al (1981)	
		σ					19	25	32			
canine (skeletal)	37	ε'					46		44	38	Schepps (1981)	
		σ					22		42	120		
canine (skeletal)	37	ε'				54		50		40	Schwan et al (1980)	75 % water
		σ				15		32		116		
rat	31	ε'	78	71	63	63	60	58	55	43	Burdette et al (1980)	*0.4 GHz in vivo Burdette's data criticised in text.
		σ	10	11	12	13	21	30	38	129		
canine	34	ε'	69	54	50*	49	47					
		σ	10	8.0	10	11	15					
canine		ε'					45*				Stuchly et al (1980)	* 2.45 GHz
		σ					11					
swine and cattle	37	ε'	71-76								Osswald (1937)	
		σ	5.6-6.5									

Tissue type		T	f(GHz):	0.1	0.2	0.5	1.0	2.0	3.0	4.0	10.0	Reference	Comments
Ocular Tissue rabbit	lens	37	ε'					49*	49^	46**	37^^	Steel and Sheppard (1986)	*2.3 GHz, ^2.8 GHz **3.7 GHz, ^^9.5 GHz
			σ					19	23	32	97		
	nucleus	37	ε'							28**	22^^		
			σ							19	63		
	cortex	20	ε'						47^	48**	38^^		
			σ						26	40	119		
	nucleus	20	ε'							28**	21^^		
			σ							23	66		
rabbit	retina	20	ε'	90	71*	67^	62	63**	62^^	57*^	48	Gabriel et al (1985)	*0.22 GHz, ^0.48GHz **1.8GHz, ^^3.2 GHZ *^4.6 GHz retina 90% water lens cortex 70% water
			σ	11	11	12	14	20	31	51	141		
	lens cortex	20	ε'	63	58*	56^	55	54**	50	46*^	33		
			σ	4.5	4.7	5.4	8.0	13	27^^	44	140		
rabbit	lens cortex	20	ε'							48*	38^	Steel et al (1984)	*3.8 GHz, ^9.5 GHz
			σ							36	119		
rabbit	retina	37	ε'	95	70*	61^	58	57**	57^^	53*^	45	Gabriel et al (1983)	*0.22 GHz, ^0.48GHz **1.8 GHz, ^^3.2 GHz *^4.6 GHz retina 89% water iris 77% water
			σ	14	16	17	19	24	35	50	122		
	iris	37	ε'	78	65*	59^	54	53**	53^^	51*^	34		
			σ	12	13	15	15	21	34	53	175		

Tissue type	T	f(GHz) :	0.1	0.2	0.5	1.0	2.0	3.0	4.0	10.0	Reference	Comments
Ocular Tissue rabbit choroid	37	ε'	80	67*	59^	56	52**	52^^	50*^	41	Gabriel et al (1983)	*0.22 GHz, ^0.48 GHz **1.8 GHz, ^^3.2 GHz *^4.6 GHz choroid 78% water cornea 75% water lens cortex 70% water lens nucleus 50% water
		σ	13	14	15	17	22	30	50	140		
cornea	37	ε'	73	62*	55^	52	51**	47^^	45*^	38		
		σ	17	18	20	21	27	34	50	160		
lens cortex	37	ε'	67	60*	55^	50	49**	48^^	47*^	40		
		σ	5.4	8.0	9.5	12	16	28	47	167		
lens nucleus	37	ε'	38	34*	31^	31	27**	26^^	24*^	19		
		σ	2.2	2.7	4.0	6.6	11	21	33	104		
rabbit lens nucleus	37	ε'	46	42		33	30*	28^	27**		Dawkins et al (1981)	*2.2 GHz, ^3.2 GHz **4.6 GHz for ε', 4.7 GHz for σ
		σ	2.1	2.6		6.4	11	15	20			
lens cortex	37	ε'	67	60		50	46	47^	42**			
		σ	5.7	6.6		10	16	19	27			
bovine lens central	32	ε'	40	30							Stuchly et al (1980)	* 2.45 GHz, ^5 GHz
		σ	4.1	4.8								
cortical	32	ε'	66	57								
		σ	7.2	7.7								
intermediate part	32	ε'	60	48								
		σ	2.2	2.9								
lens species not stated		ε'	46	42	36	32	30*	30	30^	28		
		σ	4.0	3.9	4.2	5.2	11	15	28	100		

Tissue type	T	f(GHz) :	0.1	0.2	0.5	1.0	2.0	3.0	4.0	10.0	Reference	Comments
Pancreas canine	25	ε'	76								Stoy et al (1982)	
		σ	6.9									
	37	ε'	83									
		σ	8.7									
Skin canine	20	ε'	38		45	41	40	39	34	28*	Xu et al (1987)	*9.0 GHz
		σ	2.9		5.5	6.4	12	18	19	85		
rat	32	ε'		17	12	8.8	11				Zywietz et al (1986)	in vivo 54.2% water
		σ		0.41	0.9	1.2	1.7					
Spleen bovine	24	ε'	85 (77)								Surowiec et al (1985)	77% water. Bracketed values calculated from authors' fit.
		σ	8.0 (6.8)									
rat		ε'								41*	Karolkar et al (1985)	*9.4 GHz 72% water
		σ								104		
canine	37	ε'	83								Stoy et al (1982)	
		σ	11									
	25	ε'	81									
		σ	8.1									
cat	35	ε'	80	66	59, 56*	54^	52	52	50	44**	Stuchly et al (1982a)	*0.4 GHz, ^0.9 GHz **8.0 GHz in vivo
		σ	8.1	8.1	10, 9.0	11	16	24	24	60		
rat	35	ε'			59*							
		σ			8.6							

Tissue type	T	f(GHz) :	0.1	0.2	0.5	1.0	2.0	3.0	4.0	10.0	Reference	Comments
Spleen												
cat	36	ε'	81 (69)	66 (64)	57 (59) *	54 (55) ^	53 (54)	52 (52)	50 (50)	44 (45) **	Kraszewski et al (1982)	*0.4 GHz, ^0.9 GHz **8.0 GHz in vivo Bracketed values in vitro. cat 81.8% water rat 76.3% water
		σ	8.0 (7.4)	9.4 (9.3)	10 (11)	11 (12)	18 (18)	25 (26)	31 (30)	63 (66)		
rat	32	ε'	89		57	55^	52	52	51	41		
		σ	8.5		11	12	19	25	34	101		
cat	35	ε'	71-76	59-60	51-52	50-51					Stuchly et al (1981)	in vivo
		σ	7.3-7.6	7.7-8.0	8.4-8.8	11						
canine	37	ε'					50		48*	42	Schepps (1981)	*5 GHz
		σ					22		49	110		
canine	37	ε'				52		47		38	Schwan et al (1980)	75% water
		σ				12		28		110		
swine and cattle	37	ε'	100-101								Osswald (1937)	
		σ										
Stomach												
rat		ε'								62*	Karolkar et al (1985)	*9.4 GHz 98% water
		σ								145		
Tumours												
rat	32	ε'			62	60	53				Zywietz et al (1986)	in vivo rabdomyosarcoma 78.7% water
		σ			11	13	18					
rat	37	ε'	83-110	50-69	49-64*	48-58					Peloso et al (1984)	*0.4 GHz Range for 5 mammary carcinomas + 1 rat glioma
		σ	8.7-12	8.9-13	11-15	13-25						
mouse (1)	37	ε'	89	67	60	59	55	53	46^	39	Rogers et al (1983)	*2.6 GHz for σ ^3.7 GHz for σ fibrosarcomas: (1) KHT tumour (2) RIF/1 tumour
		σ	10	11	13	16	21	25*				
(2)	37	ε'	90	65	58	56	53	48	30^			
		σ	9.0	9.5	11	15	18	22*				

Tissue type	T	f(GHz) :	0.1	0.2	0.5	1.0	2.0	3.0	4.0	10.0	Reference	Comments
Tumours canine (1)	37	ε'					50		48*	42	Schepps (1981)	*5 GHz, ^8 GHz (1) renal tubular aderosarcoma (2)splenic haematoma (3) intestinal leionyosarcoma (4) hemangio-pericyoma
		σ					21		49	110		
(2)	37	ε'					44			46^		
		σ					18			70		
(3)	37	ε'	85				58		50*	44		
		σ	11				25		55			
(4)	37	ε'	70, 65				53, 60		50*, 52*	46, 51		
		σ	11, 12				23, 28		48, 63	110, 140		

may be representative of the corresponding human tissue at microwave frequencies, but for brain tissue, lens nucleus, tumour tissues and particularly, fat, some discrepancies are apparent. An earlier paper (Surowiec et al, 1987) concluded that human tissue *does* differ from animal tissues at frequencies from 10kHz to 100MHz. This was attributed partly to higher water contents in human tissues compared to animal tissues, a disparity which would cause dissimilarity in dielectric properties at microwave frequencies also. (Water contents of various human tissues are given in Table 3.8.) Clearly more studies on human tissue are necessary.

3.4.2 *In vivo* vs *in vitro* tissue properties

It might be expected that *in vitro* properties of tissue are not representative of the living tissue, because after excision the tissue is in a physiologically abnormal state. Some groups have developed techniques for investigating radiowave and microwave dielectric properties of animal tissue *in situ* (Burdette et al, 1980; Athey et al, 1982; Zywietz et al, 1986). Their researches allow comparisons to be made between the electrical properties of tissue in the two states.

At low frequencies pronounced changes occur in tissue permittivity after excision. The α-dispersion disappears completely within a few hours of excision as noted in Section 3.3. By contrast, the β-dispersion disappears completely over a few days, due to massive disruption of the cellular membranes (Foster and Schwan, 1989). At these radio frequencies and at microwave frequencies, some controversy exists over whether the *in vitro* and *in vivo* properties of tissue differ appreciably, even for *in vitro* measurements made within a few hours of tissue excision. Burdette et al (1986a) claim that changes in the dielectric properties of brain tissue are seen immediately upon sacrifice of the experimental animal: Foster and Schwan (1989) state that any changes that occur within a few hours of animal death, or of tissue excision, are comparable to the normal variability observed within each tissue type in the same species, or between species. To illuminate this discussion, it is useful to examine the work of Kraszewski et al (1982). These authors made a comprehensive experimental comparison between

the *in vitro* and *in vivo* properties of cat brain, kidney, liver, muscle and spleen at frequencies between 0.1 and 8GHz: data from their paper is reported in Table 3.7. Above about 0.1GHz neither the permittivity nor the conductivity of any tissue *in vitro*, measured a few hours after the animal's death, was different from the *in vivo* properties within the authors' uncertainty estimations. Only at 0.1GHz was a trend observed towards a lower permittivity *in vitro*: this is likely to be associated with breakdown of cellular membranes and with electrolytic shifts between intra- and extra-cellular compartments (Foster and Schwan, 1989).

Other workers have studied dielectric properties of excised tissue as a function of time following death. Surowiec et al (1985), who studied bovine liver, kidney and spleen at frequencies between 20kHz and 0.1GHz, found that the permittivity substantially decreased and the conductivity substantially increased with time, depending on the tissue type and the length of storage (samples were stored at room temperature between measurements). Foster and Schwan (1989), on the other hand, found that refrigerated samples were stable in permittivity and conductivity at these frequencies over several hours.

In summary, it would appear that at frequencies below about 0.1GHz, marked changes *do* occur in the dielectric properties of tissue after excision, although the processes which cause this may be slowed by refrigerating the samples. Above 0.1GHz, there appears to be no observable difference in the dielectric properties of tissue *in vivo* and *in vitro*. This is not surprising: above 1GHz dielectric properties are mainly determined by the relaxation of bulk tissue water; between 0.1 and 1GHz dielectric properties are mainly determined by the relaxation of bound water. Because of this, no change, even within days, should be anticipated at microwave frequencies, provided that gross deterioration of the tissue sample is avoided.

3.4.3 Data fitting

Some caution must be observed when using data that has been calculated from an author's numerical fit, for example, to the Debye equations. It is usually inadvisable to

extrapolate data outside the frequency range of the data fit — often even the endpoints of a data fit are inaccurate representations of the experimental data. For instance, in Table 3.7, the data of Surowiec et al (1985) on bovine liver, kidney and spleen, are compared with values calculated from numerically fitted parameters. For all three types of tissue the fitted values underestimate permittivity at 100MHz by between 10 and 20%, while two of the calculated conductivities differ by 6 and 15% from the original data. These values (given in brackets in the table) were calculated from parameters fitted to data points in the frequency range 0.1 to 100MHz. Other fitted parameters were given in this paper for the frequency range 20kHz to 100MHz: these produced values at 100MHz even further removed from the original data. Since the frequency ranges used span the β-dispersions in these tissues, the fitted parameters are representative of this dispersion, but may not be considered representative of either end of the dispersion range. At the high end, about 100MHz, other processes, representative of the δ-and γ-dispersions, may affect dielectric properties.

3.4.4 Temperature coefficients

The temperature coefficients of tissue conductivity and permittivity must be discussed separately because of the influence of ionic conductivity. Below about 1GHz, tissue conductivity has the same temperature coefficient as the conductivity of simple electrolytes: this, from Table 3.4, may be calculated to be about +2%/°C. Above 1GHz, tissue conductivity shows increasingly large contributions from the dipolar loss of liquid water which has a temperature coefficient of about -2%/°C below 10GHz. Thus the temperature coefficient of tissue conductivity falls from +2%/°C at low frequencies to -2%/°C at high frequencies, with a crossover point near 2GHz. At 3GHz, the value may be calculated from Table 3.5 to be -0.3%/°C between 25 and 37°C (Foster and Schwan, 1989).

Tissue permittivity at microwave frequencies reflects that of water, which has a temperature coefficient of about -0.3%/°C (Table 3.5). At lower frequencies, tissue permittivity is expected to have a temperature coefficient of about 2%/°C, but is in fact

51

very much smaller, perhaps indicating the cancelling out of several effects (Foster and Schwan, 1989). More detailed discussion may be found in Foster and Schepps (1981) (3) who measured the permittivity and conductivity of barnacle muscle as a function of frequency and temperature. Some earlier temperature measurements on various tissues were analysed by Schwan (1957) who produced a table of temperature coefficients for different tissues at frequencies between 50 and 900MHz. These values have often been used since to convert data at lower temperatures to 37°C.

3.4.5 Tissue water contents

Water contents of various tissues are given in Table 3.8. At microwave frequencies high water content tissues, such as muscle, are characterised by large permittivities and conductivities, while low water content tissues, such as fat and bone, have low permittivities and conductivities. This largely reflects the volume of bulk water held in the tissue. Figures 3.7(a) and (b) show the permittivity and conductivity at 3GHz as a function of measured water content for high water content and animal tissues collected from the literature. Although the scatter is large, probably because many of the water contents were averages rather than exact water contents of the measured samples, there is clearly a trend towards high permittivity and conductivity with increasing water content. A rough fit was made to the permittivity data at 3GHz to aid comparisons with work presented later :

$$\varepsilon' = -11 + 0.77 \ w \qquad\qquad (3.8)$$

where w is the percentage water content by weight. To date, no water contents have been measured as part of a study of the dielectric properties of fat and bone. (Some of the data presented in Chapter 5 will rectify this omission.) Figures 3.8(a) and (b) compare high water content animal and human dielectric data at 3GHz. These figures graph conductivity versus permittivity for the collected values gathered in Tables 3.6 and 3.7, adjusted to 37°C using temperature coefficients given above (Section 3.4.5).

Tissue	Water content (% by weight)	Water content (% by volume)
Whole blood	78.5	83
Blood plasma	91	93
Blood corpuscles	68-72	73-77
Muscle	70-80	75-84
Skin	62-76	68-80
Fat	5-20	4-18
Liver	71-77	76-81
Lung	79-84	83-87
Slpeen	75-80	80-84
Kidney	78-84	82-87
Whole Brain	73-78	78-82
Brain (grey)	80-85	84-88
Brain (white)	68-73	73-78

Table 3.8   Water contents of various human organs and tissues

(1) % water contents compiled from Altman and Dittmer (1964), Best and Taylor (1950), Spells (1960), Mitchell et al (1945) and Pethig (1984). Compilation by Brown (1989).

(2) Water content by volume calculated assuming a density of 1.3 g/cm^3 for the non-water content of tissue, except for fat where a density of 0.86 g/cm^3 was used.

(a)
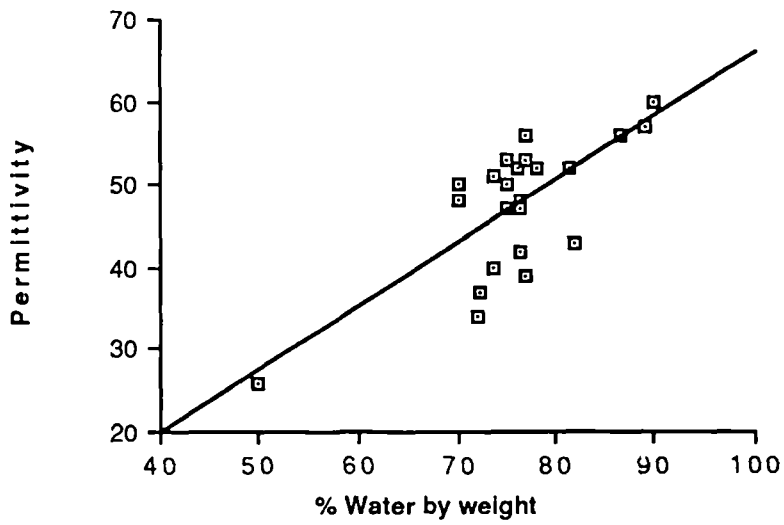
(b)
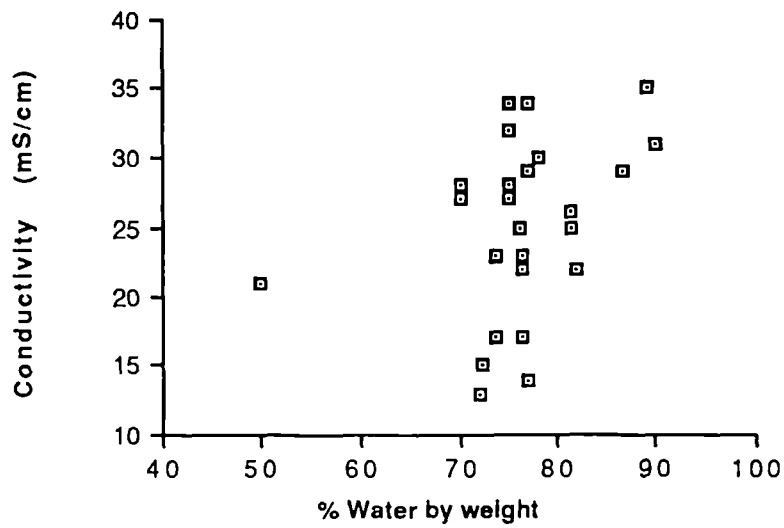
(b)

Figure 3.7   (a) Permittivity and (b) conductivity of animal tissues as a
function of water content at 3 GHz
The fit to the permittivity data is given by
$$\epsilon' = -10.6 + 0.768 \ w$$
where w is the % water content by weight.

(a)
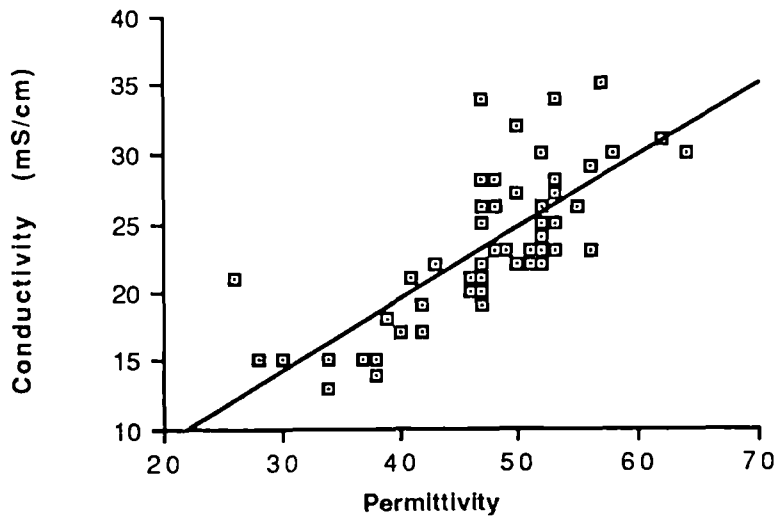
(b)
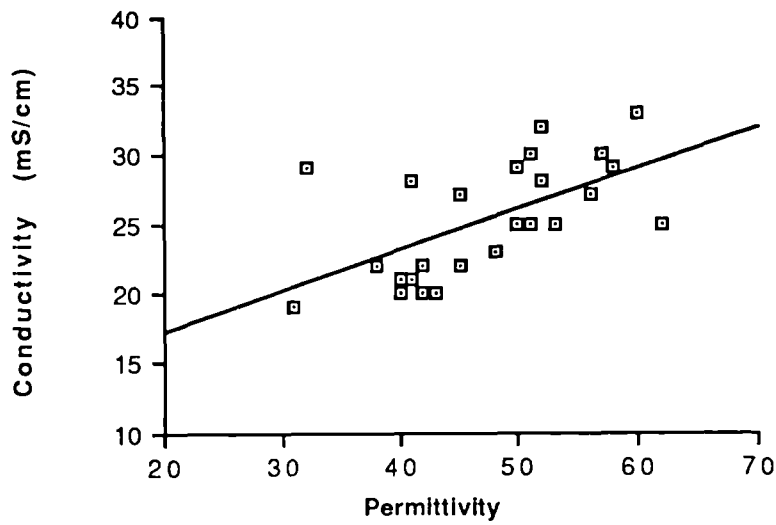
Figure 3.8   The variation of conductivity with permittivity at 3 GHz for
(a) animal and (b) human tissues
The fitted lines are

(a) $\sigma = -1.3 + 0.52\ \epsilon'$

and

(b) $\sigma = 11 + 0.29\ \epsilon'$

Empirical lines have been fitted to these data using a least squares routine; this provides a very rough guide to the expected relationship of conductivity and permittivity at 3GHz. For animal tissues,

$$\sigma \text{ (mS/cm)} = -1.3 + 0.52 \, \varepsilon' \qquad (3.9)$$

For human tissues,

$$\sigma \text{ (mS/cm)} = 11 + 0.29 \, \varepsilon' \qquad (3.10)$$

Combining both sets of data (Figure 3.9) give the empirical relation,

$$\sigma \text{ (mS/cm)} = 2.8 + 0.44 \, \varepsilon' \qquad (3.11)$$

For low water content tissues, no data on mammalian tissues are available at 3GHz. Fitting a line to the human fat and bone data (Figure 3.10) yields the empirical equation,

$$\sigma \text{ (mS/cm)} = 0.56 + 0.27 \, \varepsilon' \qquad (3.12)$$

It must be emphasised that (3.8) to (3.11) are extremely rough guides to the data. The correlation coefficient for (3.10) was as low as 0.36, although this was the worst case. The best correlation coefficient (0.68) was found to be between the conductivity and permittivity data of human fat and bone tissues at 3GHz [(3.12)].

Very few workers have examined the relationship of dielectric constant of a tissue to its total water content. Schepps and Foster (1980) fitted their data at 1 to 5GHz to a Debye dispersion in order to study the relationship of extrapolated static permittivity, ε_s, and static conductivity, σ_s, to water content by volume. Their data correlated well, but lay below the theoretical prediction calculated from the Fricke equation (2.34). These authors hoped that their empirical line would aid prediction of the dielectric properties of
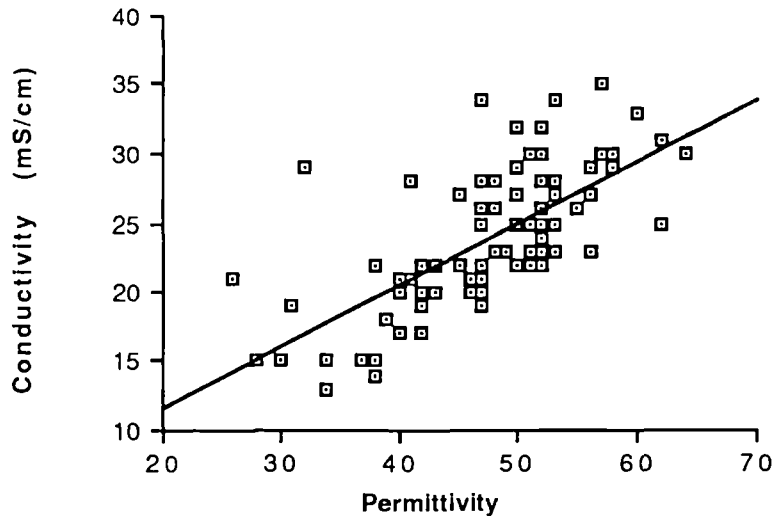
Figure 3.9   The variation of conductivity with permittivity at 3 GHz for
human and animal high water content data
The fitted line is

$$\sigma \text{ (mS/cm)} = 2.8 + 0.44 \, \varepsilon'$$
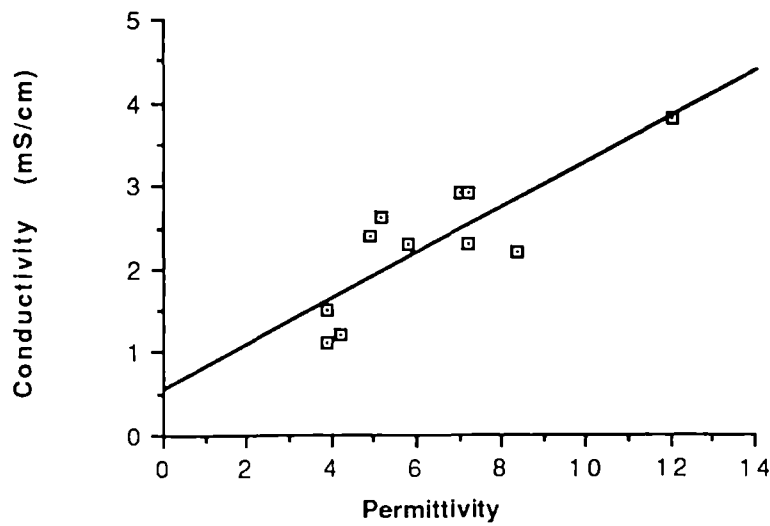
Figure 3.10   The variation of conductivity with permittivity at 3 GHz for
human fat and bone tissues
The fitted line is

$$\sigma \text{ (mS/cm)} = 0.56 + 0.27 \, \varepsilon'$$

a tissue, if its water content was known. By the principle of generalised conductivity (Section 2.5.1), mixture equations are valid at high frequency fields as well as static fields: therefore, the fitted data of Schepps and Foster may validly be extrapolated to 3GHz in order to devise empirical relationships between permittivity and water content and between conductivity and water content at this frequency. This extrapolated data is shown in Figure 3.11.

Fitting empirical equations to their high water content data yields:

$$\varepsilon' = -47 + 1.1 \, v \tag{3.13}$$

and

$$\sigma \, (mS/cm) = -76 + 1.3 \, v \tag{3.14}$$

where v is the percentage of water by volume held in the tissue. The correlation coefficients for these lines were 0.75 for (3.13) and 0.53 for (3.14).

3.5 Bound water

Water molecules which are adjacent to, and which interact strongly with, macromolecular surfaces have properties which are physically different from those molecules at a greater distance. For instance, they exhibit lower vapour pressure, lesser mobility and a reduced freezing point. Water in this state is usually referred to as bound, with any of the above properties providing a basis for definition. However, because different methods measure different physical properties they may find differing amounts of bound water. This difficulty is further compounded by the fact that the measured properties may change continuously with distance from the macromolecular surface, making determination of an amount of bound water somewhat arbitrary. Despite these problems, it is generally accepted that 'bound' water is distinguishable from 'bulk' water. Cooke and Kuntz (1974) identified three types of biological water: Type 1, 'bulk' water, forms the greatest part of biological water and is not appreciably

(a)

Relative permittivity

60
50
40
30
20
10
0

□ High water content
● Low water content

0   20   40   60   80   100
% Water by volume

(b)

Conductivity (mS/cm)

50
40
30
20
10
0

□ High water content
● Low water content

0   20   40   60   80   100
% Water by volume
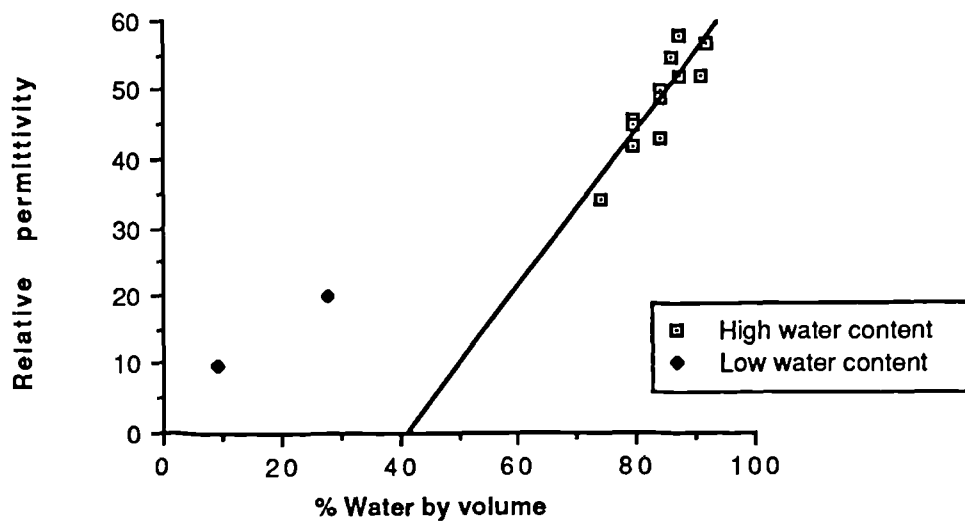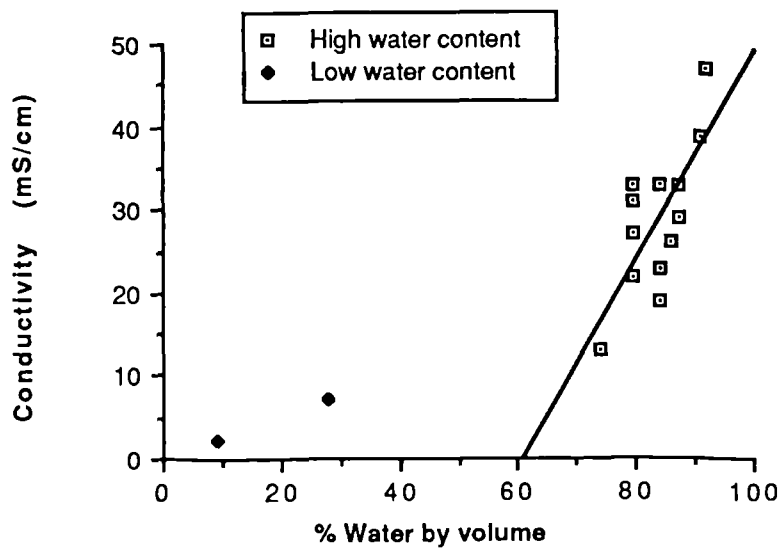
Figure 3.11   Data interpolated from Schepps and Foster (1980)
(a) Permittivity and (b) conductivity of canine tissues at 3 GHz
The fitted lines are

$$\varepsilon' = -47 + 1.1 \ w$$

and

$$\sigma \ (mS/cm) = -76 + 1.3 \ v$$

where v is the percentage water content by volume.

affected by binding to macromolecules; Type 2, 'bound' water, forms a smaller part of the system and has rotational motion, freezing point and vapour pressure significantly affected by interactions with macromolecular surfaces; Type 3, 'irrotationally bound' water, forms a very small part of the biological water system, perhaps only a monolayer or a bilayer around the macromolecule, and is 'site-bound' to the macromolecule (Fig 3.12).

Measurements on protein solutions first provided evidence of dielectrically bound water by the discovery of a dispersion between the β- and γ-dispersions (Oncley, 1943; Buchanan et al, 1952). These early discoveries prompted further studies by Grant (1965) and Grant et al (1968) on bovine serum albumin and egg albumin solutions, and by Schwan (1965) and Pennock and Schwan (1969) on haemoglobin. Results from these studies established that 'bound' water has properties somewhere between those of ice and of free water, suggesting a structure ordered somewhere between the rigidity of ice and the clustering of water molecules in free water. The dispersion of bound water showed a much flatter slope than that of water, indicating a broad distribution of relaxation times: this itself implied that a wide range of binding energies was involved (Figure 3.13). Estimates of the average relaxation frequency ranged from 300 to 850MHz, while binding energies between 7 and 16kcal/mole were calculated. [The binding energies of free water and of ice are about 4 and 13kcal/mol respectively (Pennock and Schwan, 1969).]

By its very nature, bound water cannot be studied directly, but must have its properties, and even its existence, inferred from dielectric or other measurements on solutions or tissues. Several factors make it difficult to determine absolute values to describe its physical properties: firstly, the total amount of bound water in a substance, including 'irrotationally bound' water, is likely to be only a small fraction of its total water content, so that the bound water must be observed against a large background of bulk water; also, mixture theory must be used to separate out the different types of water, so that quantities derived are dependent upon the particular equation used; uncertainties in the properties of the solid substance of the tissue or protein and of free
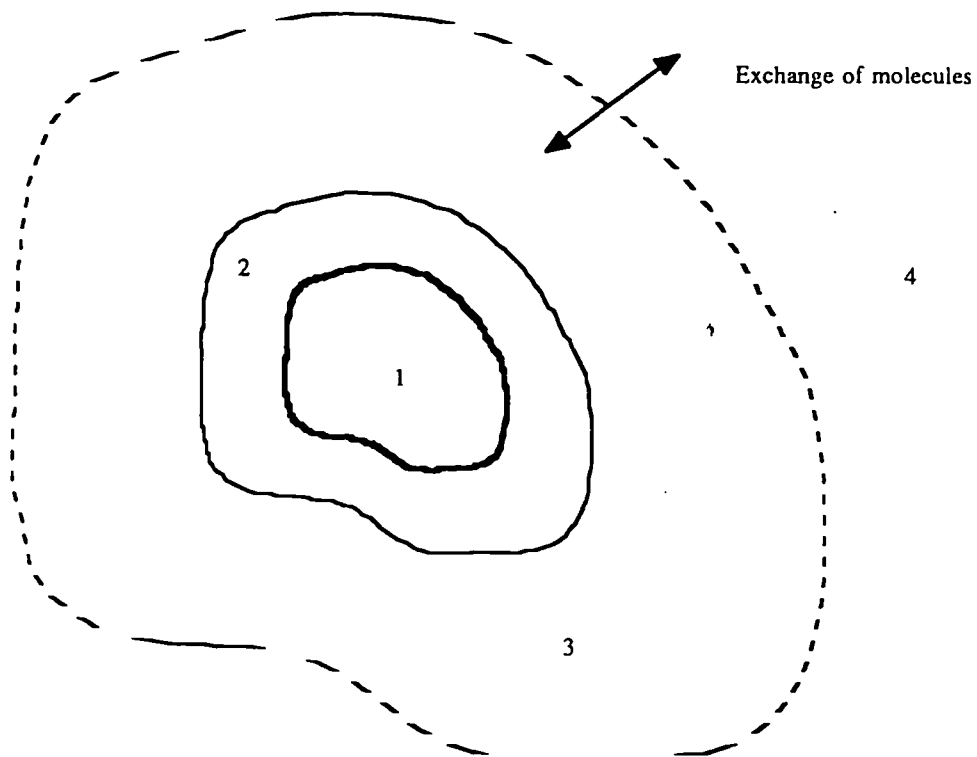
Figure 3.12   Schematic representation of the various states of binding around a protein molecule

1 Macromolecule

2 'Irrotationally bound' water which rotates with the protein

3 'Bound' water

4 Bulk water
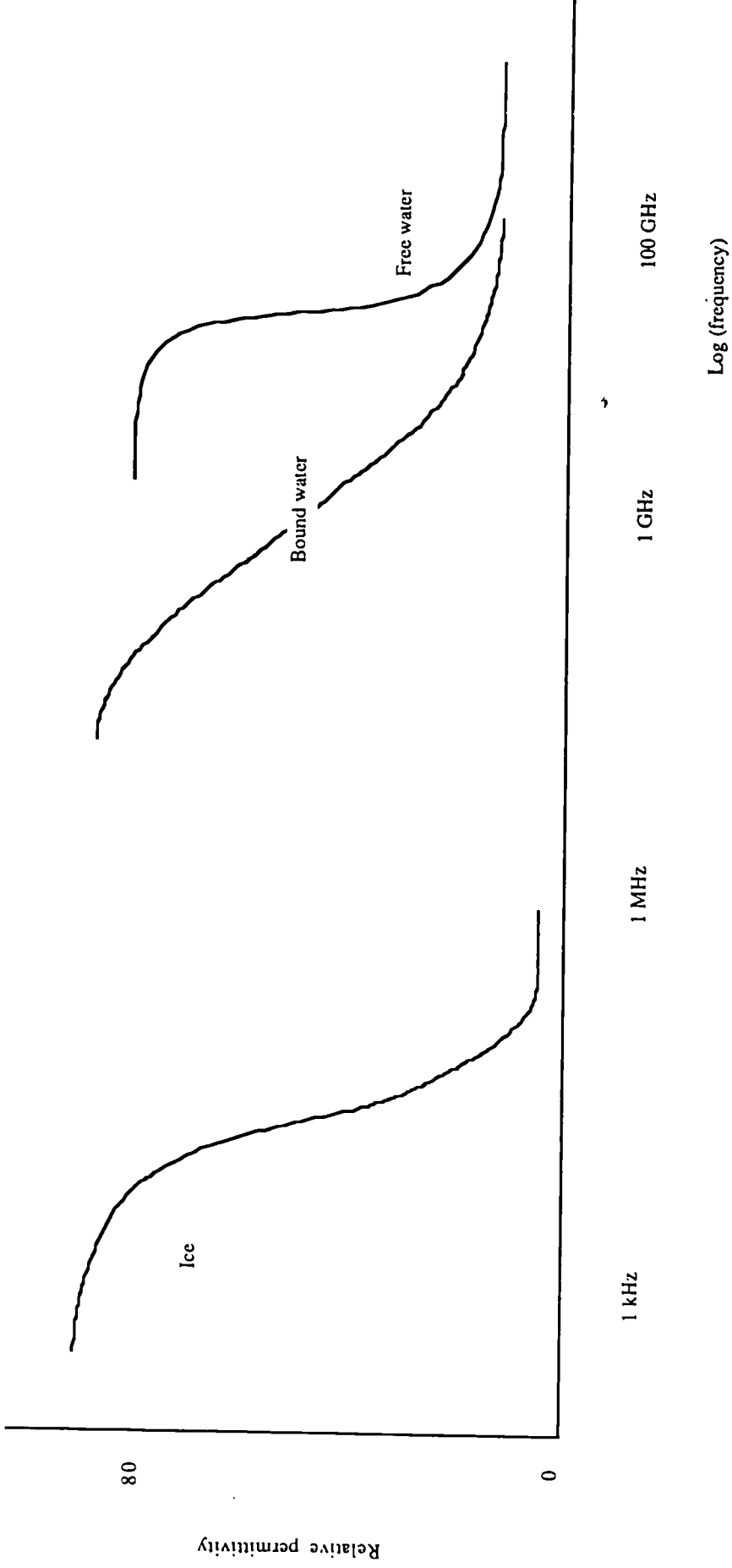
Figure 3.13   Schematic representation of the frequency variation of the permittivity of ice, bound water and free water

water introduce further errors; and finally, different dielectric methods probe different states of binding of water, so that it is not always obvious whether derived properties and volumes refer to a combination of 'irrotationally bound' and 'bound' water , or to one or the other.

Several dielectric methods have been used to measure the amounts and physical properties of bound water. Analysis of the microwave dispersions of various protein solutions and of tissues using the Debye and Cole-Cole equations [(2.14) and (2.17)] is the basis of most methods. The most common method of analysis was first set out by Schwan (1965) where a dispersion is analysed in terms of a sum of Debye relaxation processes:

$$\varepsilon^* = \varepsilon_\infty + \sum_N \frac{\Delta \varepsilon_i}{1 + j\omega\tau_i}$$

(3.15)

where N is the number of relaxation processes; $\Delta \varepsilon_i$ is the dielectric decrement and τ_i is the relaxation time of the ith relaxation process. When separating out bound and free water contributions, N = 2. Authors use (3.15) to fit their dielectric data, usually by assuming values of ε_s and ε_∞ for bound water which are close to those for ice and water (Section 3.2). This analysis, combined with use of the Maxwell-Fricke equation (2.34) allows an estimate to be made of the amount of 'bound' water in a substance. Since this technique depends upon the mobility of the bound water molecules — they are assumed to contribute to permittivity at microwave frequencies — it does not detect 'irrotationally bound' water. Authors who have analysed their data in this way include Grant et al (1978), Grant (1984), Clegg et al (1984) and Gabriel et al (1985).

A less quantitative method is to analyse a dispersion using the Cole-Cole equations (2.17): this sort of study produces Cole-Cole parameters far removed from those of free water. In particular, large values of the parameter α and lowered values of the relaxation frequency f_c are found, compared to pure water. From this it is inferred that more than one relaxation process is occurring in the substance under examination, with

the most likely explanation being the presence of an amount of bound water. This allows only a qualitative discussion of bound water. Authors who have studied tissues and protein solutions in this way include Schwan et al (1977), Gent et al (1970), Nightingale et al (1983) and Foster et al (1984).

Another method of quantifying amounts of bound water has been to fit data above 1GHz to a Debye dispersion with parameters fixed at the values for pure water, in conjunction with a mixture equation, so that an amount of free water may be calculated. This is then compared with a measured water content: the difference between the two is taken to be the 'bound' water fraction (Stuchly et al, 1982a). The reasoning behind this technique states that above 1GHz bound water cannot rotate and therefore cannot contribute to the permittivity — the permittivity should therefore follow that of pure water, if a suitable mixture equation is used to allow for the reduced volume. However, several authors (for instance Schepps, 1981; Clegg et al, 1984; Steel and Sheppard, 1985, 1986) have found evidence of bound water relaxation well above 1GHz, suggesting that this method is not sound. Even if a 'cutoff' frequency were known for bound water, above which it longer rotates, such a method would produce values for amounts of bound water which included 'irrotationally bound' water, making it unsuitable to compare with some other methods.

'Irrotationally bound' water is probed by measurements at audio and radiofrequencies of permittivity and conductivity as a function of hydration. An early example of this type of study was made by Marino et al (1967). They measured the permittivity of bone in several states of hydration at kHz frequencies. At low levels of hydration, permittivity was found to increase little with increasing hydration, until a 'critical hydration' was reached: above this value permittivity increased sharply with increasing hydration (Fig 3.14). This critical hydration, w_c, was identified with 'irrotationally bound' water: below w_c water molecules are essentially site-bound and cannot rotate in an electromagnetic field; above w_c water molecules are less tightly bound and are able to rotate. Some other authors have noted and used this effect (Buchanan et al, 1952; Grant et al, 1978; Clegg et al, 1984).
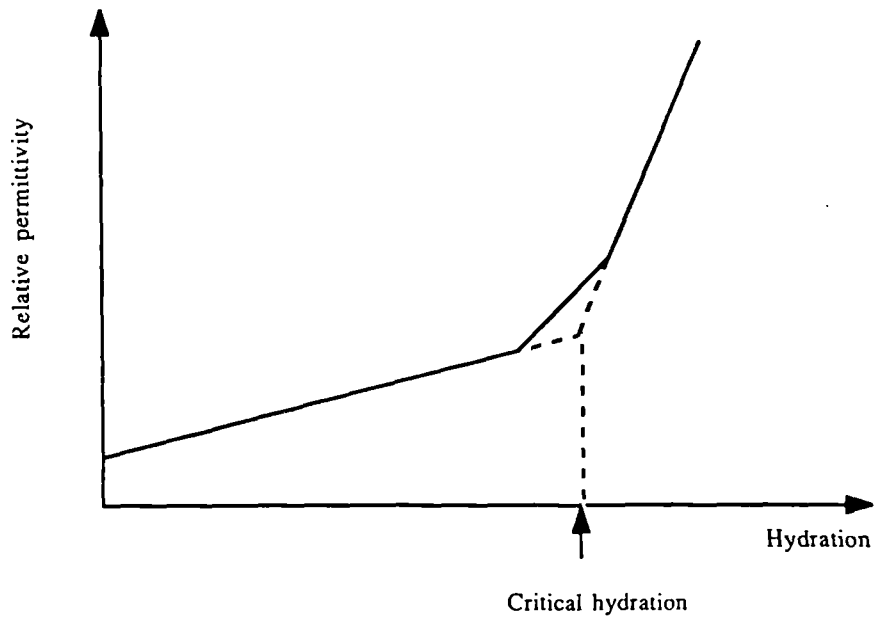
Figure 3.14   Variation of permittivity of biological materials at kHz frequencies
as a function of hydration. The critical hydration, w_c, is identified
with the amount of 'irrotationally bound' water.

Most analyses of bound water have been made on protein solutions, since these are less complex than tissues and should therefore allow fairly concrete conclusions to be drawn regarding the fraction of bound water (Buchanan et al, 1952; Grant et al, 1965, 1968, 1978; Schwan, 1965; Pennock and Schwan, 1969; Schepps, 1981; and many more). Values from these studies for the amount of bound water range from 0.30 to 0.45 g $H_2O/$ g dry protein, except for the study by Schepps (1981) which suggested values of between 0.5 and 0.6 g $H_2O/$ g dry protein. Corresponding values for tissues are more difficult to compare because they are expressed in many different types of units: these are not translateable without further information not usually provided by authors, regarding total water content, and in some cases, dry tissue density. However, some authors have expressed their data such that it may be compared. For instance, muscle contains bound water of about 0.4 g $H_2O/$ g dry weight (Schepps, 1981), brain contains about 0.4 to 0.6 g $H_2O/$ g dry weight (Schepps, 1981; Steel and Sheppard, 1985), liver contains about 0.58 g $H_2O/$ g dry weight, haematoma has 0.30 to 0.45 g $H_2O/$ g dry weight and tumours have 0.9 to 1.3 g $H_2O/$ g dry weight (Schepps, 1981).

The above values may be transformed roughly into percentages by weight of total water, assuming total water contents of the order of those in Table 3.8 for most tissues, and a value of 74% for the total water content of tumours (from measurements on breast tumours by the present author). Then 20% protein solutions may be considered to contain 6 to 9% bound water (Grant, 1965; Schwan, 1965) or 10 to 12% bound water (Schepps, 1981). Muscle, brain, liver and tumours contain 10%, 10 to 12%, 15% and 23 to 34% bound water respectively (Schepps, 1981; Steel and Sheppard, 1985).

Other authors have found that in muscle, 5 to 10% of the water is bound (Schwan and Foster, 1977; Foster et al, 1980). In ocular tissues 4 to 29% of the water is bound with nucleus containing more bound water than other lens tissues (Steel and Sheppard, 1985, 1986). Also, amounts of bound water in human ocular tissues are significantly higher than in other mammals (Dawkins et al, 1981). In normal blood, less than 2% of the water is bound, while in blood showing symptoms of disease and cancer up to 4%

of water is bound (Grant, 1984). In contrast to the values for high water content tissues, Smith et al (1985) found that bone marrow and adipose tissue contained very little bound water, but they did not attempt to quantify it.

These values above were calculated from measurements at microwave frequencies and so will be representative of amounts of Type 2, bound water: they will not contain any information about 'irrotationally bound' water.

It is interesting to note that two of the above studies found that water binding is enhanced in cancerous tissues, a fact which if confirmed, would be helpful in the calculation of energy deposition in tissues during microwave hyperthermia. Another area in which knowledge of bound water would be helpful is the study of microwave hazards. Dawkins et al (1979) pointed out that the range 0.3 to 3GHz must be treated differently for calculation of microwave bio-effects in order to account for enhanced energy absorption in this range. Steel and Sheppard (1986) noted that lens tissue is particularly susceptible to microwave radiation, which, at sufficiently high dosages, can cause cataracts. Knowledge of tissue bound water would therefore allow better safety standards to be set.

Very little modelling on tissues or other substances containing bound water has been attempted other than the simple model shown in Figure 3.12. An exception to this is a study by Spiridonov (1982) who produced a model, for the purpose of calibrating water-content meters, which allows permittivity to be calculated as a function of total water content and water binding energy. His model is an extension of that shown in Figure 3.12. It considers that each layer of water molecules surrounding a macromolecular surface becomes successively less bound, until above some extreme limit successive layers flow freely. Discrete decrements in the binding energy for each layer are estimated and a relaxation time for each layer is calculated. Integrating over all layers allows permittivity and loss factor of the whole substance to be calculated. Spiridonov found that many characteristics of wet materials could be explained qualitatively using his model, although no allowance was made for a 'critical hydration'. No further work has been done on his model: it would be interesting to

discover if it allowed better quantitative understanding of bound water characteristics in real substances, a problem which would require a corresponding experimental study.

Other interpretations of the δ-dispersion have been made. For instance, Masszi et al (1976) suggested that *all* water held in frog muscle displayed properties different to those of pure water. Their data was taken at frequencies between 2 and 4GHz, a very limited part of the microwave spectrum. Consequently, their conclusions must be treated with care because they are based on a very limited amount of information. This has also been noted by some other authors (Foster and Schwan, 1989; Grant, 1984).

A similar interpretation was made by Clegg et al (1984) with very much more justification. These authors made measurements of Artemia cysts at microwave frequencies. Artemia is a crustacean which forms cysts made up of a packed cell system with no extracellular space and surrounded by a non-cellular shell. These cysts are easily dehydrated and rehydrated so that dielectric constant may be studied as a function of hydration. Measurements were made for hydrations between 0.05 and 1.40 g H_2O / g dry weight (the maximum which could be supported by the cyst) and at frequencies between 0.8 and 70GHz. Results from the study suggested that little or no water in the Artemia cyst is free, even at high levels of hydration: the permittivity was found to level out to a minimum level at about 35GHz, a point at which pure water has completed only two thirds of its dispersion. No evidence was found of a 'critical hydration', which was explained by a particular property of the cyst whereby glycerol replaces water molecules on surfaces of cyst components at low hydrations. This type of property may be common to some other types of material, such as lipids, which do not chemically bond with water. The relaxation frequency of the cyst dispersion was found to be between 2 and 7GHz, but errors involved in its calculation meant that it was not possible to observe if the relaxation frequency changed with increasing hydration. The authors suggested that that their results may provide information on water-binding in other biological systems, although they acknowledged that cysts may magnify interactions between water and cell structures. This sort of study would certainly be more useful in the study of bound water than those studies which span only a limited

range of frequencies. One other experiment which spanned most of the γ-dispersion was made by Gabriel and Grant (1985) on ocular tissues in supercooled and frozen states: these authors found that the conventional picture of bound water, given by Cooke and Kuntz (1974) (described on p54 — 55), was adequate to explain their results. More studies over a wide frequency range would be useful in this controversial area.

In summary, it is certain that in many, if not all, biological materials, water exists in different states of mobility. A small amount is 'irrotationally bound', probably due to chemical bonding with macromolecular surfaces. A larger volume is 'bound' in the sense that its kinetic properties are reduced compared to those of free water. Estimates of amounts of 'bound water' and its relaxation frequency vary considerably, but it is established that it affects dielectric measurements at frequencies as low as 0.1GHz and as high as 5GHz, with some possibility that even higher frequencies may be affected. The greatest amount of water in a biological system is likely to be free or 'bulk' water, although in some systems this may not be the case. Clearly, great difficulties exist in detecting and quantifying bound water since the most reliable methods involve measurements over a very wide frequency range, something that is difficult to achieve with accuracy.

3.6 Summary

This chapter has described and summarised the measured dielectric properties of tissues at frequencies between 0.1 and 10GHz.

The properties of free water, which largely define the microwave dielectric properties of tissues, were discussed first, and values of ε' and σ for water and physiological saline were calculated at 3GHz for temperatures between 20 and 40°C (Tables 3.2 and 3.5).

Next, a brief description was given of the observed dielectric dispersions in tissues over the whole frequency range from audio to infrared frequencies. Using an extensive data summary (Tables 3.6 and 3.7), the work of the major groups was discussed

generally, followed by a detailed comparison of human and animal measurements. This comparison concluded that much work remains to be done on human tissues before proper comparisons can be made, but that enough discrepancies exist to make it advisable to exercise caution when using animal data as a replacement for human data.

The relative merits of *in vivo* and *in vitro* measurements were analysed; temperature coefficients were calculated; and some rough empirical equations were calculated from literature data to relate dielectric properties with water contents at 3GHz [(3.8) to (3.14)].

Finally, a discussion was given of the controversy surrounding theory, measurement, and analysis of bound water in biological systems. Some approximate amounts of bound water for different tissue types were stated.

Chapter 4

A New Resonant Cavity Perturbation Technique

4.1 Introduction

In this chapter a new experimental technique for measuring dielectric properties of small biological samples is described; theory and instrumentation are discussed, and systematic experimental errors are assessed. In Section 4.2 an introductory description of the method is given. In Section 4.3 resonant perturbation is discussed and a theoretical formula is derived for obtaining the dielectric properties of a sample using this technique. In Section 4.4 the instrumentation and the experimental procedure are described; equipment calibrations are discussed and comparisons are made between expected theoretical parameters and their measured experimental values. Section 4.5 describes the preparation of biological samples for dielectric measurement, while in Section 4.6 the procedure for measuring sample water contents is given.

4.2 Dielectric measurement technique

One of the main problems facing those who make *in vitro* dielectric measurements on human tissue is that samples available from surgery are often very small. Thus it was necessary to design a technique which allowed the use of small volumes of tissue. Another major problem is that most biological tissues are very lossy because of high water content (as discussed in Chapter 3). This presents difficulties in the measurement of sample conductivity: often the higher the conductivity of a lossy sample, the less accurate the measurement of both permittivity and conductivity.

These problems were resolved in the Microwave Physics group in the Department of Physics and Astronomy, Glasgow University, as a modification of an earlier method (Land, 1987c). A new cavity resonator technique was designed, which allows measurement at one frequency of both high and low loss biological samples of small

volume. A cylindrical resonant copper cavity operating in the Transverse Magnetic 010 (TM_{010} or E_{010}) mode at about 3GHz was chosen. This has a purely longitudinal electric field and a purely transverse magnetic field (Figure 4.1).

The cavity was 'loaded' (filled) with polytetrafluoroethylene (PTFE) and three cylindrical apertures were drilled along and parallel to the axis to form sample holders (Figure 4.2). Dielectric properties of a sample are measured by observing the change in the resonant frequency and quality factor of the cavity produced by perturbation of the cavity fields when the sample is inserted into one of the apertures. Referring to Figures 4.1 and 4.2, it is clear that samples inserted into the central aperture are at the electric field maximum, and so will strongly perturb the field. The electric field falls to zero at the cavity walls following a zero order Bessel function in the interior. (This is described mathematically in Section 4.3.2.) Therefore, by placing apertures at different radial positions, different strengths of field perturbation may be obtained. As long as the aperture is not placed too close to the cavity walls, which might cause sample images to be induced, the dielectric properties of even *very lossy* samples may accurately be measured with this technique, by suitable placement of the aperture. The three aperture positions shown in Figure 4.2, and which were used in the experiments described in this thesis, correspond to relative degrees of perturbation of about 1, 0.25 and 0.01.

In order to allow for the small sample volumes available, the cavity was designed with a length of only about 7.5mm, while the apertures were about 1.5 mm in diameter. This meant, in theory, that sample volumes of only about 10mm^3 were necessary for measurement. In practice, slightly larger volumes were necessary in order to be certain that the sample spanned the whole length of the cavity.

4.3 Resonant cavity perturbation

Cavity resonators have long been used for measurements of dielectric properties of materials at microwave frequencies (e.g. Dunsmuir and Powles, 1946; Horner et al,

(a)

(b)

E

r = 0   r

(c)

——————— Field lines of **E**

— — — — — — Field lines of **B**
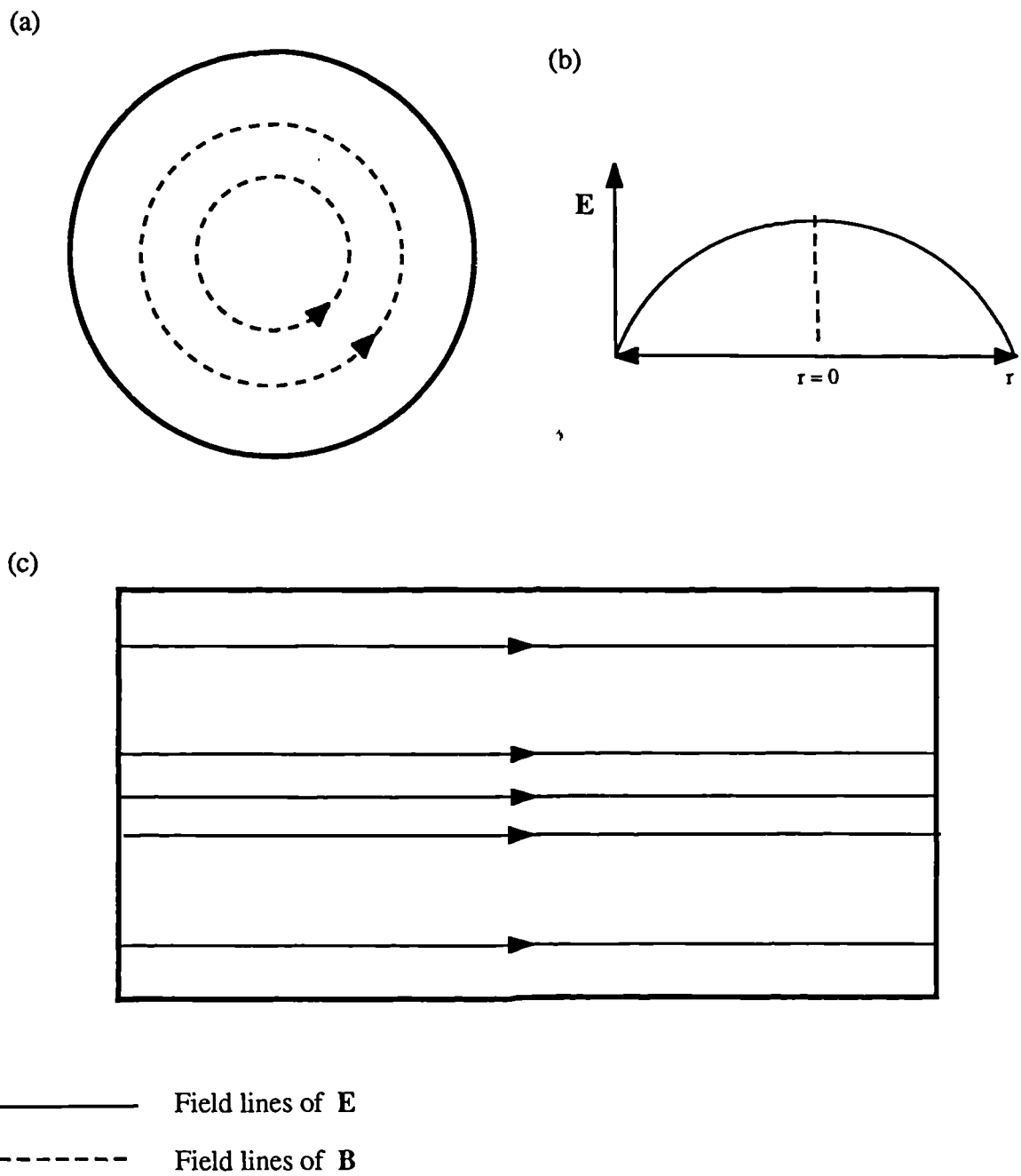
Figure 4.1   Field patterns in a TM_{010}-mode cylindrical cavity

(a) Transverse magnetic field

(b) Transverse electric field

(c) Longitudinal electric field
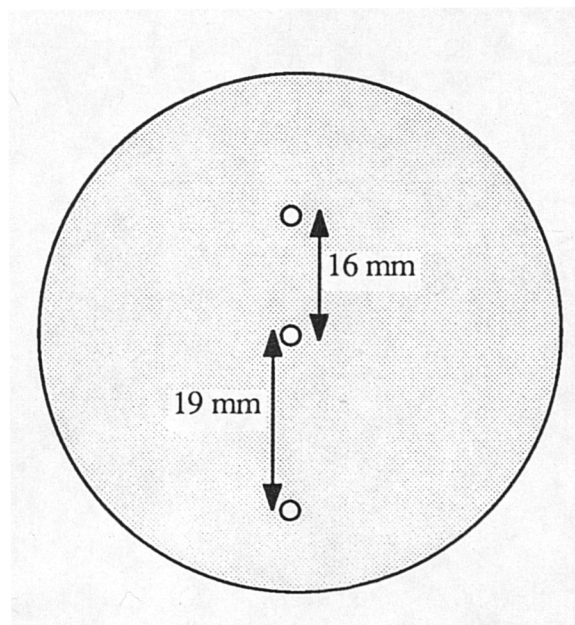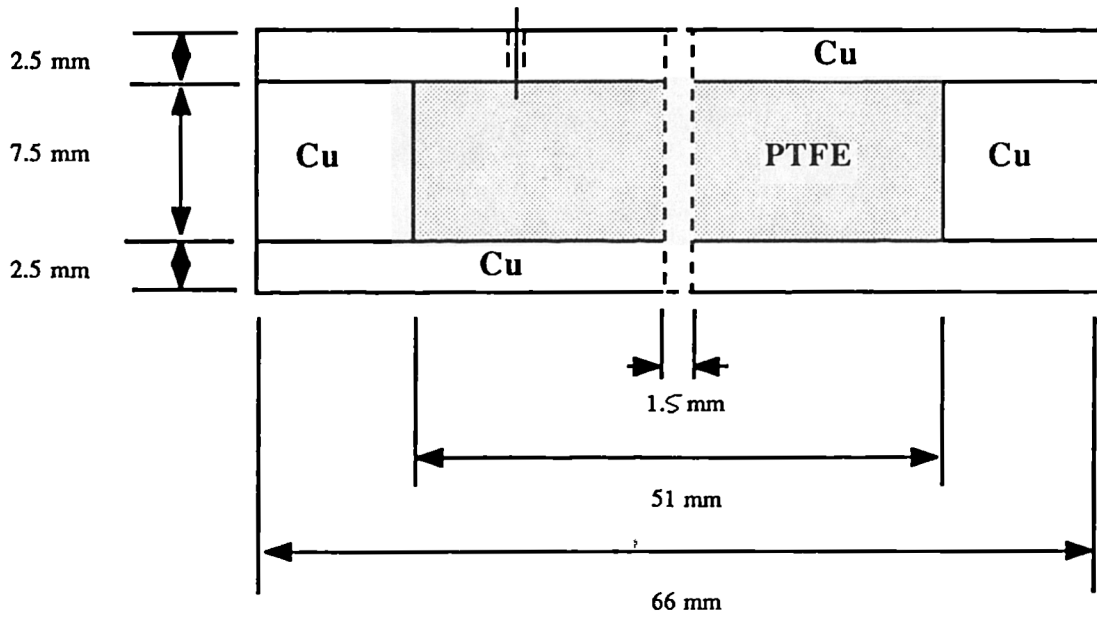
Figure 4.2   TM$_{010}$ -mode cavity used in measurements. The diagram shows

approximately the relative sizes of each component and the

relative positioning of the apertures

Cavity coupling is by a copper wire probe through an endplate

1945; Sinha and Brown, 1960; Li et al, 1981; Martinelli et al, 1985). When a piece of conducting, ferrite or dielectric material is introduced into a resonant cavity, the frequency of resonance and the shape of the resonance curve is altered. If the effect is sufficiently small it may be described by perturbation theory. Early treatments of this problem were given by Muller (1939), Bethe and Schwinger (1943), Slater (1950) and Casimir (1951).

A cavity resonator may be considered to be a waveguide with two short-circuiting planes perpendicular to the principal axis. The tangential component of the electric field, E, should be continuous across a boundary; and the gradient of the magnetic induction, B, should be zero. This, combined with the fact that $E = 0$ inside a conductor, means that the tangential component of E and the normal component of B are zero at the surface of the cavity. This is only possible if the planes are separated by an integral number of half-wavelengths, which is the case only at certain frequencies. Therefore, it is possible to excite waves inside the enclosure, but only at a certain number of discrete frequencies. In these conditions, the normal modes, the cavity resonates.

4.3.1 Derivation of the perturbation formula for a resonant cavity

Several publications give excellent, detailed derivations of perturbation formulas for cavities of different types operating in different modes (eg Harrington, 1961; Waldron 1969). In this section a general formula for the change in resonant frequency of a perturbed cavity will be derived, following Waldron (1969), so that the approximations inherent in the theory may be appreciated. This formula will be applied in Section 4.3.3 to the case of a cylindrical dielectric sample perturbing a TM_{010}-mode cavity.

Consider a cavity oscillating in one of its normal modes with electric and magnetic fields given by

$$E = E_0 e^{j \omega t}$$
$$H = H_0 e^{j \omega t}$$

(4.1)

where E_0 and H_0 are functions of position in the cavity, but not of time, t. When the cavity is perturbed slightly, by distorting the walls or by introducing material into the cavity, let the fields become

$$E' = (E_0 + E_1) e^{j (\omega + \delta\omega) t}$$
$$H' = (H_0 + H_1) e^{j (\omega + \delta\omega) t}$$

(4.2)

where $\delta\omega$ is the change in the resonant angular frequency of the cavity. The resonant frequency of the cavity has to change in order to re-establish equality of electric and magnetic stored energies (the resonance condition). Fields in the perturbed state are represented as the sum of the unperturbed fields E_0 and H_0 and additional fields E_1 and H_1.

For (4.2) to be valid it is important that the perturbation is small; otherwise higher order effects must be taken into account. This may mean a very small change in properties over a large section of the cavity volume, or a large change in properties over a very small section of the cavity volume. The additional fields, E_1 and H_1, will be small compared to the unperturbed fields, E_0 and H_0, over most of the cavity volume, but may be large, in the latter case, in the vicinity of the sample.

The fields E_0 and H_0 in (4.2) have the same configuration as E_0 and H_0 in (4.1) but may not have the same magnitudes, since these depend on the level of excitation: this may change when a sample is introduced, because of mismatch at cavity inputs and outputs. However, since the perturbation consists of a change of field configuration, it is the ratios of E_1 and H_1 to E_0 and H_0, over the volume of the cavity that matter.

To derive a perturbation formula, Maxwell's curl equations:

$$\nabla \times E = - \frac{\partial B}{\partial t}$$

(4.3)

and

$$\nabla \times H = \frac{\partial D}{\partial t} \qquad (4.4)$$

are substituted into (4.1) and (4.2), yielding

$$\nabla \times E_1 = -j [\omega B_1 + \delta\omega (B_0 + B_1)] \qquad (4.5)$$

and

$$\nabla \times H_1 = -j [\omega D_1 + \delta\omega (D_0 + D_1)] \qquad (4.6)$$

The scalar products of H_0 with (4.5) and of E_0 with (4.6) are formed. Then, using (4.3) and (4.4), taking $\partial / \partial t = j \omega$, and integrating over the whole cavity volume, V_0, the following equation may be derived:

$$j\omega \iiint_{V_0} [(E_1 \cdot D_0 - H_1 \cdot B_0) - (E_0 \cdot D_1 - H_0 \cdot B_1)] \, dV$$

$$- \iiint_{V_0} \nabla \cdot [(H_0 \times E_1) + (E_0 \times H_1)] \, dV$$

$$= j\delta\omega \iiint_{V_0} [(E_0 \cdot D_0 - H_0 \cdot B_0) + (E_0 \cdot D_1 - H_0 \cdot B_1)] \, dV \qquad (4.7)$$

Now, by Green's theorem,

$$\iiint_{V_0} \nabla \cdot [(H_0 \times E_1) + (E_0 \times H_1)] \, dV = \iint_{S_0} [(H_0 \times E_1) + (E_0 \times H_1)] \cdot n \, dS$$

where S_0 is the surface of the cavity and n is a unit vector normal to the cavity. If the cavity is perfectly conducting, E is normal to the surface, so that $E \times H$ and $H \times E$ are tangential to the surface; therefore this term vanishes. Equation (4.7) then becomes,

67

$$\frac{\delta\omega}{\omega} = \frac{\displaystyle\iiint_{V_0} \left[(\mathbf{E}_1 \bullet \mathbf{D}_0 - \mathbf{E}_0 \bullet \mathbf{D}_1) - (\mathbf{H}_1 \bullet \mathbf{B}_0 - \mathbf{H}_0 \bullet \mathbf{B}_1) \right] dV}{\displaystyle\iiint_{V_0} \left[\mathbf{E}_0 \bullet (\mathbf{D}_0 + \mathbf{D}_1) - \mathbf{H}_0 \bullet (\mathbf{B}_0 + \mathbf{B}_1) \right] dV} \qquad (4.8)$$

Equation (4.8) is exact as long as the cavity walls are perfectly conducting. If it is now assumed that $\delta\omega \ll \omega$, then $\mathbf{D}_1$ and $\mathbf{B}_1$ in the denominator may be neglected. This is justified because over most of the volume, $\mathbf{D}_1 \ll \mathbf{D}_0$ and $\mathbf{B}_1 \ll \mathbf{B}_0$; and in the neighbourhood of the sample, the contributions to the integral by $\mathbf{D}_1$ and $\mathbf{B}_1$ are small as long as V_1 and $\delta\omega$ are small. Thus (4.8) becomes

$$\frac{\delta\omega}{\omega} = \frac{\displaystyle\iiint_{V_0} \left[(\mathbf{E}_1 \bullet \mathbf{D}_0 - \mathbf{E}_0 \bullet \mathbf{D}_1) - (\mathbf{H}_1 \bullet \mathbf{B}_0 - \mathbf{H}_0 \bullet \mathbf{B}_1) \right] dV}{\displaystyle\iiint_{V_0} (\mathbf{E}_0 \bullet \mathbf{D}_0 - \mathbf{H}_0 \bullet \mathbf{B}_0) \, dV} \qquad (4.9)$$

Equation (4.9) is a general formula for the shift in frequency of a resonant cavity by a small perturbation.

If the perturbation is very small the numerator of the right hand side of (4.9) will be small compared to the denominator, so that $\delta\omega/\omega$ will also be small. In practice, the smaller $\delta\omega/\omega$, the more difficult it is to measure accurately. Thus a compromise must be made: $\delta\omega/\omega$ must be large enough so that serious errors in measurement are avoided, but small enough to avoid theoretical error due to approximations made in the analysis.

When the perturbation is due to a small change in the shape of a cavity, or the introduction of a small sample, major changes in fields occur only over the small volume, V_1, of the perturber. At distances far from the sample, the perturbations $\mathbf{E}_1$ and $\mathbf{H}_1$ are negligible; even close to the perturber, the contribution to the integral in the numerator of (4.9) is very much smaller than the contribution from the sample interior. Therefore, V_0 may be replaced by V_1 in the numerator of (4.9), so that it becomes:

$$\frac{\delta \omega}{\omega} = \frac{\iint\limits_{V_1} \int [(E_1 \cdot D_0 - E_0 \cdot D_1) - (H_1 \cdot B_0 - H_0 \cdot B_1)] \, dV}{\iint\limits_{V_0} \int (E_0 \cdot D_0 - H_0 \cdot B_0) \, dV} \qquad (4.10)$$

The denominator of (4.10) is equivalent to twice the stored energy in the cavity. In order to calculate $\delta\omega/\omega$, the numerator must be expressed in terms of E_0, D_0, H_0 and B_0, which are known for certain cavity shapes; this eliminates the need to measure the perturbed fields E_1, D_1, H_1 and B_1.

4.3.2 Fields in a TM_{010}-mode cavity

Cavity fields are derived from Maxwell's equations, using suitable boundary conditions (Waldron, 1969). Firstly the wave equations for a linear, isotropic medium are set up in cylindrical coordinates; these are solved, allowing for $_{\wedge}$electric and $_{\wedge}$magnetic (tangential) (normal) fields to be zero on the cavity surfaces. Two sets of field components are derived: Transverse Magnetic (TM-) or E-modes, where the axial component of the magnetic field, $H_z = 0$; and Transverse Electric (TE) or H-modes, where the axial component of the electric field, $E_z = 0$. The components of the fields for TM_{pqs}-modes may be written:

$$E_r = -\frac{s\,\pi}{k\,c} \, A \, J_p'(k\,r) \cos p\theta \sin \frac{s\,\pi\,z}{c}$$

$$E_\theta = \frac{p\,s\,\pi}{k^2\,r\,c} \, A \, J_p(k\,r) \sin p\theta \sin \frac{s\,\pi\,z}{c}$$

$$E_z = A \, J_p(k\,r) \cos p\theta \cos\frac{s\,\pi\,z}{c}$$

$$H_r = -\frac{j\,\omega\,\varepsilon_0\,p}{k^2\,r} \, A \, J_p(k\,r) \sin p\theta \cos \frac{s\,\pi\,z}{c} \qquad (4.11)$$

$$H_\theta = -\frac{j\,\omega\,\varepsilon_0}{k} \, A \, J_p'(k\,r) \cos p\theta \cos \frac{s\,\pi\,z}{c}$$

$$H_z = 0$$

where r, θ and z denote radial, azimuthal and axial directions; p and s are integers dependent on the mode; $J_p(x)$ is a Bessel function while $J_p'(x)$ denotes its first derivative; c is the cavity length; A is a constant; and

$$k^2 = \omega^2 \, \varepsilon_0 \, \mu_0 - \frac{s^2 \, \pi^2}{c^2} = \frac{\chi^2}{a^2}$$

The parameter a is the cavity radius and χ is a zero of $J_p(x)$. The subscript q denotes which zero of $J_p(x)$, for TM-modes, is to be taken for χ.

For TM_{010}-modes, (4.11) are written

$$E_r = E_\theta = 0 \; ; \quad E_z = A \, J_0(k \, r)$$

$$H_r = H_z = 0 \; ; \quad H_\theta = j \, \frac{\omega \, \varepsilon_0}{k} \, A \, J_1(k \, r) \tag{4.12}$$

using a simple relation between Bessel functions. These fields are shown in Fig 4.1. The characteristic equation may then be written,

$$k^2 = \omega^2 \, \varepsilon_0 \, \mu_0 = \frac{\chi^2}{a^2} \tag{4.13}$$

where $\chi = k \, a$ is the first zero of $J_0(x)$:

$$\chi = k \, a = 2.40483$$

It is noticeable from (4.12) that the fields in a cylindrical cavity operating in the TM_{010}-mode, or in fact any mode where s = 0, are independent of cavity length.

4.3.3 The TM_{010}-mode cavity with a cylindrical dielectric perturber

In order to calculate the change, $\delta\omega/\omega$, in (4.10), the fields E_1 and H_1 must be known at each point throughout the volume V_1, so that the integral in the numerator may be calculated. This integral may be performed analytically for certain special cases assuming the fields to be quasi-static. For instance, Stratton (1941) gives general

70

formulas for the fields due to conducting and dielectric spheres and ellipsoids; Maier and Slater (1952) give perturbation formulas for metallic needle, sphere and disk perturbers; and Waldron (1969) calculates perturbations due to dielectric and ferrite cylindrical perturbers.

For the case of a thin solid cylindrical dielectric sample inserted centrally along the cavity axis and flush with the end plates, the field E_1 is easily calculated. Figure 4.3a shows the field configuration in this case: the sample sits at a maximum of the electric field, with field lines running parallel to its edges. By continuity of E, therefore, the field in the perturber is the same as the field just external to it; ie, $E_0 + E_1 = E_0$, so that $E_1 = 0$, if it is assumed that the sample is very long. The displacement, D_1, is obtained by noting that

$$D_0 + D_1 = \varepsilon_0 \, \varepsilon_s \, (E_0 + E_1) = \varepsilon_0 \, \varepsilon_s \, E_0$$

where ε_s is the dielectric constant of the sample. Since $D_0 = \varepsilon_0 \, E_0$ is the electric displacement in the aperture when it is empty, it is easily seen that

$$D_1 = \varepsilon_0 \, E_0 \, (\varepsilon_s - 1)$$

The sample is non-magnetic so that $B_1 = H_1 = 0$. These facts, along with (4.12) which describe the fields in the cavity, allow the numerator of (4.10) to be evaluated:

$$\iiint_{V_1} (E_1 \cdot D_0 - E_0 \cdot D_1) \, dV = A \, \varepsilon_0 \, V_1 \, (\varepsilon_s - 1) \qquad (4.14)$$

The denominator may be evaluated by noting that,

$$E_0 \cdot D_0 - H_0 \cdot B_0 = \varepsilon_{PTFE} \, (\varepsilon_0 E_0^2 - \mu_0 H_0^2)$$

where H_0 and E_0 are the maximum field strengths at radius r, and ε_{PTFE} is the dielectric constant of the PTFE loading the cavity. The denominator may then be written
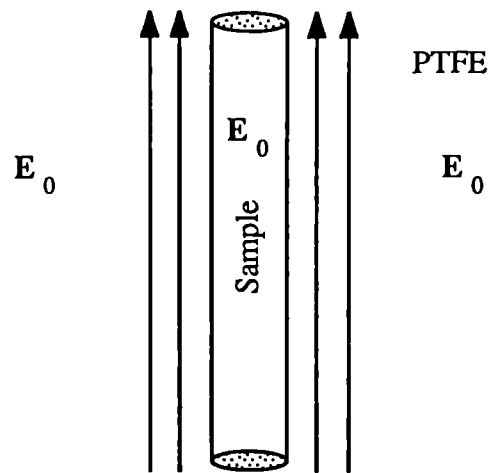
(a)   Field in sample inserted into central aperture
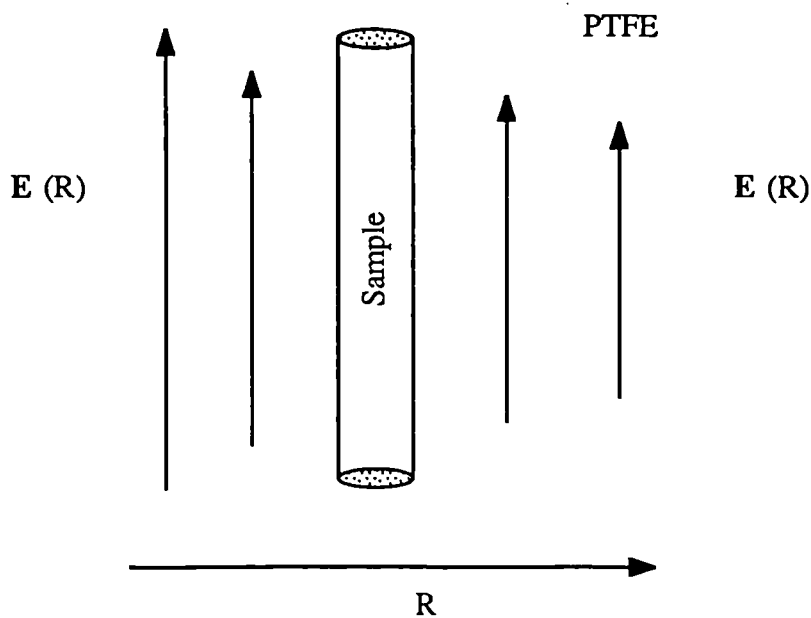
(b)   Field in sample inserted into one of the offset apertures

Figure 4.3   Fields in cavity apertures

$$\int\int\int_{V_0} (E_0 \cdot D_0 - H_0 \cdot B_0) \, dV = \varepsilon_{PTFE} \, \varepsilon_0 \int\int\int_{V_0} [\, J_0^2(kr) + J_1^2(kr) \,] \, r \, dr \, d\theta \, dz$$

$$= 2 \, \varepsilon_{PTFE} \, \varepsilon_0 \, V_0 \, J_1^2(ka) \qquad\qquad (4.15)$$

using some simple rules for Bessel functions. The right hand side of (4.15) is just twice the stored energy in the cavity.

Therefore, for this case, (4.10) may be written

$$\frac{\delta\omega}{\omega} = - \frac{V_1 \, (\varepsilon_s - 1)}{2 \, V_0 \, \varepsilon_{PTFE} \, J_1^2(ka)} \qquad\qquad (4.16)$$

When the sample is lossy, the permittivity is complex. It is convenient to define a complex frequency, Ω, using a lossy resonant circuit analogy (Waldron, 1969). The resonance condition may be written:

$$\Omega = \omega + j \frac{\omega}{2 Q_0}$$

so that,

$$\frac{\delta\Omega}{\omega} = \frac{\delta\omega}{\omega} + j \frac{1}{2} \delta\left(\frac{1}{Q_0}\right) \qquad\qquad (4.17)$$

where Q_0 is the quality factor that the cavity would have if completely uncoupled from any circuit; it is the ratio of the resonant frequency to the bandwidth, at half power, of the resonance curve; $\delta \, (1/Q_0)$ denotes the change in the inverse quality factor.

Separating out real and imaginary parts of the dielectric constant, ε_s, and converting from loss factor to equivalent conductivity, the dielectric properties of the sample are found from the following equations:

$$\varepsilon' = 1 + 2 \frac{V_0}{V_1} \varepsilon_{PTFE} J_1^{\ 2} (ka) \frac{\delta\omega}{\omega}$$

$$(4.18)$$

$$\sigma = \omega \varepsilon_0 \frac{V_0}{V_1} \varepsilon_{PTFE} J_1^{\ 2} (ka) \delta\left(\frac{1}{Q_0}\right)$$

These are exact first order theoretical formulas for a perfectly cylindrical sample axially located in a perfect, infinitely conducting cylindrical cavity. In practice, the apertures will not be drilled perfectly, the cavity may be slightly misshapen, and there will be fringing fields at the aperture edges, so that it is necessary to calibrate the cavity experimentally. Then (4.17) are written,

$$\varepsilon' = 1 + 2 C \frac{\delta\omega}{\omega}$$

$$(4.19)$$

$$\sigma = \frac{1}{\omega \varepsilon_0} C \ \delta\left(\frac{1}{Q}\right)$$

where C is a constant to be determined experimentally.

For samples placed in either of the peripheral apertures, the field is not constant across the aperture (Figure 4.3b), so that an exact calculation of the numerator in (4.10) requires a numerical integration over the sample volume V_1. To find out whether this numerical integration was really necessary for these measurements, the integral

$$\iiint_{V_1} J_0^{\ 2}(kr) \ r \ dr \ d\theta \ dz$$

was calculated numerically for each of the three apertures shown in Figure 4.2, and compared with the approximation:

$$\iiint_{V_1} J_0^{\ 2}(kr) \ r \ dr \ d\theta \ dz \approx V_1 J_0^{\ 2}(k R) \tag{4.20}$$

where R is the position of the aperture from the cavity axis.

73

Approximation (4.20) was found to be within 0.3% of the numerically calculated value. This is a small error for experiments with high loss samples, so that the approximation could be assumed for calculations. Therefore, for the peripheral apertures,

$$\varepsilon' = 1 + 2 \frac{V_0}{V_1} \varepsilon_{PTFE} \frac{J_1^2(k\,a)}{J_0^2(k\,R)} \frac{\delta\omega}{\omega}$$

$$(4.21)$$

$$\sigma = \omega\,\varepsilon_0 \frac{V_0}{V_1} \varepsilon_{PTFE} \frac{J_1^2(kR)}{J_0^2(kR)} \delta\left(\frac{1}{Q_0}\right)$$

Again, in practice, the constants in equations (4.20) must be calibrated experimentally to allow for slight deviations in the shapes of the sample and the cavity, and for fringing fields in the apertures.

4.4 Measurement system

Figure 4.4 shows a schematic diagram of the measurement system used. The pieces of equipment used were:

(1) Signal Generator — Hewlett Packard microwave signal generator model 8616A

(2) Frequency Meter — made up of (a) Hewlett Packard electronic counter, model 52454; and (b) Hewlett Packard frequency converter, model 5255A

(3) Amplitude Modulator Drive — Levell RC Oscillator model TG 200 DMP; operated at 1kHz and 7V

(4) Isolator — Racal model MESL UG 3553

(5) Directional Coupler — NARDA high directivity reflectometer coupler, model

(2) Frequency Meter

(3) Amplitude
Modulator

(1)   Microwave Oscillator

(4) Isolator

(7) Piston Attenuator

(5) Reflectometer
Coupler

(6)

(a)

(a)

(a)

Detector

-10 dB

(b)

(8)   Amplifier + Meter

(9) Cavity
+
Sample

(b)

(a)

(b)

(b)
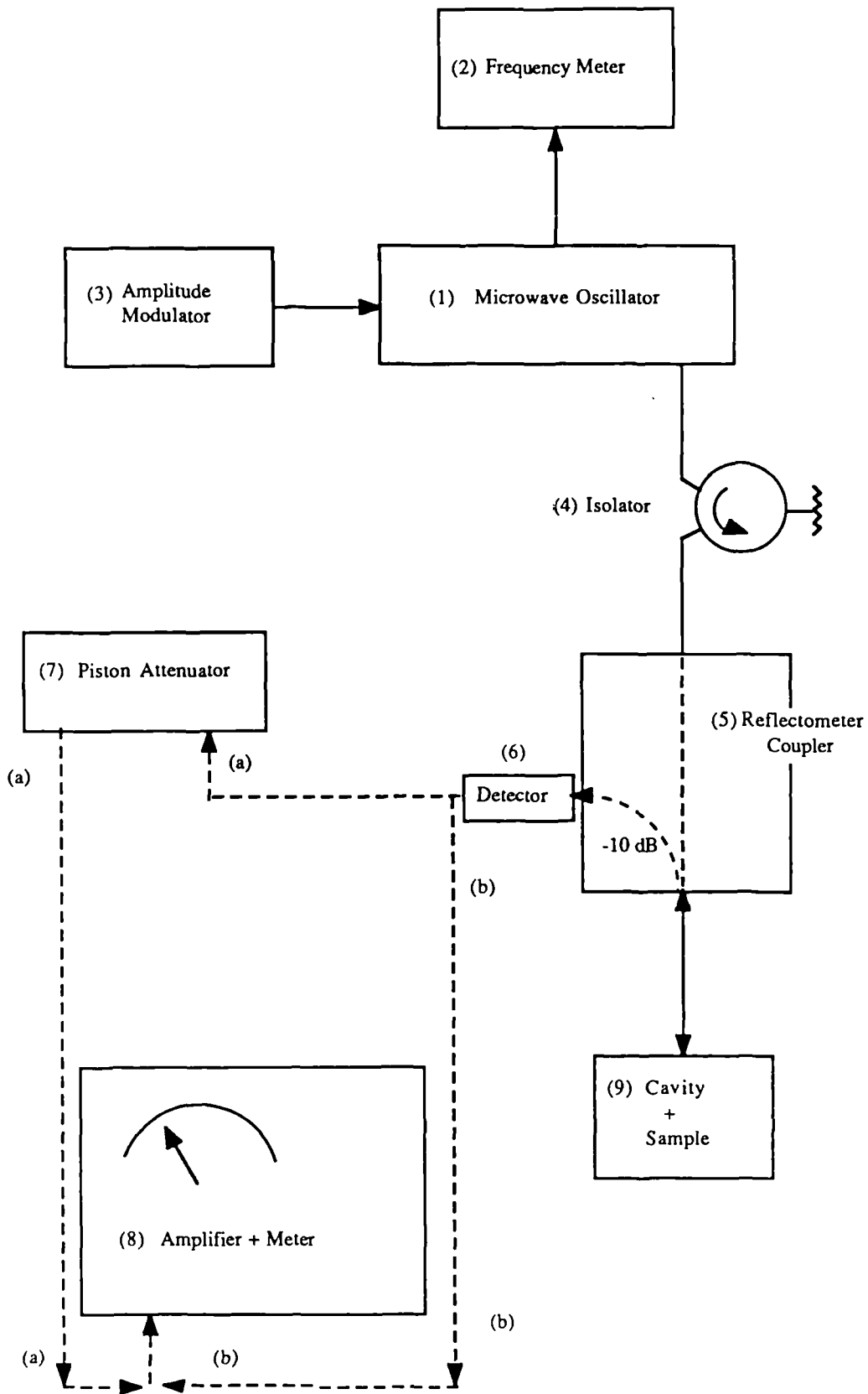
Figure 4.4   Experimental measurement system

Numbers relate to explanations in the text (Section 4.4)

Equipment was connected with coaxial cable

5073

(6) Detector — Hewlett Packard HP 423A crystal detector operated in the square law response region

(7) Attenuator — Flann piston cutoff attenuator model CA/S Ser 73; attenuation range 0 to 120dB

(8) Amplifier + meter — Sanders VSWR Amplifier MK2

(9) Resonant Cavity — As described in Section 4.2, a copper cavity operating in TM_{010}-mode; loaded with PTFE ($\varepsilon_{PTFE} = 2.02$); resonant frequency ≈ 3.18 GHz, $Q_0 \approx$ 1500 at room temperature; coupling by probe to the electric field through the end wall, such that the unperturbed cavity is almost critically coupled (See Figure 4.1)

4.4.1 Procedure

A signal at about 3.2GHz with a 1kHz amplitude modulation is reflected from the resonant cavity. About -10dB's of this signal is detected and then measured using either the microwave attenuator and the amplifier/voltmeter system, or directly by the amplifier/voltmeter system.

To find the resonant frequency, f_0, and quality factor, Q_0 of the unperturbed cavity, the oscillator output signal is set approximately to f_0 (observed as a minimum in the reflected signal). The cavity is then "detuned" by shorting it with a wire placed through one of the apertures which touches the two end-plates: this allows 100% of the input signal to the cavity to be reflected back to the detection system (which allows for any losses in the cavity coupling). Allowing the signal to follow route (a) in Fig. 4.4, ie to pass through the piston attenuator, the attenuator is tuned until maximum signal on the meter is obtained; the meter is set at a reference level $_{\wedge}$(using attenuation on the *of 30dB* Sanders Amplifier) with the attenuator on the low frequency 30dB range. The cavity short is then removed and fine frequency tuning allows a minimum to be found accurately. The reading on the frequency meter at this point is the unperturbed resonant frequency, f_0. Decreasing the attenuation until the meter is at the previous reference level allows the reflection coefficient at resonance, ρ_0, to be calculated:

$$\rho_0 = 10^{-(30 - x_0)/20}$$

(4.22)

where x_0 is the reading in dB's on the attenuator at resonance and at the reference level on the meter.

In order to find the frequencies, $f_{1/2}$ and $f_{-1/2}$, at half-power on each side of the resonance curve (Figure 4.5), it is necessary to calculate the attenuation needed to allow the reference level on the meter to be reached at these points. This may be calculated to be:

$$x_{1/2} \text{ (dB)} = 30 - \left[10 \log_{10} \left(\frac{2}{\rho_0^2 + 1} \right) \right]$$

(4.23)

Setting the attenuator at this level, the frequency of the signal is altered either side of resonance until the frequencies which give the reference level on the meter are reached.
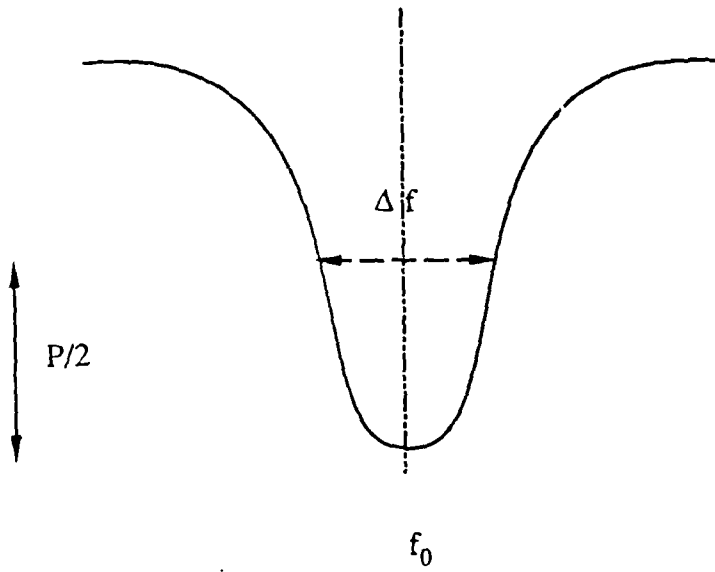
Figure 4.5   Schematic representation of the resonance curve
The loaded quality factor is $Q_L = f_0/\Delta f$ where Δf is the
bandwidth at half power (P/2)

The 'loaded quality factor', Q_L, is then calculated from,

$$Q_L = \frac{f_0}{\Delta f}$$

(4.24)

If the cavity were completely uncoupled, this would be equal to the unloaded quality factor, Q_0. However, because the cavity is coupled to the source and to the detector system, the coupling network must be taken into account. This is done using a coupling coefficient, β, which is the ratio of coupled resistance to cavity resistance (Duffin, 1980). The loaded and unloaded quality factors may be related by:

$$Q_0 = Q_L (1 + \beta)$$

(4.25)

The coupling coefficient, β, is related to the reflection coefficient at resonance ρ_0 by the equation,

$$\beta = \frac{1 - \rho_0}{1 + \rho_0}$$

(4.26)

where ρ_0 may be positive or negative. If $\beta = 1$, the coupled resistance and the cavity losses are equal, and the cavity is said to be critically coupled; if $\beta < 1$, the cavity is said to be under-coupled; if $\beta > 1$, the cavity is said to be over-coupled. Knowledge of whether β is greater or less than one allows Q_0 to be calculated from (4.25). The cavity was tested for under- or over-coupling using a procedure described in Section 4.4.2.

If the perturbation is sufficiently small, the perturbed resonant frequency, f_0', and the perturbed quality factor, Q_0', may be measured using the same procedure. However, for larger perturbations various problems are encountered. Firstly, the microwave oscillator output power level is not constant over a wide frequency range and it can be significantly different at either side of a resonance curve: this makes impractical the use of a reference level for calculation of $\rho_{1/2}$. Secondly, the piston

attenuator used has a very narrow frequency band of tuning, so that using this piece of equipment during a measurement can mean input matching it at several points through the resonance curve (Fig 4.6): this in turn means that the reference level on the meter cannot be relied on, since exactly the same matching is difficult to obtain each time. Thus it was decided that for highly lossy perturbers the resonance curve would be measured directly, without using the piston attenuator [following path (b) in Figure 4.4], while measuring V_{in}, the input level, as a function of frequency by shorting the cavity at several places across the resonance curve. An example of such a measurement curve is shown in Figure 4.7.

The curve measurements are normalised to the short circuit values and the resultant curve is fitted numerically (in a routine described in Section 4.4.6 and Appendix B) to obtain ρ_o', f_0' and Q_L' (the perturbed reflection coefficient, resonant frequency and loaded quality factor, respectively). This then allows Q_0' to be calculated.

For most measurements presented in Chapter 5, the perturbation was between 0.1 and 1%, although for one or two very lossy samples, the perturbation was slightly greater than 1%. Even this size of perturbation was sufficiently small that errors due to approximations in the theory were negligible; and even the smaller perturbations were sufficiently small that large experimental errors were avoided.

4.4.2 Test for coupling

It is necessary to know only if the cavity is under-coupled or over-coupled. The following simple procedure (Ginzton, 1957) was adopted. A system is set up consisting of source, isolator, standing wave detector and cavity (Figure 4.8). The cavity is detuned completely by shorting as described before, so that its resistance is zero and its reflection coefficient is -1. A voltage node (minimum) is located in the standing wave detector. This is called the detuned short position. The cavity is then tuned to resonance where its impedance is purely resistive. Therefore, at the detuned short position, there should be a voltage minimum or a voltage maximum. A voltage minimum implies under-coupling; a voltage maximum implies over-coupling.
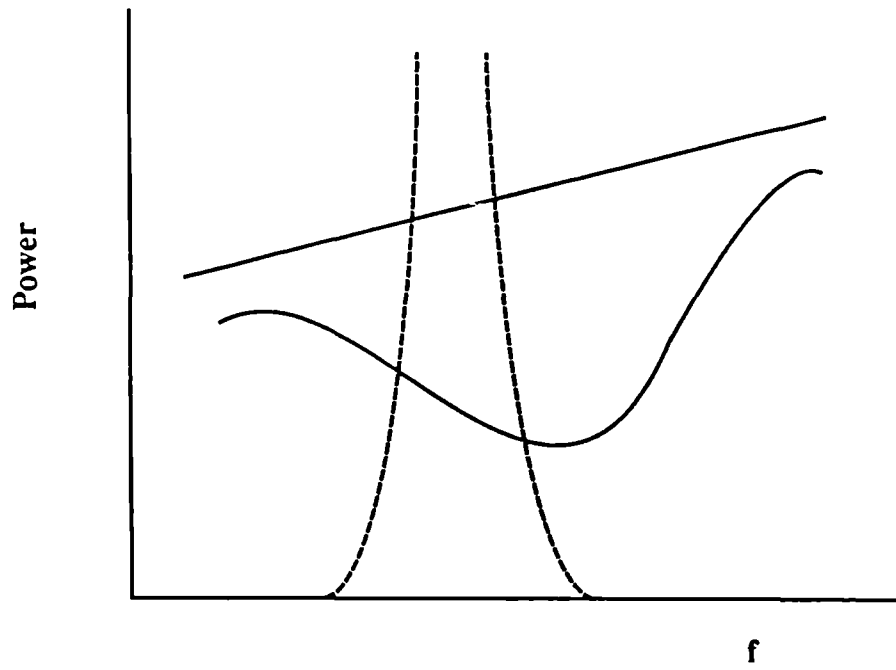
Figure 4.6   Cross-over of frequency band of attenuator tuning with
   frequency bandwidth of a lossy curve
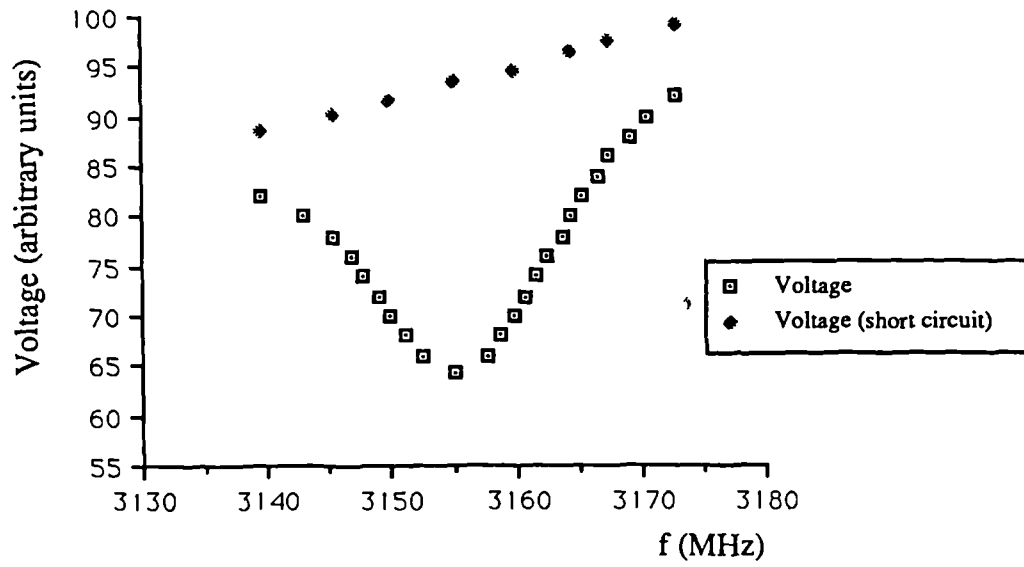
Figure 4.7   Typical measurement set
             (Sample of fibroadenoma in offset aperture)
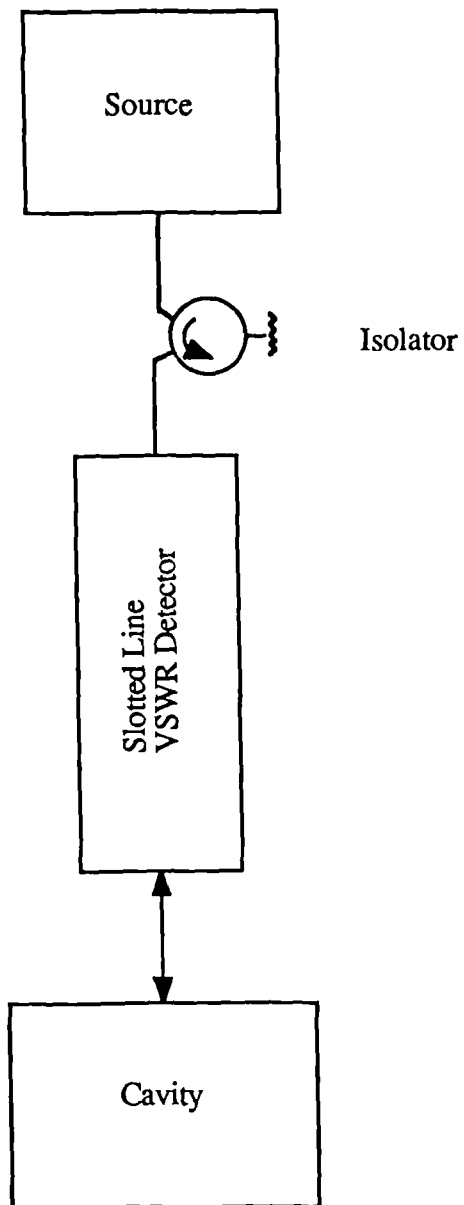
Figure 4.8   Schematic diagram showing the experimental apparatus used to determine the magnitude of cavity coupling

When this procedure was followed, for the cavity in both perturbed and unperturbed conditions, a voltage minimum was found at the detuned short position, so that the cavity was undercoupled. The coupling coefficient could then be written:

$$\beta = \frac{1 - |\rho_0|}{1 + |\rho_0|}$$

(4.27)

4.4.3 Calibrations of perturbation factor

The perturbation of the central aperture was determined absolutely using a ceramic rod whose properties were first measured in a standard TM_{010}-mode cavity of accurately known dimensions and with a resonant frequency close to 3GHz. Letting the standard cavity be denoted by subscript ST and the test cavity (to be calibrated) be denoted by subscript T, and setting

$$\frac{V_0}{V_1} = \frac{a}{r_s}$$

where a is the cavity radius and r_s is the sample radius, (4.17) may be written

$$r_{CER} \, (\epsilon_{CER} - 1) = - 2 \, J_1^{\,2}(k_{ST} \, a_{ST}) \, a_{ST}^2 \, \frac{\delta f_{ST}}{f_{0 \, ST}}$$

$$= - K \frac{\delta f_T}{f_{0T}}$$

(4.28)

where

$$K = 2 \, \epsilon_{PTFE} \, J_1^{\,2}(k_T \, a_T) \, a_T^2$$

Subscript CER refers to the ceramic rod.

When measurements were made in the $\overset{standard}{\wedge}$ cavity it was found that

$$r_{CER}^2 \, (\epsilon_{CER} - 1) = 3.164 \; mm^2$$

(4.29)

79

with about 0.2% accuracy, where r_{CER} is expressed in mm. Making the same measurement in the test cavity, and expressing rs in mm, allowed K to be calculated:

$$K = 755 \pm 4 \text{ mm}^2 \qquad (4.30)$$

Accuracy was determined by making repeated measurements and taking the standard error of the mean.

This gave an absolute calibration for the perturbation in the central aperture of the cavity. Equations (4.18) could be written:

$$\varepsilon' = 1 + \frac{755}{r_s^2} \frac{\delta f}{f_0}$$

CENTRAL APERTURE (4.31)

$$\sigma = \pi \varepsilon_0 \frac{755}{r_s^2} f_0 \, \delta\left(\frac{1}{Q_0}\right)$$

where r_s is expressed in mm.

The two outer apertures were calibrated relative to the central aperture by making repeated measurements of the frequency shift caused by various perturbers in each aperture. The ceramic rod; a glass rod; and a glass tube, empty, filled with distilled water and filled with alcohol, were used for this. These gave relative perturbations of 0.284 ± 0.006 for the mid-aperture, and 0.106 ± 0.002 for the outer aperture. Equations (4.21) may therefore be written:

$$\varepsilon' = 1 + \frac{2660}{r_s^2} \frac{\delta f}{f_0}$$

MID APERTURE (4.32)

$$\sigma = \pi \varepsilon_0 \frac{2660}{r_s^2} f_0 \, \delta\left(\frac{1}{Q_0}\right)$$

and,

$$\varepsilon' = 1 + \frac{7120}{r_s^2} \frac{\delta f}{f_0}$$

OUTER APERTURE (4.33)

$$\sigma = \pi \varepsilon_0 \frac{7120}{r_s^2} f_0 \, \delta\left(\frac{1}{Q_0}\right)$$

where r_s is again expressed in mm.

4.4.4 Comparisons of calibrations to theoretical values

Firstly, the dielectric constant of the PTFE may be calculated from the resonant frequency of the unperturbed cavity using the characteristic equation (4.13),

$$\chi^2 = \omega^2 \, \varepsilon_0 \, \mu_0 \, \varepsilon_{PTFE} \, a^2 = (ka)^2 \tag{4.34}$$

assuming that the cavity is perfectly conducting and that the influence of the apertures on the fields is negligible. Noting that $\chi = 2.4048$ is the first root of the zero order Bessel function, the relative permittivity of the cavity may be calculated to be:

$$\varepsilon_{PTFE} = 2.01 \tag{4.35}$$

which is consistent with accepted values (eg, the CRC Handbook of Physics and Chemistry states that $\varepsilon_{PTFE} = 2.01$ at 1kHz, 1MHz and 0.1GHz).

(a) Perturbation strengths

The positions of the offset apertures were measured using a travelling microscope:

$$R_{mid} = 16.022 \pm 0.013 \text{ mm}$$

$$R_{outer} = 19.230 \pm 0.015 \text{ mm}$$

These are the distances between the centre of the central aperture to the centres of the offset apertures and were in fact calculated from addition of the central aperture radius, the offset aperture radius and the distance from the edge of the central aperture to the edge of the offset aperture. The Bessel functions $J_0^2(kR)$ were evaluated, using $k = 94.67 \text{ m}^{-1}$ calculated from (4.34) and (4.35). Then,

81

$$J_0^2 \, (k \, R_{mid}) = 0.2524 \pm 0.0007$$

$$J_0^2 \, (k \, R_{outer}) = 0.1077 \pm 0.0006$$

where the stated errors correspond to experimental errors in R_{mid} and R_{outer}. The theoretical values of the constants in (4.31) to (4.33) were then calculated to be 699, 2774 and 6472 for the central, mid and outer apertures, respectively: thus the differences due to inaccuracies in cavity dimensions, and due to fringing fields, is about 8%, 4% and 10% for central, mid and outer apertures.

(b) Cavity Q

The theoretical quality factor of a cavity is a function of its dimensions and the skin depth of the cavity walls. Using the following formula (Waldron, 1969),

$$Q_0 = \frac{a \, l \, \sqrt{2 \, \omega \, \mu_0 \, \sigma_{Cu}}}{(1 + 2 \, a)} \tag{4.36}$$

where l is the cavity length and σ_{Cu} is the conductivity of copper, the theoretical value of Q_0 was calculated to be 5600. The measured value (which must be determined from the loaded quality factor, Q_L, and the coupling coefficient, β, as described in Section 4.4.1) was calculated to be about 1500 ± 200. This is different to the theoretical value probably because of a number of departures from ideal conditions: for example inaccuracies in the cavity shape, and lossiness in the PTFE.

[Dielectric loss in the PTFE is likely to be the most significant factor in reducing the quality factor. If it is assumed to be the only factor, the perturbation formula (4.10) may be used to calculate the loss factor of the PTFE, $\varepsilon'' = 4.9.10^{-4}$, which is near the lower end of published ranges $[4.2.10^{-4} - 1.2.10^{-2}$ (Moreno, 1948)].] However, as long as $Q_0 >> Q_0'$, the fact that the measured quality factor is different from the theoretical value is unimportant, because it is the change $\delta(1/Q_0)$ which matters.

4.4.5 Calibrations of aperture radii

Two different techniques were used to measure the radii of the three apertures. Initially an indirect method was used which involved placing a sample of some malleable material (eg lard) into the aperture. It was expected that the material would spread out to fill the aperture space. The material was then removed intact, placed on a glass plate, and its diameter measured using a travelling microscope (Figure 4.9a). Repeated measurements using different materials allowed a fairly accurate estimation of the radii: for example, before the main bulk of measurements commenced, r_{centre} was measured to be 0.741±0.008 mm.

A more accurate and reliable technique was used latterly. Again a travelling microscope was used, but this time the apertures were examined directly. The cavity was placed and held firmly (with blu-tak) on the microscope shelf, directly above a hole in the shelf, below which was placed a light source (Figure 4.9b). The shelf could be tilted and was set so that the flat plates of the cavity were precisely perpendicular to the axis of the microscope lens. Light therefore shone directly through the aperture to be measured, illuminating its edges. An outline of the aperture was measured by measuring in both x and y directions across the plane of the aperture. This allowed a check on the circularity of the aperture cross section; and, because the lens could be focussed up and down the length of the aperture, the consistency of this circularity and of the aperture dimensions could be estimated, and the smoothness of the aperture walls observed. Measurements around an aperture circumferences were translated to a calculation of its radius using a least squares optimisation routine for a circle written for the purpose and run on a BBC micro-computer. This allowed the radii to be determined to an accuracy of less than about 1.5%, with the main source of error being departure from circularity.

With constant use — with samples being pushed in and out — the apertures expanded slightly, radially, by about 5% over 65 measurements. Frequent measurements were made of these parameters. A typical set of measurements (eg Figure 4.10) gave results:

(a)

Glass plate

Sample

Measurement
of diameter

Measurement at several places along length

(b)

Travelling
microscope

Aperture

Cavity

Platform

Light
source
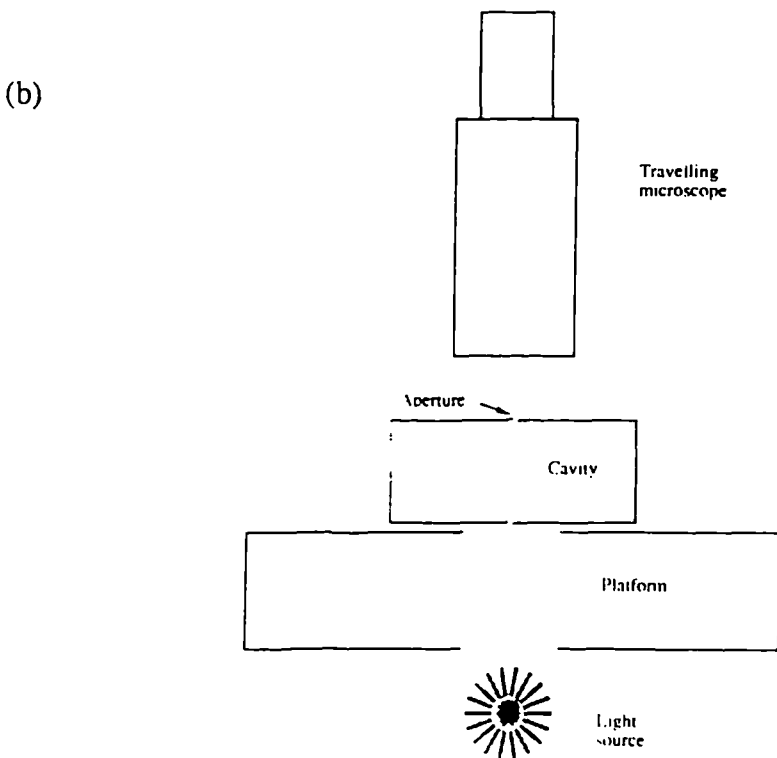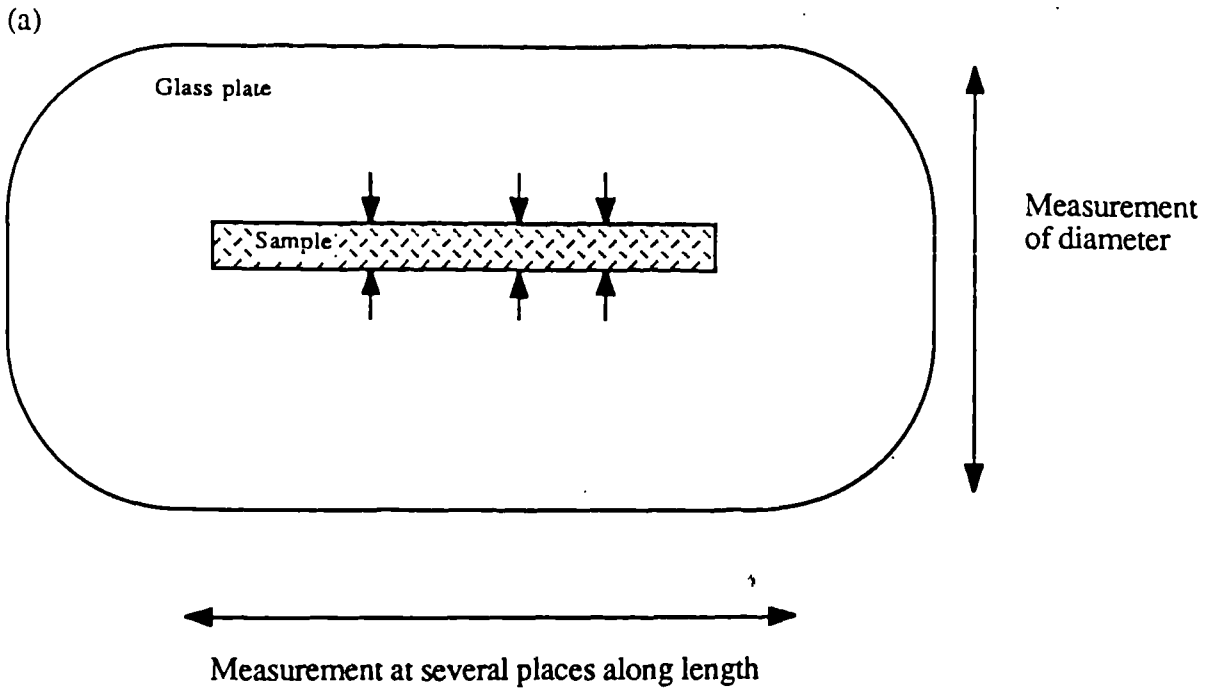
Figure 4.9   (a) Simple technique for measurement of sample diameter using
                     a travelling microscope
                     (b)Apparatus used to measure aperture radii. The platform was
                     moveable in x, y and z directions allowing focussing up and
                     down the aperture, and the aperture outline to be measured

(a)
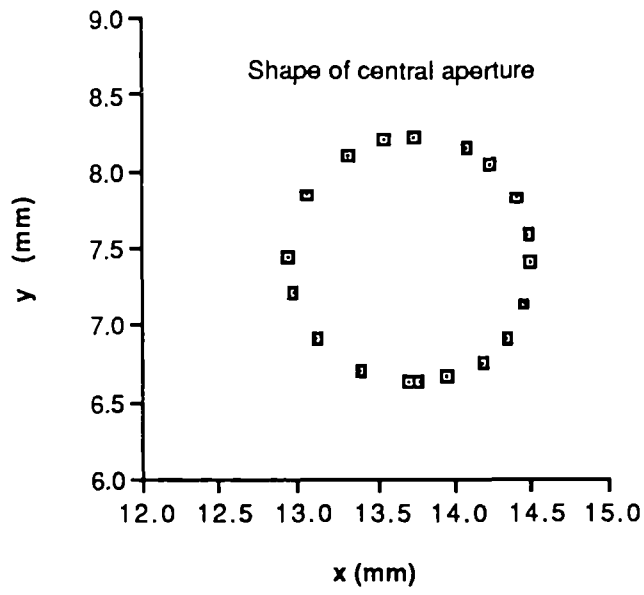
(b)
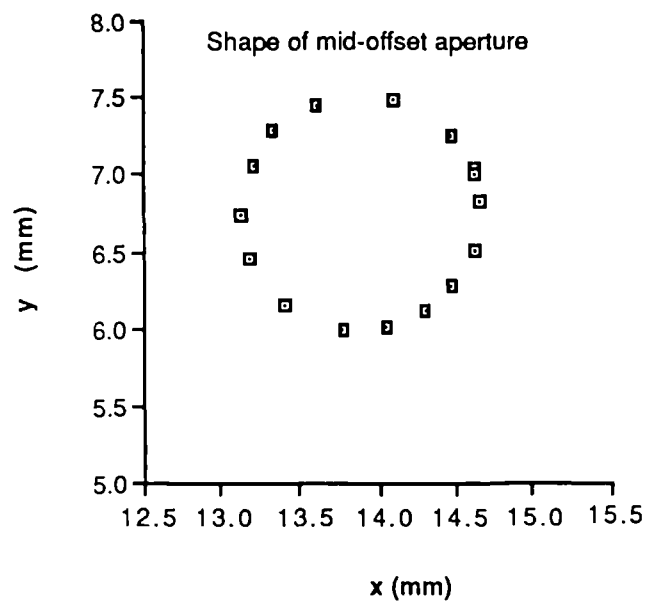
Figure 4.10   Typical data sets for the radii of (a) central and (b) mid-offset
apertures

$$r_{centre} = (0.7822 \pm 0.0098) \text{ mm}$$

$$r_{mid} = (0.7633 \pm 0.0001) \text{ mm}$$

$$r_{outer} = (0.7534 \pm 0.0018) \text{ mm}$$

where the accuracies stated are the standard errors of the best-fit parameters.

4.4.6 Curve fitting routine

In order to derive ρ_0, Q_L and f_0 from a scan of the perturbed resonance curve, the equation of the curve must be written in terms of these parameters. The voltage-frequency response of a resonant circuit may be expressed (Duffin, 1980)

$$\frac{V_{ref}}{V_{in}} = \frac{\rho_0 - j\, 2\, Q_L\, (\frac{f - f_0}{f})}{1 + 2j\, Q_L\, (\frac{f - f_0}{f})} \tag{4.37}$$

where V_{in} is the RF voltage incident on the cavity and V_{ref} is the reflected voltage. If the law of the detector is $V_{det} = V^n$ (where V is the input voltage to the detector and V_{det} is the output voltage from the detector) then the detected signal may be written

$$V_{det} = (V_{in})^n \left[\frac{\rho_0^2 + 4\, Q_L^2\, (\frac{f - f_0}{f})^2}{1 + 4\, Q_L^2\, (\frac{f - f_0}{f})^2} \right]^{n/2} \tag{4.38}$$

This curve may then be analysed to give best fit values of ρ_0, Q_L and f_0.

A FORTRAN program, CURVFIT, was written, which runs on an IBM 4361 mainframe computer, to analyse the data. The data itself consisted of two sets of numbers similar to the typical data set in Figure 4.7. In the program, a least squares routine was used to calculate a best fit line for the short-circuit data. The resonance curve data was then normalised to this best fit line and was itself fitted to obtain values of ρ_0, Q_L and f_0. A program listing is given in Appendix B along with additional

explanation.

A typical best fit curve is shown in Figure 4.11 with the normalised data points for comparison. The closeness with which the curve follows the normalised data indicates that the TM_{010}-mode cavity used in these investigations does behave as a simple resonant circuit.

4.4.7 Detector calibration

The detector was calibrated using the Flann piston attenuator (Section 4.4.1). It was found to be square law over the range of power levels used in the experiments,

$$n = 2.03 \pm 0.05$$

where n is the law of the detector. In fact the parameters of the resonance curve (4.38) are very insensitive to changes in the detector law, so that their calculated values were not affected by the above error in n.

4.4.8 Temperature dependence

The resonant frequency of the cavity, f_0, was expected to change with temperature, introducing an error to due to thermal drift. (All dielectric measurements were made at room temperature in an environment which was not temperature-controlled.) Copper has a coefficient of linear expansion:

$$\left(\frac{\Delta l}{l} \right)_T = 16.6 \ 10^{-6} / \, ^\circ C$$

(4.39)

while the dielectric constant of the PTFE has a temperature coefficient:

$$\left(\frac{\Delta \varepsilon_{PTFE}}{\varepsilon_{PTFE}} \right)_T = -7.7 \ 10^{-4} / \, ^\circ C$$

(4.40)

(CRC Handbook of Physics and Chemistry). This allows a rough calculation to be made
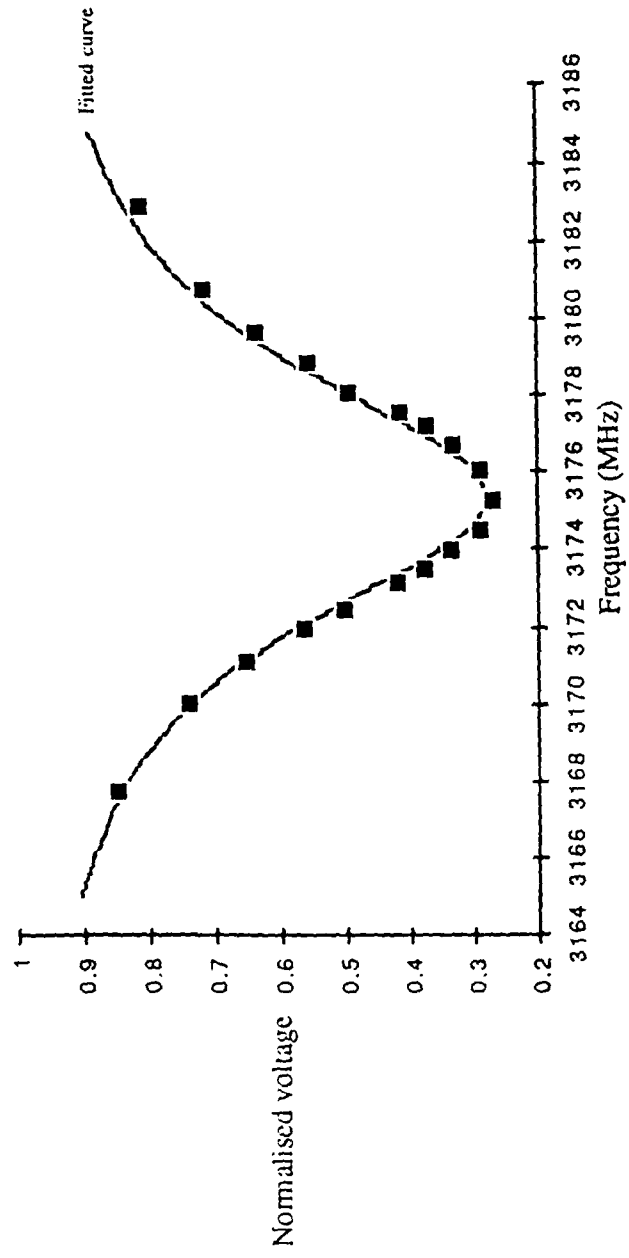
Figure 4.11   Typical normalised data set with best fit resonance curve
calculated from CURVFIT

for the expected change in the resonant frequency due to temperature:

$$\Delta f)_{PTFE} = 0.58 \, \text{MHz} \, / \, ^{\circ}\text{C} \quad \text{at} \; 3190 \, \text{MHz}$$

$$(4.41)$$

$$\Delta f)_{Cu} = -0.05 \, \text{MHz} \, / \, ^{\circ}\text{C} \quad \text{at} \; 3190 \, \text{MHz}$$

so that with a first order approximation,

$$\Delta f_T \approx 0.53 \, \text{MHz} \, / \, ^{\circ}\text{C}$$

$$(4.42)$$

where subscript T denotes change due to temperature.

The roughly observed dependence of f_0 upon T produced a slightly higher result:

$$\Delta f_T \approx 1 \pm 0.3 \, \text{MHz} \, / \, ^{\circ}\text{C}$$

$$(4.43)$$

Over a typical measurement time (1 minute)the temperature remained stable so that the error in f_c was less than 0.5MHz.

4.4.9 Cavity cleaning

Between sample measurements the aperture and sample holder were cleaned with "Genklene", a propriety cleaner, and dried with alcohol; the cleanliness and dryness of the cavity was easily checked by measurement of Q_L which clearly decreased if the cavity was contaminated. If the quality deteriorated so far that cleaning the apertures was ineffective, the whole cavity was dismantled and each part was cleaned with "Genklene". This usually happened only occasionally, when semi-liquid fat samples had been placed in the cavity; these tended to 'leak' along the upper and lower plates.

4.5 Sample preparation

Samples of human breast tissue — fat, normal and diseased tissues — were obtained from the Glasgow University Department of Surgery, Western Infirmary, Glasgow, within one or two hours of surgery. These were then kept refrigerated until

measurements were made, usually within twenty four hours of obtaining the sample.

In order to fill one of the cavity apertures with material from the sample, it had to be cut and molded into a shape suitable for insertion. The sample was placed on a clean surface; if it was bleeding it was wiped with an alcohol-soaked piece of cotton wool (this was rarely necessary). Cutting was performed with a sharp scalpel blade and the pieces of tissue removed were pushed into a sample holder designed for this purpose (Figure 4.12) until it was estimated that enough material was contained in the holder to fill the cavity aperture.

Firstly, the unperturbed resonant frequency, f_0, and quality factor, Q_L, of the cavity were measured, using the procedure outlined in Section 4.4.1. Then the sample was pushed into the cavity aperture and the perturbed resonant frequency, f_0', and the perturbed quality factor, Q_L', were measured. It was fairly easy to decide which aperture to place the tissue in: firstly, the Department of Surgery marked all samples by tissue type, so that it was clear whether the tissue was expected to be highly lossy; secondly, experience gained handling tissue allowed the likely lossiness of the tissue to be judged by malleability, colour and wetness. After measurement the sample was pushed out of the aperture and its water content was measured using a procedure described in Section 4.6.

There are some intrinsic problems with the above method of sample preparation. Firstly, cutting and pushing could cause loss of fluid from high water content tissues, which would cause the permittivity and conductivity to be underestimated. Because of this the samples were handled as little as possible, so that bleeding was rarely noticed and other fluid loss was minimised. Apart from the slight loss in fluid experienced by high water content tissues, cutting in itself would not have disturbed the tissue electrical properties at 3GHz, since the bulk properties of the tissue were not being altered. Secondly, for hard tissues (for instance, some tumours), it was necessary to prepare the sample in many small pieces, so that there was a possibility of leaving tiny pockets of air within the sample itself: this again would have an effect on the estimated dielectric properties. However, these samples in particular retained a cylindrical shape upon

10 cm

Solid steel insertion rod

4 cm

Steel sample holder

Sample

2.2 mm
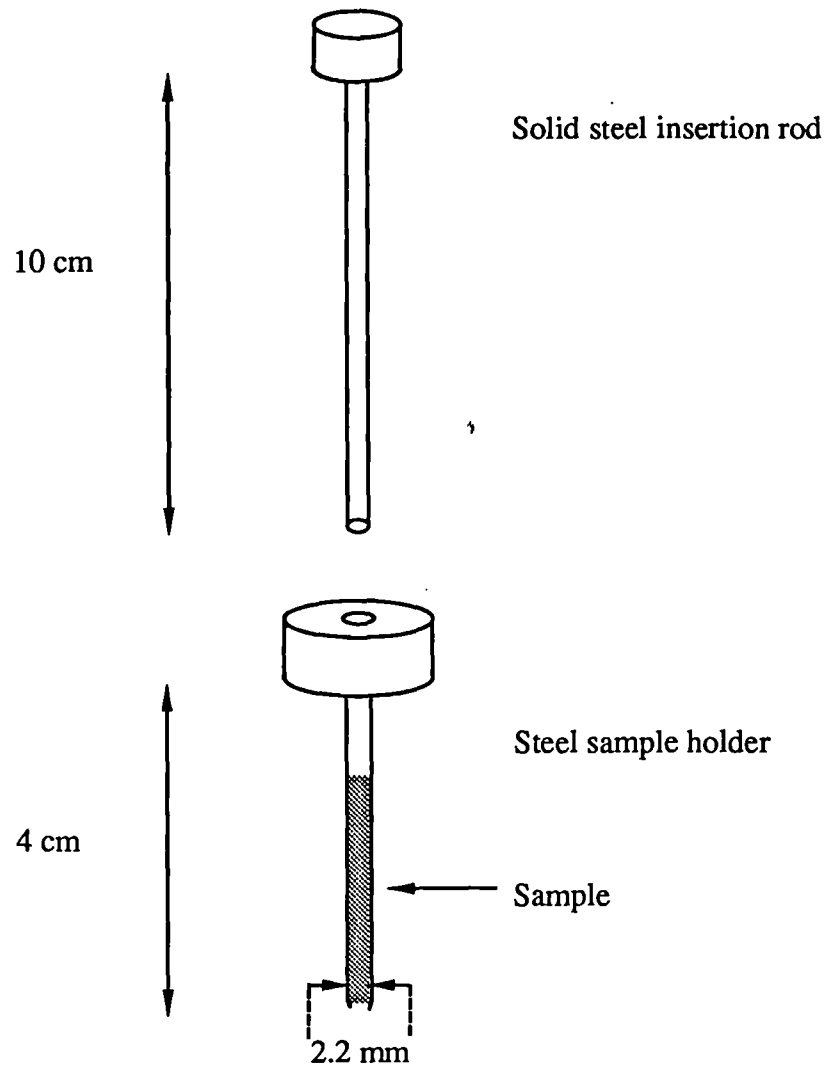
Figure 4.12   Sample holder and insertion rod

removal from the cavity so that any obvious errors in shape would be noticed and the measurement rejected. This meant that only small inhomogeneities are likely to have remained. Finally, it is possible that slight increases in tissue density were caused by pushing the sample into and out of the sample holder. Again, the effect was minimised by ensuring that the tissue was as little handled as possible.

As long as the above problems can be kept to a minimum it is believed that these are acceptable uncertainties, in order that the technique can deal with very small volumes of tissue. It is likely that inhomogeneities in each tissue and differences between individuals are greater than the uncertainties caused by sample preparation.

4.6 Water contents

After making a dielectric measurement, the sample was removed from the cavity by pushing it out onto a disposable sample container. This was made of either aluminium foil or baking parchment and had been prepared (Figure 4.13) and weighed previously. The sample was dried in an oven at 105 °C until it reached a stable weight (usually after 48 — 96 hours); its weight before and after drying was measured using an electronic precision balance with a resolution of 0.0001g. This allowed the water content by weight to be calculated. Measurement precision was about 1-2% for this procedure.

Some systematic errors must be considered when considering the accuracy of the water contents calculated. Firstly, removing the sample from the cavity, placing on the balance and measuring its 'wet' weight took about 30s. This may have allowed very high water content samples to dry out a little between the measurement of dielectric constant and the water content measurement. In order to gauge the size of this effect, the rates of drying at room temperature of two very high water content samples ($\approx$80% water) were measured. These allowed an estimate to be made of water loss, due to the time delay, of $\leq$0.5% for very high water content tissues, an error less than the precision of the water content measurements.

Another systematic error which must be considered when comparing water content

Glass Cylinder

rounded end

Sample Holder
(Aluminium foil or
greaseproof paper)

Sponge
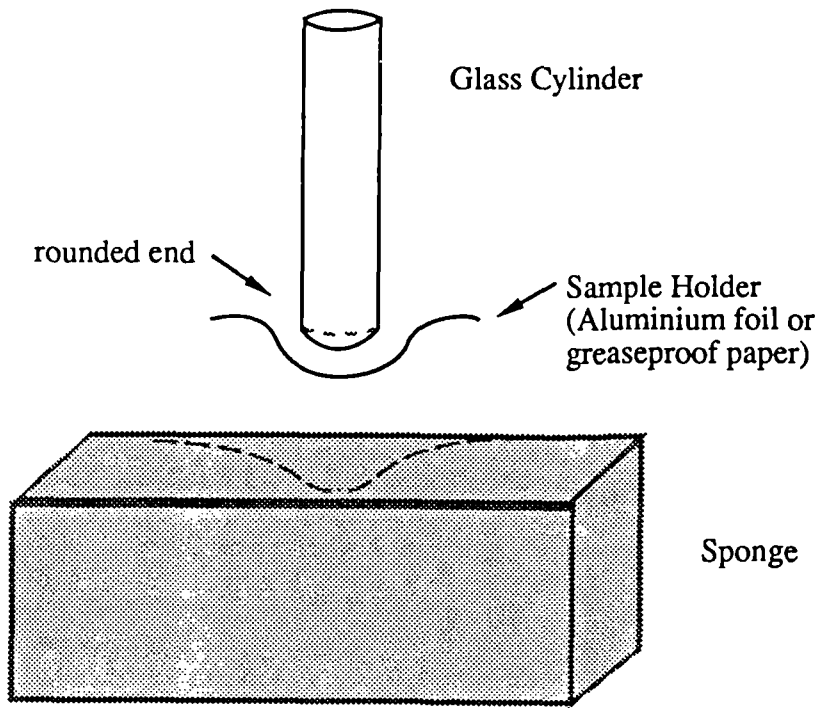
Figure 4.13   Preparation of container in which to dry sample

and dielectric measurements was that the volume of tissue used for dielectric measurements was less than that used in water content measurements. This was caused by the nature of the cavity system (Fig. 4.2). In order to be sure that the sample spanned the whole of the inner cavity length (ie the length of the PTFE) it had to be long enough to span the lengths of the two copper endpieces also, so that the sample could be seen from either side. However, this meant that the volume of tissue used in the dielectric measurement was about $10mm^3$, while that used in the water content measurement was about $17mm^3$. This is likely to have caused a loss in accuracy of at most a few percent for most tissues, because within a small volume of tissue the distribution of water is fairly homogeneous (Tables 5.1 to 5.5 give comparisons of water contents for different parts of the same tissue).

4.7 Summary

In this chapter a cavity perturbation technique was described for dielectric measurement of small biological samples at 3GHz. First order theoretical formulae were derived based on the assumptions that the cavity walls are perfectly conducting, that the change in resonant frequency is very much less than the resonant frequency of the cavity and that the sample volume is small. Instrumentation and measurement procedures were discussed and experimental calibrations were given. These calibrations were compared to theory; and the relative errors of the different system components were discussed. A description was given of sample preparation and of the procedure for measuring water contents; systematic errors in these procedures were assessed. From these discussions it is clear that the major sources of error in these experiments are inhomogeneities in the tissue samples; fluid loss in samples due to the preparation procedure and finite measurement time; departure from circularity in aperture radii; air pockets at the interface between samples and aperture walls; differences in the volumes of tissues used for dielectric and water content measurements; and temperature drift during measurement.

89

This technique may be used to make dielectric measurements at 3GHz for samples with relative permittivities ranging from 2 to 78, and with conductivities ranging from 0.2 to 50mS/cm. Accuracies in measurement are about 3 — 4% for permittivity, conductivity, and water content.

Chapter 5

Dielectric Properties of Human Tissues

5.1 Introduction

In this chapter, new dielectric data are presented on human tissues, mainly female breast tissues. Section 5.2 introduces the different types of tissue measured and gives a simple description of their biological role. Section 5.3 discusses a method of analysis which allows the estimation of some information about a possible underlying dispersion. In Section 5.4, data on low water content tissues, fat and bone, are presented and analysed. Sections 5.5 to 5.11 present and analyse data on higher water content tissues: normal breast tissue, and benign and malignant tumours. All data were measured at room temperature, 20 — 25 °C. Finally, in Section 5.12, a data summary is presented, and a discussion is given of the potential implications of the new data for future measurements and for modelling.

5.2 Anatomy of the breast

The female breast (Figure 5.1) contains a mixture of glandular (epithelial) tissue, loose connective tissue (a loose unorganised arrangement of fibres), and varying amounts of fat, blood vessels, nerves and lymphatics (see Section 2.1). The glandular structure consists of alveoli, which are small sac-like dilations, inconspicuous in the non-lactating breast. These lead into lactiferous ducts which are larger than the alveoli, and are embedded in fibrous connective tissue and fat. Each duct dilates into a sinus and opens onto a nipple. In the upper part of the breast connective tissue is thickened and well developed, such that it subdivides the fat and the glandular tissue, and also attaches these structures firmly to the skin. Connective tissue and glandular tissue in the breast are inextricably intermingled (Rehmann, 1978; Haagensen, 1986).

91

Pectoralis
major muscle

Fibrous connective
tissue bands

Lactiferous sinus

Lactiferous duct
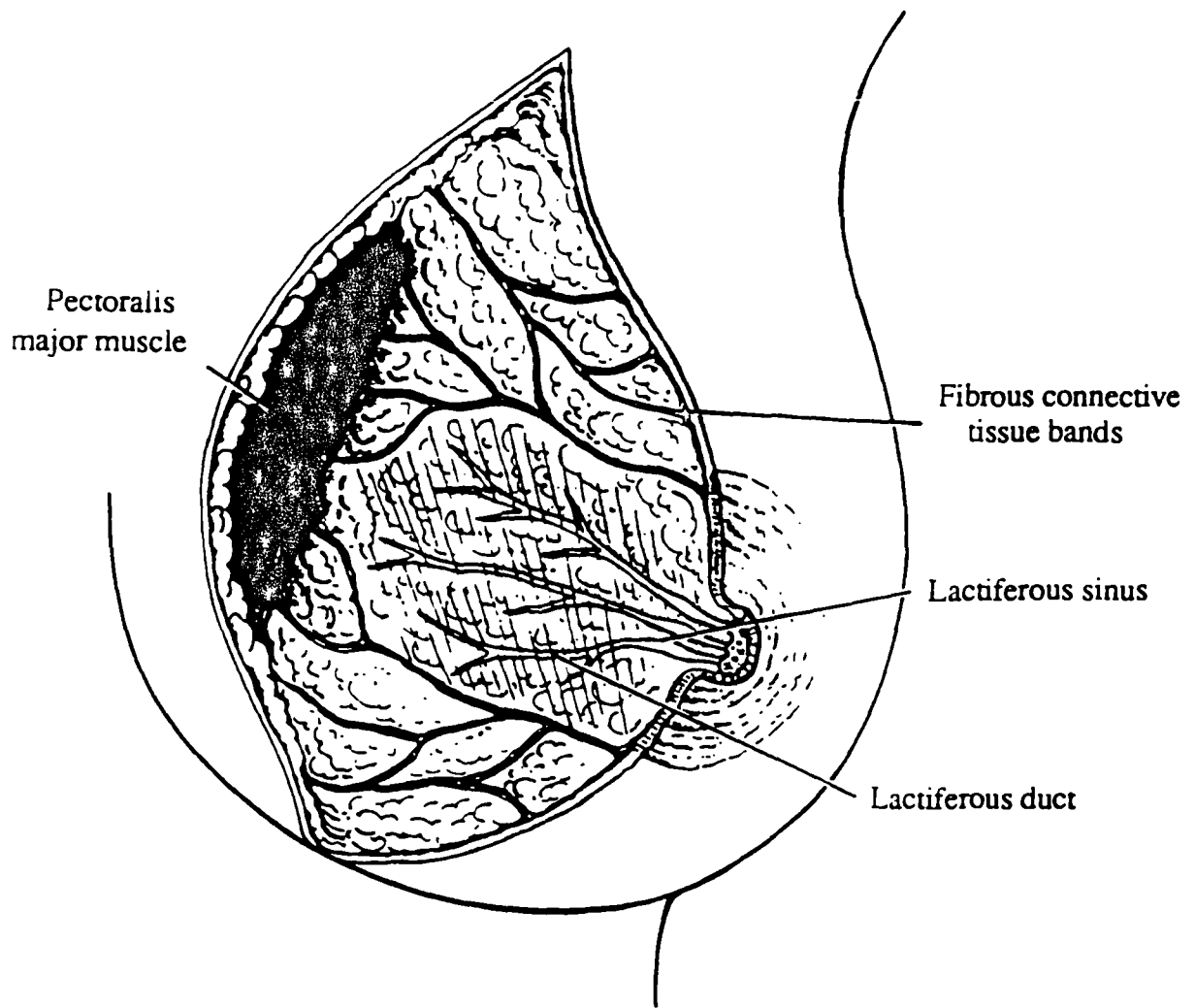
Figure 5.1   Structure of the non-lactating female breast

Adipose tissue is composed of fat cells that are dispersed within loose connective tissue. Each cell contains a large droplet of fat that squeezes and flattens the nucleus, and forces the cytoplasm of the cell into a thin ring around the periphery of the cell (Brooks and Brooks, 1980).

In adult women, breast characteristics, that is size, fullness, density and nodularity, depend on the corpulence of the individual and on whether the breasts have ever lactated. Obese women have fattier and therefore denser breasts (Haagenson, 1986). As the menopause approaches, the breast as a whole shrinks and the glandular portion involutes. In fatty individuals there is an increase in the amount of fat, and with advancing years the glandular tissue is replaced by fat. If little fat is present, or if involution is incomplete, there may be a relative increase in the amount of fibrous tissue.

Undiseased tissues measured in this work are referred to as normal and fat. Normal breast tissue is a mixture of glandular and connective tissue: it therefore contains proteins and water. The fat tissue is in fact adipose tissue, and therefore contains a mixture of lipids (fatty acids and fats), water, and small amounts of protein from cell nuclei and membranes.

5.2.1 The diseased breast

Benign lesions are by far more common than malignant ones in both male and female breasts, accounting for 60 — 80% of breast operations. In females the more common breast lesions are fybrocystic disease, carcinoma and fibroadenoma; in males gynaecomastia is the most common lesion (Pilnik and Leis, 1978). Cysts are hollow benign tumours containing fluid or soft material, and are usually the result of blockage in milk ducts due to inflammation; they are well defined and slightly mobile. It is common to aspirate cysts rather than to remove them surgically. Fibroadenomas, which occur most frequently in young women, are benign tumours composed of glandular tissue. They are mobile, firm and well-delineated, and must be removed in surgery. Benign tumours grow slowly at one spot, pressing neighbouring parts aside

but not invading them. However, many benign tumours, including all of those measured for this work, are predisposed to subsequent breast carcinoma (Haagenson, 1986).

Carcinomas are solid, poorly-delineated and immobile. Primary female breast tumours are more commonly found in the upper outer quadrant of the breast. Unlike benign tumours, cancers spread rapidly from point to point, and invade and destroy surrounding tissues.

The Tumour Nodes Metastases (TNM) system is generally used by pathologists to describe breast cancers. In this system (used in Table 5.4), tumours are graded as types I to IV, a grading which indicates the stage of advancement of the cancer. Patients with stage I disease (those with primary lesions greater than 1cm and less than 5cm, and with negative nodes) generally survive longer than those with stage II disease (small lesions and positive nodes, or large lesions and negative nodes): 90% of stage I patients survive ten years after the initial treatment, compared to 70% of grade II patients. Of patients with grade IV disease, only 2% survive ten years after the initial treatment (Robbins, 1978).

Breasts in men are small nodules of fibrous tissue with occasional simple ducts and variable amounts of fat. Gynaecomastia, the most common lesion in the male breast, is a benign and usually reversible enlargement of the breast. It is usually categorised by its tendency to peak in three different age groups. In the mature adult it is usually a mass of mammary tissue which can approximate the size and shape of a female breast: generally only one breast is increased in size, accompanied by pain and tenderness (Crichlow, 1978; Pilnik and Leis, 1978).

5.3 Relationship of permittivity and conductivity for a given tissue type

If the polarisation of a biological material at microwave frequencies may be characterised by a relaxation process, or sum of relaxation processes, then the permittivity and conductivity may be expressed by the Debye equations (2.14), with

an additional term for ionic conductivity, or by the Cole-Cole equations (3.6). If it is assumed that there is one strongly dominant process occurring at a particular frequency in all tissues of a similar type, then the relationship between the permittivity and conductivity of the tissue at that frequency   may be parameterised using (2.14) or (3.6), such that:

$$\frac{\sigma - \sigma_s}{\varepsilon' - \varepsilon_\infty} = F(\omega, \tau, \alpha) \qquad (5.1)$$

where ε_∞ is the high frequency permittivity limit of the dispersion; σ_s is the ionic conductivity; ω is the angular frequency of the imposed electromagnetic field; τ is the relaxation time; and α is a constant which characterises the spread of relaxation times in the Cole-Cole distribution. F is a function which is dependent on the model used.

In the simplest case, a strongly dominant Debye dispersion may be assumed to determine the dielectric properties of the tissue. In this case (5.1) may be written:

$$\frac{\sigma - \sigma_s}{\varepsilon' - \varepsilon_\infty} = \omega^2 \varepsilon_0 \tau \qquad (5.2)$$

Therefore, for a given tissue type at a particular frequency, a graph of conductivity versus permittivity should yield a straight line with gradient $\omega^2 \varepsilon_0 \tau$. That is, many dielectric measurements of a tissue type at a given frequency may yield some information about an underlying dispersion common to all the tissue samples, without any need to know either the ionic conductivity or the limiting high frequency permittivity.

5.4 Fat and bone tissues

Thirty nine measurements of the dielectric properties of female human breast fat were made, on seventeen different patients. The relative permittivity of these tissues was found to range from 2.8 to 7.6, the conductivity from 0.54 to 2.9mS/cm, and the

water contents from 11 to 31% by weight. Some measurements were also made on dehydrated fat (dried at 105°C), which consisted of a liquid substance, probably lipids, and a solid substance, probably dried protein. The permittivities of these samples were found to be in the range 2.5 to 2.8 and 2.0 to 2.9; their conductivities were in the range 0.25 to 0.34 mS/cm and 0.35 to 0.37 mS/cm, respectively.

To provide information on the behaviour of the other major low water content tissue, a measurement of human bone was made. This sample was part of a head of femur from a hip replacement operation on an elderly man who suffered from osteoarthritis. Its relative permittivity was about 5, its conductivity about 2 mS/cm, and its water content was 16%.

Tables 5.1a, b and c show the collected fat data and the data from the single measurement on bone. Patients are described by number in order to preserve anonymity. These tables give the relative permittivity and conductivity (with estimated errors) of each tissue sample ; the tables also contain the water contents of the samples and the age of each patient. On some samples, an 'average' water content was measured, rather than the actual water content, for which the procedure described in Section 4.6 was used: 'averaged' measurements were made on volumes of tissue much larger than the sample volume and so may not be representative of the actual sample. It is clearly indicated in the table where average values of water content were measured. All tissue samples were obtained from areas of the breast far from any diseased tissue, except in the case of patient 6 where the tissue was fat necrosis. (This is a benign tumour which occurs in superficial body fat which has been exposed to trauma.)

5.4.1 Relationship of relative permittivity and conductivity

The results of the tissue microwave dielectric measurements made here show clearly that the permittivity and conductivity of human breast fat tissue are strongly correlated (Figure 5.2). They may be related by the straight line

Table 5.1(a)　　　　The permittivity, conductivity and
water content of human breast fat

Patient number	Permittivity	Conductivity (mS/cm)	Water content (% by weight)	Age
1	4.36 ± 0.13	1.17±0.04	11 (average)	70
2	4.51 ± 0.14	1.27 ± 0.05	—	66
	3.67 ± 0.11	1.06 ± 0.06		
5	5.38 ± 0.17	1.77 ±0.06	15 (average)	46
	5.08 ± 0.16	1.79 ±0.06		
6	4.44 ± 0.14	1.20 ± 0.04	21 (average)	
	4.91 ±0.15	1.45 ± 0.05		
	5.54 ± 0.17	1.83 ± 0.06	21 (average)	48
	4.93 ± 0.15	1.52 ± 0.05		
	5.38 ± 0.16	1.74 ± 0.06	19 (average)	
	3.99 ± 0.12	1.04 ± 0.04		
9	4.51 ± 0.14	1.40 ± 0.05	11 (average)	59
	4.65 ± 0.14	1.34 ± 0.05		
	4.05 ± 0.12	1.17 ± 0.04		
11	4.17 ± 0.13	0.91 ±0.04	16	68
	4.06 ± 0.12	1.11 ± 0.04	15	
12	7.48 ± 0.23	2.93 ±0.100	19	26
	7.05 ± 0.22	2.89 ± 0.100	20	
13	4.24 ± 0.13	1.05 ± 0.04	20	
	4.32 ± 0.13	1.16 ± 0.04	21	
	4.07 ±0.13	1.00 ±0.04	18	
	5.40 ± 0.17	1.68 ± 0.06	27	49
	4.25 ± 0.13	1.21 ± 0.05	19	
	3.50 ± 0.11	0.92 ± 0.04	17	
	3.38 ± 0.10	0.79 ± 0.03	17	

Patient number	Permittivity	Conductivity (mS/cm)	Water content (% by weight)	Age
14	6.01 ± 0.18	2.26 ± 0.08	22	94
18	5.08 ± 0.16	1.49 ± 0.05	28	66
20	4.30 ± 0.10	1.16 ± 0.04	15	
	6.93 ± 0.21	2.10 ± 0.07	24	46
	5.70 ± 0.17	2.08 ± 0.07	20	
23	4.50 ± 0.14	1.30 ± 0.04	22	54
	6.39 ± 0.20	2.14 ± 0.07	—	
30	5.78 ± 0.18	1.97 ±0.06	22	65
34	4.21 ± 0.14	0.99 ± 0.03	18	38
35	4.47 ± 0.14	1.13 ±0.04	15	53
	2.79 ± 0.10	0.54 ± 0.02	23	
37	7.55 ± 0.23	2.43 ± 0.08	31	80
38	3.58 ± 0.12	0.68 ± 0.03	21	73
	4.42 ± 0.14	1.19 ± 0.04	21	

Table 5.1(b)   The permittivity and conductivity of human hip bone

Patient number	Permittivity	Conductivity (mS/cm)	Water content (% by weight)	Age
39	5.33 ±0.16	1.83 ±0.06	16	85

Table 5.1(c)   The permittivity and conductivity of
dehydrated human fat from patient 9

Type of substance	Permittivity	Conductivity (mS/cm)
lipid	2.73 ±0.10	0.34 ± 0.02
lipid	2.80 ± 0.10	0.33 ± 0.02
lipid	2.53 ± 0.10	0.25 ±0.02
protein	2.03 ± 0.09	0.37 ± 0.02
protein	2.90 ± 0.10	0.35 ±0.02
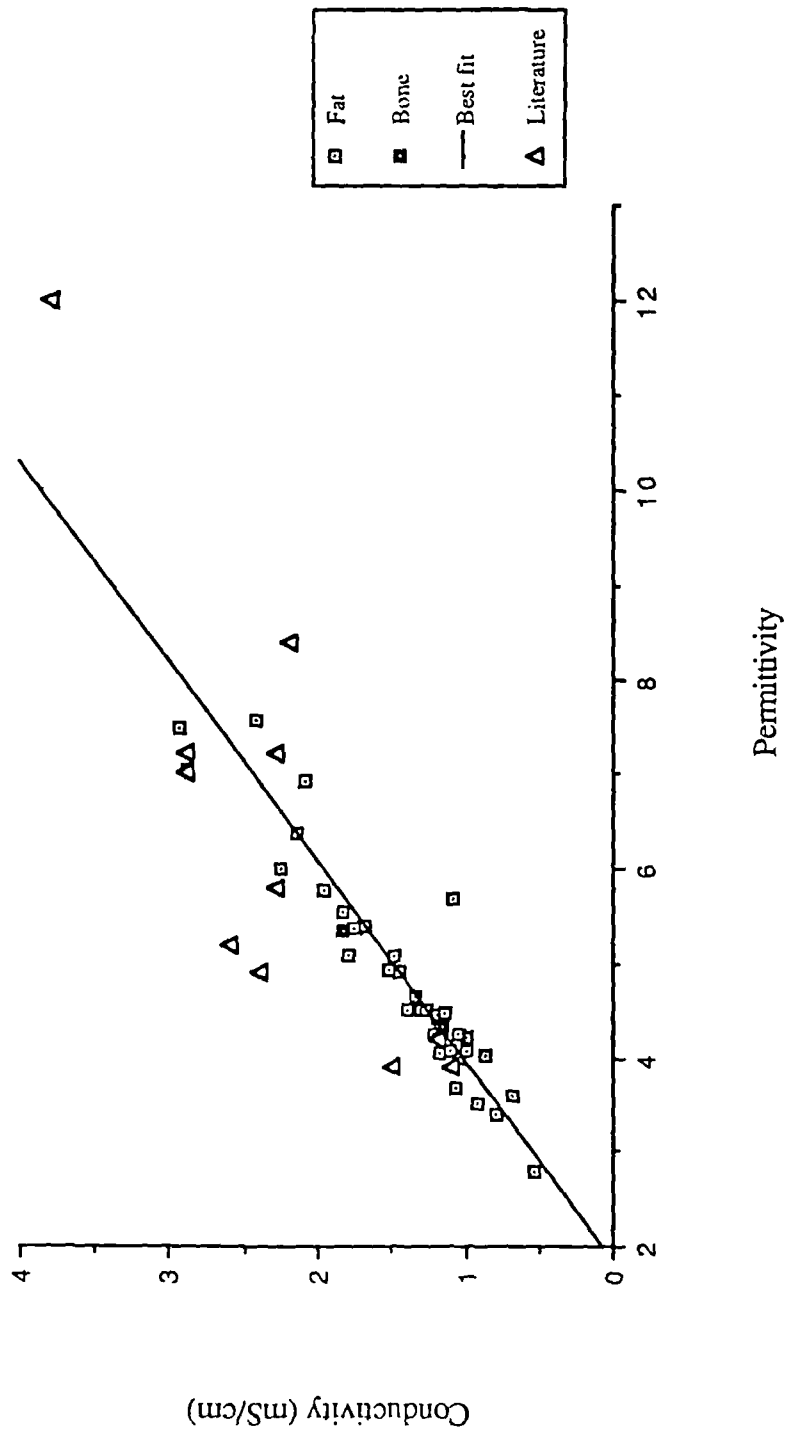
Figure 5.2   Variation of conductivity with permittivity for fat and bone tissues

$$\sigma \ (\text{mS/cm}) = m_{fat} \, \varepsilon' + c_{fat} \qquad\qquad (5.3)$$

where $\quad m_{fat} = 0.478 \pm 0.002$ mS/cm

$$c_{fat} = -0.864 \pm 0.008 \text{ mS/cm}$$

which is the least squares best fit line through all the fat and bone data, taking into account errors in σ and in ε'. Errors on data are too small to show in Figure 5.2. Equation (5.3) may be compared with (3.12), the least squares best fit of human permittivity and conductivity from the literature:

$$\sigma \ (\text{mS/cm}) = 0.27 \ \varepsilon' + 0.56 \qquad\qquad (5.4)$$

This line was calculated for only 11 points taken from different experiments: the data correlation coefficient for this fit was only 0.68 in comparison with the correlation coefficient for (5.3) which was 0.96. Although both of these correlation coefficients indicate that permittivity and conductivity are not independent [using the Spearman rank correlation coefficient test (Hayslett and Murphy, 1968)], the new data strongly suggest that the dependence is linear. When the actual data points from the literature are compared with the data from Table 5.1 (Figure 5.2), they are seen to be reasonably consistent.

The gradient, m_{fat}, may be used to calculate a value for τ from (5.2). This parameterises a Debye distribution:

$$\tau = \frac{m_{fat}}{10} \frac{1}{\omega^2 \, \varepsilon_0} = 1.34.10^{-11} \text{ s} \qquad\qquad (5.5)$$

taking into account that the gradient of the graph was calculated for the conductivity in mS/cm. A value for the relaxation frequency of fat may then be calculated:

$$f_c = 12 \text{ GHz}$$

This is lower than the relaxation frequency of saline at room temperature and 3 GHz (f_c = 20GHz). It perhaps indicates that other processes (for instance dielectric relaxation of bound water and interfacial polarisation dispersion) are contributing to the dielectric properties at this frequency, which combine to lower the estimated

relaxation frequency.

5.4.2 Relationship of ε' and σ in individual patients

In two cases, patients 6 and 13, it was possible to make a number of measurements on the fat tissue. Data from these measurements show that within individual patients, permittivity and conductivity are strongly correlated. For patient 6 (Figure 5.3):

$$\sigma \text{ (mS/cm)} = m_6 \, \varepsilon' + c_6$$

where $m_6 = 0.515 \pm 0.002$ (mS/cm)

and $c_6 = -1.04 \pm 0.01$ (mS/cm)

The correlation coefficient for this line is 0.99. For patient 13 (Figure 5.4):

$$\sigma \text{ (mS/cm)} = m_{13} \, \varepsilon' + c_{13}$$

where $m_{13} = 0.399 \pm 0.003$ mS/cm

and $c_{13} = -0.55 \pm 0.01$ mS/cm

The correlation coefficient of this line is 0.96.

The range of values of permittivity and conductivity obtained in these two experiments gives some idea of the heterogeneity of breast fat within individual patients. For patient 6, ε' ranges from 4.0 to 5.4 and σ from 1.0 to 1.8 mS/cm; for patient 13, ε' ranges from 3.4 to 5.4 and σ from 0.8 to 1.7 mS/cm. It is interesting to observe that the data from patient 6 on fat necrosis are more strongly correlated than the data from patient 13 on fat. The errors on the data for patient 6 are also apparently too large. There is no reason to assume that errors in making measurements on the fat necrosis were any less than errors made on other fat measurements. There are three possible reasons for the errors for patient 6 looking too large: errors on all the data are too large, and a real effect is being seen in the stronger correlation of data in fat necrosis (ie conductivity and permittivity in fat necrosis is more strongly linearly related than permittivity and conductivity in fat); or the data from patient 6 were more accurately measured, and the stronger correlation would be observed in all breast fat if all measurements were as accurate as this set; or the errors are correctly estimated, and
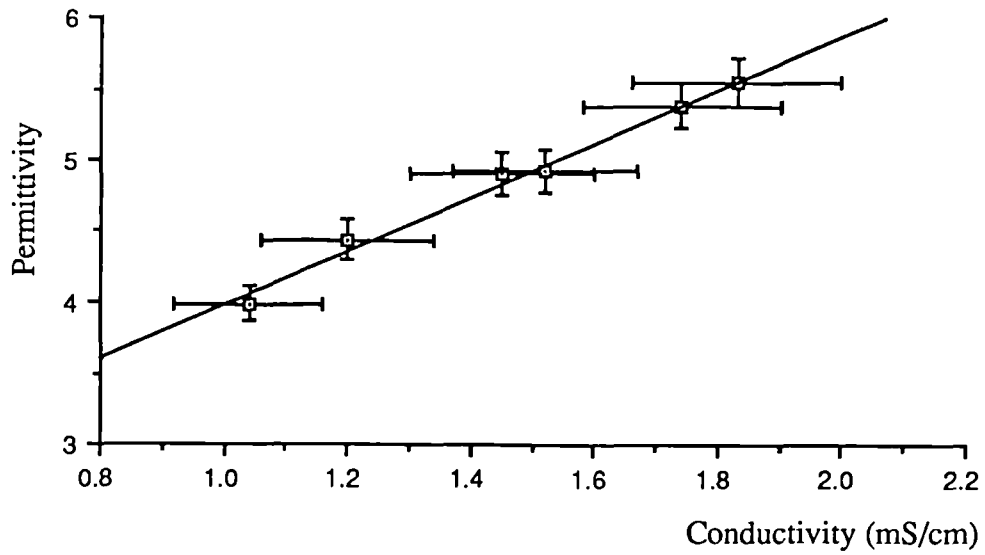
Figure 5.3   Patient 6 — Variation of permittivity with conductivity
for fat tissue
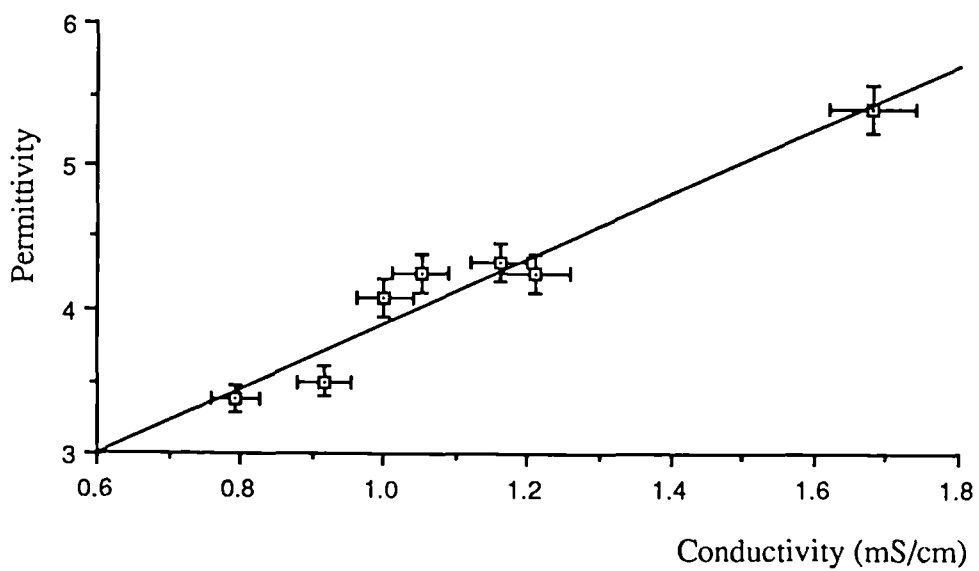
Figure 5.4   Patient 13 — Variation of permittivity with conductivity
for fat tissue

the data were correctly measured, so that the strong correlation is caused by a statistical anomaly.

5.4.3 Water contents in individual patient samples

Water content measurements were made on the individual samples of fat from patient 13. Figures 5.5a and b show the relationships between permittivity and water content, and between conductivity and water content for these fat samples. The errors on the water content are set at $\pm 1\%$ for all data points, which is an estimate of the measurement precision (Section 4.6). Clearly, there is a trend towards higher conductivity and permittivity with increasing water content. The data are correlated and may be fitted to straight lines with a correlation coefficient of about 0.94. Water contents ranged from 17% to 27% by weight.

A study was also made of the water content of fat from patient 6. Although larger 'average' water contents were measured, a number of tissues samples were used weighing between 0.07 and 0.4 g: their water contents ranged from 14% to 25%.

These ranges of water contents in individual patients are probably representative of the variation of water content in normal breast fat.

5.4.4 Dehydrated fat

In one case, patient 9, measurements were made of the dielectric properties of the liquid and solid substances, probably lipids and protein, left after drying the tissue at 105°C (Figure 5.6). This allowed an estimate to be made of the dielectric properties of the non-water content of breast fat tissue:

$$\varepsilon' \ (0\% \ \text{water}) = 2.57 \pm 0.10$$

$$\sigma \ (0\% \ \text{water}) = 0.325 \pm 0.024 \ \text{mS/cm} \tag{5.6}$$

5.4.5 Water contents

Figures 5.7a and b show scatter plots of permittivity and conductivity against water content by weight for all the fat and bone data from Table 5.1. The points are

(a)

(b)
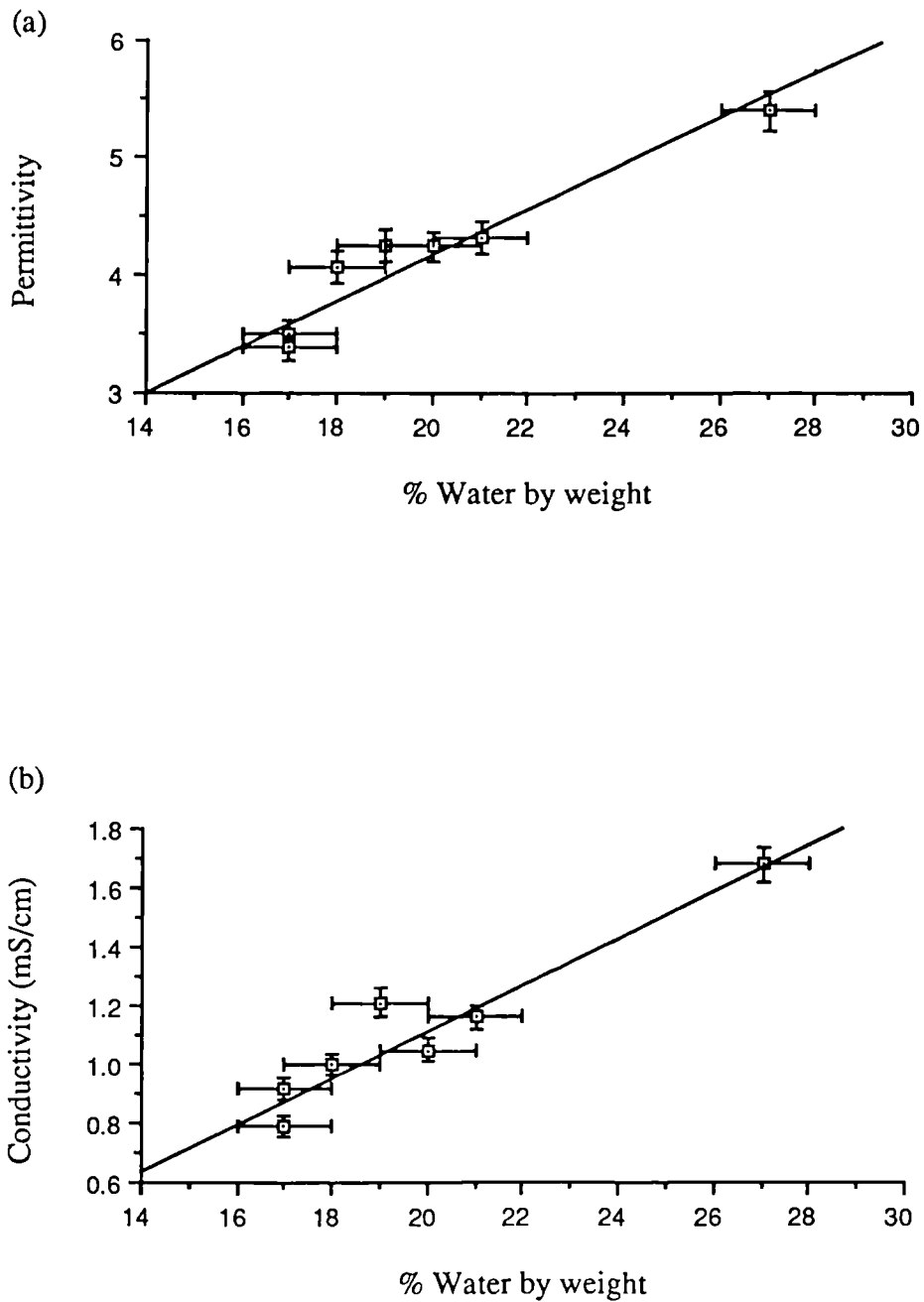
Figure 5.5   Variation of (a) permittivity and (b) conductivity with water content for the fat of patient 13. The fitted lines are:

$$\varepsilon' = 0.195 \ w + 0.28$$

$$\sigma = 0.079 \ w - 0.476$$

where w is the percentage water by weight and conductivity is in mS/cm.
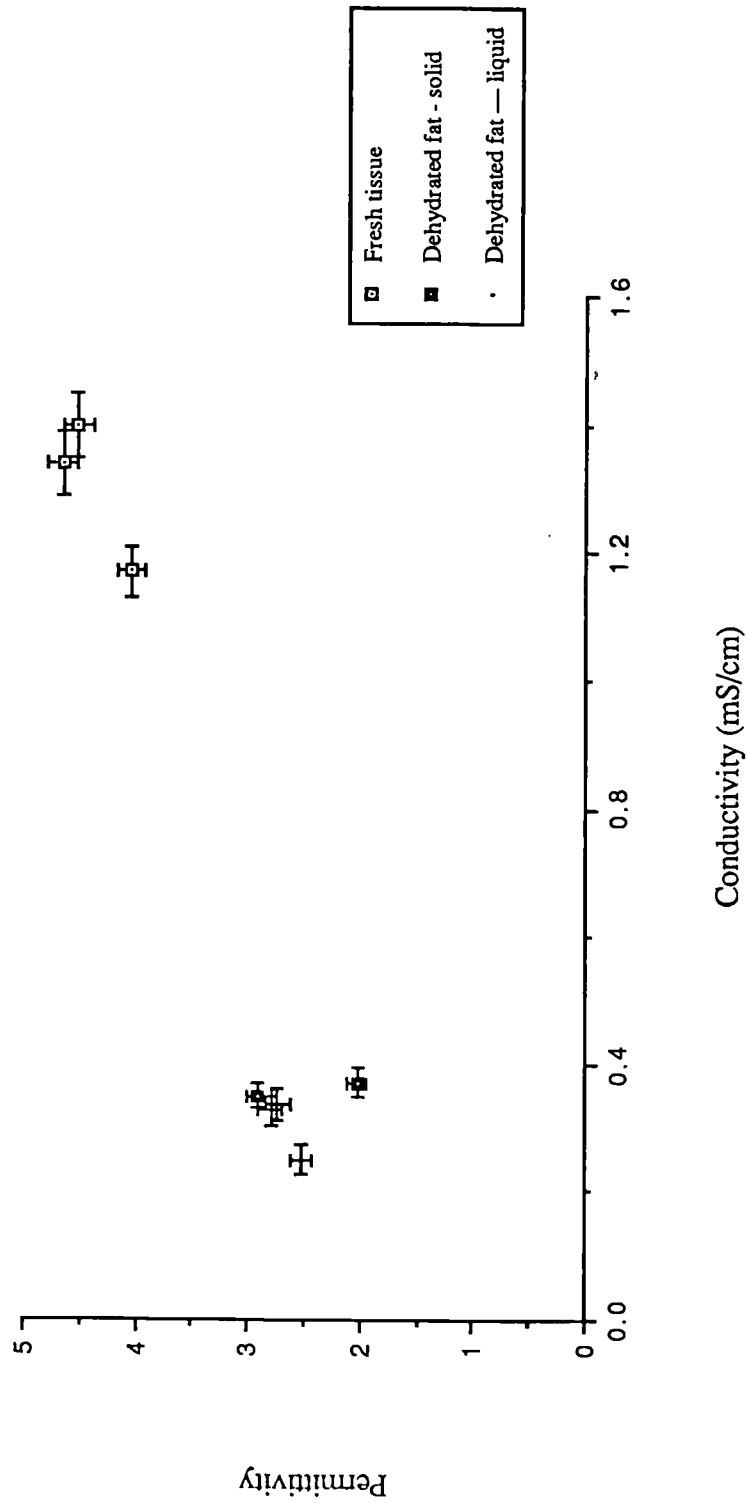
Figure 5.6   Variation of permittivity and conductivity for fresh and dehydrated fat

(a)

Fat — actual water content
Fat — averaged water content
Bone — actual water content

(b)
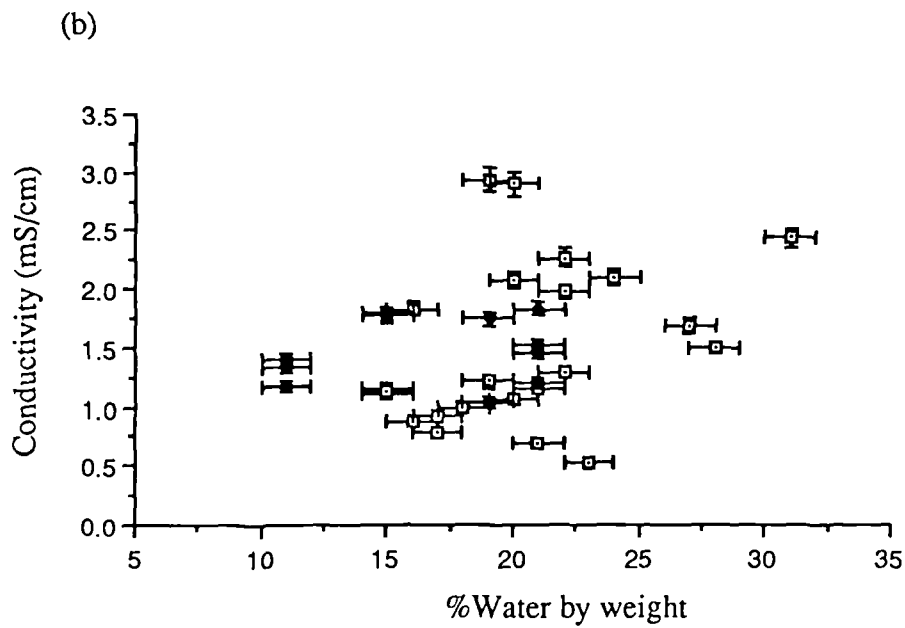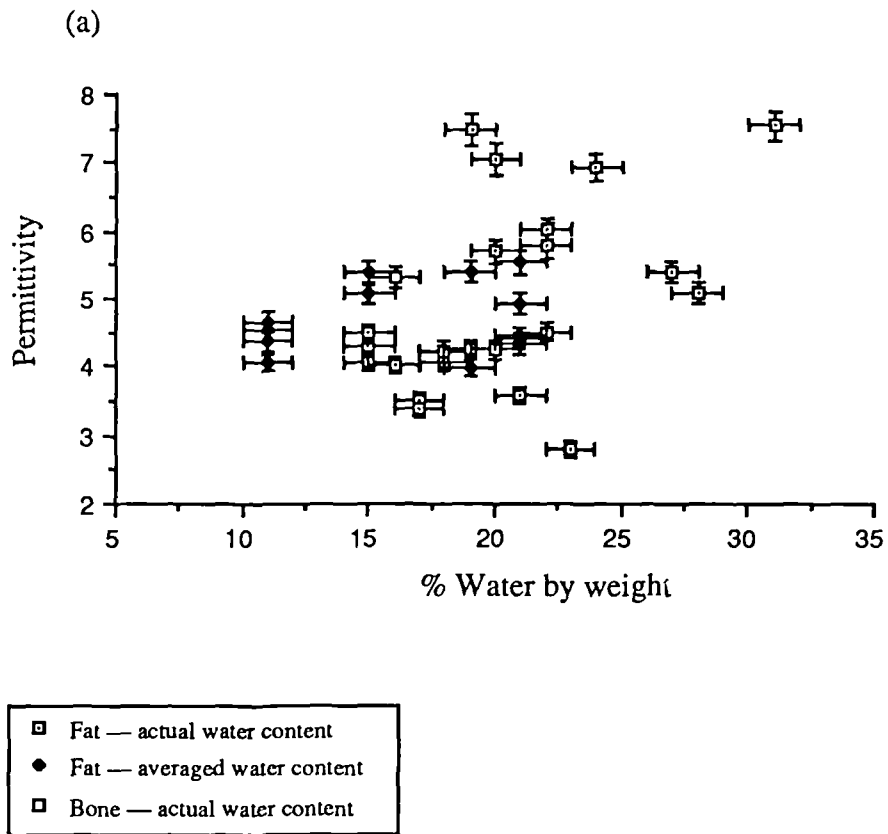
Figure 5.7   The variation of (a) permittivity and (b) conductivity
              for fat and bone tissue (including data with averaged
              water contents

completely uncorrelated, unlike the data shown in Figure 5.5, and appear to convey little information. However they may be compared with some of the models discussed in Chapter 2. Using values of dielectric constant for the non-water content tissue from (5.6), and values for physiological saline at 25°C from Table 3.5, the limiting conditions for a mixture of water in fat were calculated from (2.28) and (2.29). These series and parallel solutions, and Hashin-Shtrikman bounds, are compared with data in Figures 5.8a and b; water contents by volume have been converted to water contents by weight, using 0.86 g/cm^3 for the density of the non-water content of fat (Smith and Foster, 1985). Also shown on this graph are two points from Schepps and Foster (1980) interpolated from their empirical model at 1 — 5GHz (Section 3.4.6 and Figure 3.11); their lower point was data taken on fat, and their upper point shows data from a sample of lipoma.

Most of the new data fall within the limits imposed by the Hashin-Shtrikman (1961) equations, and are nearer the lower bound than the upper, for permittivity in particular. This contrasts with the interpolated data from Schepps and Foster (1980) which lie either outside (permittivity) or on (conductivity) the upper bound.

Comparing Figures 5.5 and 5.7, it seems that a model may be adopted for the relationship of dielectric properties and water content only within the data from an individual patient. Clearly, because the scatter is so large, a choice of one particular model for all the data is impossible. This implies that different processes occur in the fat of different patients at microwave frequencies. There may be unpredictable variations in bound water between patients: it is likely from the reduced value of the relaxation frequency (12GHz compared to 20GHz) that a component of bound water does exist. (See the discussion of bound water in Section 3.5.)

5.4.6 Choice of values

In addition to knowing the ranges over which data are spread, it is very desirable when modelling tissues to be able to choose particular values for permittivity, conductivity and water content. It is possible for human breast fat to choose values
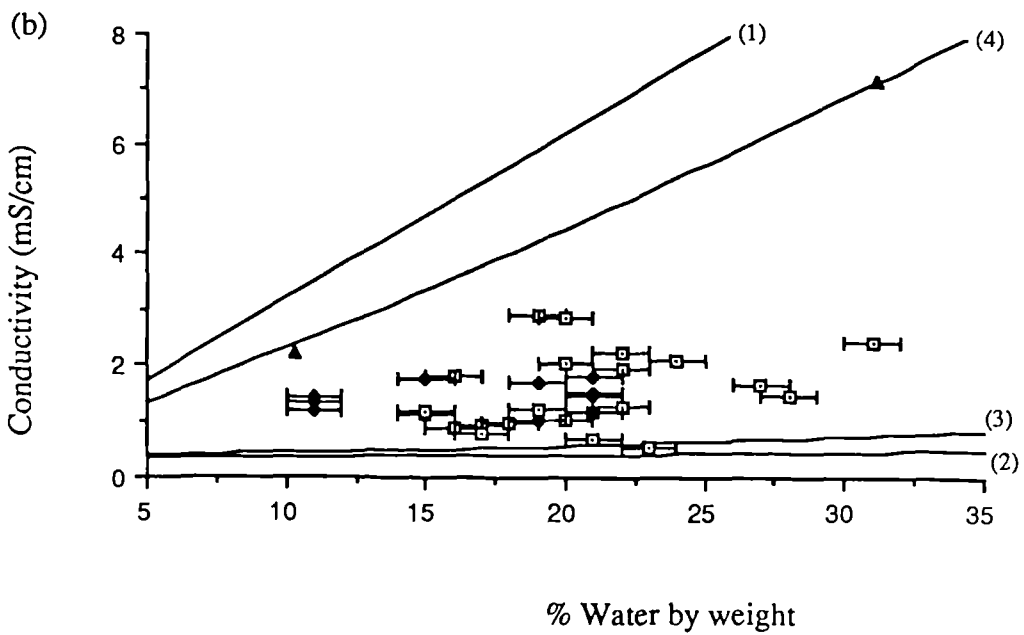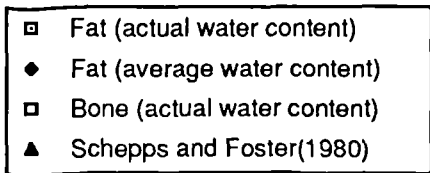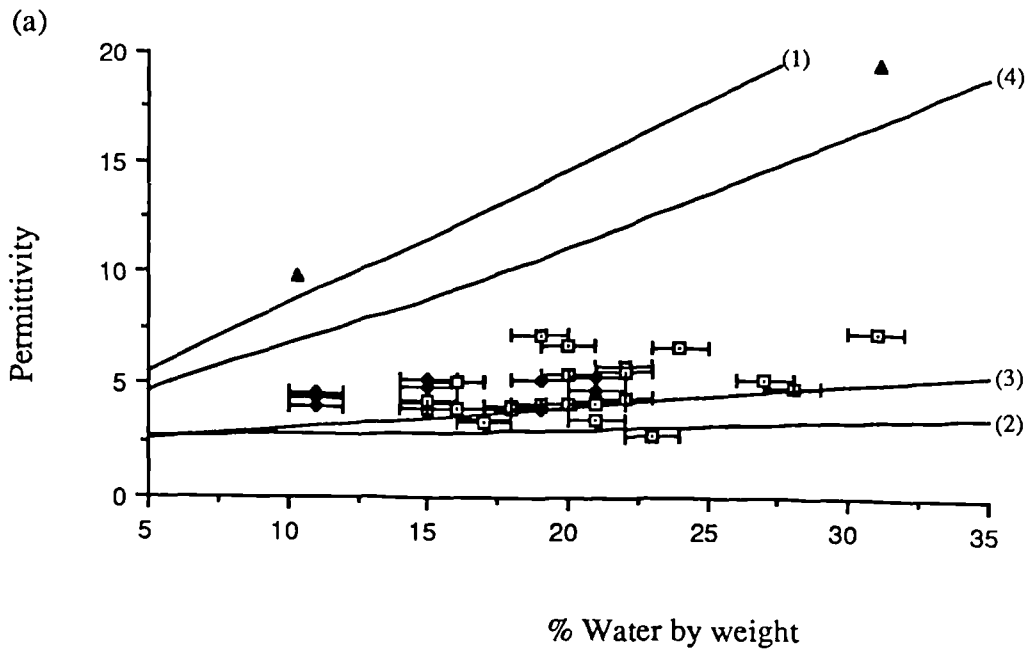
Figure 5.8   The variation of (a) permittivity and (b) conductivity
with water content for fat and bone tissues. The lines
are:
(1) Series solution (2.28)
(2) Parallel solution (2.28)
(3) Maxwell / Hashin Shtrikman lower limit (2.33)
(4) Hashin Shtrikman upper limit (2.29)

which are most likely. Figures 5.9a, b and c show histograms of the frequency of occurrence of permittivity, conductivity and water content. These graphs show clearly that ε' is most likely to lie in the range 4 — 4.5, and that σ is most likely to lie in the range 1.1 — 1.4 mS/cm. The two parameters should also be chosen to be consistent with (5.3).

The histogram of water contents (which are for particular samples, not averages) shows a peak distribution in the range 21 — 23%. However it is a less pronounced maximum and the overall distribution is not as clear as for Figures 5.9a and b. If values of water content are needed for breast fat, a value could be chosen anywhere in the region 15 — 23%.

5.5 Normal breast tissue

Twenty two measurements of the dielectric properties of female normal breast tissue were made, on eleven different patients. The relative permittivity was found to range from 9.8 to 46, the conductivity from 3.7 to 34 mS/cm, and the water contents from 41 to 76% water by weight. Table 5.2 shows the collected normal data, giving the permittivity, conductivity and water contents of each sample, and the age of the patient.

5.5.1 Relationship of permittivity and conductivity

As with breast fat, the permittivity and conductivity of normal breast tissue are linearly correlated (Figure 5.10). They may be related by the equation:

$$\sigma \text{ (mS/cm)} = m_{normal} \, \varepsilon' + c_{normal} \qquad (5.7)$$

where $\quad m_{normal} = 0.677 \pm 0.061$ (mS/cm)

$\quad\quad c_{normal} = -3.13 \pm 0.91$ (mS/cm)

which is the least squares fit through the data, taking into account errors in σ and in ε'.
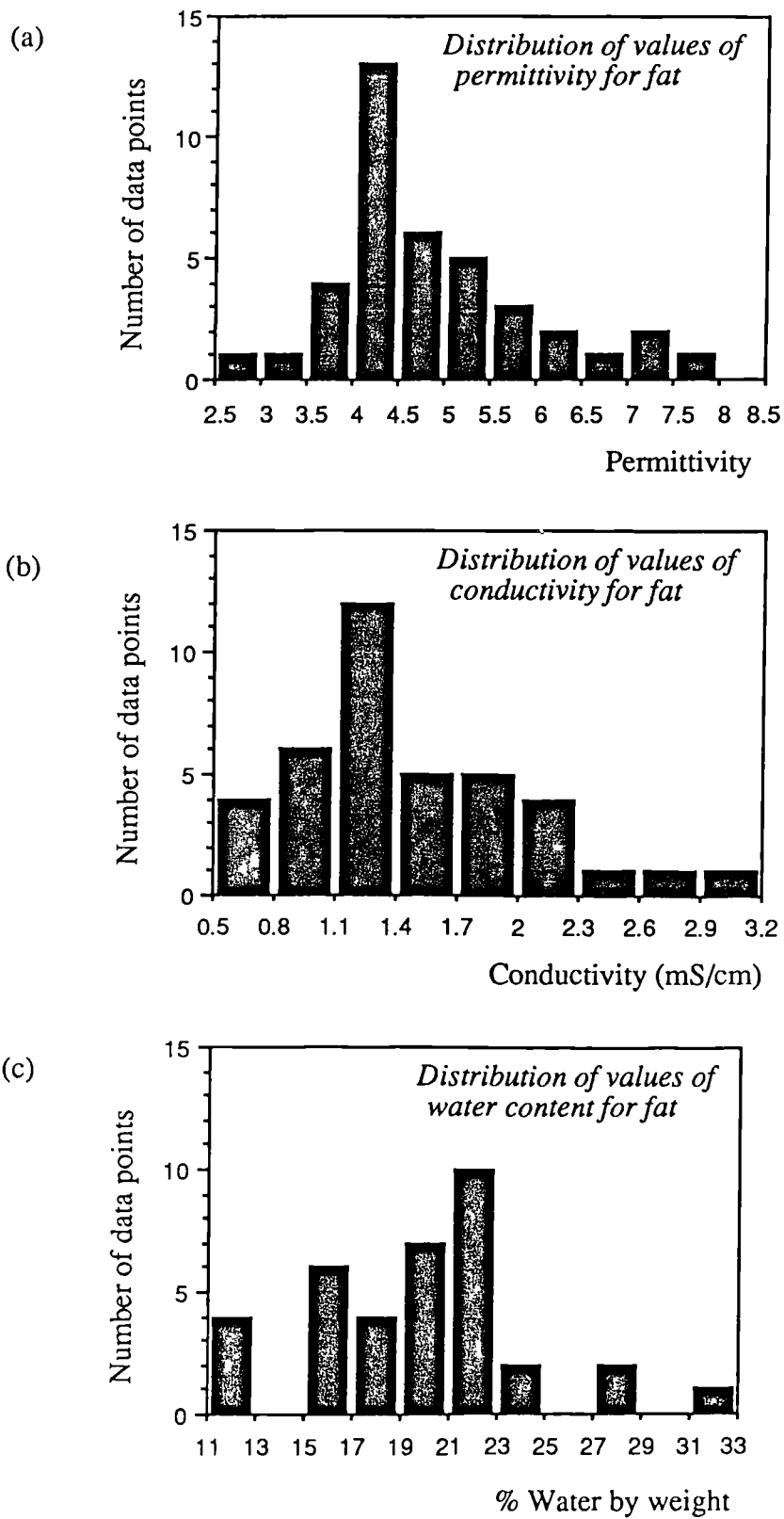
Figure 5.9   Histograms of the frequency of occurence of values of (a) permittivity, (b) conductivity and (c) water content of human breast fat

Table 5.2   The permittivity, conductivity and water
             content of normal human breast tissue

Patient number	Permittivity	Conductivity (mS/cm)	Water content (% by weight)	Age
2	13.9 ± 0.4	8.07 ± 0.30	50 (average)	66
3	29.3 ± 0.9 16.5 ± 0.5	12.7 ±0.4 7.66 ±0.24	62 (average	43
4	23.1 ± 0.7	8.53 ±0.30	65 (average)	37
9	24.7 ± 0.9 10.0 ± 0.3	13.5 ±0.5 6.45 ±0.24	46 (average)	59
10	41.4 ±1.5 13.6 ± 0.5	27.0 ± 1.2 5.58 ± 0.23	66 47	36
11	23.4 ± 0.9 16.1 ± 0.5	13.1 ± 0.5 8.31 ±0.35	47 46	68
18	32.4 ± 1.2 17.7 ± 0.7	22.2 ± 0.9 7.91 ± 0.32	63 57	66
20	51.3 ± 1.6 16.5 ± 0.6	33.6 ± 1.1 3.98 ± 0.32	72 76	46
23	33.9 ± 1.3 44.7 ± 1.7 45.7 ± 1.4 38.5 ± 1.2	20.8 ±0.8 33.0 ± 1.4 29.7 ± 0.9 24.6 ± 0.8	67 67 68 68	54
36	17.9 ± 0.6	6.70 ± 0.30	59	42
37	10.3 ± 0.5 25.1 ± 0.9 9.8 ± 0.4	4.47 ± 0.21 13.9 ±0.5 3.65 ± 0.15	49 52 41	80
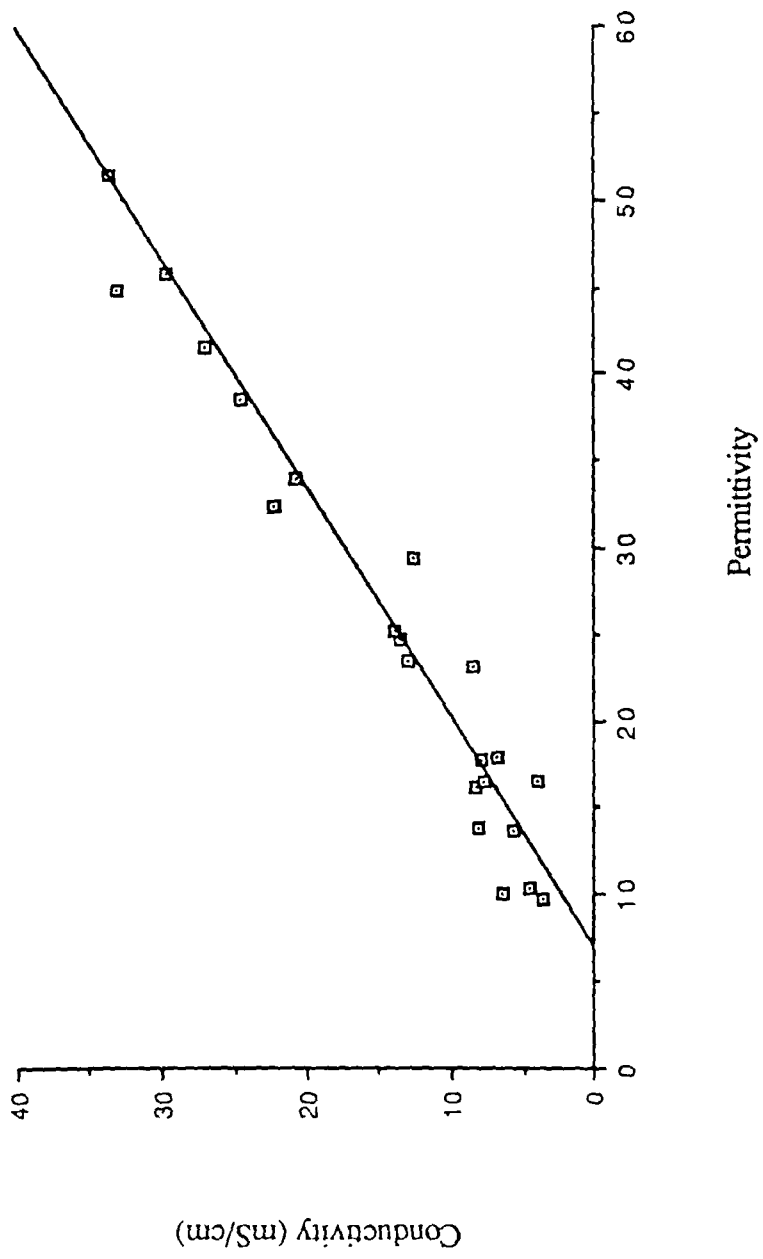
Figure 5.10   Variation of permittivity with conductivity for all normal breast tissue

The correlation coefficient for this data is 0.92.

Using (5.2) a Debye time constant may be calculated, which may describe an average of the dispersion processes involved:

$$\tau = 1.9.10^{-11} \text{ s}^{-1}$$

The relaxation frequency which parameterises the dispersion may be calculated:

$$f_c = 8 \text{GHz}$$

Again , this is below the relaxation frequency of saline (20GHz), which indicates that processes are involved other than the dielectric dispersion of saline.

5.5.2 Normal tissue in individual patients

For patient 23 it was possible to make four measurements of normal tissue (Figure 5.11). The relationship between permittivity and conductivity in the data from this patient show that within individual patients, these parameters are probably correlated. These data also give some indication of the range of permittivity and conductivity that can be expected within normal tissue with a homogeneous distribution of water (the four samples had water contents 67 — 68% by weight): permittivity ranges from 34 to 46, while conductivity ranges from 21 to 33 mS/cm.

Data from other patients shows that a much wider range of permittivity and conductivity may be expected in tissue with a heterogeneous distribution of water. In tissue from patient 37, permittivity ranged from 10 to 25, conductivity from 4 to 14 mS/cm and water contents from 41 to 52% by weight. The two measurements on normal tissue from patient 10 showed widely differing properties: permittivities of 14 and 41, conductivities of 6 and 27 mS/cm, and water contents of 47 and 66% by weight.

5.5.3 Water contents

Figures 5.12a and b show plots of permittivity and conductivity against water content by weight, for all normal tissue from Table 5.2. These graphs also show series and parallel solutions calculated from (2.28), for a mixture of protein in a saline
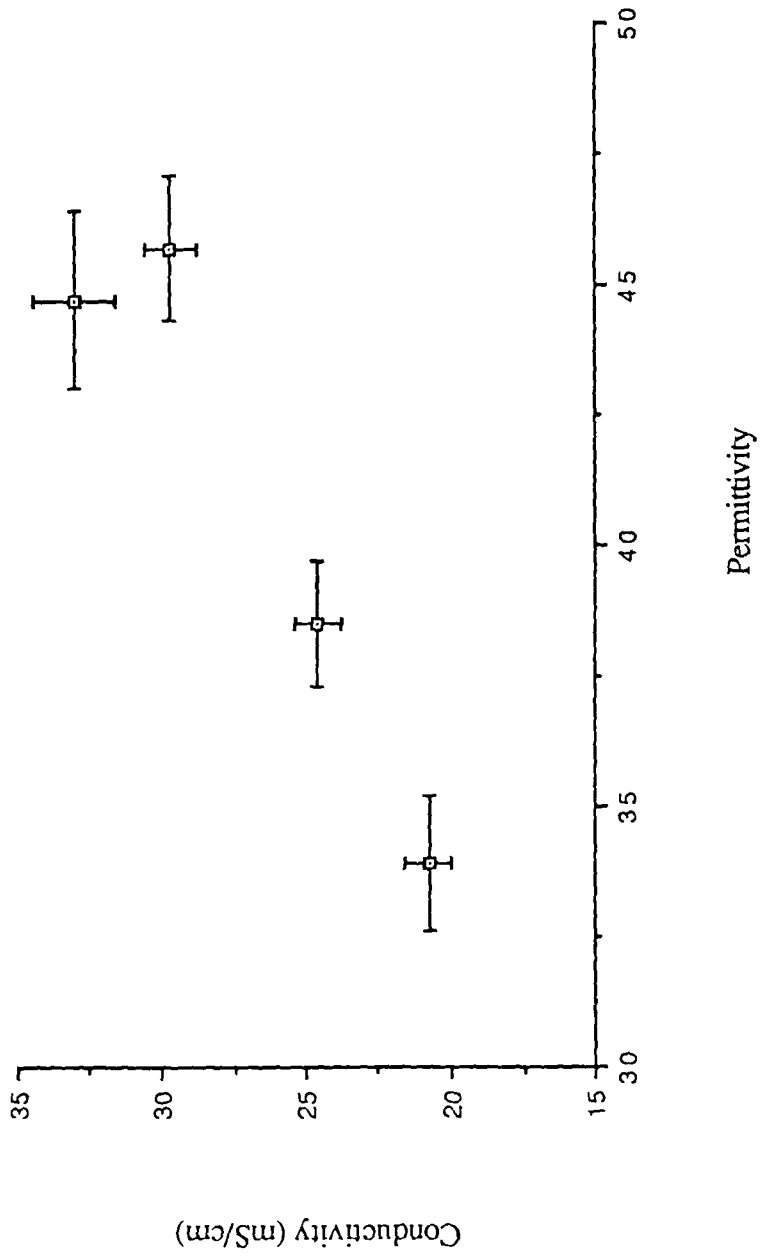
Figure 5.11   The variation of conductivity with permittivity in normal tissue from patient 23

(a)

(b)
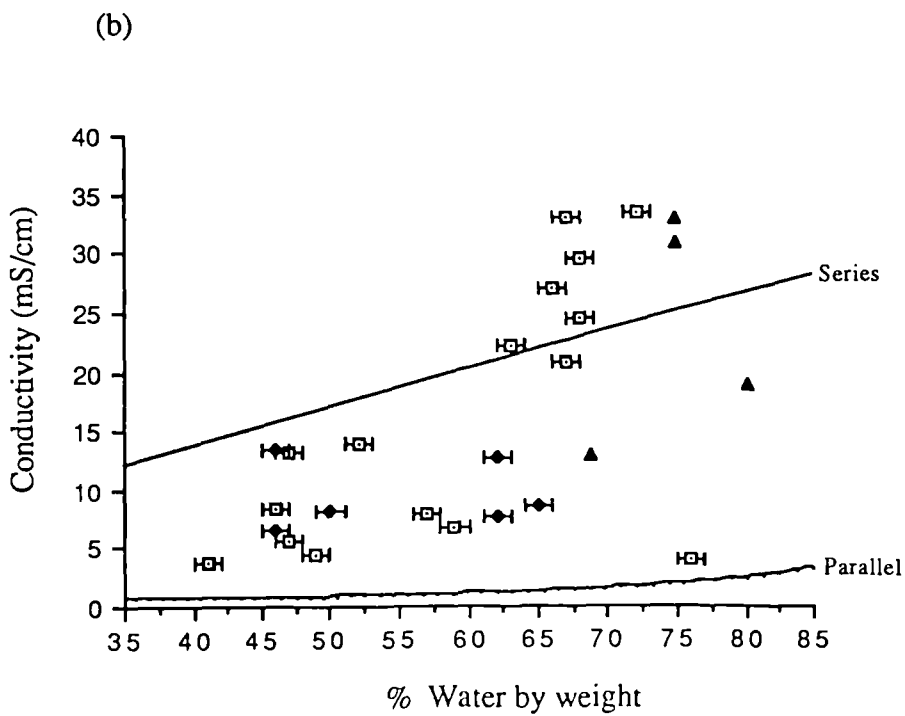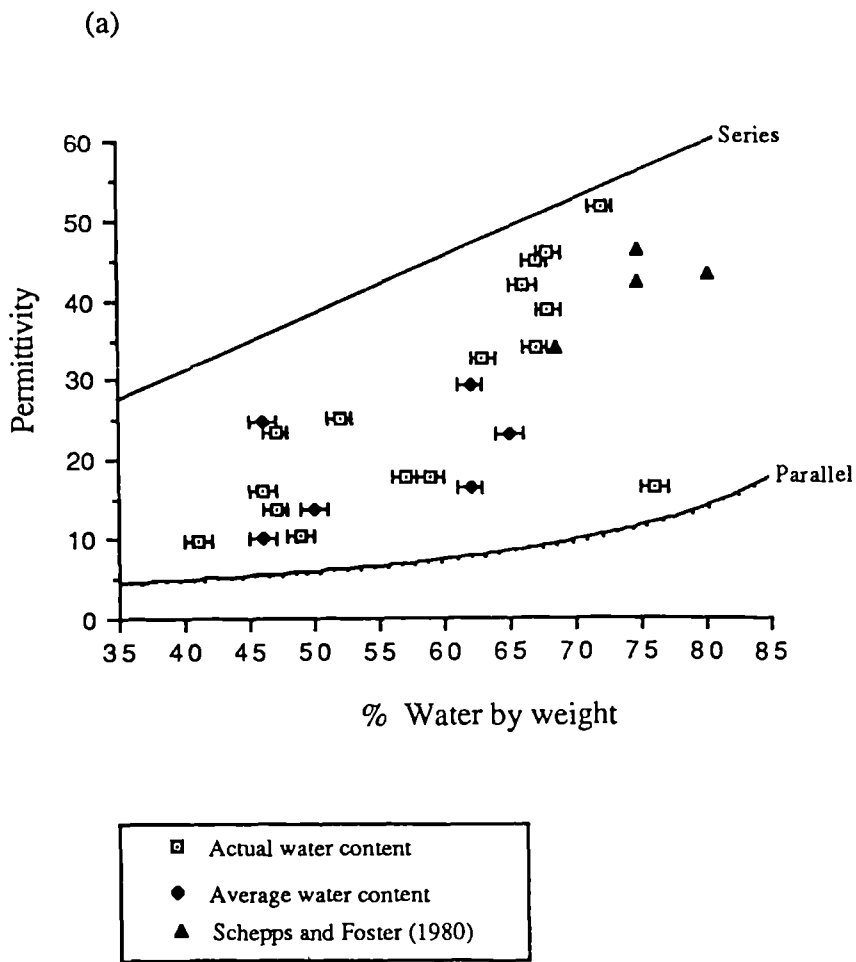
Figure 5.12   The variation with water content of (a) permittivity
and (b) conductivity of new data on normal tissues

continuum. The permittivity and conductivity of protein were taken to be those values in (5.6). These values are similar to those adopted by other modellers (Hasted, 1973). Water contents by volume were converted to water contents by weight using 1.3 g/cm^3 for the density of the non-water content of the tissue (Smith and Foster. 1985).

The permittivity data all lie within the theoretical limits and are scattered randomly between the bounds. The conductivity data show many data points which lie outside the limits: for several points conductivities are far in excess of expected values. Experimental data interpolated from Schepps and Foster (1980) are also shown in this figure: these data follow a similar pattern. The data which lie outside the bounds have about 70% water content and are close to the maximum conductivity possible in the models (33.5 mS/cm, the conductivity of saline at 3GHz and room temperature). This indicates that some other conductive process is occurring, in addition to the ionic conductance of the saline.

One possibility is that the conductivity of intracellular water, which comprises 67% of the total body water (Section 2.2), cannot in fact be approximated as physiological saline. Its ionic profile (Table 2.1) is different from plasma and interstitial water, containing more potassium ions. In Section 3.2 conductivity differences between the different body waters were discussed; it was concluded that because Na^+ and K^+ have similar dielectric decrements, the conductivities of the various body waters should be similar. However it is possible that the various proteins in intracellular water contribute more to the conductivity at 3GHz than is presently believed. This contradicts indirect evidence from Cook (1951) who suggested that the conductivity of intracellular water is less than that of physiological saline.

5.5.4 Choice of values

Figures 5.13a, b and c show histograms of the frequency of occurrence of permittivity, conductivity and water content for normal tissues. There is no clear distribution of dielectric data, although permittivity and conductivity both peak at
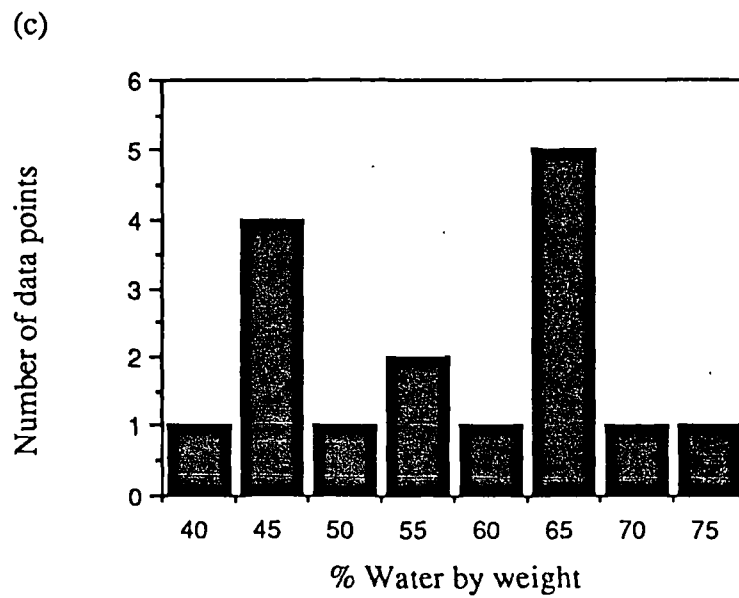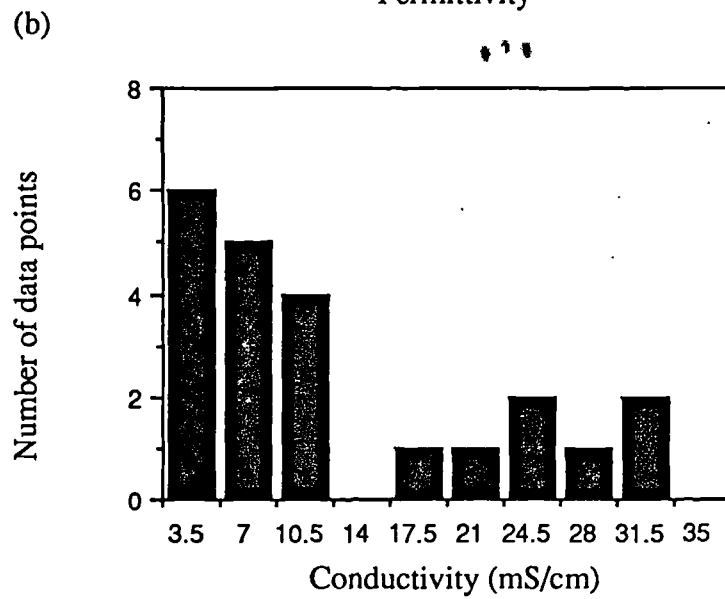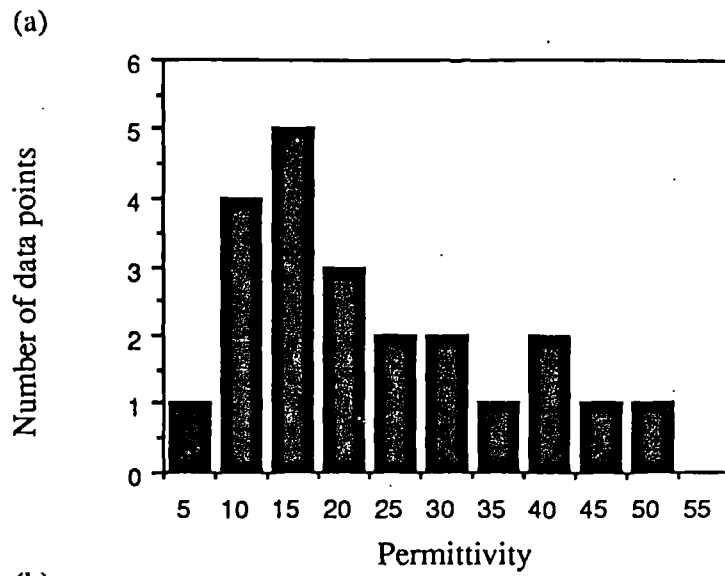
Figure 5.13 Frequency of the occurence of values of (a) permittivity,
(b) conductivity and (c) water content for normal tissues

lower values: permittivity from 10 to 20, and conductivity from 3.5 to 14mS/cm. The water content data is doubly peaked at around 45 to 50% and 65 to 70% water by weight. If values of permittivity, conductivity and water content are to be chosen, two typical ranges are possible: $\varepsilon' = 10 — 25$, $\sigma = 3.5 — 10.5$, % water = 45 — 50; and $\varepsilon' = 25 — 55$, $\sigma = 17.5— 35$, % water = 65— 70. Values of permittivity and conductivity should be chosen such that (5.7) is obeyed.

5.6 Benign breast tumours

Eighteen measurements of the dielectric properties of benign tumours of the female breast were made on seven different patients. Relative permittivities ranged from 15 to 67, conductivities from 7 to 49mS/cm, and water contents from 62 to 84% by weight. Table 5.3 shows the collected benign tumour data, including permittivity, conductivity, water content and pathology of the sample, and age of the patient. Three of the tumours were fibroadenomas, one was fibrosis, one epitheliosis, one adnosis and one fibroadrosis. These all are tumours containing mainly glandular tissue and are predisposed to subsequent breast cancer (Haagensen, 1986).

5.6.1 Relationship of permittivity and conductivity

As with other types of tissue, the conductivity and permittivity are closely correlated (Figure 5.14) and may be related by the equation:

$$\sigma \text{ (mS/cm)} = m_{benign}\,\varepsilon' + c_{benign} \qquad (5.8)$$

where $\quad m_{benign} = 0.698 \pm 0.060$ (mS/cm)

$\quad\quad\quad c_{benign} = -3.8 \pm 1.4$ (mS/cm)

The data have a correlation coefficient of 0.97. This line is consistent with (5.7), which relates the permittivity and conductivity of normal breast tissue. Using (5.2) values may be calculated for the Debye time constant and the relaxation frequency of

Table 5.3   Permitivity, conductivity, water content and pathology of benign breast tumours

Patient number	Permitivity	Conductivity (mS/cm)	Water content (% by weight)	Age	Pathology
7	34.1 ± 1.3	19.5 ± 0.7	75 (average)	27	Fibroadrosis Lump — 10 mm diameter No evidence of malignancy
	34.5 ± 1.3	23.4 ± 0.9	72 (average)		
8	15.4 ± 0.6	6.95 ± 0.28	36 (average)	43	Adnosis 2 lumps — 40mm and 20mm diameter No evidence of malignancy
	14.8 ± 0.5	7.66 ± 0.24	35 (average)		
	21.1 ± 0.8	10.7 ± 0.4	47 (average)		
	15.7 ± 0.6	7.51 ± 0.30	33 (average)		
12	43.5 ± 1.6	25.9 ± 1.2	67	26	Fibrosis Lump — no record of diameter No evidence of malignancy
	31.7 ± 1.2	17.8 ± 0.7	70		
	48.2 ± 1.8	32.8 ± 1.6	62		
	42.8 ± 1.3	28.5 ± 1.3	63		
15	23.0 ± 0.9	10.7 ± 0.4	62	40	Epitheliosis Lump — no record of diameter No evidence of malignancy
	27.8 ± 1.0	15.2 ± 0.6	60		

Patient number	Permittivity	Conductivity (mS/cm)	Water content (% by weight)	Age	Pathology
17	59.9 ± 2.3	34.5 ± 1.8	82	18	Fibroadenoma Lump — no record of diameter No evidence of malignancy
	55.3 ± 1.7	34.2 ± 1.2	84		
19	43.7 ± 1.7	32.5 ± 1.5	67	41	Fibroadenoma Lump — 5 mm diameter No evidence of malignancy
	55.9 ± 1.7	32.9 ± 1.2	72		
28	33.9 ± 1.0	14.8 ± 0.5	83	21	Fibroadenoma Lump — no record of diameter No evidence of malignancy
	67.3 ± 2.0	48.6 ± 1.5	83		
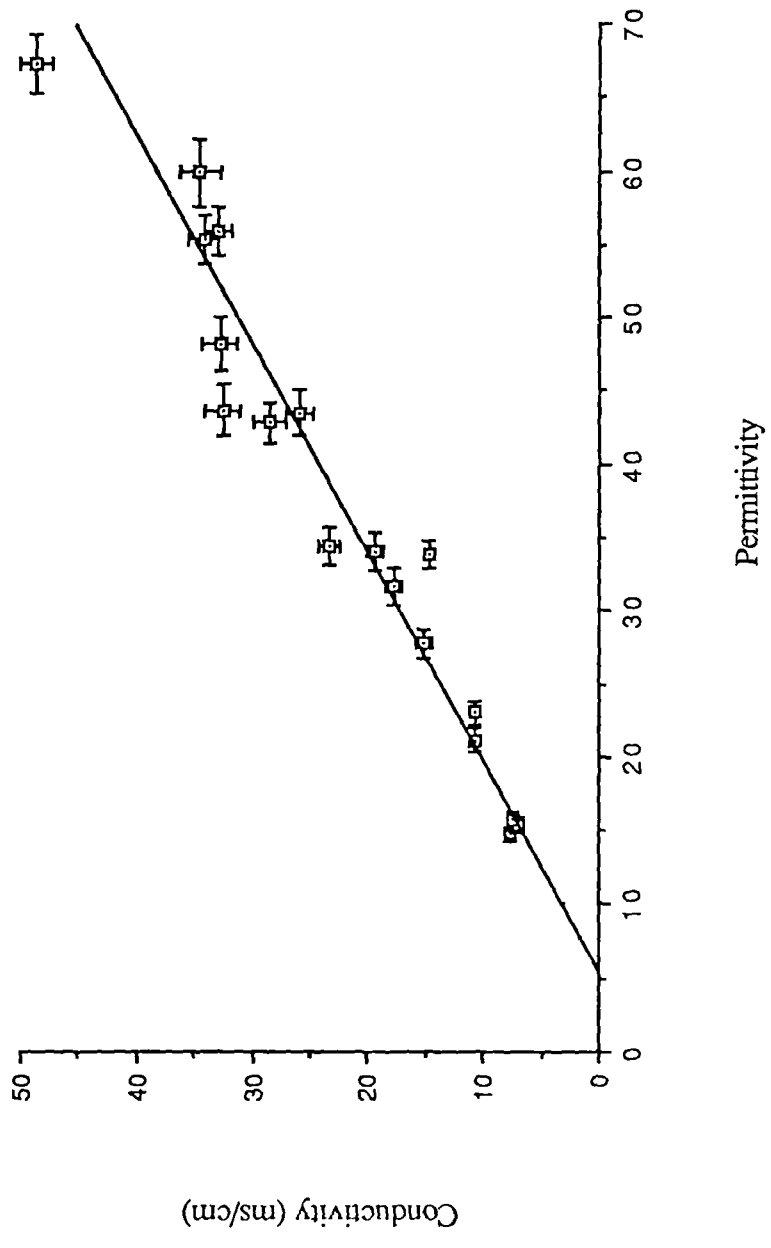
Figure 5.14   Variation of conductivity with permittivity for benign tumours

the underlying dispersive process:

$$\tau = 2.0.10^{-11} \text{ s}^{-1}$$

$$f_c = 8\text{GHz}$$

which are consistent with the values calculated for normal tissue.

5.6.2 Benign tumours in individual patients

Data from the adnosis of patient 8 is plotted in Figure 5.15, showing a strong correlation between conductivity and permittivity. One point on this graph, not shown in Table 5.3, is from tissue which was allowed to dry out for ten minutes at room temperature before measurement. Although few data points are available, and although water contents of individual sample were not measured for this patient, the linear relationship shown in the graph does suggest that it is the dielectric relaxation of tissue water which is the main process occurring at 3GHz in this adnosis. However, a rough value of relaxation frequency for the dielectric dispersion may be calculated to be 8 — 9GHz, so that if water is the main contributor to the dielectric properties, it may exist on various states of binding which reduce the relaxation frequency of the observed dispersion.

Four sets of data were taken on fibroadenoma from patient 12 (Figures 5.16a, b and c). This conductivity and permittivity data are strongly correlated, but permittivity and conductivity show negative correlations with water content.

The relationship of permittivity and conductivity to water content appears to be highly complex and may be completely different in different tissue types.

5.6.3 Water contents

Figures 5.17a and b show plots of permittivity and conductivity against water contents for all the benign data from Table 5.3. These graphs also show series and parallel solutions calculated for a mixture of protein in physiological saline. Most of the permittivity data lie within the bounds imposed by these models. As with normal tissue, a large proportion of the conductivity data lie outside the bounds, again
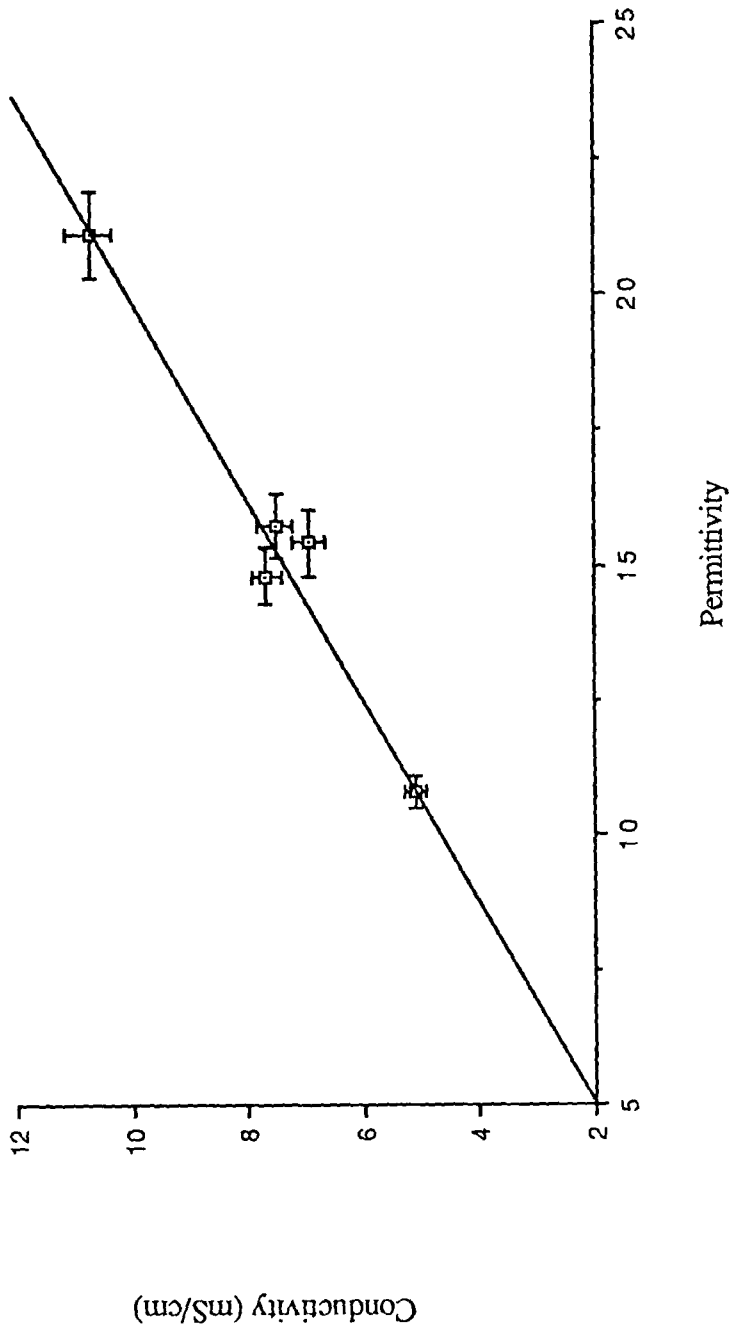
Figure 5.15   Variation of conductivity with permittivity for benign tumour· from patient 8

·One sample(the lowest data point) was left to dry for 5 minutes at room temperature.
Its dielectric properties were then remeasured.
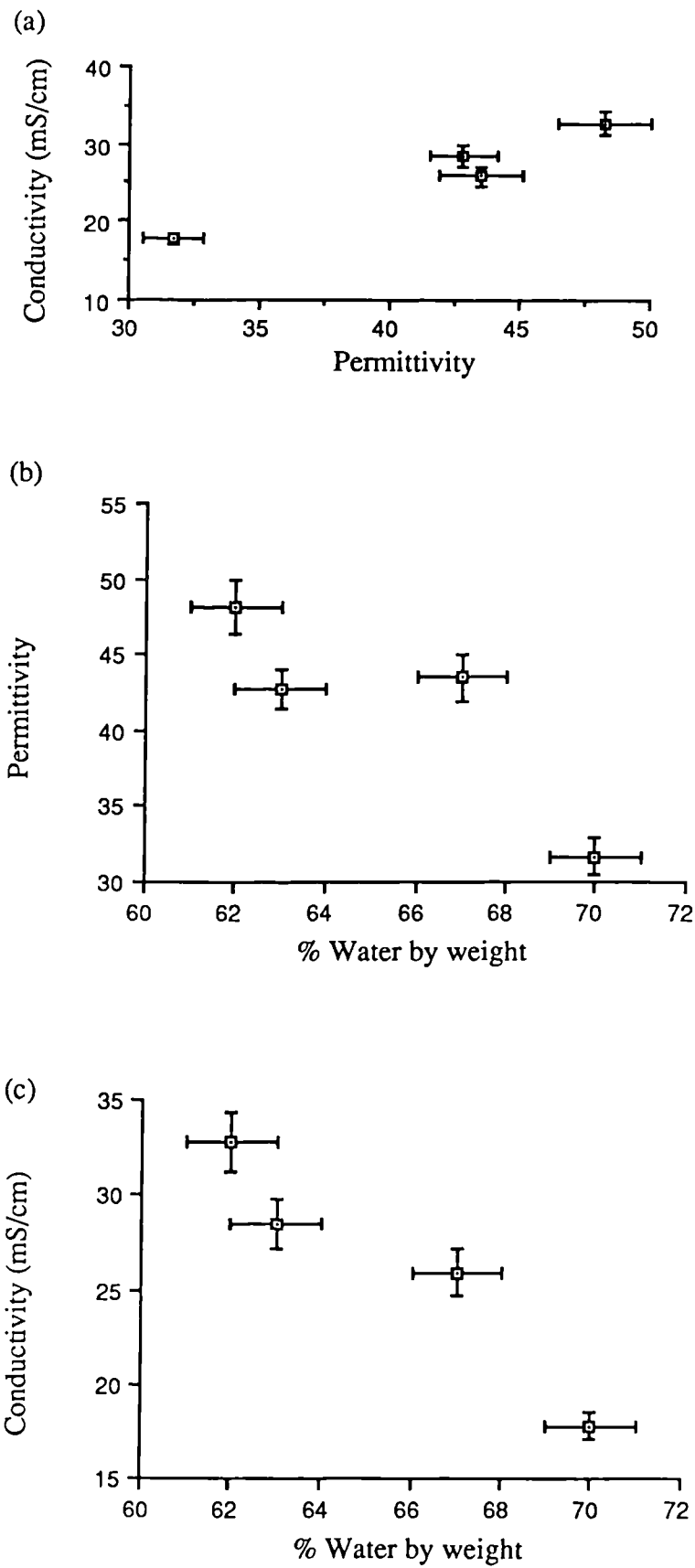
Figure 5.16   The variation of (a) conductivity with permittivity,
(b) permittivity with water content and (c) conductivity
with water content, for benign tumour from patient 12
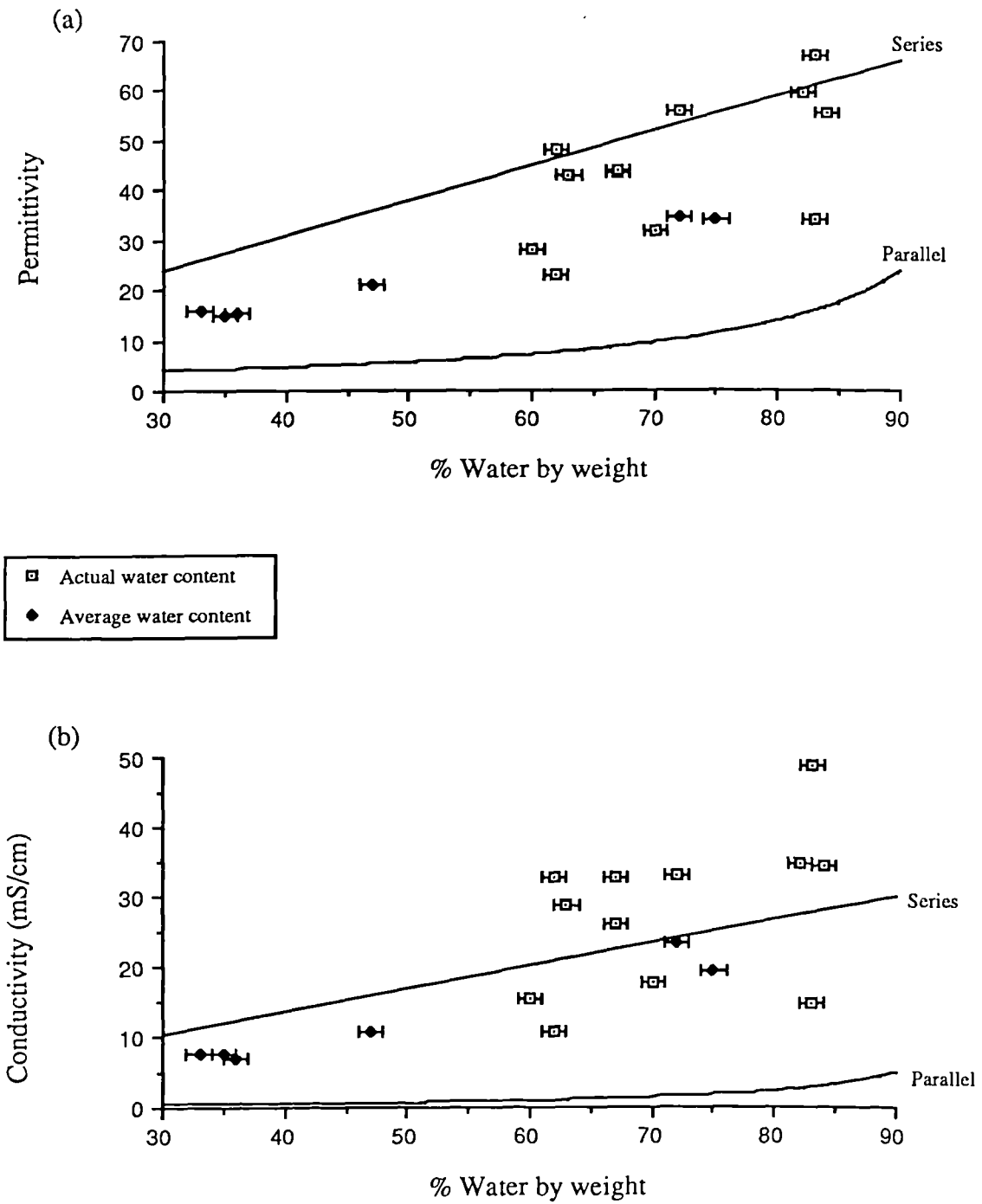
Figure 5.17   Variation of (a) permittivity and (b) conductivity
               with water content for benign tumour tissues

suggesting that some other conductive mechanism is occurring at microwave frequencies, in addition to the conductance of saline.

5.6.4 Choice of values

Figures 5.18a, b and c show histograms of the frequency of occurrence of permittivity, conductivity and water content. There is a very broad distribution of permittivity and conductivity values, and a doubly peaked distribution of water contents. Fibroadenomas are likely to have higher permittivities and conductivities than other benign tumours. Values should be chosen which relate to tissue type and which have permittivities and conductivities related by (5.8). The best range for permittivity is 10 to 50; for conductivity, 10 to 40 mS/cm; and for water content, 60 to 90% by weight.

5.7 Malignant breast tumours

Twenty three measurements were made of the dielectric properties of female breast carcinomas from nine different patients. Permittivities and conductivities showed a very wide spread of values, ranging from 9 to 59 in permittivity, and from 2 to 43mS/cm in conductivity. Water contents ranged from 66 to 79% by weight. In Table 5.4, the data collected on malignant tumours is presented: this table includes permittivities, conductivities, water contents and pathologies of samples, and patient ages. Two samples of tumour from patient 26 were stored frozen in liquid nitrogen before measurement. This is unlikely to have caused a significant change in dielectric properties compared to fresh tissue: Peloso et al (1984) measured the difference in dielectric properties at 0.1 to 1GHz of fresh and previously frozen rat muscle, and found the differences to be less than the experimental error on his measurements.

5.7.1 Relationship of conductivity and permittivity

Figure 5.19 shows the relationship of conductivity and permittivity for breast

(a)

(b)

(c)
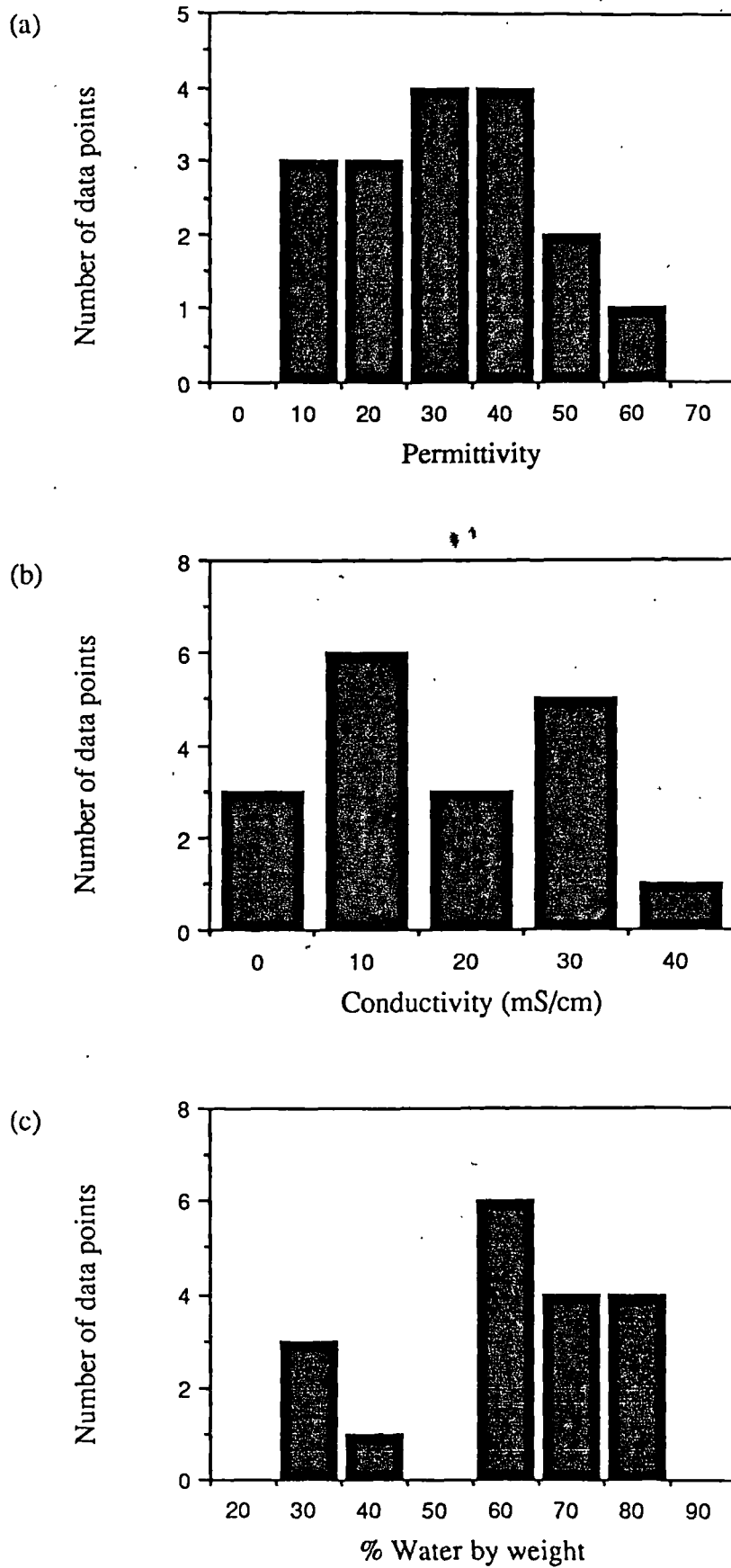
Figure 5.18   Frequency of occurence of (a) permittivity,
               (b) conductivity and (c) water content
               for benign tumours

Table 5.4   Permittivity, conductivity, water content and pathology of malignant breast tumours

Patient number	Permittivity	Conductivity (mS/cm)	Water content (% by weight)	Age	Pathology
21	45.1 ± 1.4	20.1 ± 0.7	66	71	Ca III This tissue — necrotic tissue
	37.9 ± 1.4	25.4 ± 1.1	67		
22	18.5 ± 0.7	7.1 ± 0.3	77	Not recorded	Ca I Diameter not recorded 0 +ve nodes, 4 -ve nodes
	55.5 ± 2.1	39.2 ± 2.0	78		
24	58.7 ± 1.8	43.2 ± 1.4	77	64	Infiltrating Ductal Ca I Lump — 30mm diameter 0 +ve nodes, 11 -ve nodes
	56.7 ± 1.7	42.7 ± 1.4	75		
27	53.5 ± 1.6	36.5 ± 1.2	77	68	Not available
29	55.2 ± 1.7	36.5 ± 1.3	77	61	Not available
31	50.1 ± 1.5	31.6 ± 1.0	79	86	Ca (stage not recorded) Lump — 30mm diameter 1 +ve node, 0 -ve nodes
	13.1 ± 0.5	9.78 ± 0.34	75		
	10.7 ± 0.4	2.49 ± 0.18	79		
	31.4 ± 1.2	16.9 ± 0.7	75		

Patient number	Permittivity	Conductivity (mS/cm)	Water content (% by weight)	Age	Pathology
26	51.7 ±1.6	32.7 ± 1.0	77	65	Ca II Lump — 30mm diameter 7 +ve nodes, 11 -ve nodes (a) These samples were frozen in liquid nitrogen and defrosted before measurement
	25.9 ±0.9	10.8 ± 0.4	74		
	18.2 ±0.6	5.6 ± 0.2	77		
	39.5 ± 1.5	25.8 ± 1.1	69		
	(a) 8.9 ± 0.4	2.3 ± 0.2	76		
	(a) 18.7 ± 0.7	6.3 ± 0.3	75		
	50.0 ± 1.9	34.4 ± 1.6	73		
	22.1 ± 0.8	9.0 ± 0.3	74		
37	50.2 ± 1.5	36.1 ± 1.1	70	80	Not available
	47.4 ± 1.4	33.6 ± 1.1	67		
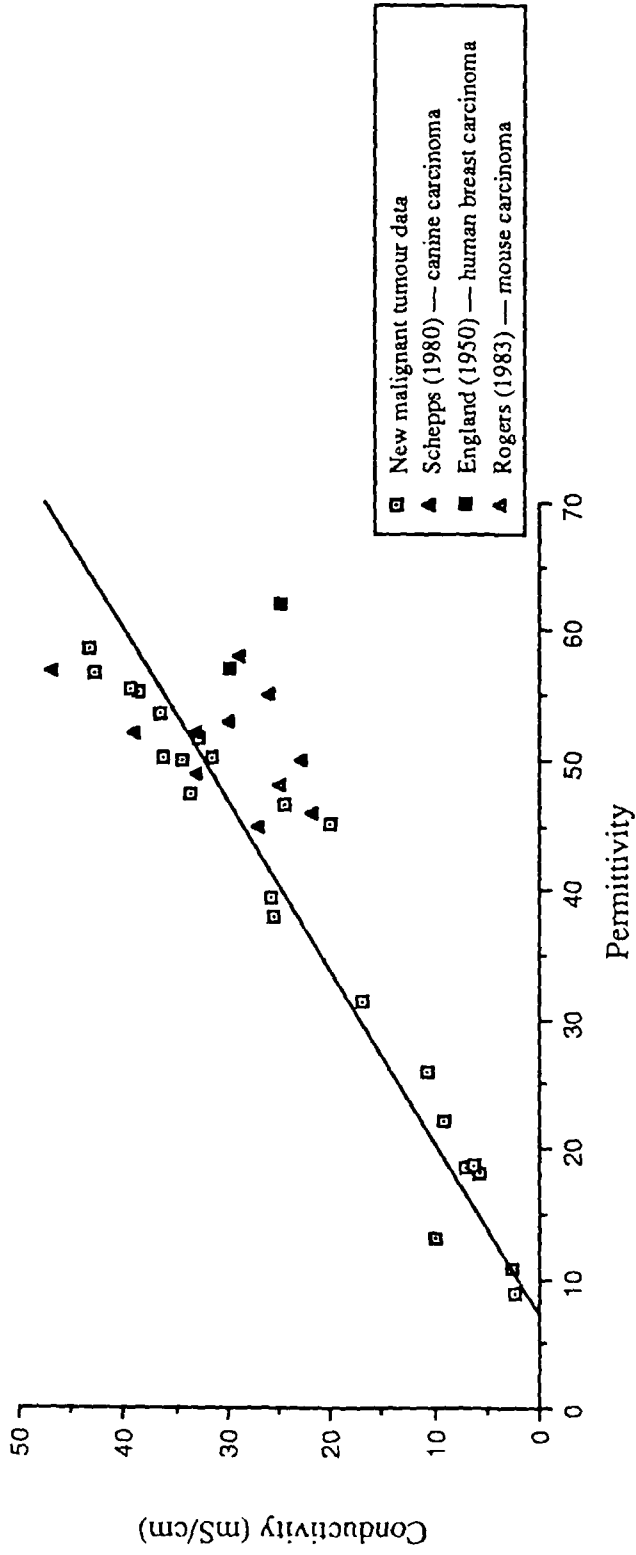
Figure 5.19   Variation of conductivity with permittivity for new malignant
tumour data with comparisons from the literature

carcinomas. The data are strongly correlated and may be related by the equation:

$$\sigma \text{ (mS/cm)} = m_{malignant}\varepsilon' + c_{malignant} \qquad (5.9)$$

where $\qquad m_{malignant} = 0.755 \pm 0.059 \text{ (mS/cm)}$

$$c_{malignant} = -5.6 \pm 1.2 \text{ (mS/cm)}$$

This equation is consistent with (5.7) and (5.8) which relate the conductivity and permittivity of normal tissue and benign tumours respectively. Values for the Debye time constant and for the relaxation frequency may be calculated:

$$\tau = 2.1.10^{-11} \text{ s}^{-1}$$

$$f_c = 8\text{GHz}$$

which are consistent with values calculated for normal tissues and benign tumours.

Malignant tumour data from the literature is also shown on this graph, taken from Tables 3.6 and 3.7; malignant tumour data interpolated from Schepps and Foster (1980) are also shown. The new data are clearly consistent with previously measured data, which show a greater spread. Only two previous measurements on human female breast carcinoma exist, published in 1950; these data lie below the empirical line (5.9). This is to be expected: because the new measurements were made at 3.2GHz, they would be expected to have higher conductivities than measurements at 3GHz, and slightly decreased values of permittivity. (See Figures 3.3a and b, which show slightly decreasing permittivity and rapidly increasing conductivity of malignant tumours above 3GHz.)

5.7.2 Tumour data in individual patients

Carcinomas from three patients, 22, 26 and 31, displayed a very large spread in values of conductivity and permittivity (Figure 5.20) without a corresponding spread in values of water content (Figures 5.21a and b). Section of tumours obtained in these cases were cross-sections of larger tumours and exhibited different consistencies of tissue within the one tumour. Tumour tissues which exhibited the expected high
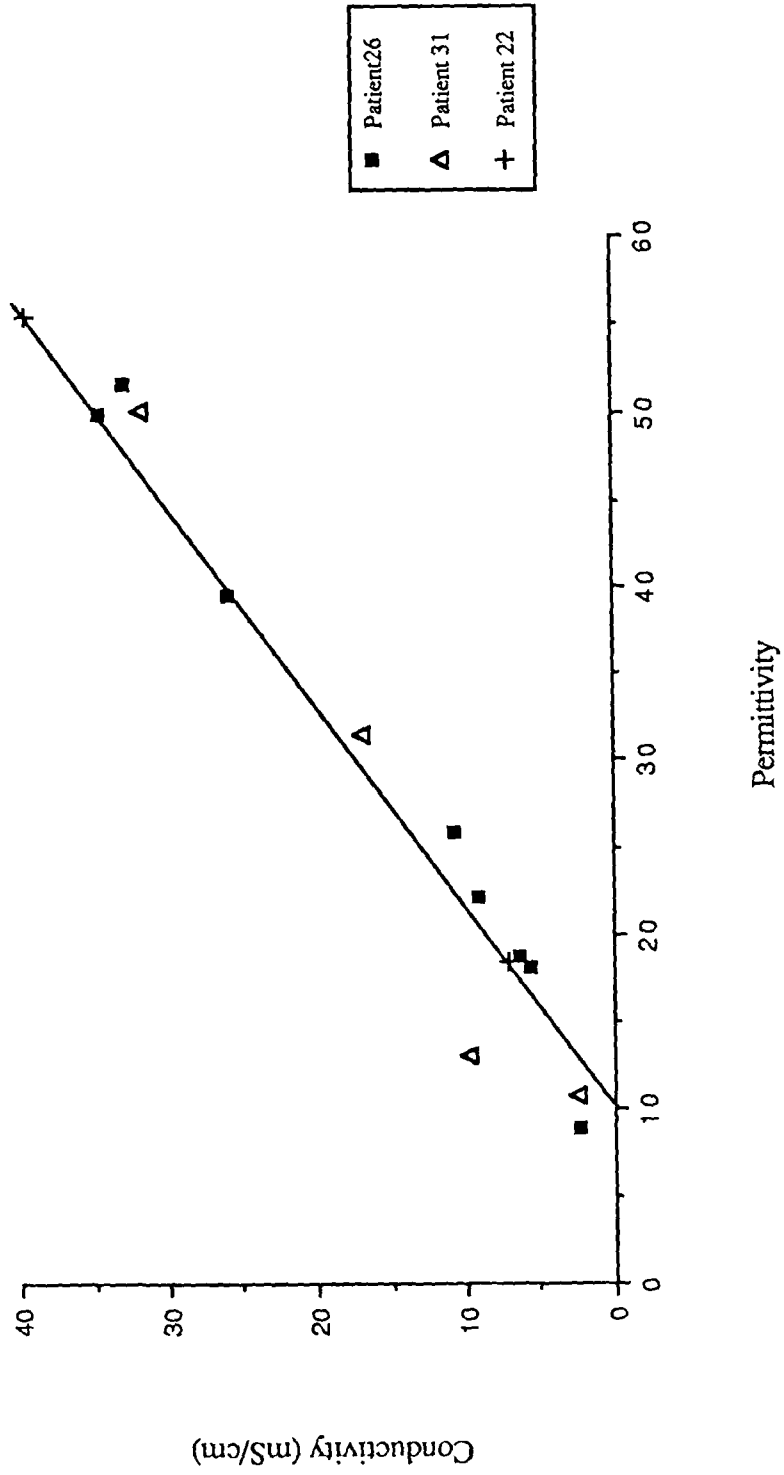
Figure 5.20   Variation of conductivity with permittivity for tumours from patients 22, 26 and 31
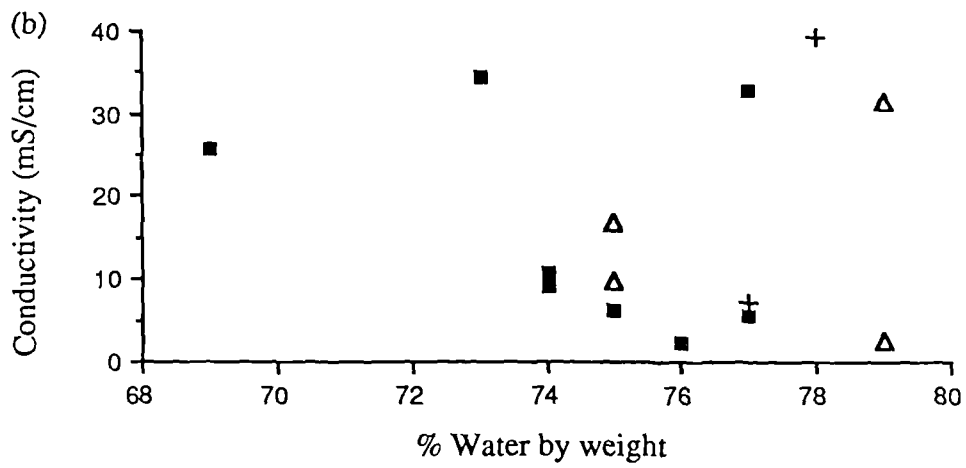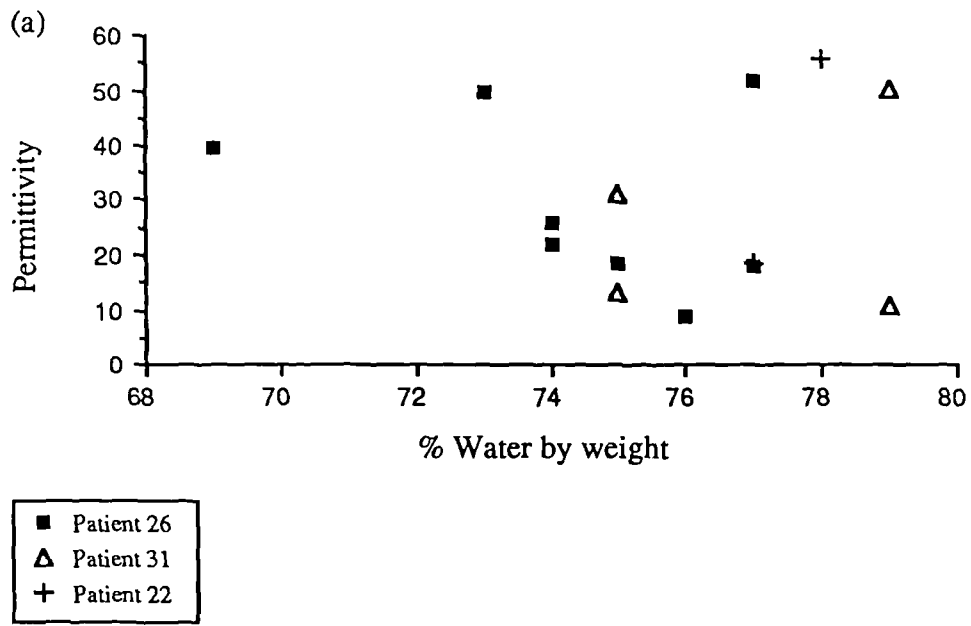
Figure 5.21   Variation of (a) permittivity and (b) conductivity
                      with water content for patients 22, 26 and 31

values of conductivity and permittivity were observed to be solid and hard, and to reduce to a powdery substance when dried. Tumour tissue which exhibited unexpectedly low values of permittivity and conductivity were soft and malleable, and reduced to a semi-solid viscous substance when dried. Surowiec et al (1988) also found tissues of widely varying properties within one type of human breast carcinoma, although their measurements were in a different frequency range (below 100MHz). They suggested that different properties probably reflected different stages of tumour development. This may also explain the widely varying properties observed at 3GHz. Samples with low permittivity and conductivity may have contained large amounts of necrotic tissue with most water molecules strongly bound and unable to rotate in the microwave field; or less probably, fibres from these tissues were aligned, by chance when forming the sample, along the sample axis so that they lay parallel to the electric field, thus reducing the observed dielectric constant.

Another possible explanation is that large or small pockets of air were held within the sample at the time of measurement because of difficulties in sample formation. However, these samples were malleable and easy to form, so that it seems unlikely that such a large number of similar errors would be made in sample formation. In all cases, the mass of tissue removed from the cavity was consistent with those of other samples, so that the volume of tissue could not have been greatly reduced in in these particular measurements. A test was made on a similar tissue (a high water content tumour) to discover how much the volume of tissue would have to be reduced in order to produce an effect of the order of that observed in patient 22 ($\varepsilon' = 16$, compared to $\varepsilon' = 56$). By inserting small amounts of tissue from each side of the cavity, an air pocket was produced inside the sample volume. It was found that the tissue volume had to be greatly reduced (by about a half to a third) in order to observe a comparably low value of permittivity. This reduction in sample volume was not observed in the tissue samples of patients 2, 26 and 31.

When the water content data are compared with those from other tumour data and with the series and parallel solutions (Figures 5.22a and b), most data from patients

22, 26 and 31 are seen to fall within the two limiting models.

5.7.3 Water contents

Figures 5.22a and b show plots of the variation of permittivity and conductivity with water content, compared to the bounds predicted by series and parallel solutions. Malignant tumour data interpolated from Schepps and Foster (1980) are also shown on this graph. As before, most of the permittivity data lie within the the two limits; but most of the conductivity data lie outside the bounds, with conductivities far in excess of those expected from a simple saline/protein mixture. The data points from Schepps and Foster confirm that this is a real effect, and not an anomaly of this particular technique.

5.7.4 Choice of values

Figures 5.23a, b and c show histograms of the frequency of occurrence of permittivity, conductivity and water content. Two distinct peaks can be observed in both the permittivity and conductivity histograms, and one peak in the water content graph. A choice of values is difficult and should depend on the type of modelling and the size of tumour to be modelled. From the data presented here, breast carcinomas are tissues with water contents in the range 75 to 80% water by weight; part of the tumour may have a high permittivity of about 45 to 60, and a high conductivity of about 30 to 40mS/cm; part of the tumour may have a low permittivity, of about 10 to 20, and a low conductivity of about 0. to 10mS/cm. These ranges perhaps reflect two extremes in tumour development.

5.8 Other tissue data

Two measurements were made on cartilage removed during a hip replacement operation on an elderly man who suffered from osteoarthritis. Cartilage is a specialised fibrous connective tissue which functions as a structural support while

(a)

(b)
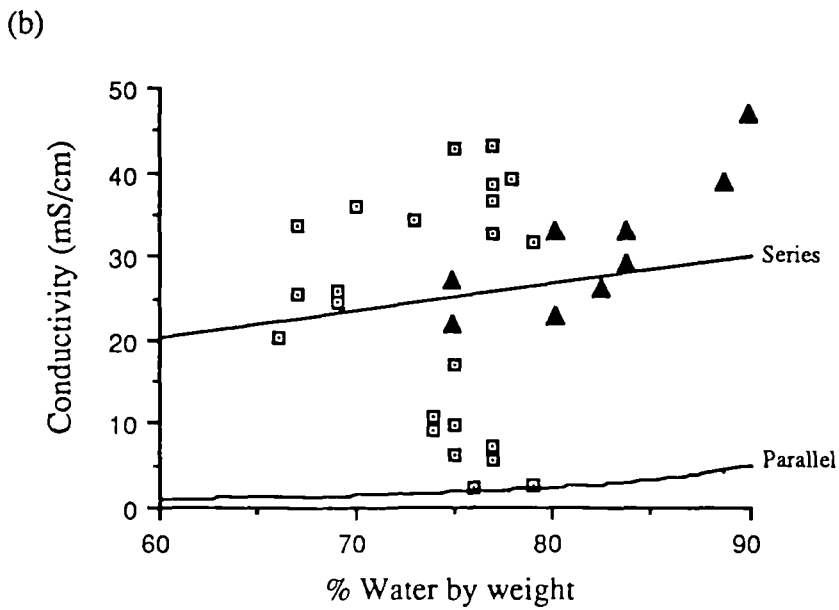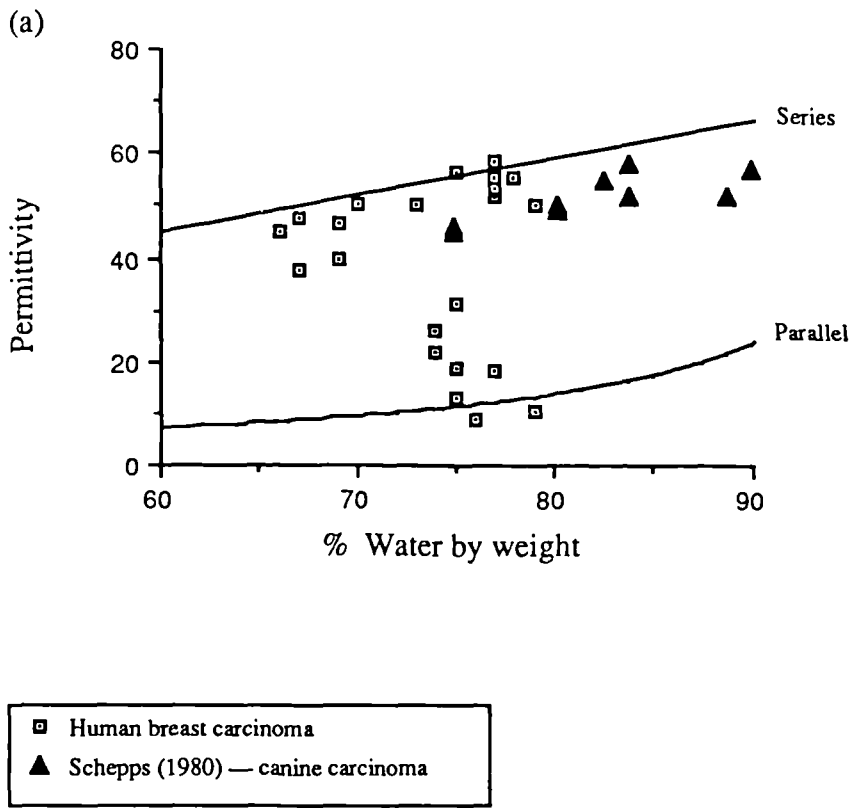
Figure 5.22   Variation of (a) permittivity and (b) conductivity
with water content for human breast carcinoma
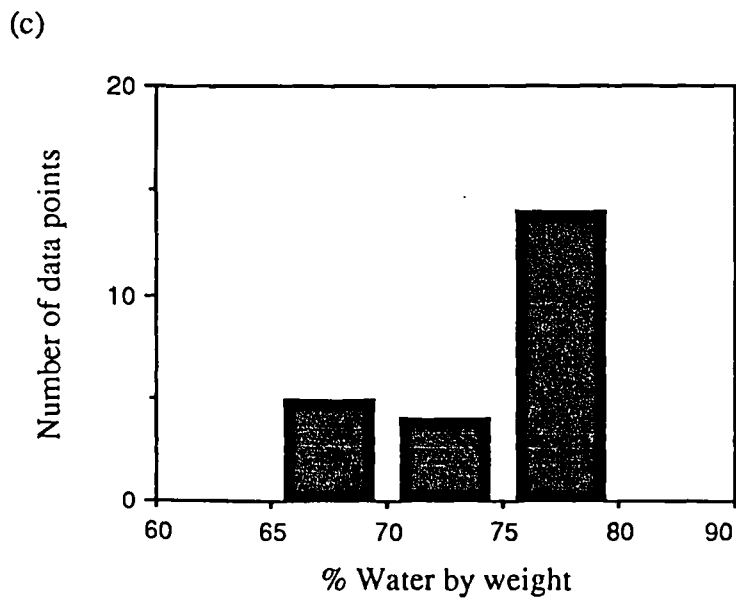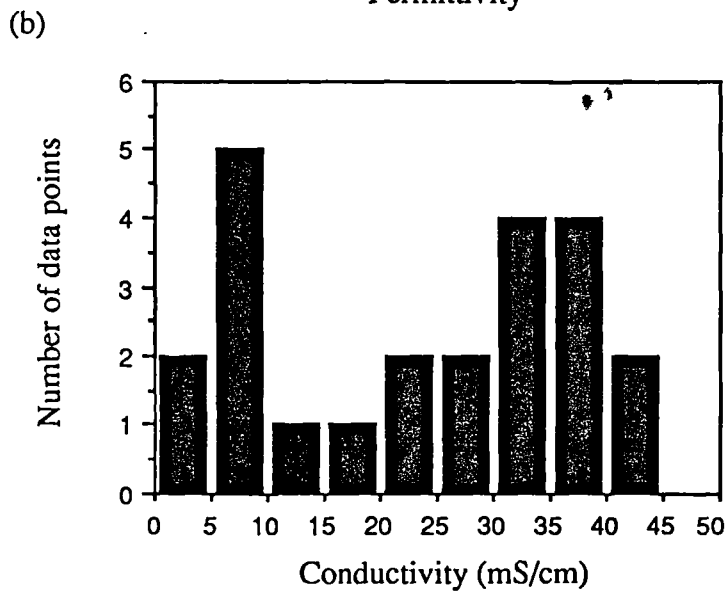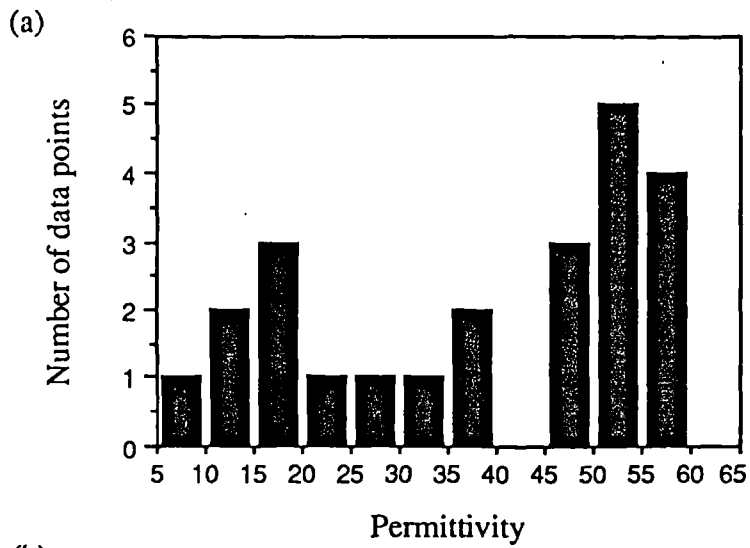
Figure 5.23   Frequency of occurence of (a) permittivity
(b) conductivity and (c) water content
for tumour tissues

remaining flexible. The cartilage at a synovial joint, such as the hip, hyelin cartilage, covers bones in a thin layer. Data from the two measurements are presented in Table 5.5.

Two data sets were taken on a sample of gynaecomastia from one patient, aged 51. The gynaecomastia was characterised by low permittivies and conductivities and a water content of about 40% by weight. These data are also presented in Table 5.5.

5.9 Comparisons between tissue types

For several patients (9, 11, 18, 20 and 23), data are available on both normal and fat breast tissues (Figures 5.24a—e). In all cases, normal tissue shows higher permittivity and conductivity than fat, although within normal tissue widely varying properties can be observed. It is clear that within one individual, fat and normal tissues are distinguishable by dielectric measurement.

For one patient (12), data are available on both fat and fibroadenoma (Figure 5.25). The benign tumour data show very much higher conductivities and permittivities than the fat data. The two tissues are clearly distinguishable by dielectric measurement.

Carcinoma, normal and fat tissue measurements were made on the breast tissue of patient 37. The carcinoma exhibited only high dielectric properties, which are clearly distinguishable from from the other tissue types (Figure 5.26). Despite the observed wide range of permittivities and conductivities in normal data from this patient, the highest value of permittivity and conductivity from this tissue is about half of the values observed for tumour tissue.

5.10 All non-fatty breast tissues

Information from Tables 5.2 to 5.5 have been combined to give an overall picture of the dielectric properties of non-fatty breast tissue. Figure 5.27 shows a plot of

Table 5.5   Permittivity, conductivity, water content and pathology of cartilage and gynaecomastia

| Tissue type	Patient number	Permittivity	Conductivity (mS/cm)	Water content (% by weight)	Age
Cartilage	39	36.7 ± 1.1 45.5 ± 1.7	30.2 ± 1.0 35.4 ± 1.8	62 66	85
Gynaecomastia	16	8.14 ± 0.52 9.99 ± 0.31	2.73 ± 0.25 3.44 ±0.12	40 39	51

(a)

(b)
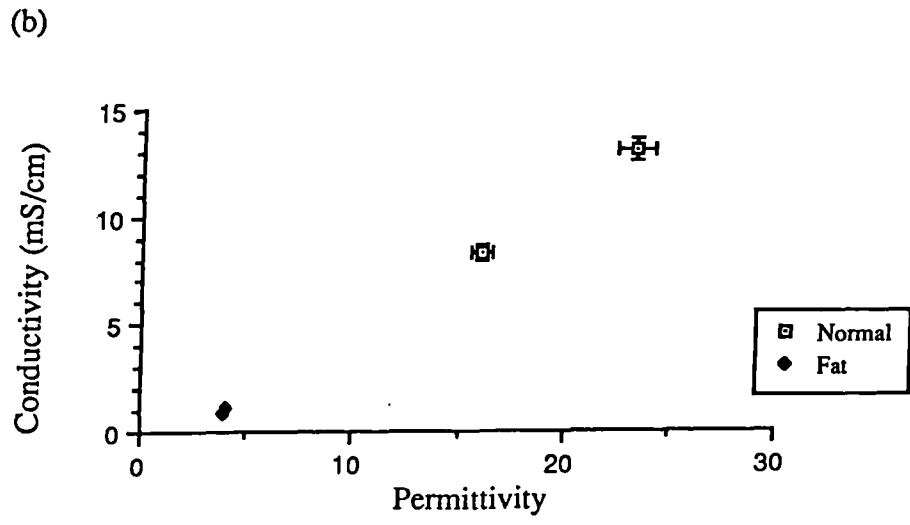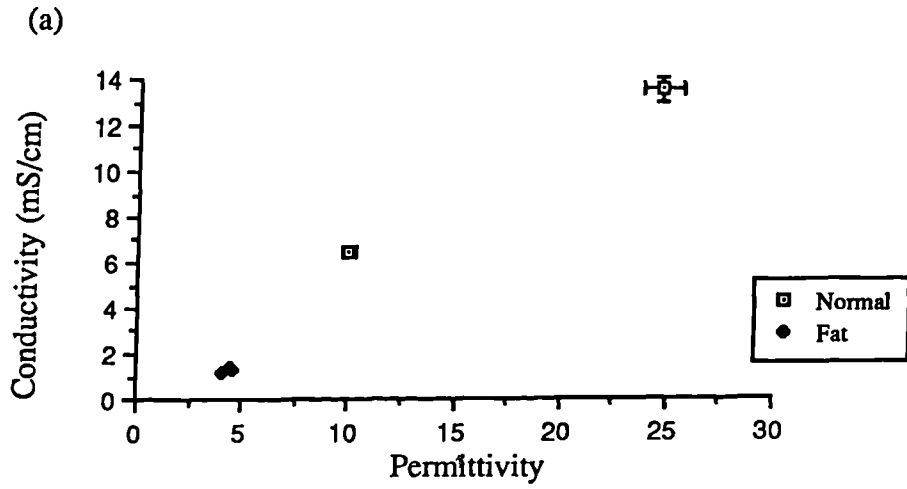
Figure 5.24   Comparison of normal and fat tissue

from patients (a) 9 and (b) 11

(c)
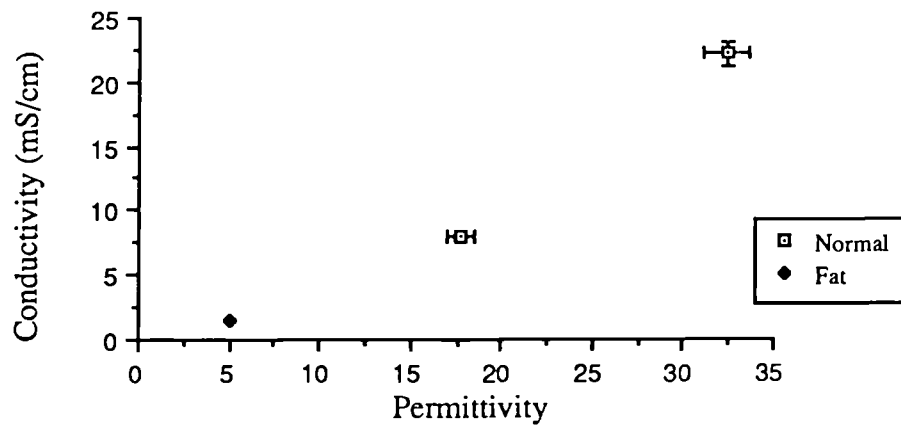
(d)
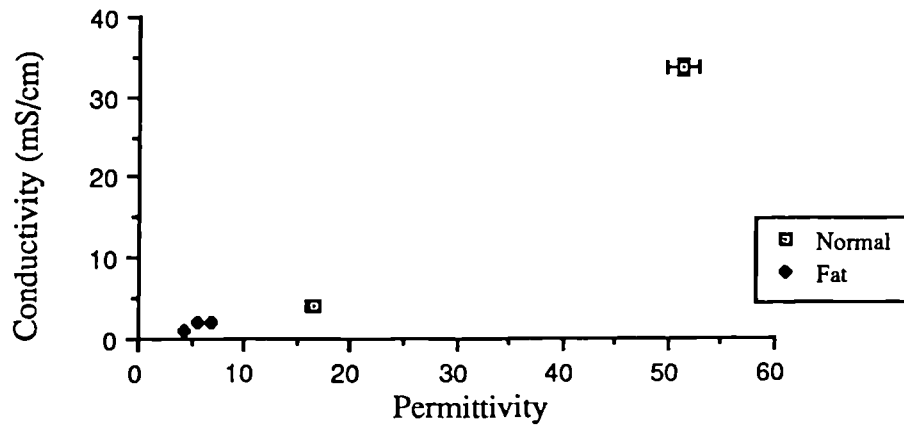
Figure 5.24   Comparison of normal and fat tissue
from patients (c) 18 and (d) 20

(e)
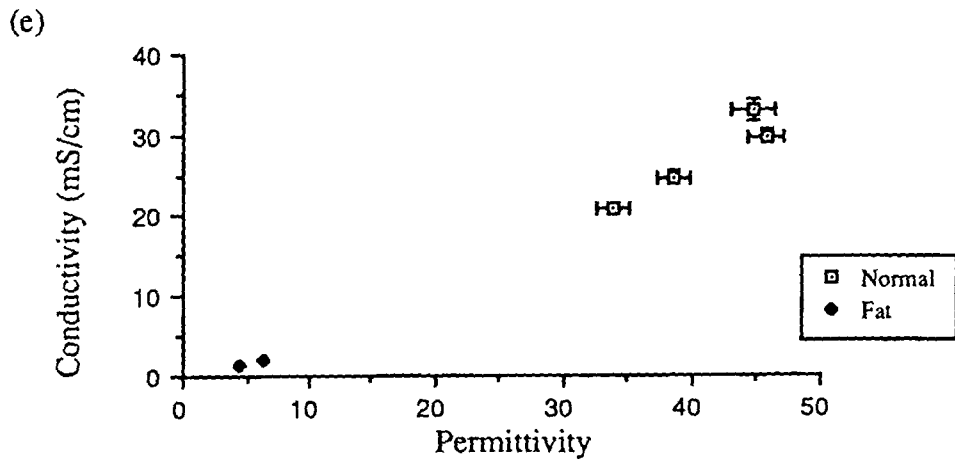

Figure 5.24   Comparison of normal and fat tissue
from patient (e) 23
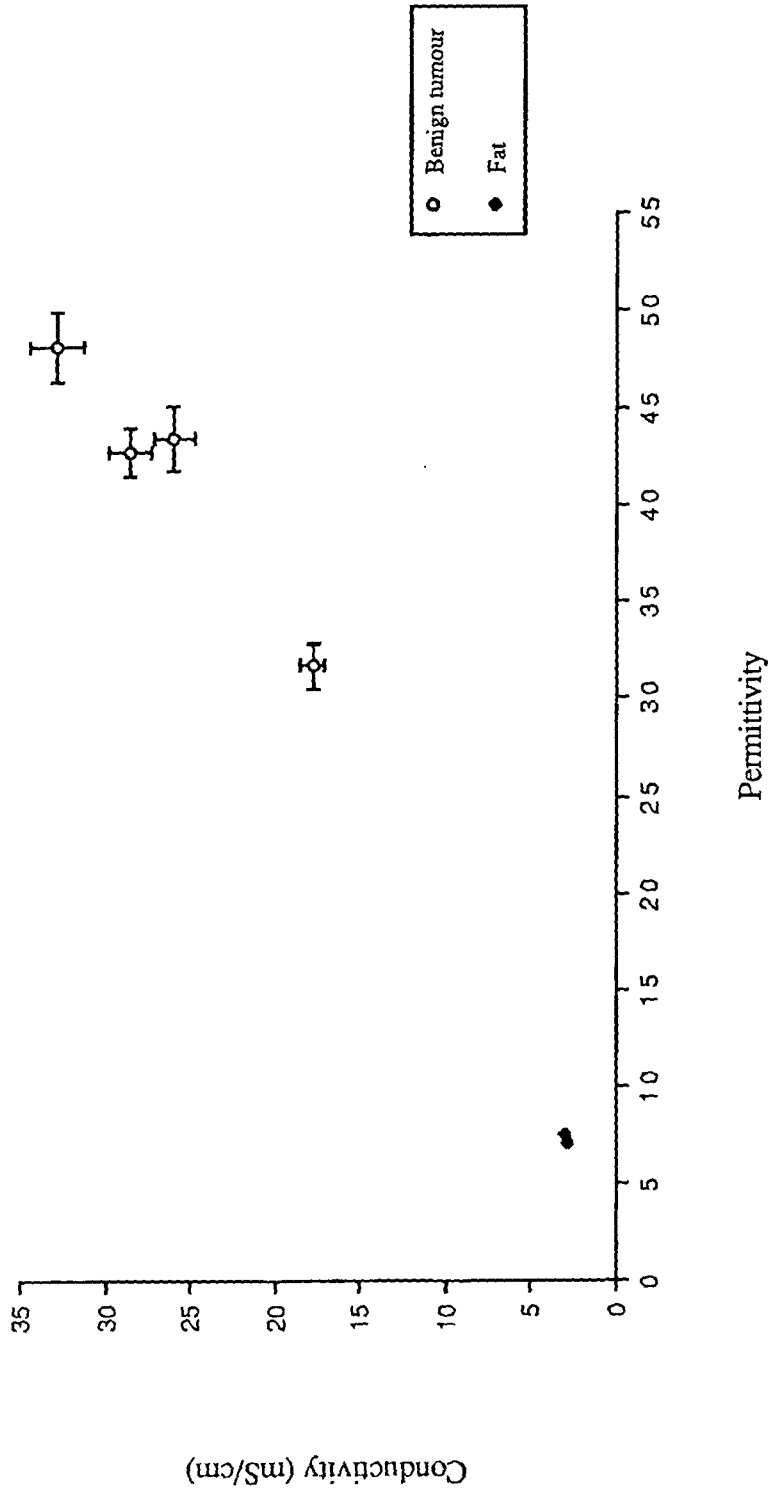
Figure 5.25   Comparison of benign tumour and fat tissue from patient 12
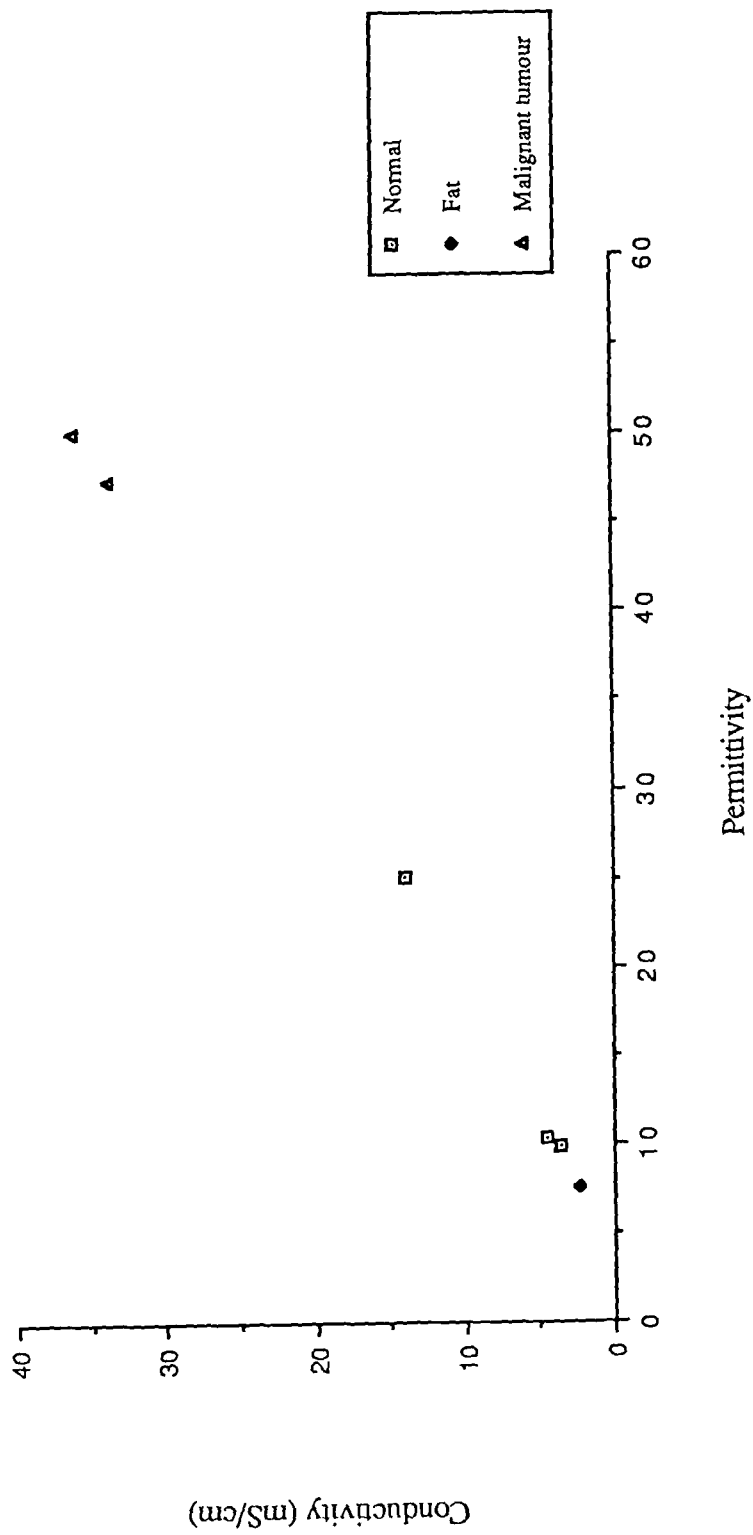
Figure 5.26   Comparison of normal, fat and tumour tissues from patient 37
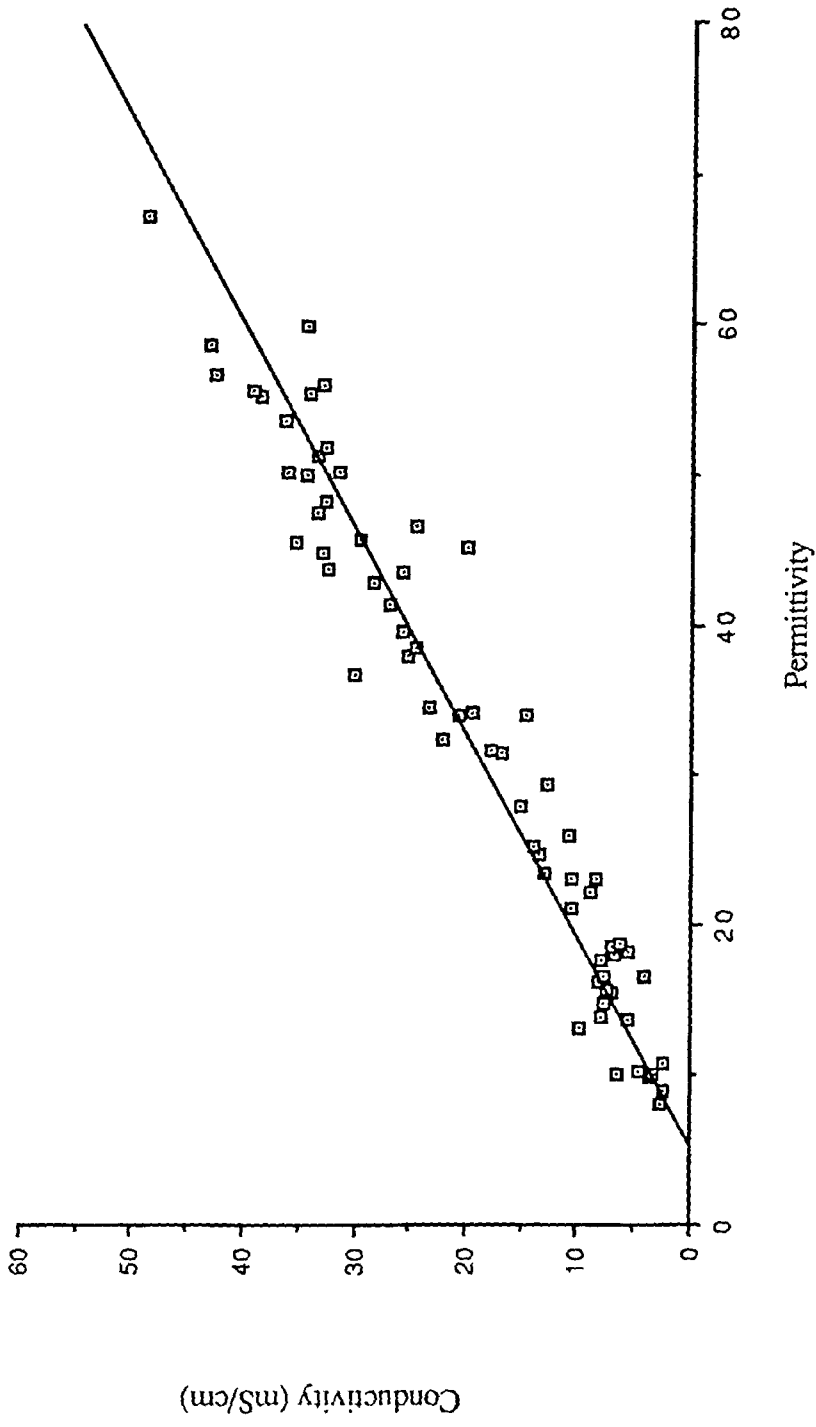
Figure 5.27   Variation of conductivity with permittivity for all new data except fat and bone

conductivity against permittivity which shows a strong correlation, independent of tissue type. Therefore, any non-fatty breast tissue at 3.2GHz has dielectric properties which are related by the formula:

$$\sigma \text{ (mS/cm)} = m_{non-fat}\varepsilon' + c_{non-fat} \qquad (5.10)$$

where $\quad m_{non-fat} = 0.731 \pm 0.039$ (mS/cm)

$\quad\quad\quad c_{non-fat} = -4.12 \pm 0.55$ (mS/cm)

with corresponding values of the Debye time constant and of the relaxation frequency:

$$\tau = 2.0.10^{-11} \text{ s}^{-1}$$

$$f_c = 8\text{GHz}$$

Figure 5.28 shows a comparison of the collected non-fat data and all high water content data gathered from the literature and presented in Tables 3.6 and 3.7. The literature data is widely spread and poorly correlated: it is a collection of data from many experiments over the last forty years, so that the scatter perhaps reflects the scatter of errors in these experiments as well as the variation between species and between individual animals. The literature data lie slightly below the data gathered in this work, which is to be expected because of the slightly higher frequency used in the present measurements. (See Figures 3.2, 3.3, 3.5 and 3.6 which show a small decrease in permittivity and a rapid rise in conductivity above 3GHz.) Taking this into account, the new data set is reasonably consistent with previous measurements.

The relationship of permittivity and conductivity to water content for all non-fatty breast tissues are shown in Figures 5.29a and b. As expected from the same plots for individual tissues, the permittivity data lie within the limits set by series and parallel models, (2.28), while the conductivities of a large number of points are very much higher than predicted by these models.
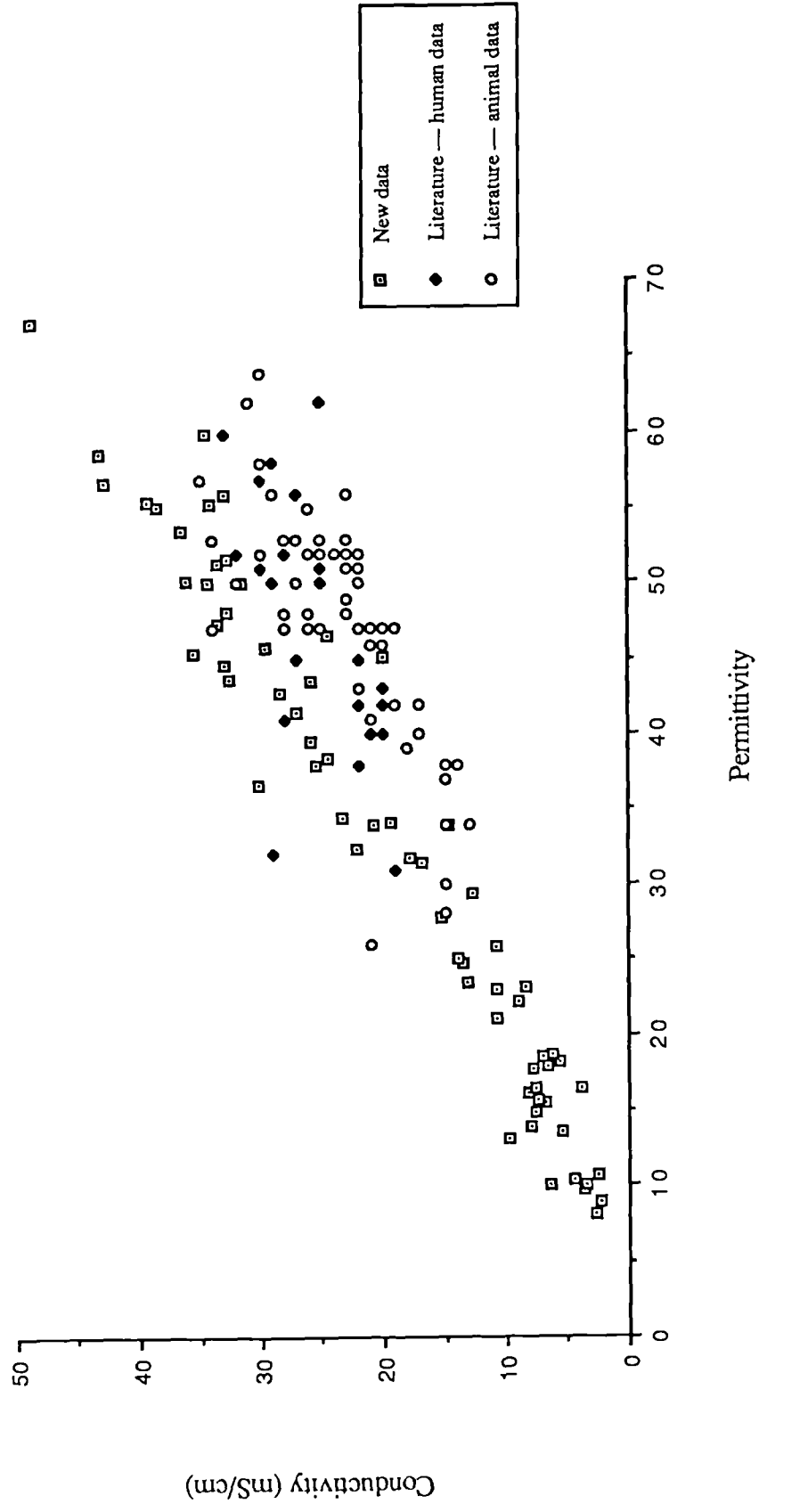
Figure 5. 28   Variation of conductivity with permittivity for all data
except fat and bone — comparison with literature

(a)

(b)
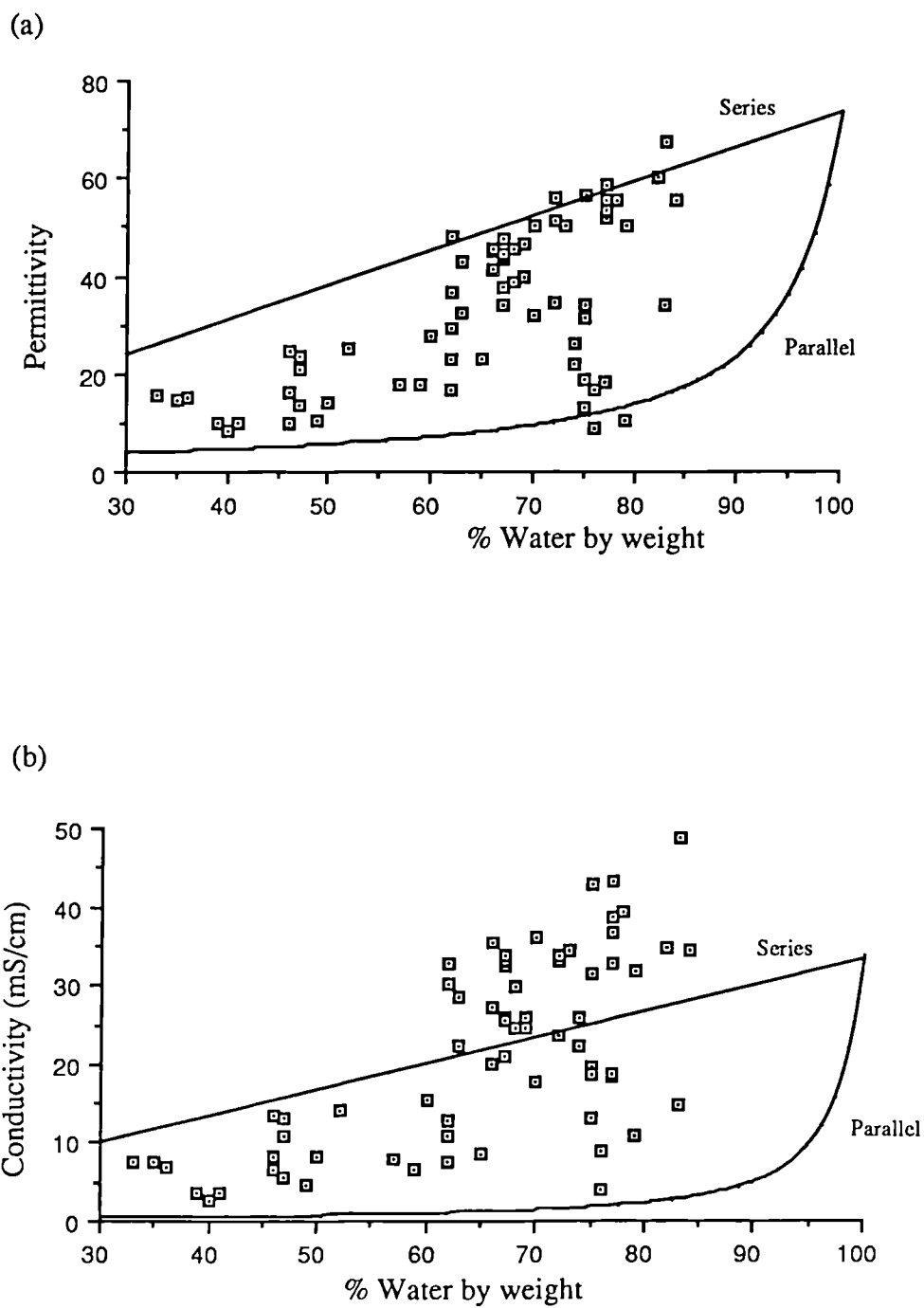

Figure 5.29   Variation of (a) permittivity and (b) conductivity with
water content for all new data except fat and bone

5.11 Patient ages

It might be expected that the pre-menopausal and the post-menopausal breast would have different characteristics: in particular the post-menopausal breast was expected to be more dense, and possibly to contain less water than the breast of younger women. Figures 5.30a, b and c show plots of average water contents of normal and fat tissues and benign tumours against patient age. Fat data display no correlation. Although the data on younger women are scarce, normal and benign tissues show a trend towards decreasing water content with age, as expected. No data were available for carcinomas of younger women — all patients for whom breast carcinoma samples were received were post-menopausal.

5.12 Summary and discussion

Information from this chapter is summarised in Table 5.6. This table contains data ranges and best choices of values for modelling, for fat and normal breast tissue and for benign and malignant breast tumours.

Clearly, more work is needed in this area, as a number of problems remain unsolved. The mechanisms of dielectric dispersion are unclear, for they do not seem to be dictated wholly by the dielectric properties of physiological saline: the strong correlations observed between permittivity and conductivity indicate that one dominant process, or combination of processes, is occurring in fatty (low water content tissue) and another in non-fatty (higher water content) tissues. These data correlations should be very reliable: for each (ε', σ) data set, the same sample was measured in the same apparatus with the same geometrical dependence. It may be that a large component of water in non-fatty tissues is bound, which reduces the observed relaxation frequency. If this is the case, in fat less water appears to be bound, a conclusion also drawn by Smith et al (1985) (see Section 3.5). Bound water in human tissues would be better studied by measurements over a wider frequency range on tissues with a wide range of water contents.
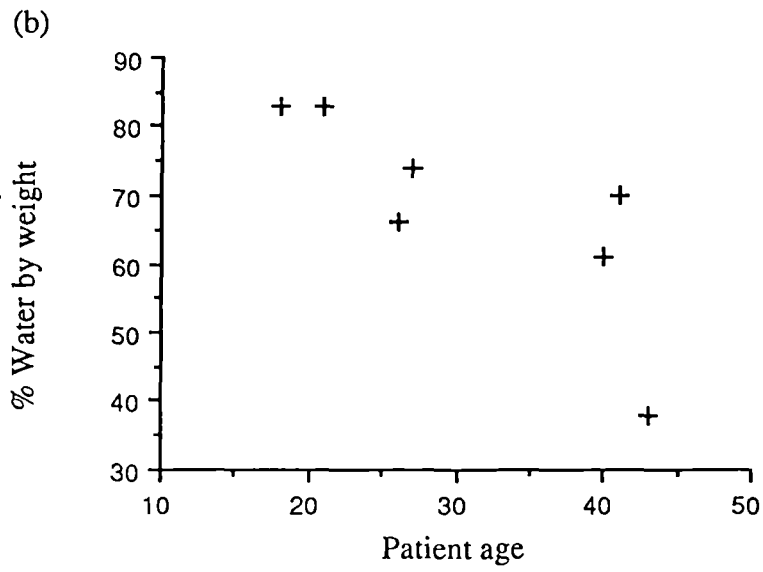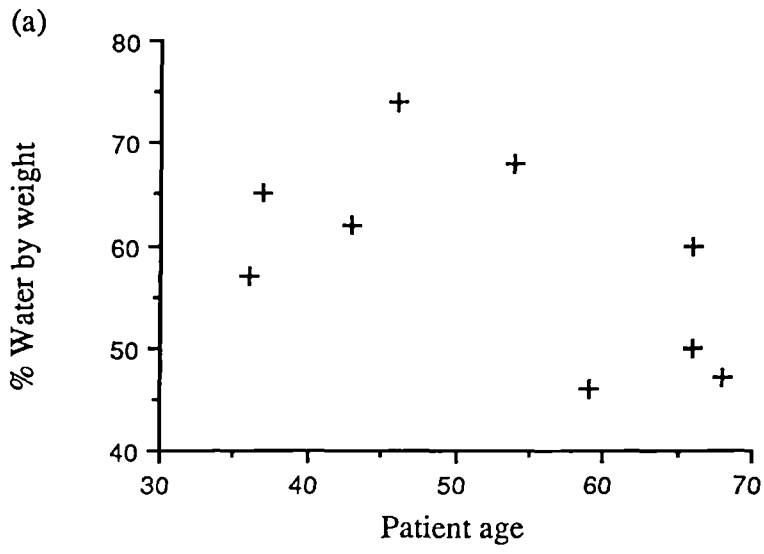
Figure 5.30   Variation of water content with age for
(a) normal and (b) benign tissues

(c)
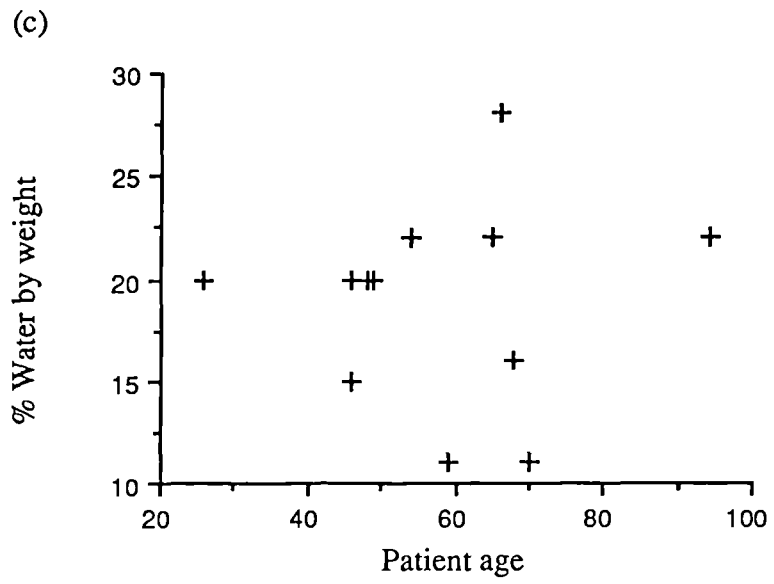
Figure 5.30   Variation of water content with age for (c) fat tissues

Table 5.6   Ranges and best choice of values for the dielectric properties and
                     water contents of fat and normal breast tissues, and of benign and
                     malignant breast tumours. For normal tissue and malignant
                     tumours a choice of best values are given.

Tissue type	Parameter	Range of data	Best values (1)	(2)
Fat (a)	Permittivity	2.8 — 7.6	4 — 4.5	
	Conductivity (mS/cm)	0.5 — 2.9	1.1 — 1.4	
	% water by weight	11 — 31	15 — 23	
Normal (b)	Permittivity	9.8 — 46	10 — 25,	25 — 55
	Conductivity (mS/cm)	3.7 — 34	3.5 — 10.5,	18 — 35
	% water by weight	41 — 76	45 — 50	65 — 70
Benign Tumour (b)	Permittivity	15 — 67	10 — 50	
	Conductivity (mS/cm)	7 — 49	10 — 40	
	% water by weight	62 — 84	60 — 90	
Malignant Tumour (b)	Permittivity	9 — 59	45 — 60,	10 — 20
	Conductivity (mS/cm)	2 — 43	30 — 40,	0 — 10
	% water by weight	66 — 79	75 — 80,	75 — 80

(a) For fat tissues,

$$\sigma \ (mS/cm) = 0.478 \ \varepsilon' - 0.864$$

[See (5.3)]

(b) For all other tissues,

$$\sigma \ (mS/cm) = 0.731 \ \varepsilon' - 4.12$$

[See (5.10)]

It is clear that particular mixture models cannot be applied to the tissues measured here, because they exhibit such widely varying properties even within one tissue type. However, the permittivity data largely fall within limits imposed by mixture theory; whereas conductivity data often fall outside the upper bound. Discovery of an additional mechanism may be necessary to explain the very high conductivities observed in non-fatty tissues. This mechanism may be a higher conductivity of intracellular water than is presently believed, or some other process such as dispersion caused by interfacial polarisation.

More comparisons of tissue types within individuals are needed, particularly carcinomas and benign lesions with normal tissues, if a dielectric imaging system for cancer detection is to be designed and used as a diagnostic tool (See Section 1.3). Dielectric properties of carcinomas should be studied in much more detail: the gross heterogeneity of some malignant tumours measured in this work indicate that for thermal and dielectric imaging, major problems could arise in temperature or dielectric retrieval. Another potentially serious problem for dielectric retrieval is that properties of benign and malignant tumours may not be distinguishable dielectrically, so that more studies of the differences between these tissues are necessary.

The data on fat tissues present fewer new problems. As with higher water content tissues, the data cannot be parameterised by one particular mixture model. However, the conductivity data of fat *do* fall within limits imposed by mixture theory, indicating that presently known processes are probably sufficient to explain data from this tissue type.

Chapter 6

Conclusions

Knowledge of the microwave properties of tissues is essential for the understanding and development of medical microwave sensing and imaging techniques. In particular, microwave thermography relies on processes fundamentally determined by the high frequency electromagnetic properties of human tissues. The most promising applications of microwave thermography are in screening of women for breast cancer and in monitoring temperatures for microwave hyperthermia. Temperature retrieval for these applications will be improved by better knowledge of the dielectric properties of human breast tissue. A specific aim of this work was to provide detailed information at the frequency of operation of the Glasgow microwave thermography equipment, 3 — 3.5GHz. In order to understand the measured data other related areas were studied — theoretical descriptions of dielectric properties of materials; experimental data on other human and animal tissues — and a new technique was devised in the Glasgow group which allows measurement of lossy samples of small volume.

The frequency variation of the dielectric properties of tissues at microwave frequencies may be described by the Cole-Cole equation (2.17). This semi-empirical equation parameterises data from complex substances, in which a number of dielectric processes are occurring at the same frequencies (causing a broadening of the resonance curve). The simpler Debye equation (2.14) may serve to parameterise simpler materials. It may also be used to parameterise data from a single tissue type at a given frequency, if is assumed that one dominant dispersion process, or set of dispersion processes, is occurring in all tissues of the same type. Less information will be gained about the underlying dispersion from measurements at a single frequency, but an approximate resonant frequency may be calculated. In biological materials the dipolar

relaxation of tissue water is believed to be the dominant process at microwave frequencies.

A number of theories have been derived for simple two phase mixtures which attempt to describe the 'generalised conductivity' of the mixture in terms of the 'generalised conductivities' and volume fractions of its component parts. These mixture equations have not been examined in the literature in sufficient experimental detail to make the choice of any one compelling for any particular type of mixture. The most useful models are likely to be those by Maxwell (1881), Fricke (1925) and Bruggeman (1935), despite more recent research. Further experimental studies examining the dependence of any 'generalised conductivity' upon the volume fractions of its components would be helpful in determining the ranges of applicability of each model. Biological tissues are very complex materials and cannot be categorised as two phase mixtures. However, mixture theories, in particular, limits from mixture theory, are useful in providing a qualitative guide to tissue structure.

The first step in providing dielectric information at microwave frequencies was to examine the data available in the literature. Until now these have been scattered among many different journals, covering a period of about forty years. Although a fairly comprehensive data table was compiled by Stuchly and Stuchly (1980), so many new data have been published over the last ten years that it was decided to compile new data tables (Tables 3.6 and 3.7) for human and animal tissues: these subsume the earlier table and correct some mistakes. They will be useful, not only for temperature retrieval in microwave thermography, but for instrumentation design in microwave hyperthermia, for development of phantom materials, for better calculation of microwave hazards, and for dielectric retrieval in microwave tomographic systems.

Tables 3.6 and 3.7 allow a detailed examination of the available tissue dielectric data. A comparison was made of animal and human tissues, for it has been widely

assumed that dielectric properties of animal tissues are representative of similar human tissues, even although the evidence for such a claim has not been examined until now. For most tissues the assumption may be correct. However, there are discrepancies for some tissue types (fat, malignant tumours, brain tissue and lens nucleus). For all tissue types there was found to be too little data available on human tissue for any certain conclusion to be drawn. Comprehensive studies of the dielectric properties of human tissues over a range of frequencies, and at specific frequencies (such as the study described in Chapter 5) are necessary before conclusions on these important comparisons can be made with any certainty.

The relative merits of *in vivo* and *in vitro* measurements were examined using data from Tables 3.6 and 3.7. It was found that although differences between these types of measurement exist at frequencies below 0.1GHz, above these frequencies there is no observable difference between *in vivo* and *in vitro* measurements, provided that gross deterioration of the tissue sample is avoided.

Water exists in various states of binding in biological materials, which may strongly affect dielectric properties between 0.1 and 5GHz. Because of its nature, bound water cannot be studied directly, but must have its existence and properties inferred from dielectric or other measurements on tissue. A quantitative method of analysis is to consider the observed dispersion as a sum of Debye relaxation processes: this allows an estimate to be made of the volume fraction of bound water in a system. A more qualitative method is to estimate a relaxation frequency from data parameterised by the Cole-Cole equations. This relaxation frequency, if much lower than that of physiological saline, is assumed to imply that bound water is present, but allows no estimation of it volume fraction. (A similar method was used in Chapter 5 to deduce that human breast tissues contain an amount of bound water.) It is possible that water binding is enhanced in some cancerous tissues. This is an area deserving more study, for deeper knowledge of water binding in tissues could be very helpful

for calculation of energy deposition in tissues for microwave hyperthermia and for studies of microwave hazards.

To fulfill the need for new dielectric data on human breast tissues, a new resonant cavity perturbation technique was designed which allows measurements at 3.2GHz on samples of very small volume ($\approx$17mm^3). This technique can measure relative permittivities ranging from 2 to 78 and conductivities ranging from 0.2 to 50mS/cm. The major sources of error were found to be tissue heterogeneity, fluid loss due to sample preparation, departure from circularity in cavity apertures, potential air pockets at the tissue/cavity wall interface, and temperature drift. In measuring the water contents of the samples the major source of error is probably the difference in the volume of tissue illuminated for dielectric measurement and the volume used for the water content measurement. Considering all these sources of error, accuracies in measurement of biological tissues are about 3 — 4%, much better than was recommended by a recent workshop which discussed temperature measurement for hyperthemia (Bardati et al, 1989).

This new technique was used to make *in vitro* measurements on human tissues, mainly female breast tissues. 102 measurements of female breast tissue were made on 37 different patients.

39 of these measurements were on fat tissues, which greatly increases the number of data available for both modelling in thermometry (Bardati et al, 1989) and for human/animal comparisons [see Section 3.4.1(a)]. The relative permittivities of these fat tissues ranged from 2.8 to 7.6, the conductivities lay between 0.54 and 2.9mS/cm and the water contents ranged from 11 to 31%.

22 of the measurements were made on normal breast tissue. This data is essential for modelling purposes. Normal tissues displayed relative permittivities between 9.8 and 47, conductivities between 3.7 and 34mS/cm, and water contents between 41 and 76%.

18 measurements were made on benign breast tumours. These are the first reported measurements of this tissue type at microwave frequencies. Relative permittivities ranged from 15 to 67, conductivities ranged from 7 to 49mS/cm, and water contents lay between 62 and 84%.

23 measurements were made of the dielectric properties of breast carcinomas. This data set greatly increases the available data for modelling and other purposes. Relative permittivities of these tissues ranged from 9 to 59, conductivities ranged from 2 to 43mS/cm and water contents were between 66 and 79%. Some tumours displayed very heterogeneous dielectric properties.

Each data set was parameterised using the Debye equation in order to calculate an equivalent characteristic frequency. For fat this frequency was calculated to be 12GHz, and for all other tissues 8GHz. It may be concluded from this that all the human breast tissues measured in this work contain an amount of bound water. Fat probably contains less bound water than other tissue types.

Comparing the data sets to some of the mixture equations discussed in Chapter 2 produced the interesting result that although permittivity data fall within limits set by mixture theory, conductivity data often have values far in excess of that expected (except for fat). The conductivities of some tissues measured were in fact greater than that of saline at the same temperature, the theoretical upper limit. This implies either that physiological saline is *not* a good approximation to all the body waters (as assumed in Section 3.2) or that some additional process is occurring (for instance, interfacial polarisation may have a stronger effect at microwave frequencies than is presently believed). Clearly more experimental and theoretical work is required in this area in order that these results be understood.

Development of microwave hyperthermia systems requires that values and ranges of the dielectric properties of tissues be established (Section 1.2). Appropriate values and ranges for the tissue types measured here are presented in Table 5.6.

Development of passive (thermographic) and active (tomographic) imaging systems requires information about the differences between dielectric properties of different tissue types within an individual. Comparisons of the new normal and benign tumour data, normal and malignant tumour data, and of normal and fat data within individual patients show that these tissue are distinguishable by dielectric measurement. However it is probable that malignant and benign tumours do not have properties sufficiently different to distinguish them by dielectric measurement only: this would constitute a severe drawback for the development of an active imaging system for the detection and diagnosis of breast disease. Passive thermography would not be affected in the same way, because the received signal is dependent on both dielectric and thermal properties of the underlying tissues.

For both types of imaging system the gross heterogeneity of some malignant tumours measured here would present major problems in their detection.

Appendix A

Theoretical solution of Bruggeman's equation

Bruggeman's formula for the complex permittivity of a mixture is:

$$\left(\frac{\varepsilon_1^* - \varepsilon_2^*}{\varepsilon_1^* - \varepsilon^*}\right)^3 \frac{\varepsilon^*}{\varepsilon_2^*} = \frac{1}{(1-\phi)^3} \tag{A1}$$

which may be solved analytically for any of the complex permittivities ε_1^*, ε_2^*, or ε^* in terms of the other two permittivities and ϕ, the volume fraction of the disperse phase (ε_1^*). If a solution for $\varepsilon^* = \varepsilon^*(\varepsilon_1^*, \varepsilon_2^*, \phi)$ is required, setting:

$$x = \varepsilon_1^* - \varepsilon^*$$

$$\varepsilon^* = \varepsilon_1^* - x \tag{A2}$$

allows (A1) to be expressed in the form:

$$x^3 + px = q \tag{A3}$$

where x , p and q are complex:

$$p = \frac{(\varepsilon_1^* - \varepsilon_2^*)^3}{\varepsilon_2^*} (1 - \phi)^3 \qquad (A4)$$

$$q = \frac{\varepsilon_1^*}{\varepsilon_2^*} (\varepsilon_1^* - \varepsilon_2^*)^3 (1 - \phi)^3 = \varepsilon_1^* \, p \qquad (A5)$$

Similarly, if ε_2^* is the unknown, setting:

$$x = \varepsilon_1^* - \varepsilon_2^*$$

$$\qquad (A6)$$

$$\varepsilon_2^* = \varepsilon_1^* - x$$

allows (A1) to be expressed in the form A3 with coefficients:

$$p = \frac{1}{\varepsilon^*} \frac{(\varepsilon_1^* - \varepsilon^*)^3}{(1 - \phi)^3} \qquad (A7)$$

$$q = \varepsilon_1^* \, p \qquad (A8)$$

Finding a substitution for ε_1^* is more complicated. First (A1) must be expressed in the form:

$$(\varepsilon_1^*)^3 + b \, (\varepsilon_1^*)^2 + c \, \varepsilon_1^* + d = 0 \qquad (A9)$$

where b, c and d are complex:

$$b = \frac{-3 \, \varepsilon_2^* \, \varepsilon^* \, (1 - \phi)^3 + 3 \, \varepsilon^* \, \varepsilon_2^*}{\varepsilon^* \, (1 - \phi)^3 - \varepsilon_2^*} \tag{A10}$$

$$c = \frac{3 \, (\varepsilon_2^*)^2 \, \varepsilon^* \, (1 - \phi)^3 - 3 \, (\varepsilon^*)^2 \, \varepsilon_2^*}{\varepsilon^* \, (1 - \phi)^3 - \varepsilon_2^*} \tag{A11}$$

$$d = \frac{(\varepsilon_2^*)^3 \, \varepsilon^* \, (1 - \phi)^3 - (\varepsilon^*)^3 \, \varepsilon_2^*}{\varepsilon^* \, (1 - \phi)^3 - \varepsilon_2^*} \tag{A12}$$

Then, a substitution of the form:

$$x = \varepsilon_1^* + \frac{b}{3} \tag{A13}$$

allows (A9) to be expressed in the form (A3) with coefficients:

$$p = c - \frac{b^2}{3} \tag{A14}$$

$$q = d + \frac{b}{3} \left(\frac{2 \, b^2}{27} - c \right) \tag{A15}$$

Equation (A3) has a known solution (Stewart, 1973$^{(4)}$) which is found by setting:

$$x = u + v \tag{A16}$$

so that

$$x^3 - 3 \, u \, v \, x = u^3 + v^3 \tag{A17}$$

Then the coefficients may be written:

121

$$p = -3\,u\,v \qquad\qquad q = u^3 + v^3 \qquad\qquad\qquad \text{(A18)}$$

Solving (A18):

$$u^3 = \frac{q}{2} \pm \sqrt{\frac{p^3}{27} + \frac{q^2}{4}} \qquad\qquad\qquad \text{(A19)}$$

$$v^3 = \frac{q}{2} \pm \sqrt{\frac{p^3}{27} + \frac{q^2}{4}} \qquad\qquad\qquad \text{(A20)}$$

In order that (A10) is satisfied, the correct solution for u^3 and v^3 must take the positive square root in either of equations (A19) or (A20) and the negative square root in the other.

In this application the coefficients p and q are complex: solutions for the cubic are documented only for real coefficients. However this problem is easily overcome by expressing u^3 and v^3 in polar form:

$$u^3 = a\,e^{j\,\alpha}$$

$$\qquad\qquad\qquad \text{(A21)}$$

$$v^3 = h\,e^{j\,\eta}$$

The angles α and η may also take the values $\alpha + 2\,\pi$, $\alpha + 4\,\pi$; $\eta + 2\,\pi$, $\eta + 4\,\pi$, thus giving the three possible solutions each for u and v:

$$u_1 = a^{1/3}\,e^{j\,\alpha/3} \; ; u_2 = a^{1/3}\,e^{j\,(\alpha + 2\pi)/3} \; ; u_3 = a^{1/3}\,e^{j\,(\alpha + 4\pi)/3} \qquad\qquad \text{(A22)}$$

$$v_1 = h^{1/3}\,e^{j\,\eta/3} \; ; v_2 = h^{1/3}\,e^{j\,(\eta + 2\pi)/3} \; ; v_3 = h^{1/3}\,e^{j\,(\eta + 4\pi)/3} \qquad\qquad \text{(A23)}$$

From equations (A22) and (A23) it is easily seen that there are nine possible combinations of u_i and v_j. Only three of these combinations are correct, and these may be calculated from the condition:

$$u_i v_j = - \frac{p}{3}$$

(A24)

[from (A18)]. Using (A24) the nine possible combinations may be subdivided into three sets of three combinations:

$$\left\{ u_1, v_1 \; ; \; u_2, v_3 \; ; \; u_3, v_2 \right\}$$

(A25)

$$\left\{ u_1, v_3 \; ; \; u_2, v_2 \; ; \; u_3, v_1 \right\}$$

(A26)

$$\left\{ u_1, v_2 \; ; \; u_2, v_1 \; ; \; u_3, v_3 \right\}$$

(A27)

Only one of these is the correct set of solutions. One calculation from each set is sufficient to determine which solution set (A25), (A26) or (A27) is correct e.g a calculation of $\{ [u_i v_i + p/3] \; ; \; i = 1, 2, 3 \}$.

This method is completely general and may be applied to any combination of real and complex coefficients.

The above procedure allows the three possible solutions of (A1) to be calculated. However, only one of these three is the physical solution. The other two solutions may be eliminated using two conditions: firstly, the permittivity and the loss factor must both be positive when the complex permittivity is written in the form (2.11); and secondly, the permittivity and loss factor of the mixture must lie within limits set

by the continuum and the disperse system. These two conditions are sufficient to determine the physical solution to the Bruggeman equation.

Appendix B

Curve Fitting Routine

A group of programs (MINUIT), written at the CERN computer centre (CERN Computer Centre Reports, 1977, 1978), was chosen. This set of programs is designed to estimate unknown parameters in almost any function, by minimising the difference between theory and experimental data, using chisquare as the function to be minimised. This may be written, for statistically independent data points as:

$$\text{Chisquare} = \sum_i \frac{[\,M_i - F_i(p_j)\,]^2}{e_i^2}$$

where M_i is the measured value of the function; $F_i(p_j)$ is the fitted value of the function as a function of the parameters p_j; and e_i are the errors associated with M_i. This method is also known as weighted least squares. The package also calculates errors on the best fit parameters.

The particular commands of MINUIT used in the program CURVFIT are:

(1) MINTSD which accesses the package

(2) MIGRAD which performs the minimisation and gives local and global correlation coefficients for the parameters

(3) CONTOUR which plots out chisquare contours in the space of any two parameters; this gives a detailed description of the sensitivity of the fit to the parameters

(4) MINOS which calculates true confidence intervals on the parameters by determining the exact behaviour of the chisquare function over an interval, taken in CURVFIT to be (the default value) that interval corresponding to one standard

deviation

(5) PRINTOUT which is merely used to limit the amount of printout from each of the above routines

The program, CURVFIT, consists of two separate routines, both of which access the package MINUIT. Firstly, a least squares best fit line is calculated for the short circuit data using routine MIGRAD. Routine MINOS is used to calculate errors of one standard deviation on the best fit parameters. Next, in the main program, data from the resonance curve is normalised to the best fit line. The normalised data is fitted to function (4.38) using MIGRAD. Contour plots are drawn using CONTOUR to test the sensitivity of each set of variables, and to look for local minima, which would indicate either experimental errors or that the wrong function has been chosen. Finally, MINOS is used to calculate errors on each of the three parameters. Experimental data and starting values are copied into the program for each new run.

```
//MT03UNP  JOB MT03,ANNE,CLASS=M,MSGLEVEL=(0,0),TIME=2
// EXEC FVCLG,LIB4='LIBR.GENLIB',CPRINT=YES
//*************************************************************
//* Read in the data for the straight line Y = AX + B and
//* fit the best straight line.
//* Output on unit one the values of A and B.
//*************************************************************
//C.SYSIN DD *
       COMMON/AB/ X
       DOUBLE PRECISION X(2)
C--
C--Call the fitting routine for the line Y = AX + B
C--
       CALL MINTSD
       STOP
       END
       SUBROUTINE FCN(NPAR,G,F,X,IFLAG)
C--
C--IMPLICIT DOUBLE PRECISION statement for FORTRAN 77
C--
       IMPLICIT DOUBLE PRECISION (A-H,O-Z)
       DOUBLE PRECISION NAM
C--
C--Input number of data points in short circuit line
C--
       PARAMETER (NDATA =8)
C--
C--X is the number of parameters used for the minimisation
C--FREQ are the observed frequencies
C--VDET are the observed voltages
C--VERR are the estimated errors on VDET
C--
       DIMENSION X(2),FREQ(NDATA),VDET(NDATA),VERR(NDATA)
       DATA    INIT/0/
C--
C--To fit experimental data to theory with free parameters
C--
       IF (IFLAG .GT. 1)  GO TO 100
C--
C--Read in data (experimental distribution for the straight line)
C--
       IF (INIT .NE. 0)  GO TO 100
       INIT = 1
       DO 50 I= 1,NDATA
    50 READ (5,700) FREQ(I),VDET(I),VERR(I)
   700 FORMAT (3F10.0)
C--
C--Calculate theoretical distribution
C--
   100 CONTINUE
       IF (IFLAG .EQ. 3)  GO TO 300
       F = 0.D0
       DO 200 I= 1, NDATA
       FUN = 0.D0
       T = FREQ(I)
C--
C--Contribution to CHISQUARE
C--
       FUN = X(1) + (X(2)*T)
   200 F = F + (( VDET(I) -  FUN )/VERR(I))**2
       GOTO 1000
C--
C--
   300  CONTINUE
C--
C--Output to temporary data set, values to be used in the next step
C--for normalisation
C--
       WRITE(1,*) X
C--
  1000 RETURN
       END
/*
//L.MINUIT DD DSN=USER.MGLIB,DISP=SHR
   INCLUDE MINUIT(MINUITSD)
```

```
        ENTRY MAIN
//G.FT01F001 DD DISP=(,PASS),DSN=&&AXPB,UNIT=3350,
// DCB=(RECFM=VBS,BLKSIZE=6233,LRECL=32760),SPACE=(TRK,(1,1),RLSE)
//G.SYSIN DD *
FIT TO STRAIGHT LINE Y = AX + B
          1   A         -1108.      110.
          2   B          0.38       0.038
              BLANK
 3172.75     99.2      1.0
 3167.55     97.5      1.0
 3164.42     96.5      1.0
 3159.80     94.5      1.0
 3155.09     93.5      1.0
 3149.91     91.5      1.0
 3145.37     90.1      1.0
 3139.45     88.5      1.0

MIGRAD
MINOS
EXIT
/*
//*•••••••••••••••••••••••••••••••••••••••••••••••••••••••••••••••••••••
//*   Now read in the fitted values for the straight line
//*   Y = AX + B, calculate the data points (X,Y) for the normalised
//*   curve and fit the three parameters, RHOSQRD, 4QLSQRD, F0.
//*   Plot all curves at the end of the fitting routines.
//*•••••••••••••••••••••••••••••••••••••••••••••••••••••••••••••••••••••
// EXEC FVCLG,LIB4='LIBR.GENLIB'
//C.SYSIN DD *
C—
C—COMMON space for HBOOK
C—
        COMMON // HMEMOR(10000)
C—
C—HBOOK CALLS
C—
        CALL HLIMIT(10000)
        CALL BOOKA
C—
C—Call the main fitting routine for the normalised curve
C
        CALL MINTSD
        STOP
        END
        SUBROUTINE FCN(NPAR,G,F,X,IFLAG)
C—
C—IMPLICIT DOUBLE PRECISION statement for FORTRAN 77
C—
        IMPLICIT DOUBLE PRECISION (A-H,O-Z)
        DOUBLE PRECISION NAM
C—
C—Number of experimental data points on curve
C—
        PARAMETER (NDATA = 24)
C—
C—Z are the data from the straight line fit. XFF, YFF, XFFL, YFFL are
C—data for the histograms. X are the parameters to be fitted. VST are
C—the best fit short circuit data evaluated at the curve points.
C—VNORM are the normalised data points
C—
        DIMENSION Z(2)
        DIMENSION XFF(100),YFF(100)
        DIMENSION XFFL(100),YFFL(100)
        DIMENSION X(3),FREQ(NDATA),VDET(NDATA),VERR(NDATA)
        DIMENSION VST(NDATA),VNORM(NDATA)
        DATA    INIT/0/
C—
C—POW allows for the law of the detector to be different from 2
C—
        POW = 2.02 / 2.D0
C—
C—To fit experimental distribution to theory with free parameters
C—
        IF (IFLAG .GT. 1)  GO TO 100
C—
```

```
C—Read in data (experimental distribution)
C—
      IF (INIT .NE. 0)  GO TO 100
      INIT = 1
      DO 50 I= 1, NDATA
   50 READ (5,700) FREQ(I), VDET(I), VERR(I)
  700 FORMAT (3F10.0)
C—
C—Read in the constants for the straight line
C—
      READ(1,*) Z
      A = Z(1)
      B = Z(2)
C—
C Calculate points along the straight line and the normalised data points
C Scale the errors
C
      DO 80 K = 1,NDATA
            VST(K) = B*FREQ(K) + A
         VNORM(K) = VDET(K)/VST(K)
            VERR(K) = VERR(K)*VNORM(K)/VDET(K)
   80    CONTINUE
C—
C—Calculate theoretical distribution
C—
  100 CONTINUE
      IF (IFLAG .EQ. 3)  GO TO 300
      F = 0.D0
      DO 200 I= 1,NDATA
      FUN = 0.D0
      T = FREQ(I)
C—
C—Contribution to CHISQUARE
C—
      FUN = X(1) +     X(2)*(ABS((1.D0-(X(3)/T)))**2.D0)
      FUN = FUN/( 1.D0 + X(2)*(ABS((1.D0-(X(3)/T)))**2.D0))
      FUN = (FUN)**POW
  200 F = F + (( VNORM(I) -  FUN )/VERR(I))**2
      GOTO 1000
C—
C—
  300 CONTINUE
C—
C—
C—Plot some X-Y curves
C—
      DO 77 K = 1,NDATA
            CALL HFILL(1,FREQ(K),VNORM(K),1.0)
   77       CONTINUE
C—
C—Plot the final curves from the fit
C—
      DDX = ( FREQ(1) - FREQ(NDATA) ) / 100.
      DX = 0.D0
      FF = 0.D0
      DO 250 K = 1,100
            DX = DX + DDX
            XFFL(K) = FREQ(NDATA) + DX
            XFF(K)  = XFFL(K)
            YFFL(K) = ( B * XFFL(K) ) + A
            CALL FUNN(X,3,XFF(K),FF)
            YFF(K) = FF
            CALL HFILL(2,XFFL(K),YFFL(K))
            CALL HFILL(3,XFF(K),YFF(K))
  250       CONTINUE
      CALL HISTDO
C—
C—Final values of the variables
C—
            RHO = DSQRT( X(1) )
            F0  = X(3)
            QL  = DSQRT( X(2) ) / 2.D0
C—
            WRITE(6,122)
            WRITE(6,124)
```

```
              WRITE(6,123)
              WRITE(6,*) RHO,QL,F0
              WRITE(6,124)
 122          FORMAT(1H1)
 124          FORMAT(////)
 123          FORMAT(9X,' RHO',25X,'QL',25X,'F0')
C—
C—Print the HISTOGRAMS
C—
 1000 RETURN
       END
       SUBROUTINE BOOKA
       CALL HBOOK2(1,'X F PLOT$',40,3135.0,3175.0,70,0.0,1.0)
       CALL HBOOK2(2,'X Y LINE FIT$',40,3135.0,3175.0,80,60.0,100.0)
       CALL HBOOK2(3,'X F PLOT FIT$',40,3135.0,3175.0,70,0.0,1.0)
       RETURN
       END
       SUBROUTINE FUNN(X,N,T,F)
       DOUBLE PRECISION X,T,F,POW
       DIMENSION X(N)
       POW = 2.02 / 2.D0
C—
       F = X(1) +    X(2)*(ABS((1.D0-(X(3)/T)))**2.D0)
       F = F/( 1.D0 + X(2)*(ABS((1.D0-(X(3)/T)))**2.D0))
       F = (F)**POW
C—
       RETURN
       END
/*
//L.MINUIT DD DSN=USER.MGLIB,DISP=SHR
   INCLUDE MINUIT(MINUITSD)
   ENTRY MAIN
//G.FT01F001 DD DSN=&&AXPB,DISP=(OLD,DELETE)
//G.SYSIN DD *
FIT TO FREQUENCY RESPONSE
        1   RHOSQRD     0.69      0.1E-02
        2   4QLSQRD     1.2E005   100.
        3   F0          3155.09   0.01
            BLANK
3172.75     92.0        1.0
3170.45     90.0        1.0
3169.14     88.0        1.0
3167.55     86.0        1.0
3166.49     84.0        1.0
3165.28     82.0        1.0
3164.42     80.0        1.0
3163.76     78.0        1.0
3162.40     76.0        1.0
3161.58     74.0        1.0
3160.66     72.0        1.0
3159.80     70.0        1.0
3158.78     68.0        1.0
3157.71     66.0        1.0
3155.09     64.2        1.0
3152.54     66.0        1.0
3151.15     68.0        1.0
3149.91     70.0        1.0
3149.06     72.0        1.0
3147.74     74.0        1.0
3146.78     76.0        1.0
3145.37     78.0        1.0
3143.08     80.0        1.0
3139.45     88.5        1.0

MIGRAD
CONTOUR     1.          2.
CONTOUR     2.          3.
CONTOUR     3.          1.
PRINTOUT    0.
MINOS
EXIT
/*
```

References

Abdul-Razzak, M.M. et al ; 1987, "Microwave thermography for medical applications", Proc.IEE, **134**, 171

Aitmedhi, R., Anderson, A.P. and Sali, S. ; 1986, "Non-invasive measurement of volumetric loss distribution by microwave phase tomography", IEEE Colloquium on industrial and medical applications of microwaves, 9th May, 1986, Digest no 1986/73

Altman, P.L. and Dittmer, D.S. ; 1964, *The biology data handbook*, Fed.Amer.Soc.Exptal.Biol., Washington D.C.

Asami, K., Hanai, T. and Koizumi, N. ; 1980, "Dielectric analysis of Escherichia Coli suspensions in the light of the theory of interfacial polarisation", Biophys.J., **31**, 215

Athey, T.W., Stuchly, M.A. and Stuchly, S.S. ; 1982, "Dielectric properties of biological substances in vivo ar radio frequencies. Part I — Measurement method", IEEE Trans. Mic.Th.Tech., **MTT-30**, 82

Atkinson, E.R. ; 1983, "Hyperthermia techniques and instrumentation", in *Hyperthermia in Cancer Therapy*, G.K. Hall, Boston

Bardati, F., Brown, V.J., Chive, M., Fredericsen, F., Land, D.V., Leroy, Y., and Uzunoglu, N. ; 1989, "Microwave radiometry for noninvasive thermometry", Report of workshop on Non-Invasive Thermometry (NIT) in Clinical Hyperthermia, Nov 24 — 25 1989, Viturbo, Italy

Barford, N.C. ; 1976, *Experimental measurements:precision, error and truth*, Addison-Wesley, London

Barrett, A.H., Myers, P.C. and Sadowsky, N.L. ; 1980, "Microwave thermography in the detection of breast cancer", Am.J.Roent., **134**, 365

Benadda, M.D., Carru, J.C., Amoureux, J.P., Castelain, M. and Chapoyon, A. : 1982, "Experimental and theoretical study of the dielectric properties of 1-

cyanoadamantane ; spectrum of the compact crystal from measurements on powder", J.Phys.D: Appl.Phys., **15**, 1477

Best, C.H. and Taylor, N.B. ; 1950, *The physiological basis of medical practice*, 5th ed., Bulliere, Tindal and Cox, London

Bethe, H.A. and Schwinger, J. ; 1943, "Perturbation theory for cavities, NRWC Report **D1-117**, Cornell Univ., Ithaca, New York

Bianco, B. Drago, G.P., Marchesi, M., Martini, C., Mela, G.S. and Ridella, S. ; 1979, "Measurements of complex dielectric constant of human sera and erythrocytes", IEEE Trans.Ins.Meas., **IM-28**, 290

Blamey, R.W. ; 1984, "The current controversy in breast cancer: an update to 1984", in *Breast Cancer*, Seminar Series, ed. Blamey, R.W., Update, London

Bocquet, B., Leroy, Y., Mamouni, A. and Van de Velde, J.C. ; 1988, "Microwave imaging process by multiprobe radiometry — present state of the exploration of tumours of the breast", IEE Colloquium on medical applications of microwaves, Monday 25 April 1988, Digest No. 1988/60

Bolomey, J.C. ; 1986, "Active and passive microwave imaging: complementary approaches to remote thermal sensing in hyperthermia treatments", IEE Colloquium on industrial and medical applications of microwaves, 9th May 1986, Digest No. 1986/73

Bolomey, J.C., Jofre, L., Peronnet, G. and Pichot, C. ; 1984, "Microwave tomography and its potential application to the control of hyperthermia treatments", IEE Colloquium on electromagnetic techniques for detection and treatment of malignant disease, 2 April 1984, Digest No. 1984/36

Boned, C. and Peyrelasse, J. ; 1983, "Some comments on the properties of ellipsoids dispersed in continuum media", J.Phys.D: Appl.Phys., **16**, 1777

Bottcher, C.J.F. ; 1945, "The dielectric constant of crystalline powders", Rec.Trav.Chim., **64**, 47

128

Brady, M.M., Symons, S.A. and Stuchly, S.S. ; 1981, "Dielectric behaviour of selected animal tissues in vitro at frequencies from 2 to 4 GHz", IEEE Trans.Biom.Eng., **BME-28**, 305

Brooks, S.M. and Brooks, N.P- ; 1980, *The human body*, CV Mosby, St. Louis

Brown, V.J. ; 1989, "Development of computer modelling techniques for microwave thermography", Ph.D. Thesis, University of Glasgow

Brown. W.F. ; 1955, "Solid mixture permittivities", J.Chem.Phys., **23**, 1514

Bruggeman, D.A.G. ; 1935, "Berechnung verscheidener physkalischer Konstanten von heterogenen Substanzen", Annalen.Physik., **24**, 637

Buchanan, T.J., Haggis, J.B., Hasted, J.B. and Robinson, B.G. ; 1952, "The dielectric estimation of protein hydration", Proc.Roy.Soc.A, **213**, 379

Burdette, E.C., Cain, F.L. and Seals, J. ; 1980, "In vivo probe measurement technique for determining dielectric properties at UHF through microwave frequencies", IEEE Trans.Mic.Th.Tech., **MTT-28**, 414

Burdette, E.C., Cain, F.L. and Seals, J. ; 1986a, "In-situ tissue permittivity at microwave frequencies: perspective, techniques, results.", in *Medical applications of microwave imaging*, eds. Larsen, E.L. and Jacobi, J.H., IEEE, New York

Burdette, E.C., Freiderich, P.G., Seaman, R.L. and Larsen, L.E. ; 1986b, "In situ permittivity of canine brain: regional variations and postmortem changes", IEEE Trans.Mic.Th.Tech., **MTT-34**, 38

Burn, I. ; 1984, "The diagnosis and treatment of early breast cancer", Practitioner, **228**, 563

Casimir, H.B.G. ;1951, "On the theory of electromagnetic waves in resonant cavities", Phil.Res.Rep., **6**, 162

CERN Computer Centre Program Library ; 1977, 1978, Long write-ups D506, D516 [adapted and updated from CERN IDD internal report 75/20 which was published in Comp.Phys.Comm., **10** (1975), 343]

Cetas, T.C. ; 1983, "Physical modes (phantoms) in thermal dosimetry" in *Hyperthermia in Cancer Therapy*, G.K. Hall, Boston

Chiew, Y.C. and Glandt, E.D. ; 1983, " The effect of structure on the conductivity of a dispersion", J.Coll.Inter.Sci., **94**, 90

Cichoki, B. and Felderhof, B.U. ; 1988, "Dielectric constant of polarisable, non-polar fluids and suspensions", J.Stat.Phys., **53**, 499

Clausse, M. ; 1983, "Dielectric properties of emulsions and related systems" in *Encyclopedia of Emulsion Technology* , ed. Becher, P., Marcel-Dekker, N.Y.

Cleary, S.F. ; 1983, "Bioeffects of microwave and radiofrequency radiation", in *Hyperthermia in Cancer Therapy*, G.K. Hall, Boston

Clegg, J.S., McClean, V.E.R., Szwarnowski, S. and Sheppard, R.J. ; 1984, "Microwave dielectric measurements (0.8 — 70GHz) on Artemia cysts at variable water content", Phys.Med.Biol., **29**, 1409

Cole, K.S. and Cole, R.H. ; 1941, "Dispersion and absorption in dielectrics I. Alternating current characteristics", J.Chem.Phys., **9**, 341

Cole, K.S. and Cole, R.H. ; 1942, "Dispersion and absorption in dielectrics II. Direct current characteristics", J.Chem.Phys., **10**, 98

Cole, K.S., Li, C.-L. and Bak, A.F. ; 1969, "Electrical analogues for tissues", J.Exp.Neur., **24**, 459

Cole, R.H. ; 1957, "Induced polarization and dielectric constant of polar liquids", J.Chem.Phys, **27**, 33

Cook, H.F. ; 1951, "The dielectric behaviour of some types of human tissues at microwave frequencies", Brit.J.App.Phys., **2**, 295

Cook, H.F. ; 1952, "A comparison of the dielectric behaviour of pure water and human blood at microwave frequencies", Brit.J.Appl.Phys., **3**, 249

Cooke, R. and Kuntz, I.D. ; 1974, "The properties of water in biological systems", Ann.Rev.Biophys.Bioeng., **3**, 95

CRC ; 1977—78, *Handbook of Chemistry and Physics*, CRC, Cleveland, Ohio

Crichlow, R. W. ; 1978, "Diseases of the male breast", in *The Breast*, eds. Gallagher, H.S., Leis H.P., Reuven, R.K. and Urban, J.A., CV Mosby, St. Louis

Davidson, D.W. and Cole, R.H. ; 1951, "Dielectric relaxation in glycerine", J.Chem.Phys., **18**, 1417

Davis, D.L., Hoel, D., Fox, J. and Lopez, A. ; 1990, "International trends in cancer mortality in France, West Germany, Italy, Japan, England and Wales, and the USA", Lancet, **336**, 474

Dawkins, A.W.J., Gabriel, C., Sheppard, R.J. and Grant, E.H. ; 1981, "Electrical properties of lens material at microwave frequencies", Phys.Med.Biol., **26**, 1

Dawkins, A.W.J., Nightingale, N.R.V., South, G.P., Sheppard, R.J. and Grant, E.H. ; 1979, 'The role of water in microwave absorption by biological material with particular reference to microwave hazards", Phys.Med.Biol., **24**, 1168

Debye, P. ; 1929, *Polar Molecules*, Chemical Catalogue Co., New York.

Dickson, J.A. and Calderwood, S.K. ; 1983, "Thermosensistivity of neoplastic tissues in vivo", in *Hyperthermia in Cancer Therapy*, G.K. Hall, Boston

du Bois-Reymond, E. ; 1849, *Untersuchungen uber tierische Elektricitat*, G Reimer, Berlin

Duffin, W.J. ; 1980, *Electricity and Magnetism*, 3rd edition, McGraw-Hill, London

Dukhin, S.S. ; 1971, "Dielectric properties of disperse systems", Sur.Coll.Sci., 3, 83

Dukhin, S.S. and Shilov, V.N. ; 1974, *Dielectric phenomena and the double layer in disperse systems and polyelectrolytes*, John Wiley and Sons, New York.

Dunsmuir, R. and Powles, J.G. ; 1946, "A method for the measurement of the dielectric properties of liquids in the frequency range 600 — 3,200 Mc/sec (50 — 9.4 cm)", Phil.Mag., **37**, 747

Edeiken, S. ; 1988, "Mammography and palpable cancer of the breast", Cancer, **61**, 263

Edrich, J. ; 1979, "Centimeter and millimeter wave thermography: A survey of tumor detection"", J.Mic.Pow., **14**, 95

England, T.S. ; 1950, "Dielectric properties of the human body for wavelengths in the 1-10 cm range", Nature, **166**, 480

England, T.S. and Sharples, N.A. ; 1949, "Dielectric properties of the human body in the microwave region of the spectrum", Nature, **163**, 487

Forrest, P.F. et al ; 1986, *Breast cancer screening*, Department of Health and Social Security, London

Foster, K.R. and Schwan, H.P. ; 1986, "Dielectric properties of tissues", Part I of *CRC Handbook of the biological effects of electromagnetic fields*, eds. Polk,C. and Postow, E., CRC Press, Boca Riton, Florida

Foster, K.R. and Schwan, H.P. ; 1989, "Dielectric properties of tissues and biological materials: a critical review", Crit.Rev.Biomed.Eng, **17**,25

Foster, K.R., Cheever, E. and Leonard, B. ; 1984, "Transport properties of polymer solutions", Biophys.J., **45**, 975

Foster, K.R., Schepps, J.L. and Schwan, H.P. ; 1980, "Microwave dielectric relaxation in muscle. A second look", Biophys.J., **29**, 271

Foster, K.R., Schepps, J.L., Stoy, R.D. and Schwan, H.P. ; 1979, "Dielectric properties of brain tissue between 0.01 and 10GHz", Phys.Med.Biol., **24**, 1177

Fricke, K. ; 1924, "A mathematical treatment of the electric conductivity and capacity of disperse systems. Part I", Phys.Rev., **24**, 575

Fricke, K. ; 1925a, "A mathematical treatment of the conductivity of disperse systems. Part II", Phys.Rev., **26**, 678

Fricke, K. ; 1925b, "The electrical capacity of suspensions of red corpuscles of a dog", Phys.Rev., **26**, 682

Fricke, K. ; 1955, "The complex conductivity of a suspension of stratified particles of spherical or cylindrical form", J.Phys.Chem., **59**, 168

Fricke, K. and Morse, S. ; 1925, "An experimental study of the electrical conductivity of disperse systems. I Cream", Phys.Rev., **25**,361

Frohlich, H. ; 1949, *Theory of dielectrics*, Oxford University Press, Oxford

Gabriel, C. and Grant, E.H. ; 1985, "Dielectric properties of ocular tissues in the supercooled and frozen states", Phys.Med.Biol., **30**, 975

Gabriel, C., Sheppard, R.J. and Grant, E.H. ; 1983, "Dielectric properties of ocular tissue at 37 °C", Phys.Med.Biol., **28**, 43

Gent, W.L.G., Grant, E.H. and Tucker, S.W. ; 1970, "Evidence from dielectric studies for the presence of bound water in myelin", Biopolymers, **9**, 124

Ginzton, E.L. ; 1957, *Microwave Measurements*, McGraw-Hill, New York

Grant, E.H., Keefe, S.E. and Takashima, S. ; 1968, 'The dielectric properties of aqueous solutions of bovine serum", J.Phys.Chem., **72**, 4373

Grant, E.H., Sheppard, R.J., and South, G.P. ; 1978, *Dielectric behaviour of molecules in solution*, Oxford University Press, Oxford

Grant, J.P. ; 1984, "Measurement, medical significance and applications of the dielectric properties of biological materials", Ph.D. Thesis, Surrey University

Grant. E.H. ; 1965, 'The structure of water neighbouring proteins, peptides and amino acids as deduced from dielectric measurements", Ann.Rev.N.Y.Acad.Sci., **125**, 418

Gunther, K. and Heinrich, D. ; 1965, "Dielektrizitatskonstante, Permeabilitat, elektrische Leitfahigkeit, Warmeleitfahigkeit und Diffusionskonstante von Gemischen mit kugelformigen Teilchen (gitterformige and statistiche Anordnung)", Z.Physik., **185**, 345

Guy, A.W. and Chou, C. -K. ; 1983, "Physical aspects of localised heating by radiowaves and microwaves" in *Hyperthermia in Cancer Therapy*, G.K. Hall, Boston

Haagensen, C.D. ; 1986, *Diseases of the breast*, W.B.Saunders, Philadelphia

Hanai, T. ; 1968, "Electrical properties of emulsions" in *Emulsion Science*, ed. Sherman, P., Academic Press, London

Hanai, T. and Koizumi, N. ; 1975, "Dielectric relaxation of W/O emulsions in particular reference to theories of interfacial polarisation", Bull.Inst.Chem.Res., Kyoto Univ., **53**, 153

Hanai, T., Asami, K. and Koizumi, N. ; 1979, "Dielectric theory of concentrated suspensions of shell-covered spheres in particular reference to the analysis of biological cell suspensions", Bull.Inst.Chem.Res., Kyoto Univ., **57**, 297

Hanai, T., Kita, Y. and Koizumi, N. ; 1980, " Dielectric relaxation profiles in a theory of interfacial polarisation developed for concentrated disperse systems of spherical particles", Bull.Inst.Chem.Res., **58**, 534

Hand, J.W. ; 1987, "Hyperthermia. Challenging applications in cancer therapy", Phys.Bull., **38**, 111

Harrington, R.F. ; 1961, *Time-harmonic electromagnetic fields*, McGraw-Hill, New York

Hashin, Z. and Shtrikman, S. ; 1961, "Note on the effective constants of composite materials", J.Franklin Inst., **271**, 423

Hasted, J.B. ; 1972, "Liquid water: dielectric properties", in *Water: A comprehensive treatise*, Vol 1, chapter 7, ed. Francks, Plenum, New York

Hasted, J.B. ; 1973, *Aqueous dielectrics*, Chapman and Hall, London

Havriliak, S. and Watts, D.G. ; 1986, "Comparing graphical and statistical methods for analysing dielectric dispersions of polymers represented in the complex plane", Polymer, **27**, 1509

Hawley, M.S., Conway, J. and Anderson, A.P. ; 1988, "Effects of tissue layering on microwave thermography", IEE Colloquium on Medical Applications of Microwaves, 25 April 1988, Digest no. 1988/60

Hayslett, H.T. and Murphy, P. ; 1968, *Statistics made simple*, W.H. Allen, London

Hey-Shipton, G.L., Matthews, P.A. and McStay, J. ; 1982, "The complex permittivity of human tissue at microwave frequencies", Phys.Med.Biol., **27**, 1067

Hoque, M. and Gandhi, O.P. ; 1988, "Temperature distributions in the human leg for VLF — VHF exposures at the ANSI-recommended safety levels", IEEE Trans.Biom.Eng., **BME-35**, 442

Horner, F., Taylor, T.A., Dunsmuir, R., Lamb, J. and Jackson, W. ; 1945, "Resonance methods of dielectric measurement at centimetre wavelengths", J.IEE, **XC111**, 53

Irimajiri, A., Hanai, H. and Inouye, A. ; 1979, "A dielectric theory of 'multi-stratified shell' model with its application to a lymphoma cell", J.Theor. Biol, **78**, 251

Jenkins, S., Clarke, R.N., Horrocks, M. and Preece, A.W. ; 1989, "Dielectric measurements on human tissues between 100MHz and 3GHz", presented at *Advances in medical and microwave imaging* conf., University of Lille, Paris

Jofre, L., Broquetas, A., Hawley, M.S ; 1988, "Active microwave imaging: a cylindrical system for biomedical applications", IEE Colloquium on medical applications of microwaves, 25 April, Digest no. 1988/60

Karolkar, B.D., Behari, J. and Prim, A. ; 1985, "Biological tissues characterisation at microwave frequencies", IEEE Trans.Mic.Th.Tech., **MTT-30**, 64

Kirkwood, J.G. ; 1936, "On the theory of dielectric polarization", J.Chem.Phys., **4**, 592

Kisdnasamy, S. and Neelakantaswamy, P.S. ; 1984, "Complex permittivity of a dielectric mixture: modified Fricke's formula based on Lichtenecker's logarithmic law of mixing", Elec.Lett., **21**, 270

Kosterich, J.D., Foster, K.R. and Pollack, S.R. ; 1983, "Dielectric permittivity and electrical conductivity of fluid saturated bone", IEEE Trans.Biom.Eng., **BME-30**, 81

Kraszewski, A., Stuchly, M.A., Stuchly, S.S. and Smith, A.M. ; 1982, "In vivo and in vitro dielectric properties of animal tissues at radiofrequencies", Bioelectromagnetics, **3**, 421

Kraus, J.D. ; 1984, *Electromagnetics*, McGraw-Hill, Tokyo

Land, D.V ; 1987c, "Improved method for resonant-frequency perturbation methods", Elec.Lett., **23**, 1166

Land, D.V. ; 1987a, "A clinical microwave thermography system", Proc.IEE, **134**, 193

Land, D.V. ; 1987b, "Subcutaneous temperature measurement by microwave thermography", in *Chronobiotechnology and chronobiological engineering*, NATO ASI Series E: Applied Sciences, eds. Scheving, L.E., Halberg, M.D., and Ehret, C.F., Martinus Nijhoff, Dordrecht

Land, D.V., Fraser, S. and Shaw, R. ; 1986, "A review of the clinical experience of microwave thermography", J.Med.Eng.Tech. (Supp.: Recent developments in medical and physiological imaging), 109

Landau, L.D. and Lifshitz, E.M. ; 1959, *Electrodynamics of continuous media*, Pergamon, Oxford (Translated from Russian edition: Fizmatgitz, Moscow)

Landau, L.D. and Lifshitz, E.M. ; 1984, *Electrodynamics of continuous media*, 2nd ed., Pergamon, Oxford

Lewin, L. ; 1947, "The electrical constants of a material loaded with spherical particles", J.Inst.Elec.Eng., **94**, 65

Li, S., Akyed, C. and Bosisio, R.g. ; 1981, "Precise calculations and measurements of the complex dielectric constant of lossy materials using TM_{010} cavity perturbation techniques", IEEE Trans.Mic.The.Tech., **MTT-29**, 1041

Lichtenecker, K. ; 1929, "Mischkopertheorie als Wahrscheinlichkeitsproblem", Physik.Zeitschr., **30**, 805

Lichtenecker, K. and Rother, K. ; 1931, "Dieherleitung des logarithmischenMischumgenesetzes eus allgemeinen Prinzipien der stationaren Stromung", Physik.Zeithschr., **32**, 255

Lin, J.C. ; 1975, "Microwave properties of fresh mammalian brain tissue at body temperature", IEEE Trans.Biomed.Eng., **BME-22**, 74

Looyenga, H. ; 1965, "Dielectric constants of heterogeneous mixtures", Physica. **31**, 401

Lorraine, P. and Corson, D. ; 1970, *Electromagnetic fields and waves*, WH Freeman & Co, San Francisco

Maier, L.C. and Slater, J.C. ; 1952, "Field strength measurements in resonant cavities", J.App.Phys., **23**, 68

Malmberg, C. G. and Maryott, A. A. ; 1956, "Dielectric constant of water from 0°C to 100°C", J.Res.Nat.Bur.Stand., **56**, 1

Mamouni , A., Van de Velde, J.C., Hochedez-Robillard, M., Dujardin, B., Bocquet, B. and Leroy, Y. ; 1986, "Present state of microwave radiometry for medical applications", IEE Colloquium on industrial and medical applications of microwaves, Friday 9th May 1986, Digest No., 1986/73

Marino, A.A., Becker, R.O. and Bachman, C.H. ; 1967, "Dielectric determination of bound water of bone", Phys.Med.Biol., **12**, 367

Martinelli, M., Rolla, P.A. and Tombari, E. ; 1985, "A method for dielectric loss measurements by a microwave cavity in fixed resonance condition", IEEE Trans.Mic.Th.Tech., **MTT-33**, 779

Masszi, G., Zzijarto, Z. and Grof, P. ; 1976, "Investigations on the ion- and water-binding of muscle by microwave measurements", Acta.Biochim.et.Biophys.Acad.Sci.Hung., **11**, 129

Maxwell, J.C. ; 1881, *A treatise on electricity and magnetism*, 2nd ed., Clarendon Press, London

Meredith, R.E. and Tobias, C.W. ; 1960, "Resistance to potential flow through a cubic array of spheres", J.App.Phys., **31**, 1270

Mitchell, H.H., Hamilton, T.S., Steggerda, F.R. and Bean, H.W. ; 1945, "The chemical composition of the human body and its bearing on the biochemistry of growth", J.Biol.Chem., **158**, 625

Moreno, T. ; 1948, *Microwave transmission design data*, Dover, New York

Muller, J. ; 1939, "Untersuchung uber elektromagnetische Holraume", Hochfreq.Elektroakust., **54**, 157

Neelakantaswamy, P.S., Chowdari, B.V.R. and Rajaratnam, A. ; 1983, "Estimation of the permittivity of a compact crystal by dielectric measurement on its powder: A stochastic mixture model for the powder dielectric", J.Phys.D:Appl.Phys., **16**, 291

Neelakantaswamy, P.S., Turkman, R.I. and Sarkar, T.K. ; 1985, " Complex permittivity of a dielectric mixture: corrected version of Lichtenecker's logarithmic law of mixing", Elec.Lett, **21**, 270

Nightingale N.R.V., Goodridge, V.D., Sheppard, R.J. and Christie, J.L. ; 1983, "The dielectric properties of the cerebellum , cerebrum and brain stem of mouse brain at radiowave and microwave frequencies", Phys.Med.Biol., **28**, 897

Nightingale, N.R.V., Dawkins, A.W.J., Sheppard, R.J., Grant, E.H., Goodridge, V.D. and Christie, J.L. ; 1980, "The use of time domain spectroscopy to measure the dielectric properties of mouse brain at radiowave and microwave frequencies", Phys.Med.Biol., **25**, 1161

Oncley, J.L. ; 1943, *Proteins, amino acids and peptides*, eds. Cohn, E.J. and Edsall, J.T., Reinhold, New York

Onsager, L. ; 1936, "Electric moments of molecules in liquids", J.Am.Chem.Soc., **58**, 1486

Osswald, K. ; 1937, "Hochfrequenzleitfaehigkeit und dielektrizitaetskonstate von biologischen Geweben und Fluessigkeiten", Hochfrequenz.Elektroakustik, **49**, 40

Peloso, R., Tuma, D.T. and Jain, R.K. ; 1984, 'Dielectric properties of solid tumours during normothermia and hyperthermia", IEEE Trans.Biom.Eng., BME-**31**, 725

Pennock, B.E. and Schwan, H.P. ; 1969, "Further observations on the electrical properties of haemoglobin-bound water", J.Phys.Chem., **73**, 2600

Pethig, R. ; 1984, "Dielectric properties of biological materials: biophysical mechanisms and medical applications", IEEE Trans. Elec.Ins., EI-**19**, 453

Pethig, R. and Kell, D.B. ; 1987, "The passive electrical properties of biological systems: their significance in physiology, biophysics and biotechnology", Phys.Med.Biol., **32**, 933

Pilnik, S. and Leis, H.P. ; 1978, "Clinical diagnosis of breast lesions" in *The Breast*, eds Gallagher, H.S., Leis H.P., Reuven, R.K. and Urban, J.A., CV Mosby, St. Louis

Polder, D. and van-Santen, J.H. ; 1946, "The effective permeability of mixtures of solids", Physica, **12**, 25

Rajewsky, B. ; 1938, *Ultrakurzwellen, Ergebnisse der biophysikalischen Forschung*, Vol 1, George Thieme, Leipzig

Rayleigh, Lord ; 1892, "On the influence of obstacles arranged in rectangular order upon the properties of a medium", Phil.Mag., **34**, 481

Rehmann, I ; 1978, "Embryology and anatomy of the breast", in *The breast*, eds. Gallagher, H.S., Leis H.P., Reuven, R.K. and Urban, J.A., CV Mosby, St. Louis

Robbins, G.F. ; 1978, "Staging end-result reporting for patients with breast carcinoma", in *The Breast*, eds. Gallagher, H.S., Leis H.P., Reuven, R.K. and Urban, J.A., CV Mosby, St. Louis

Roebuck, E.J. ; 1986, "Mammography and breast screening for breast cancer", Brit.Med.J., **292**, 223

Rogers, J.A., Sheppard, R.J., Grant, E.H., Bleehen, N.M. and Hones, D.J. ; 1983, "The dielectric properties of normal and tumour mouse tissue between 50MHz and 10GHz", Brit.J.Rad., **56**, 335

Rotherberg, L.N. ; 1986, "Mammography and medical physics", Physics Today, S45

Runge, I. ; 1925, "Zur elektrischen Leitfahigkeit metallischer Aggregate", Zeitschr.F.Tech.Physik., **6**, 61

Schepps, J.L ; 1981, "The measurement and analysis of the dielectric properties of normal and tumor tissues at UHF and microwave frequencies", Ph.D. Thesis, University of Pennsylvania

Schepps, J.L. and Foster K.R. ; 1980, "The UHF and microwave dielectric properties of normal and tumour tissues: variation in dielectric properties with tissue water content", Phys.Med.Biol., **25**, 1149

Schwan, H.P and Li, K. ; 1956, "Hazards due to total body irradiation by radar", Proc.IRE, **44**, 1572

Schwan, H.P. ; 1957, "Electrical properties of tissue and cell suspensions" in *Advances in biological and medical research*, 5, Academic, New York

Schwan, H.P. ; 1964, "Electrical characterisitics of tissues: a survey", Biophysik, **1**, 198

Schwan, H.P. ; 1965, "Electrical properties of bound water", Ann.N.Y.Acad.Sci., **125**, 344

Schwan, H.P. ; 1981, "Electrical properties of cells: principles, some recent results and some unresolved problems" in *Biophysical approach to excitable systems*, eds. Adelman W.S. and Goldman D., Plenum, New York

Schwan, H.P. and Foster, K.R ; 1980, "RF-field interactions with biological systems: electrical properties and biophysical mechanisms", Proc.IEEE, **68**, 104

Schwan, H.P. and Foster, K.R. ; 1977, "Microwave dielectric properties of tissue. Some comments on the rotational mobility of tissue water", Biophys.J., **17**, 193

Schwan, H.P. and Li, K. ; 1953, "Capacity and conductivity of body tissues at ultrahigh frequencies", Proc. IRE, **41**, 735

Sihvola, A. ; 1989, "Macroscopic permittivity of dielectric mixtures with application to microwave attenuation of rain and hail", Proc.IEEE.M. (Micr.Antenn.Prop.), **136**, 24

Sihvola, A. and Lindell, I.V. ; 1990, "Polarizability and effective permittivity of layered and continuously inhomogeneous dielectric ellipsoids", J.Elec.Waves.App., 4,1

Sinha, J.K. and Brown, D. ; 1960, "A new cavity-resonator method for measuring permittivity", Proc.IEE, **107**(B), 522

Slater, J.C. ; 1950, *Microwave electronics*, (Bell Laboratory Series), Van Nostrand, Princeton

Smith, G.S. and Scott, J.R. ; 1990, "The use of emulsions to represent dielectric materials in electromagnetic scale models", IEEE Trans.Ant.Prop., APP-38, 323

Smith, S.R. and Foster, K.R. ; 1985, "Dielectric properties of low water content tissues", Phys.Med.Biol., 30, 965

Smythe, C.P. ; 1955, Dielectric behavior and structure, McGraw-Hill, New York

Spells, K.E. ; 1960, "The thermal conductivities of some biological fluids", Phys.Med.Biol, 5, 139

Spiegel, R.J., Fatmi, M.B.A., Stuchly, S.S. and Stuchly, M.A. ; 1989, "Comparison of finite difference time-domain SAR calculations with measurements in a heterogeneous model of man", IEEE Trans.Biom.Eng., BME-36, 849

Spiridonov, V.I. ; 1982, "A relaxation model for the dielectric properties of water in heterogeneous mixtures", Meas.Tech., 25, 448

Steel, M., Sheppard, R.J. and Grant, E.H. ; 1984, "A precision method for measuring the complex permittivity of solid tissue in the frequency domain between 2 and 18GHz", J.Phys.E.: Sci.Instrum., 17, 30

Steel, M.C. and Sheppard, R.J. ; 1988, "The dielectric properties of rabbit tissue, pure water and various liquids suitable for tissue phantoms at 35GHz", Phys.Med.Biol., 33, 467

Steel, M.C. and Sheppard, R.J., 1985, "Dielectric properties of mammalian brain tissue between 1 and 18GHz", Phys.Med.Biol., 30, 621

Steel, M.C. and Sheppard, R.J., 1986, "Dielectric properties of lens tissue at microwave frequencies", Bioelectromagnetics, 7, 73

Stogryn, A. ; 1971, "Equations for calculating the dielectric constant of saline water", IEEE Trans.Mic.The.Tech., MTT-19, 733

Storm, F.K. ; 1983, "Background, principles and practice" , in Hyperthermia in Cancer Therapy, G.K. Hall, Boston

Stoy, R.D., Foster, K.R. and Schwan, H.P. ; 1982, "Dielectric properties of mammalian tissues from 0.1 to 100 MHz: a summary of recent data", Phys.Med.Biol., 27, 501

Stratton, J.A. ; 1941, *Electromagnetic theory*, McGraw-Hill, New York

Stuchly, M.A. and Stuchly, S.S. ; 1980, "Dielectric properties of biological substances - tabulated", J.Mic.Pow., 15, 19

Stuchly, M.A., Athey, T.W., Samaras, G.M. and Taylor, G.E. ; 1982b, "Measurement of radio frequency permittivity of biological tissues with an open-ended coaxial line: Part II — experimental results", IEEE Trans. Mic.Th.Tech., MTT-30, 87

Stuchly, M.A., Athey, T.W., Stuchly, S.S., Samaras, G.M. and Taylor, G. ; 1981, "Dielectric properties of animal tissuès in vivo at frequencies 10MHz to 1GHz", Bioelectromagnetics, 2, 93

Stuchly, M.A., Kraszewski, A., Stuchly, S.S. and Smith, A.M. ;1982a, "Dielectric properties of animal tissue in vivo at radio and microwave frequencies: comparison between species", Phys.Med.Biol., 27, 927

Surowiec A.J., Stuchly, S.S. and Swarup, A. ; 1985, "Radiofrequency dielectric properties of animal tissues as a function of time following death", Phys.Med.Biol., 30, 1131

Surowiec, A., Stuchly S.S., Eidus, L. and Swarup, A. ; 1987, "In vitro dielectric properties of human tissues at radiofrequencies", Phys.Med.Biol., 32, 615

Surowiec, A.J., Stuchly, S.S., Barr, J.R., and Swarup, A ; 1988, "Dielectric properties of breast carcinoma and the surrounding tissues", IEEE Trans. Biom.Eng., BME-35, 257

Tanabe, E. and Joines, W.T. ; 1976, "A nondestructive method for measuring the complex permittivity of dielectric materials at microwave frequencies using an open transmission line resonator", IEEE Trans.Instrum.Meas., IM-25, 222

Thurai, M., Goodridge, V.D., Sheppard, R.J. and Grant, E.H ; 1984, "Variation with age of the dielectric properties of mouse brain cerebrum", Phys.Med.Biol., 29, 1133

Velick, S. and Goran, M. ; 1940, "The electrical conductance of suspensions of ellipsoids and its relation to the study of avian erythrocytes", J.Gen.Physiol., **23**, 251

Von-Hippel, A.R. ; 1954, *Dielectric materials and applications*, Chapman-Hall, London

Wagner, K.W. ; 1914, "Erklarung der dielektrischen Nachwirkungsvorgange auf Grund Maxwellscher Vorstellungen", Archiv Electrotechnik, **2**, 371

Waldron, R.A. ; 1969, *Theory of electromagnetic waves*, Van Nostrand Reinhold, London

Wiener, O. ; 1912, "Herkunft und Stellung der Aufgabe", Abh.Sachs.Akad.Wiss., Math-Phys.Kl., **32**, 509

Windle, W.F. ; 1976, *Textbook of histology*, 5th edition, McGraw-Hill, New York

Xu, D., Liping, L. and Zhiyan, J. ; 1987 "Measurement of the dielectric properties of biological substances using an improved open-ended coaxial line resonator method", IEEE Trans.Mic.Th.Tech., **MTT-35**, 1424

Zywietz, F. and Knochel, R. ; 1986, "Dielectric properties of Co-γ irradiated and microwave-heated rat tumour and skin measured in vivo between 0.2 and 2.4GHz", Phys.Med.Biol., **31**, 1021

(1) Schwan H.P., Sheppard R.J. and Grant E.H. ; 1976, "Complex permittivity of water at 25°C", J.Chem.Phys., 64, 2257

(2) Chaudhary S.S., Mishra R.K., Swarup A. and Thomas J.M. ; 1984, "Dielectric properties of normal and malignant human breast tissues at radiowave and microwave frequencies", Ind.J.Biochem. Biophys., 21, 76

(3) Foster K.R. and Schepps J.L. ; 1981, "Dielectric properties of tumor and normal tissues at radio through microwave frequencies", J.Mic.Pow., 16, 107

(4) Stewart I. ; 1973, *Galois Theory*, Chapman & Hall, London